UNIVERSITY OF CALIFORNIA, SAN DIEGO

SAN DIEGO STATE UNIVERSITY

An Analysis of Autophagy in the Aging Murine Heart

A dissertation submitted in partial satisfaction of the requirements for the degree Doctor of Philosophy

in

Biology

by

Michael Allen Gurney, Jr.

Committee in Charge:

University of California, San Diego

Professor Stephen M. Hedrick
Professor Hemal H. Patel

San Diego State University

Professor Roberta A. Gottlieb, Chair
Professor Phyllis-Jean Linton, Co-Chair
Professor Greg L. Harris
Professor Tom Huxford

2014

The Dissertation of Michael Allen Gurney, Jr. is approved, and it is acceptable in quality and form for publication on microfilm and electronically:

_____

_____

_____

_____

_____
Co-Chair

_____
Chair

University of California, San Diego

San Diego State University

2014

DEDICATION

Foremost, I would like to dedicate this work to my family, Amber, Trevor, and Calvin Gurney. I would not have been able to complete this project without their continued love, support, and sacrifice. Additionally, I would also like to dedicate this dissertation to my brother Mark and my mother Wilda for their support as well.

Furthermore, I would like to dedicate this dissertation to my Grandmother Lila and my late Grandfather, Keith C. Kelly. They made me the man I am and I thank them for it. Someday all my family will meet again in heaven - in the log cabin by the babbling brook that Grand and Pa are building for us.

Finally, I would also like dedicate this thesis to the officers and crew of the U.S.S. Benfold (DDG-65), both past and present. I thank you for your courage, your steadfast devotion to honor, and commitment to duty and I dedicate this work to those of you that work so hard and sacrifice so much, but will never see your names in print. Fair Winds and Following Seas, Benfold. Onward with Valor!

EPIGRAPH

Do. Or do not. There is no try.

&

Always pass on what you have learned.

Jedi Master Yoda

TABLE OF CONTENTS

LIST OF ABBREVIATIONS

MA – Macroautophagy

CMA – Chaperone Mediated Autophagy

ROS – Reactive Oxygen Species

FBS – Fetal Bovine Serum

SDS – Sodium dodecyl sulfate

AKT – Gene Name (Synonymous with Protein Kinase B)

AMPK – 5’ Adenosine monophosphate-activated protein kinase

ATG – Autophagy Gene

TBST – Tris Buffered Saline with Tween 20

DMSO – Dimethyl sulfoxide

DMEM – Dulbecco’s Modified Eagle Medium

PBS – Phosphate Buffered Saline

RIPA – Radioimmunoprecipitation Assay

TETN – Tris, EDTA, Triton X-100, NaCl

IF – Intermittent Fasting

AL – Ad Libitum

LIST OF FIGURES AND TABLES

ACKNOWLEDGMENTS

I would like to take this opportunity to thank my mentors Drs. Phyllis-Jean Linton and Roberta A. Gottlieb for their tremendous assistance and guidance in completing this dissertation. I know reading over multiple drafts of dissertation and proposal papers, abstracts, posters, and Graduate Student Seminars took a lot of time and effort and I appreciate it. I could not have achieved what I have and come this far without their assistance.

Additionally, I would like to thank Dr. Kim Finley for her assistance with ImageJ and the initial p62/ubiquitin western blots and Lillian Li with her assistance during the early times. Additionally, I would like to thank Dr. Marylyn Thoman for her assistance with some of the later experiments. I would also like to thank some of the undergraduates that assisted with washing western blots: Ian, Nancy, Tianna, Charlene, Julie, Sarah, and Sarah. I would also like to thank the additional members of my committee: Drs. Hedrick, Patel, Huxford, and Harris for their valuable insights and suggestions.

Finally, I would like to thank Drs. Stark, Tobin, and Burnette for developing western blot technology. Without them I would not have had the opportunity to run hundreds and hundreds and hundreds and hundreds of western blots.

Chapter I, in part, is currently being prepared for submission for publication of this material. Gurney, M.A., Gottlieb, R.A., and Linton, P.J. The dissertation author was the primary investigator and author of this material.

Chapter II, in part, is currently being prepared for submission for publication of this material. Gurney, M.A., Gottlieb, R.A., and Linton, P.J. The dissertation author was the primary investigator and author of this material.

Chapter III, in part, is currently being prepared for submission for publication of this material. Gurney, M.A., Linton, P.J., and Gottlieb, R.A. The dissertation author was the primary investigator and author of this material.

VITA

Education:

Fire Control 'A' School (US Navy Service School Command, Great Lakes, IL), 1994

Fire Control 'C' School (Aegis Training Center, Dahlgren, VA), 1995

Grossmont Community College (El Cajon, CA)
Associates of Arts – University Transfer Studies, 2003

University of California, San Diego (La Jolla, CA)
Bachelor of Science – Biochemistry and Cell Biology, 2006

San Diego State University (San Diego, CA)
Master of Science – Cell and Molecular Biology, 2009, with Dr. Kelly Doran
Thesis Title: *Role of Surface Expressed Pili and Fibrils in the Pathogenesis of Group B Streptococcal Disease*

San Diego State University/University of California, San Diego (San Diego, CA)
Doctor of Philosophy in Biology, 2014 with Drs. P.J. Linton and R.A. Gottlieb
Dissertation Title: *An Analysis of Autophagy in the Aging Murine Heart*

Honors and Awards:

Awarded the Donald P. Shiley Scholarship (2013-2014)

Finalist in the Idea to Product Competition at the California State University Program for Education and Research in Biotechnology (Fluormidine) (2013)

Achievement Rewards for College Scientists (ARCS) Scholar (2012-2014)

Graduated Magna cum Laude from the University of California San Diego (2006)

UCSD Provost Honors

Graduated with Honors from Grossmont Community College (2003)

Grossmont College President's List

Certificate of Recognition for Volunteer Math Tutoring, Emerald Middle School (2003)

Honorable Discharge from the US Navy (1999)

Navy Achievement Medal, US Navy (1999, 1996)

Good Conduct Medal, US Navy (1999, 1996)

Letter of Appreciation, Commanding Officer Aegis Training Center (1994)

Association Memberships:

American Heart Association (2012-2013)

San Diego Microbiology Group (2008 – Present)

American Association for the Advancement of Science (2008 – 2013)

San Diego State University Student Veterans Organization (2007 – Present)

American Society for Microbiology (2007 – 2010)

Phi Beta Kappa Honor Society (2006 - Present)

Phi Sigma Theta Honor Society (2004 – Present)

Professional Experience:

(2009-Present) **PhD Student in the Laboratories of Dr. Phyllis Linton and Dr. Roberta Gottlieb, Department of Biology, San Diego State University, San Diego, California.**
Determining how autophagy changes across a lifespan with respect to mouse strain (C57BL/6 vs. BALB/c), tissue (brain, heart, spleen, liver, lymph node, and thymus), and gender. Observing if a substantially less severe form of caloric restriction (intermittent fasting) in middle-aged animals can reverse the age-related decline in autophagy and restore immune function or improve cardiac recovery following heart attack. Investigating the role of autophagy in aging immune cell populations. Investigating the interrelation between inflammation on autophagy in the context of aging, specifically in the heart and spleen. Optimization of flow cytometry analysis of autophagy in cells (Fluormidine)

2007- 2009 **Graduate Student in the Laboratory of Dr. Kelly Doran, San Diego State University, San Diego, California (Master's Student).**
Project: *Investigating the Role of Group B Streptococcus Proteins on Host Immunity.* Invasion/adherence assays, RNA extraction, real-time PCR, production of a knock-out mutant, cloning, ELISA, cell culture, protein isolation/purification, lab maintenance, safety officer, lab manager.

2007- Present **Teaching Assistant, San Diego State University, San Diego, California.**
Fundamentals of Microbiology (Bio210/211) Lab Section (8x)
General Microbiology (Bio350) – Spring 2014

2006-2007 **Biological Sciences Laboratory Technician with Dr. Theo Kirkland**
The Veterans Medical Research Foundation, La Jolla, California.
Coccidioidides and *Leptospira* research (infectious disease). RNA Extraction, real-time PCR, cloning, transfection, FACS, LAL assay, western blots, ELISA, intraperitoneal macrophage activation, cell culture, and small animal handling, injections, and tissue harvesting

2004 **Volunteer Laboratory Assistant with Dr. Doug Bartlett**
The Scripps Institute of Oceanography, La Jolla, California
Cholera research. Prepared mini/maxipreps, PCR, cloning, and gel electrophoresis

2003-2004 **Laboratory Assistant for Dr. Lisa Stowers and Dr. Uli Mueller**
The Scripps Research Institute: Department of Cell Biology, La Jolla, California
Prepared mini/maxipreps, single cell picking, PCR, cloning, gel electrophoresis, making competent cells, antibody purification, washing glassware, making stock solutions, and general lab maintenance

2003 **Junior High Math Tutor for Americorp Program**
Tutored junior high children in remedial math, assisted in homework club tutoring Algebra and English

2002 **Physics Paper Grader**
Grossmont College, El Cajon, California
Graded Physics 110 and 140 papers

1999-2000 **Final Test Technician at Delta Design, Kearney Mesa, California**
Performed component-level trouble-shooting, maintenance, alignments, and repair of both Summit and Flex Pick and Place Handlers. Analyzed, trouble-shot, and repaired faults using schematics, specialized tools and test equipment

1999 **Final Test Technician for @TECH/APPLE ONE TEMPORARY AGENCY, Mira Mesa, California**
Contracted to Delta Design as a Final Test Technician.

1993-1999 **U.S. Navy Fire Controlman (Secret Clearance)**
Performed component-level trouble-shooting, alignments, maintenance, and repair of the AEGIS Display and Computer Systems. Micro/mini soldering techniques to repair faulty components. Work Center Supervisor. Qualified: Combat Systems

Officer of the Watch, Combat Systems Duty Officer, Officer of the Deck, Enlisted Surface Warfare Specialist.

Professional Presentations:

(Oct., 2014) Oral Dissertation Defense: "An Analysis of Autophagy in the Aging Murine Heart." San Diego, California.

(May, 2014) Poster Presentation at Keystone Symposia - Autophagy: Fundamentals to Disease. Austin, Texas.

(Apr., 2014) Poster Presentation at the San Diego State Graduate Student Symposium, San Diego, California.

(Mar., 2014) Poster Presentation at the San Diego State Student Research Symposium, San Diego, California.

(Dec., 2013) Oral Presentation: "Autophagy and Inflammation in the Aging Murine Heart." Graduate Student Seminar. San Diego, California.

(Apr., 2013) Poster Presentation at the San Diego State Graduate Student Symposium, San Diego, California.

(Mar., 2013) Poster Presentation for SDCSB Symposium at the Sanford Consortium Auditorium, La Jolla , California.

(Mar., 2013) Poster Presentation at the San Diego State Student Research Symposium, San Diego, California.

(Mar., 2013) Oral Presentation: "An Analysis of Autophagy and the NLRP3 Inflammasome in the Aging Murine Heart." La Jolla, California.

(Jan., 2013) Oral Presentation: "Autophagy, Aging, and Fluormidine." Graduate Student Seminar. San Diego, California.

(Jan., 2013) Oral Presentation: "Autophagy and Aging." for the ARCS Winter General Membership Meeting, San Diego, California.

(Jan., 2013) Oral Presentation/Question and Answer Period on Fluormidine at the I2P Competition at the CSUPERB Conference, Anaheim, California.

(July, 2012) Poster Presentation at the American Heart Association Basic Cardiovascular Science Conference, New Orleans, Louisiana.

(Apr., 2012) Poster Presentation at the Cell and Molecular Biology Graduate Student Symposium, San Diego, California.

(Feb., 2012) Oral Presentation: "Autophagy Changes Across a Lifetime: A Tale of Two Mice" Graduate Student Seminar, San Diego, California.

(Mar., 2011) Oral Presentation: "Visualization and Characterization of Autophagosomes by a Cadaverine Conjugated Dye." Graduate Student Seminar, San Diego, California.

(Jun., 2009) Poster Presentation at the 15th Annual Conference on Gram Positive Microorganisms, La Jolla, California.

(May, 2009) Oral Thesis Defense: "The Role of Surface Expressed Pili and Fibrils in the Pathogenesis of Group B Streptococcal Disease." San Diego State University, San Diego, California.

(May, 2009) Poster Presentation at the San Diego Microbiology Group The Scripps Institute of Oceanography, La Jolla, California.

(Apr., 2009) Poster Session at the Molecular Biology Graduate Student Symposium, San Diego, CA.

(Nov., 2008) Oral Presentation: "The Host Response to Group B Streptococcus." San Diego, CA

(May, 2008) Poster Presentation at the San Diego Microbiology Group, The Scripps Institute of Oceanography, La Jolla, California.

(Apr., 2008) Poster Session at the Molecular Biology Graduate Student Symposium, San Diego, California.

Publications:

van Sorge, N.M., Quach, D, **Gurney, M.A.,** Sullam, P.M., Nizet V. and Doran, K.S. 2009. *The Group B Streptococcal Serine Rich Repeat 1 Glycoprotein Mediates Penetration of the Blood-Brain Barrier.* Journal of Infectious Disease. May 15: 199(10):1479-87.

Gurney, M.A., Lembo, A., Burnside, K., Banerjee, A., de los Reyes, M., Connelly, J.E., Wan-Jun, L., Jewel, K.A., Vo, A., Renken, C.W., Doran, K.S., and L. Rajagopal. 2010.

Regulation of CovR expression in Group B Streptococcus impacts blood-brain barrier penetration. Molecular Microbiology. 77(2):431-443.

Banerjee, A., Kim, B.J., Carmona E.M., Cutting, A.S., **Gurney, M.A.**, Carlos, C., Feuer, R., Prasadarao, N.V., and K.S. Doran. 2011. *Bacterial Pili exploit integrin machinery to promote immune activation and efficient blood-brain barrier penetration*. Nature Communications. Sep. 6: 2:462.

Burnside, K., Lembo, A., Harell, M.I., **Gurney, M.A.,** Xue, L., Binh-Tran, N.T., Connelly, J.E., Jewel, K.A., Schmidt, B.Z., de los Reyes, M., Tao, W.A., Doran, K.S., and L. Rajagopal. 2011. *Serine/Threonine Phosphatase Stp1 Mediates Post-transcriptional Regulation of Hemolysin, Autolysis, and Virulence of Group B Streptococcus*. Journal of Biological Chemistry. Dec. 23: 286(51):44197-44210.

Gurney, M.A., Gottlieb, R.A., and P.J. Linton. 2012. *Autophagy in the Aging Heart*. Circulation Research (Abstract). Aug 30: 111:A302. < http://circres.ahajournals.org /cgi/content/meeting_abstract/111/4_MeetingAbstracts/A302>.

Gurney, M.A., Muralidhar, G., and P.J. Linton. 2013. Autophagy in the Immune System. In Roberta A. Gottlieb (Ed.) *Autophagy in Health and Disease* (pp. 41-55). London, U.K., Elsevier.

Viriyakosol, S., del Pilar Jimenez, M., **Gurney, M.A.**, Ashbaugh M.E., and J. Fierer. 2013. *Dectin-1 is Required for Resistance to Coccidioidomycosis in Mice.* mBio. Feb. 4(1):e00597-12.

Gurney, M.A., Huang, C., Ramil, J.M., Ravindran, N., Andres, A.M., Sin, J., Linton., P.J., and R.A. Gottlieb. 2014. *Measuring Cardiac Autophagic Flux in vitro and in vivo*. In Gil Mor and Ayesha Alvero (Eds.) *Apoptosis and Cancer: Methods and Protocols (Methods in Molecular Biology)*. (In Press).

Huang, C., Hiraumi, Y., Ramil, J.M., Zhang, X., Ratliff, E.P., **Gurney, M.A.**, Lee, P., Hernandez, G., Sin, J., LaRue, J., Doran, K.S., Gustafsson, A.B., and R.A. Gottlieb. 2014. *G-CSF Prevents Doxorubicin-Induced Late-Onset Cardiomyopathy through Mobilization of c-kit+ Stem Cells and Stimulation of VEGF Production*. Journal of Clinical Investigation. (Submitted).

Andres, A., Ramesh, M., Hernandez, G., Lee, P., **Gurney, M.A.**, Islam, M.J., Linton, P.J., and R.A. Gottlieb. *Mitophagy protects against statin-mediated cell death in C2C12 skeletal muscle cells.* (In Preparation)

Ratliff, E., Kotzebue, R., Mauntz, R., Gonzalez, A., Achal, M., Barekat, A., Garza, S., Sparhawk, J., Finley, K., **Gurney, M.**, Linton, P., Herr, D., Harris, G., and K. Finley. 2014. *The Regulation Neural Aging by Intermittent Fasting, Autophagy and Insulin Signaling Pathways in Drosophila.* Aging Cell. (Submitted).

Gurney, M.A., Li, L. Gottlieb, R.A., and P.J. Linton. 2014. *Characterization of Autophagy in the Aging Murine Heart.* (In Preparation).

Gurney, M.A., Gottlieb, R.A., and P.J. Linton. 2014. *Characterization of Strain-Related Differences in Autophagy in the Murine Heart: C57BL/6 vs. BALB/c.* (In Preparation).

American Society of Microbiologists Blog:

Gurney, M.A., Schwarzberg, K., Youle, M., and M. Schaechter. American Society of Microbiology. May 17, 2010. *You Are What You Eat.* Small Things Considered (American Society for Microbiology Blog). <http://schaechter.asmblog.org/schaechter/2010/05/you.html >.

Gurney, M.A., Schwarzberg, K., Gurfield, A. N., Youle, M., and M. Schaechter. American Society of Microbiology. June 21, 2010. *Our Counterintelligence Staph.* Small Things Considered (American Society for Microbiology Blog). < http://schaechter.asmblog.org/schaechter/2010/06/our-counterintelligence-staph.html>.

ABSTRACT OF THE DISSERTATION

An Analysis of Autophagy in the Aging Murine Heart

by

Michael Allen Gurney, Jr.

Doctor of Philosophy in Biology

University of California, San Diego, 2014
San Diego State University, 2014

Professor Roberta A. Gottlieb, Chair
Professor Phyllis-Jean Linton, Co-Chair

Although macroautophagy (MA) has been shown to decline with age, whether these changes are manifest differently in a shorter-lived (BALB/c) vs. longer-lived (C57BL/6) mouse strain remains unclear. Several parameters of basal MA were measured in cardiac tissue from mice aged 2.5-3 and 24-25 months: LC3-II and a Triton-insoluble fraction containing p62/SQSTM1 and ubiquitinated proteins. We observed a decrease in LC3-II coupled with an increase in p62 and ubiquitinated proteins, confirming a decline

in MA in aged C57BL/6 mice. In contrast, old BALB/c mice demonstrated increased LC3-II, reduced p62, and no change in ubiquitinated proteins. Further analysis in aged C57BL/6 revealed a significant decline in Atg5 and an increase in the upstream autophagy regulator, pAKT-Ser473. In contrast, aged BALB/c mice demonstrate an increase in the autophagy proteins, pULK1-Ser757, Atg3, Atg7, Atg5, Atg12, Beclin-1, Atg4D, and Parkin, and an increase in the upstream autophagy regulators, pAKT-Thr308, pAKT-Ser473, pAMPK-Thr172, pFoxO3a-Ser253, and SirT1. This demonstrates a dysregulation in autophagy since molecules that enhance as well as inhibit autophagy are altered with age. Importantly, as suggested by the data with aged mice, MA is manifest differently in these strains. Comparing young C57BL/6 and BALB/c mice confirmed differences in autophagy and its upstream regulatory proteins. Young BALB/c mice demonstrate higher levels of pULK1-Ser757, p62, Atg7, Atg12, Atg5/12, Beclin-1 (Atg6), Parkin, and pAMPK-Thr172 in addition to reduced expression of LC3-II, indicating a dysregulation in the autophagy pathway and depressed autophagy compared to its C57BL/6 counterpart. Moreover, when subjected to an acute stress (a fast), LC3-II levels increased in young and old mice of both strains. However, compared to young C57BL/6, maximal levels of LC3-II were attained later in aged C57BL/6 and in all BALB/c, suggesting defective flux. To confirm this, fasted mice were chloroquine-treated, which prevents autophagosome/lysosome fusion and favors LC3-II accumulation. Whereas LC3-II accrued in young C57BL/6, we found no increase in the aged C57BL/6 or in young or old BALB/c. Thus, the aged can mount an acute response, albeit with reduced flux. In order to make autophagy detection clinically viable, we developed and validated a reagent that appears to detect autophagy in peripheral blood.

INTRODUCTION TO THE DISSERTATION

Autophagy is a cellular process that has been demonstrated to play an important role in an array of age-related diseases such as neurodegenerative disorders[1], muscle disorders[2], cancer[3,4], cardiovascular disease[5], metabolic syndrome[6,7], obesity[7], infection[8-10], and many, many others. It is generally assumed in the literature that autophagy declines with increasing age; however, no one to date has done a comprehensive analysis of how changes in autophagy are manifest in the aged by observing both basal and induced or stimulated autophagy.

In order to get an indication of how autophagy is manifest in a variety of murine tissues (the brain, heart, liver, spleen, thymus, lymph node, and lung) under basal conditions with age, the expression of a variety of autophagy-related proteins was analyzed in aged versus young C57BL/6 (a longer lived strain – average lifespan 30 months) and BALB/c (a shorter lived strain – average lifespan 24 months) mice (Figure I.1 and Figure 2.1). The study demonstrated two interesting things. First, the overall trend in the expression of several autophagy proteins in each tissue in the same mouse strain suggests a decline in autophagy with increasing age, but how each specific tissue ages with respect to autophagy differs between tissues. This observation reaffirms that autophagy could be a contributing factor to some age-related diseases, since all of the aforementioned diseases have a substantial autophagic component in their underlying etiologies. Second, a comparison of the age-associated change in autophagy protein profiles for any specific tissue in the C57BL/6 to its BALB/c counterpart revealed substantial differences. This implies marked strain-related differences in the autophagy pathway in aging mice that could impact susceptibility to or the progression of a variety

of aging associated diseases. The focus of this dissertation is on the heart so the majority of the study will be limited to the heart. These observations led us to ask the following questions.

First, if there is a difference in the autophagic protein profile between a variety of aging tissues across mouse strains, is there a strain-related difference in the manifestation of autophagy in the hearts of young C57BL/6 versus BALB/c or is it the autophagic difference the result of a difference in the way the mouse strains age? Also, if there is a difference in autophagy between the two mouse strains, how would autophagy be manifest in the progeny of these mice? This is an important line of research because it describes a strain-related difference in an important cellular pathway (or its upstream regulatory components) that communicates with virtually every other pathway in the cell. Consequently, changes in autophagy between mouse strains or parent/progeny could have a profound effect on disease studies, the reproducibility of data, and the viability of extrapolating *in vivo* data to a human population that may or may not match the autophagy profile of the animal.

Second, does autophagy change in the aging murine heart, and if it does how are those changes manifest? It is well documented that autophagy is important for limiting the mortality and morbidity associated with myocardial infarct in the elderly. The primary focus of this research is to determine if/how autophagy changes in the aged heart in order to design future therapeutics or interventions that can restore or partially restore autophagy in the elderly and ameliorate injury from a heart attack.

If we are to determine autophagic state in patients in order to design or test therapeutics, we require a method of detecting autophagy *in vivo* without using invasive methods. In place of repeated heart biopsies, an *in vitro* assay, preferably with a high throughput format is desirable. In fact, one of the primary limitations of applying autophagy research to a drug design or translational/diagnostic/therapeutic setting is a lack of reagents capable of detecting autophagy reliably, rapidly, and reproducibly on a variety of platforms (plate reader/microscopy for high throughput drug screens and flow cytometry for real-time diagnostic and therapeutic purposes in the clinic and *in vivo* research in the laboratory). We believe that we have developed a staining protocol that utilizes a combination of reagents AlexaFluor-488^{TM}-cadaverine (fluorescent dye) and the polyamine (spermidine) that addresses this demand. We have given the product the brand name Fluormidine, which labels puncta that we believe to be autophagosomes.

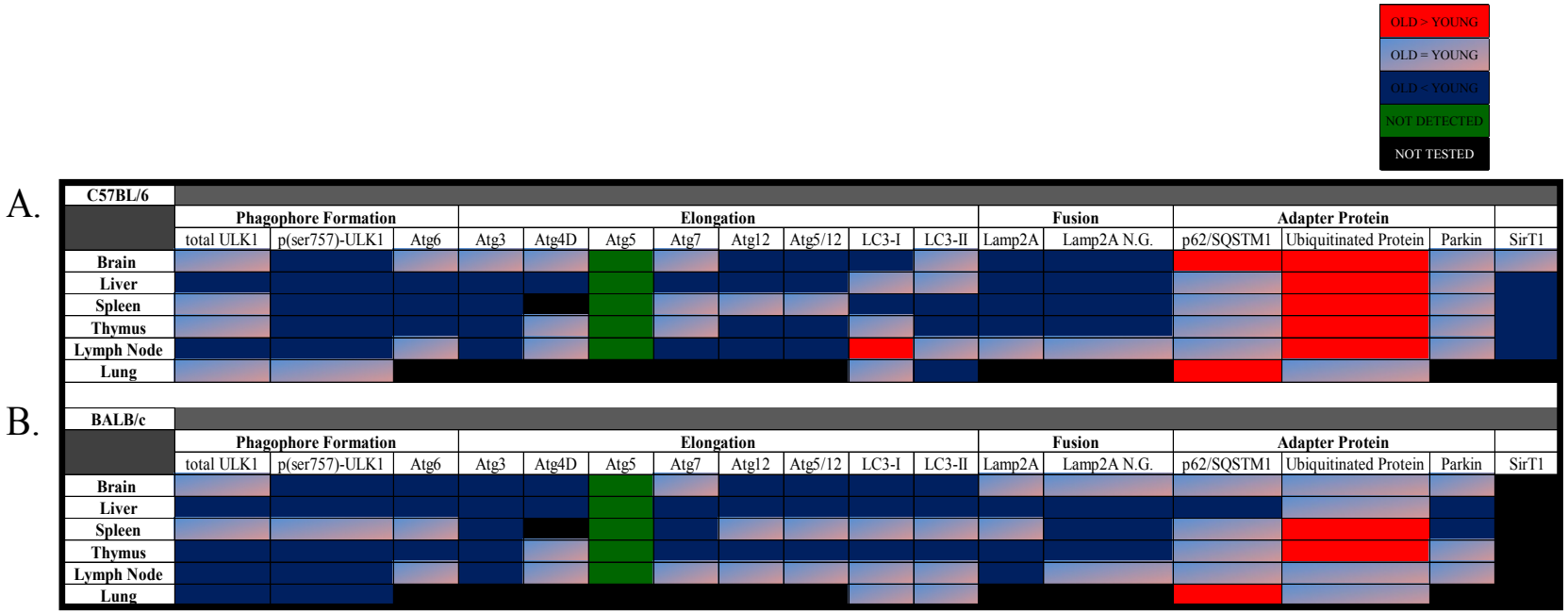

Figure I.1: Age-Related Changes in Autophagy with Respect to Tissue and Strain Differences. Color map depicting significant changes in autophagy protein levels. The brains, livers, spleens, thymuses, lymph nodes, and lungs of 2.5-3 and 24/25 month old (n=3 or n=4) C57BL/6 (A) and BALB/c (B) mice, respectively, were removed and subjected to western blot analysis. 30 µg of total protein extracted in TETN buffer was loaded onto a 10-20% Tris-HCl gel, transferred to PVDF and probed with the following antibodies: rabbit α-total ULK-1, rabbit α-phospho-ULK1 (Ser-757), rabbit α-Atg6, rabbit α-Atg3, rabbit α-Atg4D, rabbit α-Atg5, rabbit α-Atg7, rabbit α-Atg6/Beclin-1, rabbit α-Atg12, rabbit α-LC3, rabbit α-LAMP2A, and mouse α-actin. Additionally, 30 µg of total protein derived from the Triton-X 100 insoluble/2% SDS soluble fraction (See Common Methods) was loaded onto a 4-12% Bis-Tris gel, transferred to PVDF and probed with the following antibodies: guinea pig α-p62/SQSTM1, mouse α-ubiquitin, and mouse α-actin. Protein expression was normalized to its actin control and significance was established by $p<0.05$ by Student's T Test. Red and Blue indicate a significant increase or decrease in protein expression respectively. Source data (original blots and graphs derived from ImageJ quantification) are found in Appendix 1.

INTRODUCTION TO AUTOPHAGY

Autophagy is characterized by the delivery of intracellular components to the lysosome, which can be accomplished via three different mechanisms that are thought to operate simultaneously in most cell types[11], microautophagy, chaperone-mediated autophagy, and macroautophagy. Microautophagy is a constitutive process by which random invaginations in the lysosomal or vacuolar (plants) membrane deliver cytoplasm to the lysosomal lumen via single membrane vesicles, resulting in the degradation of cytoplasmic material[12,13]. The microautophagy pathway is important during nutrient starvation[14], targeting glycogen to the lysosome[15], and selective degradation of peroxisomes, mitochondria, and parts of the nucleus (yeast)[12]. Chaperone-mediated autophagy (CMA) is characterized by lysosomal targeting, translocation across the lysosomal membrane, and subsequent degradation of specific, predominantly cytosolic proteins containing a pentapeptide motif biochemically related to KFERQ[16]. A process solely identified in mammals, CMA does not require the formation of a membrane; instead, a cytosol-borne heat shock cognate protein of 70 kDa, Hsp70, binds the target, and ferries it to a complex consisting of LAMP2A (Lysosome-Associated Membrane Protein 2A) and Hsp90 embedded in the lysosomal membrane, promoting protein unfolding[17]. The LAMP2A complex multimerizes and threads the protein into the lysosomal lumen where the protein is destroyed[17]. CMA is thought to be constitutive in most cell types in order to maintain homeostasis by clearing non-functional proteins[17]. It has been shown to respond to starvation (although its response is somewhat delayed compared to macroautophagy[18]) and increased ROS levels[19], and has been shown to decline with age[20-22]. Finally, macroautophagy (MA) is a form of autophagy that relies on the de novo formation of a double membrane vesicle (autophagosome) around the cargo

to be degraded. This constitutive process has been shown to greatly increase in times of stress, e.g. starvation[23], heart attack[24], and infection[8]. Of the three autophagy pathways, MA is the best characterized and is the focus of this dissertation and is discussed in greater detail below.

Autophagy is regulated by several different kinases (mammalian Target of Rapamycin (mTOR), AKT (also known as Protein Kinase B), and AMPK (5' Adenosine Monophosphate-Activated Protein Kinase) and a deacetylase called Sirtuin 1 (SirT1)). These proteins sense a variety of cellular stresses, such as metabolic, energy, hypoxic, and oxidative stress, and coordinate responses that facilitate homeostasis, autophagy being one. The pathways in which mTOR, AKT, AMPK and SirT1 overlap and regulate autophagy are depicted in Figure I.2.

mTOR is a major component of a nutrient sensing complex that acts to coordinate cellular growth, metabolism, differentiation, and stress responses/cell survival (reviewed in Betz & Hall, Bracho-Valdez et al., and Jewel & Guan)[25-27]. mTOR is a serine/threonine kinase that exists in two independent and distinct complexes, mTORC1 and mTORC2. mTORC1 is associated with a myriad of accessory proteins such as Raptor (regulatory-associated protein of mTOR) and PRAS40 (proline-rich AKT/PKB substrate of 40 kDa), which control its activation state[25-27]. Considering the role of mTOR in the cell, it is no surprise that mTORC1 activity is regulated by a variety of factors including growth factors, hypoxia, cellular stress, and energy/metabolic/nutrient state[27]. Once activated, mTORC1 promotes autophagy suppression via phosphorylation of ULK1 at Serine-757 (See Below)[28,29]. Additionally, mTORC1 activity promotes

cellular growth by activating a myriad of proteins including those associated with protein synthesis[30,31], synthesis of viral biomolecules such as lipids[32-34] and nucleotides[35,36], mitochondrial biogenesis[37], lysosome biogenesis[38], ribosome biogenesis[39], and so on. In all, under conditions of "plenty", mTORC1 is activated, which promotes growth and inhibits autophagy.

mTORC2 is identified by its binding partner, Rictor (rapamycin-insensitive companion of mTOR) (reviewed in Oh et al. and Brancho-Valdes et al.)[26,40]. Much remains unknown about mTORC2, prompting questions like "Is there interconversion between mTORC1 and mTORC2?", "Why is it found in the nucleus?", etc. According to the literature, mTORC2 is activated by growth factors[27]. More importantly, mTORC2 regulates AKT activity (see next paragraph) which in part, may be why mTORC2 is associated with a variety of pro-growth and survival mechanisms such as "metabolism, growth, migration, proliferation, and angiogenesis.[26]" To date there is no evidence that mTORC2 is involved in any direct regulation of autophagy, although it does indirectly act to suppress autophagy via AKT activity.

mTORC1 activity is regulated by the kinases AMPK and AKT. AMPK is a vital player in the maintenance of homeostasis during cellular stress or energetic/nutritional crisis. Upon activation, AMPK promotes the upregulation of pathways associated with ATP production (i.e., autophagy) and then represses or suppresses cellular pathways that expend ATP (i.e., growth, differentiation, and migration) (AMPK regulation is reviewed in Wang et al. and Sridharan et al.)[41,42]. AMPK is a heterotrimeric protein that is sensitive to both increasing AMP/ATP ratios (resulting in a slight increase 2-5 fold in

AMPK activity) and activation by upstream regulatory kinases, such as Liver Kinase B1 (LKB1), Calcium/Calmodulin-dependent protein kinase kinase β (CaMKKβ) and possibly other molecules that are active during cellular stress[41]. The regulators phosphorylate AMPK at Threonine-172, thus activating AMPK[43], which in turn initiates autophagy by phosphorylating the ULK1 complex at either Serine-555 or Serine-777 & Serine-317[44,45]. Additionally, AMPK phosphorylates both the TSC1/TSC2 complex and Raptor, inactivating the mTORC1 complex and initiating autophagy (See Below)[46,47].

Conversely, AKT activity accomplishes the opposite of AMPK; by facilitating AKT activity, a variety of pro-growth and survival mechanisms that regulate "metabolism, growth, migration, proliferation, and angiogenesis[26]" ensues. The regulation and activation of AKT is a highly complex process (Reviewed in Ravikumar et al., Kumar et al., and Sridharan et al.)[42,48,49]. Briefly, it is thought that the presence of growth factors promotes formation of the mTORC2 complex, which then phosphorylates Serine-473 of AKT; additionally, a variety of signals converge on and activate PDK1 (an effector protein in the insulin/growth factor pathway)[29], which then phosphorylates AKT at Thr-308[48]. There is some controversy in the literature concerning activation of AKT with some suggesting that phosphorylation at Serine-473 promotes phosphorylation at Threonine-308 and others suggesting that only phosphorylation at Serine-473 or Threonine-308 is important[49-51]. In any case, activated AKT binds the TSC1/TSC2 complex promoting its dissociation and subsequent activation of mTORC1[52]. Also, activated AKT phosphorylates PRAS40, resulting in its dissociation from mTORC1 and promoting mTORC1 activation[53,54] and the ultimate suppression of autophagy.

AMPK and AKT not only modulate autophagy through direct and indirect interaction with mTOR, they also assist in the activation and localization of the transcription factor FoxO3a in conjunction with SirT1. SirT1, one of seven members of a family of NAD-dependent deacetylases, is associated with environmental stress, namely nutrient stress (increased NAD^+/NADH ratio)[55-58] and longevity (Reviewed by Salminen & Kaariranta[59,60] and Speakman & Mitchell[61]). Under basal conditions, SirT1 has been shown *in vitro* to associate with and acetylate the autophagy proteins LC3, Atg7, and Atg5. Upon fasting these proteins are deacetylated, presumably by SirT1[56], thus establishing a role for acetylation in autophagy regulation. Additionally, SirT1 has also been demonstrated to deacetylate the transcription factor FoxO3 and promote expression of genes associated with cell stress and autophagy in skeletal muscle *(atg8a, atg8b,* and *bnip3*)[62-64]. The activation of AKT results in the phosphorylation of FoxO3 at three sites (Threonine-32, Serine-253, and Serine-315)[65], which promotes 14-3-3 protein binding (prevents AKT dephosphorylation/retention and degradation[66] in the cytoplasm), translocation out of the nucleus, and the suppression of FoxO3a-mediated autophagy transcription (described below)[67,68]. The specific role of AMPK in this process remains unclear. AMPK has been shown to phosphorylate six sites on FoxO3a (Thr166, Ser399, Ser413, Ser321, Thr463, and Ser466), at least *in vitro,* and initiate FoxO3a transcriptional activity, not localization[69]. However, recent data has elucidated an AMPK-SirT1 pathway where AMPK can activate SirT1, which can then activate FoxO3a-mediated expression[70-72]. In all, AKT phosphorylation results in nuclear exclusion of FoxO3a, while SirT1 and AMPK promote FoxO3a-mediated transcription of some stress response

and autophagy genes. SirT1 also acts to promote "activation" of key autophagy proteins, Atg5, Atg7, and LC3[28].

To promote cell survival when confronted with nutrient deprivation, oxidative stress (reviewed in van der Vos & Coffer[73]; Pietrocola et al.[74]), and hypoxic stress[75], the FoxO's regulate a variety of cellular processes such as cell cycle arrest, apoptosis, metabolism and proliferation. FoxO3a acts to maintain homeostasis in part by promoting the upregulation of stress-response genes (such as manganese superoxide dismutase[76] and catalase[76]) and autophagy. When autophagy is upregulated, FoxO3a controls the transcription of several autophagy genes such as *Atg4B*[77], *Atg12*[64,78], *Atg14*[79], *Beclin-1*[64], *Bnip3*[64], *GABARAPL1*[78], *MAP1LC3 (Atg8)*[64], the PI3 kinase *VPS34 (PI3KCA & PI3KC3)*[64,80], and *ULK2*[64]. It is crucial to note that FoxO3a is not the sole transcription factor associated with stress response and autophagy (for a list of transcription factors see Pietrocola et al)[74].

The MA pathway consists of 36 identified proteins of which 16 are considered part of the essential core machinery[81]. For a schematic overview of the macroautophagy pathway refer to Figure I.2. There are a variety of excellent reviews of the autophagy pathway and its regulation: Kroemer et al.[28], He et al.[29], and Ravikumar et al.[49]. As shown in panel A, the initiation of autophagy is accomplished through the inactivation of mTOR[29,82]. mTOR maintains Ulk1 (Atg1 in yeast) in the phosphorylated form (pUlk1-Ser-757) that prevents the formation of the Ulk1·Atg13·FIP200·Atg101 complex needed for autophagy initiation[29]. Autophagy-inducing stimuli release mTOR repression of the ULK1 complex, such that the ULK1 complex binds and activates the Beclin-1 (PPI3K)

complex and translocates to specific regions (likely the ER membrane)[83]. The Beclin-1 (Atg6 in yeast) complex in addition to other autophagy proteins assist in phagophore nucleation and the recruitment of proteins associated with phagophore elongation[83,84]. The origin of the membrane is still being elucidated, however, it appears that the ER (the primary site of autophagosomal assembly)[85-87], the mitochondrial membrane[88], and the plasma membrane[89] are the likely sources.

Elongation of the phagophore requires ubiquitin-like conjugation systems that help to convert LC3 into the LC3-II form that is incorporated in the autophagosomal membrane (Figure 1B). One system utilizes Atg7 and Atg10 to create the irreversible covalent linkage between Atg5-Atg12, which then associates with Atg16L1 to form a complex required for membrane elongation[29]. A second ubiquitin-like conjugating system is required for the incorporation of LC3-II into the autophagosomal double membrane[29]. Atg4 cleaves the terminal amino acid(s) from LC3, yielding LC3-I[29]. The activities of the ubquitin-like proteins Atg3 and Atg7 in conjunction with or without the Atg5-12-16L1 complex facilitate the addition of phosphatidylethanolamine to LC3-I, resulting in LC3-II and subsequent incorporation of LC3-II into the autophagosomal membrane[29,90]. LC3-II is incorporated into both faces (convex and concave) of the cup-shaped phagophore double membrane structure[29]. Upon formation of the autophagosome, Atg5-Atg12-Atg16L1 dissociate from the autophagosomal double membrane and LC3-II is recycled from the outer leaflet and converted to LC3-I again by Atg4 (LC3-II incorporated into the inner leaflet is eventually degraded by lysosomal hydrolases following autophagolysosome creation)[29]. The autophagosomes can fuse with

other autophagosomes, with endosomes (amphisome), or with lysosomes (autolysosome or autophagolysosome)[91].

LAMP2A, expressed on the lysosomal surface, mediates lysosomal fusion with the autophagosome and the formation of the autophagolysosome (Figure 1A)[29]. Lytic lysosomal-borne enzymes catalyze the degradation of the inner autophagosomal membrane along with its protein/organelle cargo[29]. In order to target specific substrates for degradation, the autophagy system relies on a handful of adapter proteins of which p62/SQSTM-1 is the best characterized in the context of targeting protein aggregates to the autophagy pathway[92]. P62 possesses domains for binding both LC3 and ubiquitin, meaning that it binds ubiquitinated substrates and targets them to the autophagy pathway via its LC3 binding domains[93]. Therefore, if the autophagic pathway is functioning normally, levels of p62 and ubiquitin-tagged proteins should not increase. Since the role of p62 in autophagy is aggregate association, studies of p62 require the use of 1% Triton-X 100 extraction to remove soluble proteins followed by solubilization of the aggregates (and cytoskeletal components) with 2% SDS prior to western blot analysis[92].

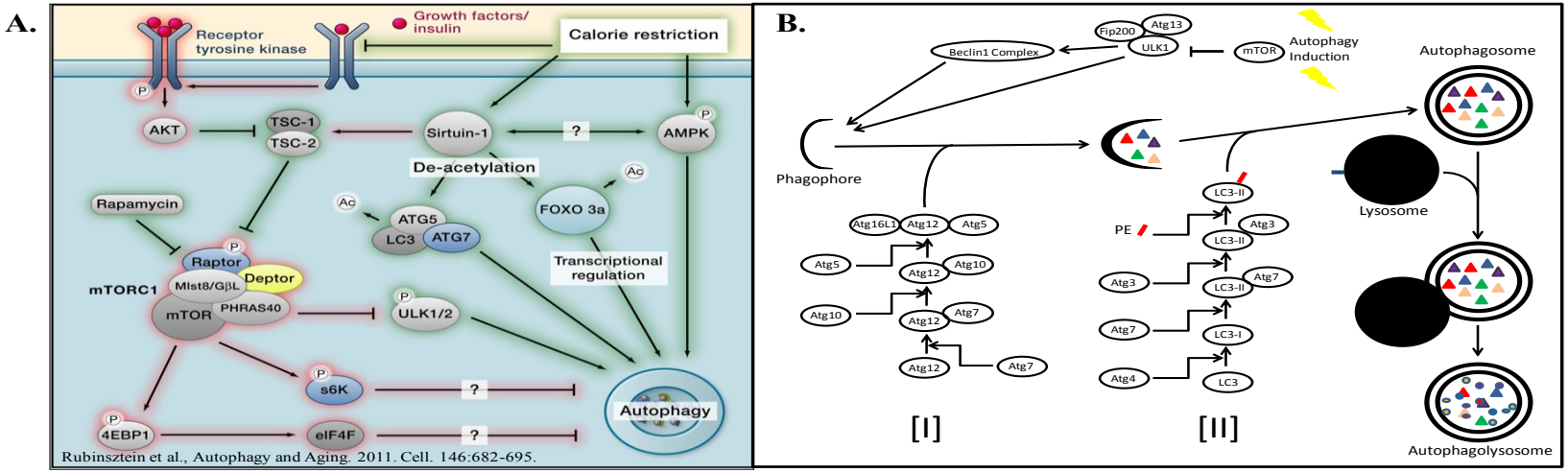

Figure I.2. Schematic Overview of Autophagy. Panel A focuses on the upstream molecules that impact autophagy, whereas Panel B is an overview of the autophagy pathway. Panel A: A variety of signals converge on the mammalian Target of Rapamycin (mTOR) complex, modulating autophagy. AKT activity, typically associated with senescence, cell growth, inflammation, and insulin signaling, activates mTOR complex. An activated mTOR complex promotes the suppression of the ULK1, preventing autophagy induction. Conversely, AMPK, associated with metabolic stress, is triggered by high AMP/ATP ratios and represses the mTOR complex. This releases ULK1 complex repression, allowing autophagy to proceed. Also, high NAD^+/NADH ratios induce Sirtuin1, activating the transcription factor FoxO3a to transcribe *ulk2, Beclin-1, vps35, atg8(lc3), atg12, gabarap1, & atg4b*[94] (See text). Panel B: The loss of ULK1 complex repression leads to its binding and activating the Beclin complex promoting nucleation and recruitment of proteins associated with phagophore elongation. Two ubiquitin-like conjugation systems are involved in phagophore elongation. The ubiquitin-like conjugation system utilizing Atg7 & Atg10 to create the Atg5-Atg12-Atg16L1 complex [I] is required for phagophore membrane elongation. The second ubiquitin-like conjugating system [II] required for the incorporation of LC3-II into the autophagosomal double membrane. Atg4 cleaves the terminal amino acid from LC3, yielding LC3-I. The activity of the ubiquitin-like proteins Atg3 and Atg7 result in the addition of phosphatidylethanolamine (in red) to LC3-I, resulting in LC3-II and subsequent incorporation of LC3-II into the autophagosomal membrane, likely via the Atg5-Atg12-Atg16L1 complex. Upon autophagosome formation, LAMP2 (in blue) expressed on the surface mediates lysosomal fusion with the autophagosome, forming the autophagolysosome. Lytic lysosomal-borne enzymes catalyze the degradation of the inner autophagosomal membrane and the protein/organelle cargo enclosed by the autophagolysosome (See text).

COMMON METHODS USED IN ALL CHAPTERS

The methods described in detail in this chapter are used throughout the dissertation. Individualized protocols and methods specific to the individual chapters are detailed in their respective chapters.

Animals

C57/BL6 and BALB/c mice were bred in-house or obtained from the NIA Colony maintained by Charles River Laboratories (Wilmington, MA). Mice were acclimated at least two weeks prior to experimentation. All mice were housed in a temperature controlled room under a 12 hr. light/dark cycle (6 P.M. to 6 A.M. Dark Cycle). Mice were allowed free access to food (Teklad, 8604 Rodent Diet) and water unless otherwise specified. All experiments were performed at 10 AM to avoid any complications from circadian rhythms (except for the chloroquine studies, which were performed at 11 AM). Basal autophagy was assessed using unmanipulated mice. All studies with animals were approved by the San Diego State University Institutional Animal Care and Use Committee.

Tissue Lysis and Preparation for Gene and Protein Analysis

Tissues were removed, wrapped in aluminum foil, snap frozen in liquid nitrogen, and stored at -80°C. Tissues were divided on dry ice for either total RNA (RT-qPCR Analysis of Autophagy Gene Expression section - See Below) or protein extraction. Total protein was extracted either in TETN (Tris, EDTA, Triton X-100, NaCl), 1% Triton-X 100/2% SDS Buffer, or RIPA (Radioimmunoprecipitation Assay) Buffer.

TETN Buffer: Tissues were homogenized using a mortar and pestle (USA Scientific, 1415-5390) in the presence of ice-cold TETN Buffer (50 mM Tris Base - pH=7.4, 150 mM NaCl, 1 mM EGTA, 1 mM EDTA, and 1% Triton-X 100) supplemented with 1X Complete Protease Inhibitors (Roche, 11873580001), 1 mM $NaVO_4$ (Stock 200 mM), 10 mM NaF (Stock 1M), and 17.5 mM sodium β-glycerophosphate (Stock 500mM) in a 1.7 mL microfuge tube. The samples were centrifuged at a minimum of 12,000-14,000 rpm at 4°C for 10 minutes in a table top centrifuge, supernatants were divided into aliquots, and frozen at -80°C.

1% Triton-X 100/2% SDS Buffer: Tissue lysates were prepared as previously described[95]. Briefly, tissues were homogenized using a mortar and pestle (USA Scientific, 1415-5390) in the presence of the soluble protein extraction buffer (1% Triton-X 100, 1X PBS, and 1X Complete Protease Inhibitor (Roche, 11873580001)) in a microfuge tube. Samples were then centrifuged for 10 minutes at 12,000-14,000 rpm at 4°C. The supernatant was carefully removed and saved as the Triton-Soluble Fraction. The pellet was resuspended in 1 mL protein extraction buffer and centrifuged at 12,000-14,000 rpm for 10 minutes at 4°C. The supernatant was discarded. The pellet was resuspended in the protein insoluble buffer (2% SDS, 50 mM Tris Base - pH=7.4 and Complete Protease Inhibitors (Roche, 11873580001)), sonicated briefly, and centrifuged for 10 minutes at 12,000-14,000 rpm at 4°C. The resulting supernatant fraction is collected, aliquoted, and saved as the Triton X-100 insoluble/2% SDS soluble fraction at -80°C.

RIPA Buffer: Tissues were homogenized using a mortar and pestle (USA Scientific, 1415-5390) in the presence of ice-cold RIPA Buffer (50 mM Tris Base - pH=8.0, 150 mM NaCl, 0.1% SDS, 0.5% sodium deoxycholate, 1% NP-40) supplemented with 1X Complete Protease Inhibitors (Roche, 11873580001), 1 mM $NaVO_4$ (Stock 200 mM), 10 mM NaF (Stock 1M), and 17.5 mM disodium β-glycerophosphate (Stock 500mM) in a 1.7 mL microfuge tube. The samples were centrifuged at a minimum of 12,000-14,000 rpm at 4°C for 10 minutes at 4°C in a table top centrifuge, divided into aliquots, and frozen at -80°C.

SDS-PAGE and Western Blot Analysis

Samples were thawed on ice. Total protein concentrations of all samples were normalized to total protein concentration using a Lowry Assay[96] in accordance with the manufacturer's instructions (BioRad, DC Protein Reagent A [500-0113], DC Protein Assay Reagent B [500-0114], DC Protein Assay Reagent [500-0115]) using Bovine Serum Albumin as a standard (Thermo Scientific, 23209). Total protein was quantified using a plate reader (Molecular Devices Spectra Max Plus 384). 30 µg total protein was prepared in 1X SDS Sample Buffer (supplemented with 10% β-mercaptoethanol), and water. Samples were centrifuged, boiled for 6 minutes, allowed to cool, quickly centrifuged, and loaded onto a protein gel (BioRad Criterion 4-12% Bis-Tris Gels [345-0124] in 1X XT MOPS Running Buffer [161-0788XTU] for Triton-X 100 soluble/insoluble Analysis; Criterion BioRad 4-20% or 10-20% Tris-HCl [345-0033 or 345-0043, respectively]) in 1 X SDS Running Buffer for TETN or RIPA analysis. Precision Plus Protein Standards (BioRad, 161-0373) were used as weight markers.

Gels were run at 90-120V until 10 kDa band was just visible at bottom of gel. An Amersham Hybond-P PVDF Transfer Membrane (GE Healthcare, RPN303F) was submerged in 100% methanol and equilibrated several minutes in Transfer Buffer. The gel was transferred for 16.75 hrs at 20 mA at 4°C. Blots were trimmed with scissors and incubated in 5% non-fat milk dissolved in Tris Buffered Saline/Tween-20 (TBST) for at least 1 hour at room temperature with rocking.

Blots were quickly washed two or three times in 1X TBST. Antibodies, prepared in 5% Bovine Serum Albumin (Sigma, A-7906) in 1X TBST with 0.02% sodium azide, were poured on blots and incubated at 4°C overnight on a rocker. Blots were washed three times with 1X TBST for 6-10 minutes at room temperature with rocking. A 1:2500 dilution of affinity purified peroxidase labeled goat-α-rabbit, goat-α-mouse, or goat-α-guinea pig antibody (KPL 074-1516, KPL 074-1806 or Jackson Research Labs 106-035-003, respectively) in 5% non-fat powdered milk/1X TBST was added for 60-75 minutes at room temperature with rocking. Blots were washed three times for 5-10 minutes in 1X TBST at room temperature with constant rocking. The blots were developed with SuperSignal West Dura Extended Duration Substrate (Thermo Scientific, 34076) on Molecular Imager Gel Doc XR+ System with Quantity One Software (Bio-Rad, 170-8195). When necessary, blots were stripped with Restore PLUS Western Blot Stripping Buffer (Thermo Scientific, 46430), re-blocked with 5% non-fat milk in 1X TBST for 1 hr., quickly washed with 1X TBST, and re-probed with another antibody overnight at 4°C with constant rocking. Densitometry was performed using ImageJ software (NIH,

http://rsb.info.nih.gov/ij) using β-actin as a loading standard. Data analysis and statistics was done with GraphPad Prism 5 software.

The following are the recipes for the reagents referred to in the above section. SDS Running Buffer: 1 L; 3.003 g Tris Base, 14.41 g Glycine, 1 g SDS, pH=8.3; Transfer Buffer: 25 mM Tris, 192 mM Glycine, and 10% methanol; Tris Buffered Saline/Tween-20 [TBST]: 20X Stock – 2 M NaCl, 200 mM Tris-HCl pH=7.4, 2% Tween-20. 5X Laemmli Buffer (Sample Buffer): 10% SDS, 0.05% bromophenol blue, 40% glycerol, 250 mM Tris pH=6.8 (supplemented with 10% β-mercaptoethanol just before use).

RT-qPCR Analysis of Autophagy Gene Expression

Total RNA extracted from the hearts of C57BL/6 and BALB/c mice were used in studies that determined strain-related differences using young mice and in those studies of age-related differences in basal autophagy with the two murine strains. Briefly, the heart was divided on dry ice with one half for RT-qPCR and the other for protein analysis by western blot. RNA was isolated using a NucleoSpin RNA II kit (E & K Scientific, 740955-250) in accordance with the manufacturer's instructions. cDNA was prepared using an iScript Reverse Transcription Supermix for RT-qPCR (BioRad, 170-8841). Primer sets, their respective sequences, and their efficiencies for each of the autophagy genes are listed in Common Methods Table 2. RT-qPCR analysis was performed for the following genes: *atg1 atg3, atg5, atg6, atg7, atg4a, atg4b, atg4c, atg4d, atg8a, atg8b, atg12, atg16l1, LAMP2a, parkin, p62/sqstm1,* and *nrf2* with *β-actin* used as a housekeeping gene. The 20 μL reaction mixture was assembled using 1 μL cDNA

template, 300 nM each primer set, the iTaq Universal SYBR Green Supermix (BioRad, 172-5124) and the following conditions were used: 30 sec at 95°C; 40 cycles of 10 sec at 95°C and 30 sec at 60°C; and a melt curve (CFX96 Real Time System and C1000 Touch Thermal Cycler, BioRad). The Pfaffl Method[97] was used to calculate fold change with a greater than >2 or less than a <0.4 fold change being considered significant. The data was independently verified using the $\Delta\Delta C_t$ method to ensure no gross mathematical errors.

Carbonylation

Relative protein carbonylation was determined using an OxiSeclect Protein Carbonyl Immunoblot Kit (Cell BioLabs inc., STA-308). Briefly, RIPA extracted heart lysates were prepared from C57BL/6, BALB/c, and CB6F1/J mice, subjected to PAGE, and transferred to a PVDF membrane (See Above). The remainder of the assay was performed in accordance with the manufacturer's instructions.

Table I.1: Antibodies Used for the Dissertation

Name	Cat. #	Manufacturer	Dilutio	Secondary
Atg3	3415	Cell Signaling	1:1000	goat-α-rabbit
Atg4D	AP1811b	Abgent	1:1000	goat-α-rabbit
Atg5	2630	Cell Signaling	1:1000	goat-α-rabbit
Beclin-1	3738	Cell Signaling	1:1000	goat-α-rabbit
Atg7	2631	Cell Signaling	1:1000	goat-α-rabbit
LC3AB	4108	Cell Signaling	1:1000	goat-α-rabbit
Atg12	2011	Cell Signaling	1:1000	goat-α-rabbit
LAMP2A	PA1-655	Thermo Scientific	1:1000	goat-α-rabbit
Parkin	2132	Cell Signaling	1:1000	goat-α-rabbit
p62/SQSTM1	5114	Cell Signaling	1:1000	goat-α-rabbit
p62/SQSTM1	03-GP62-	American Research	1:2000	goat-α-guinea
Ubiquitin	3936	Cell Signaling	1:1000	goat-α-mouse
Total Ulk1	A7481	Sigma-Aldrich	1:1000	goat-α-rabbit
pULK1-Ser757	6888	Cell Signaling	1:1000	goat-α-rabbit
Actin	A1978	Sigma-Aldrich	1:1000	goat-α-mouse
CoxIV	4844	Cell Signaling	1:1000	goat-α-rabbit
SirT1	2028	Cell Signaling	1:1000	goat-α-rabbit
SirT3	2627	Cell Signaling	1:1000	goat-α-rabbit
FoxO3a	2497	Cell Signaling	1:1000	goat-α-rabbit
pFoxO3a-	9466	Cell Signaling	1:1000	goat-α-rabbit
AKT	9272	Cell Signaling	1:1000	goat-α-rabbit
pAKT-Thr308	9275	Cell Signaling	1:1000	goat-α-rabbit
pAKT-Ser473	9271	Cell Signaling	1:1000	goat-α-rabbit
AMPKα	2532	Cell Signaling	1:1000	goat-α-rabbit
pAMPKα-	2535	Cell Signaling	1:1000	goat-α-rabbit

Table I.2: RT-qPCR Primer Sets & Efficiencies of Autophagy Genes

Name	Forward Primer	Reverse Primer	Efficiency (%)
atg1	TTCTCTCGCAAGGACCTGAT	TTGATTTCCTTTCCCAGCAG	93.6
atg3	ATGGGCTACAGGGGAAGAAT	TATCTACCCATCCCCCATCA	96.6
atg5	CACTGGGACTTCTGCTCCTG	TCCTTCAACCAAAGCCAAAC	94.2
atg6	GGCCAATAAGATGGGTCTGA	TGCACACAGTCCAGAAAAGC	99.5
atg7	TCCGTTGAAGTCCTCTGCTT	CCACTGAGGTTCACCATCCT	99.2
atg4a	CCGGATACAGATGAGCTGGT	CATCAGATGAAGGGCCTGTT	103.5
atg4b	CCAGGATGTCCTGAACCTGT	AGGTCTGGGTTCTCAAAGCA	90.5
atg4c	ATGGAGGCTTCAGGAACAGA	CAGGCAACATCTTGCTTTCA	100.3
atg4d	CCAGCTTCAGCAAGATCTCC	ATACATCCCCAGCCACAGTC	103.1
atg8a	TCAGTCCCCAGTGGATTAGG	CAAAAGAGCAACCCGAACA	97.0
atg12	GGCCTCGGAACAGTTGTTTA	TTTGCAGTAATGCAGGACCA	104.6
atg8b	GCGACTGGAGAGCCTGTTTCT	GTGAGCCAAGTCTGGAGCAT	99.2
atg16l1	GGAGAACCAGGAACTGGTCA	CGGGAGAGGTCTCTTCTGTG	89.9
lamp2A	CACCCACTCCAACTCCAACT	TTGTGGCAGGGTTGATGTTA	90.6
18s	AAACGGCTACCACATCCAAG	CCTCCAATGGATCCTCGTTA	103.9
parkin	TTCTGACACCAGCATCTTGC	CTTCTCCTCCGTGGTCTCTG	93.1
gapdh	GTGTCCGTCGTGGATCTGA	CCTGCTTCACCACCTTCTTG	100.6
β-actin	TGTTACCAACTGGGACGACA	GGGGTGTTGAAGGTCTCAAA	101.5
p62/ sqstm1	ACAGATGCCAGAATCGGAAG	AGAAACCCATGGACAGCATC	93.8
nrf-2	GGACATGGAGCAAGTTTGGC	GGAACAGCGGTAGTATCAGCC	97.4

CHAPTER I:

Strain-Related Differences in Cardiac Autophagy: C57BL/6 vs. BALB/c

INTRODUCTION

There is evidence for differential autophagy regulation between different mouse strains (primarily with respect to infection and inflammation), but nothing concrete is known about strain-related autophagy differences in the hearts of C57BL/6 and BALB/c mice, two commonly used mouse strains. However, there is mounting evidence pointing to a direct interrelation between autophagy and cholesterol in macrophages in the development and progression atherosclerosis (extensively reviewed in Maiuri et al.)[98]. To our knowledge, the only autophagy study specifically looking at strain differences in the cardiovascular system focuses on cholesterol metabolism in bone marrow-derived macrophages in the AKR and DBA strains[99], which has implication in the development of cardiovascular disease, namely the arterial lesions associated with atherosclerosis. In this study Robinet et al., found that differential autophagic flux contributed to accumulation of cholesterol esters in macrophages from DBA/2 mice[99]. Specifically, they found that a reduction in autophagy can promote the transformation of arterial macrophages into the foam cells (macrophages filled with cholesterol esters) that are associated with early atherosclerotic plaques[100,101]. Moreover, Paigen and colleagues report that C57BL/6 mice are more susceptible to aortic lesions than their BALB/c counterparts with C57BL/6 developing lesions much earlier (7 weeks vs. 1 year) following the initiation of a pro-atheroscleric diet[102], potentially due to autophagy differences between C57BL/6 and BALB/c mice. Consequently, the observations in the above DBA & AKR cholesterol metabolism and C57BL/6 & BALB/c atherosclerosis

studies may highlight strain-related differences in autophagy in the cardiovascular system, at least in macrophages.

Additionally, strain-related differences in autophagy may have an effect on tissue repair as demonstrated by differential tissue fibrosis following heart attack in C57BL/6 and BALB/c mice[103]. An analysis of the hearts of these mice following a 28 day recovery post myocardial infarction (coronary artery occlusion) demonstrated a large degree of fibrosis in the C57BL/6 relative to the BALB/c[103,104]. In this case, autophagy has been demonstrated to modulate cardiac fibrosis, with an upregulation in autophagy and autophagic flux promoting increased collagen degradation (reviewed in Przyklenk et al.)[105]. The authors conclude that there may be a dual role for autophagy regulation in wound healing post MI, with upregulation of autophagy at the periphery of the infarcted site leading to less collagen disposition and maintenance of cardiac function and down-regulation of autophagy in the fibroblasts associated with the damaged site to promote collagen disposition and scar formation[105]. With fibrogenesis displaying such a dependence on autophagy, then strain-related differences in autophagy most likely play a role in the observed difference in fibrogenesis between the C57BL/6 and BALB/c mice[103].

It appears that there are likely strain-related differences in autophagy (directly and indirectly) in the cardiovascular system, at least with respect to fibroblasts and macrophages, but nothing is known about the whole tissue under basal conditions. This prompted us to ask the following questions: Are there strain-related differences in basal autophagy protein expression in the heart ventricles? If so, how are these differences

manifest? Finally, how is basal autophagy manifest in the progeny of cross between a BALB/c and C57BL/6?

METHODS

Basal Autophagy Studies in Young C57BL/6, BALB/c, and CB6F1/J Mice

Hearts were removed from 2.5-4 month old female C57BL/6 and BALB/c mice. We also examined CB6F1/J (2.5 month old) mice that were obtained from the NIA Colony at Charles River Labs. Animal housing, cardiac sample preparation, PAGE, western blot and carbonylation analyses, as well as gene expression analysis were as described the Common Methods section.

RESULTS

Strain-Related Differences in Autophagy in the Hearts of Young C57BL/6 and BALB/c Mice

To understand potential differences in autophagy between the murine strains, we analyzed basal autophagy as well as upstream proteins that regulate autophagy. To do so, the hearts (ventricles) of 2.5-3 month old C57BL/6 and BALB/c mice (n=4) were subjected to analysis by western blot using antibodies to proteins associated with the initiation of autophagy, phagophore elongation, autophagosome/lysosome fusion, autophagosome targeting, upstream regulation of autophagy, and oxidative damage (Common Methods Table 1). Protein levels were analyzed and differences in protein expression between the two strains were considered significant if $p<0.05$ (See Figure 1.1, Appendix 2).

We found no significant difference between the strains in their expression of the autophagosome proteins: total ULK1 (associated with the autophagy initiation complex), Atg3 (part of the LC3 ubiquitin-like conjugation system), Atg4D (associated with GABARAP processing and mitochondrial targeting), Atg5 (part of the Atg5/12/16 complex), and LAMP2A (facilitates autophagosomal-lysosomal binding). Additionally, the protein levels of ubiquitin, isolated from the Triton X-100 insoluble/2% SDS soluble fraction (an indication of autophagic flux), were similar between the two mouse strains. Finally, there were no differences observed in the autophagic regulatory protein levels between the C57BL/6 and BALB/c mice with respect to total-AKT, pAKT-Thr308 (a kinase suppressor of autophagy), pAKT-Ser473 (autophagy suppressive kinase), total-

AMPK (kinase sensitive to metabolic state of the cell that associated with activation of autophagy) , total-FoxO3a (transcription factor associated with some autophagy genes), and pFoxO3a-Ser253 (AKT substrate resulting in the nuclear exclusion of FoxO3a and a decline in autophagy gene transcription).

However, the BALB/c mice demonstrated increased levels of pULK1-Ser757 (the inactive or suppressed form of ULK1) and Atg6/Beclin-1 (PI3K complex member associated with nucleation of the autophagosome) ($p<0.0267$ and $p<0.0146$, respectively). Additionally, the BALB/c mice demonstrated significantly higher levels of Atg7 (associated with both ubiquitin-conjugation systems), Atg12 (component of the atg5/12/16 complex), and Atg5/12 (part of the elongation complex) ($p<0.0072$, $p<0.0007$, and $p<0.0064$, respectively). Furthermore, the BALB/c mice showed greater expression in both p62/SQSTM1 (Triton X-100 insoluble/2% SDS soluble fraction – cargo adapter protein associated with autophagic flux) and Parkin (an E3-ubiquitin ligase associated with mitophagy) ($p<0.0001$ and $p<0.0445$, respectively). Moreover, BALB/c mice showed significantly more pAMPK-Thr172 (the activated form of the kinase AMPK) and SirT1 (a deacetylase associated with the FoxO3a transcription factor) ($p<0.0041$ and $p<0.0329$, respectively). Finally, relative to the C57BL/6 mice, BALB/c mice demonstrated significantly greater amounts of oxidative damage (with a carbonylated protein assay) to cellular proteins ($p<0.0019$). (See Figure 1.1, Appendix 2).

We found that the C57BL/6 mice showed increased levels of LC3-I (the non-membrane associated form of LC3) and LC3-II (the autophagosomal membrane-

incorporated, lipidated LC3-form) autophagy proteins ($p<0.0092$ and $p<0.0030$, respectively).

RT-qPCR Analysis of Autophagy Genes in Young C57BL/6 and BALB/c Mouse Hearts

As shown above, C57BL/6 and BALB/c mice demonstrate substantial differences in the basal expression of proteins throughout the autophagy pathway as well as in proteins that regulate the pathway. We sought to determine if comparable differences were present in basal autophagy gene expression between the two strains. The same tissue samples used for protein expression were subjected to analysis by RT-qPCR using the primer sets listed in Common Methods Table 2. We found no significant differences between the C57BL/6 and BALB/c mice in their expression of a*tg1, atg3, atg5, atg6, atg7, atg4a, atg4b, atg4c, atg4d, atg8b, atg12, atg16l1, LAMP2a, parkin, p62/sqstm1,* and *nrf2* (data not shown). However, there was an approximate 8830 fold increase in *atg8a* message in C57BL/6 relative to the young BALB/c mice (See Figure 1.2).

Basal Autophagy Protein Profile in the Hearts of CB6F1/J Mice Compared to C57BL/6 and BALB/c Mice

To understand potential differences in autophagy between the C57BL/6 and BALB/c strains and their offspring, we analyzed basal autophagy as well as its upstream regulatory proteins. To do so, the hearts (ventricles) of 2.5-3 month old C57BL/6 and BALB/c mice (n=4) and 4 month old CB6F1/J mice (n=6) were subjected to analysis by western blot using antibodies to proteins associated with phagophore formation during

the initiation of autophagy, phagophore elongation, autophagosome/lysosome fusion, autophagosome targeting, upstream regulation of autophagy, and oxidative damage (Common Methods Table 1). The individual autophagy proteins of the CB6F1/J mice were compared to the parental strains and categorized as being more similar to either one or both parents, intermediate between the parents, or significantly dissimilar to either parent (Figure 1.3; Appendix 2).

The overall autophagic protein expression in the CB6F1/J mice was unique in that there was no discernible pattern in the expression of the autophagy proteins relative to one parental strain or the other. We found that there were no differences observed in protein levels between C57BL/6, BALB/c, and CB6F1/J mice with respect to Atg3 and LAMP2A. There were no differences observed in protein levels between C57BL/6, BALB/c, and CB6F1/J mice with respect to the Triton X-100 insoluble/2% SDS soluble ubiquitin. Finally, there were no observed differences in protein levels between C57BL/6, BALB/c, and CB6F1/J mice with respect to total-AKT, pAKT-Thr308, total-AMPK, and total-FoxO3a.

Furthermore, some of the autophagy proteins analyzed in the CB6F1/J mice demonstrated intermediate levels of some proteins, meaning that CB6F1/J expression levels ranged between those observed in the parents. Examples of this were Parkin and pULK1-Ser757.

Additionally, some of the observed autophagy protein levels were more like one parent than the other. Atg6 (Beclin-1) analysis showed that the CB6F1/J mice were more similar to the C57BL/6 parent (BALB/c to CB6F1/J $p<0.0048$; C57BL/6 to CB6F1/J

p=n.s.). Atg4D (BALB/c to CB6F1/J p<0.0260; C57BL/6 to CB6F1/J p=n.s.), Atg12 (BALB/c to CB6F1/J p<0.0051; C57BL/6 to CB6F1/J p=n.s.), LC3-I (BALB/c to CB6F1/J p<0.0166; C57BL/6 to CB6F1/J p=n.s.), LC3-II (BALB/c to CB6F1/J p<0.0174; C57BL/6 to CB6F1/J p=n.s.), and the amount of the glycosylated form of LAMP2A (BALB/c to CB6F1/J p<0.0270; C57BL/6 to CB6F1/J p=n.s.) were more similar to a C57BL/6 mouse. Furthermore, pAKT-Ser473 (BALB/c to CB6F1/J p<0.0255; C57BL/6 to CB6F1/J p=n.s.), pAMPK-Thr172 (BALB/c to CB6F1/J p<0.0201; C57BL/6 to CB6F1/J p=n.s.), and SirT1 (BALB/c to CB6F1/J p<0.0060; C57BL/6 to CB6F1/J p=n.s.) expression profiles were more similar to a C57BL/6 mouse. The carbonylation assay, a measure of oxidative damage to a variety of cellular proteins, demonstrated a degree of oxidative damage similar to the C57BL/6 mouse (BALB/c to CB6F1/J p<0.0001; C57BL/6 to CB6F1/J p=n.s.), which corresponds to less damage than that observed in the BALB/c mice. Conversely, we also found that CB6F1/J mice were more similar to BALB/c mice in just one instance, pFoxO3a (BALB/c to CB6F1/J p=n.s.; C57BL/6 to CB6F1/J p<0.0487) (Figure 1.3; Appendix 2).

We also noted that CB6F1/J mice demonstrated significantly less total-ULK1 than its parental strains (BALB/c to CB6F1/J p<0.0063; C57BL/6 to CB6F1/J p<0.0340). Additionally, Atg5 (BALB/c to CB6F1/J p<0.0042; C57BL/6 to CB6F1/J p<0.0021), Atg7 (BALB/c to CB6F1/J p<0.0008; C57BL/6 to CB6F1/J p<0.0072), and Atg5/12 (BALB/c to CB6F1/J p<0.0003; C57BL/6 to CB6F1/J p<0.0468) were significantly dissimilar to either the C57BL/6 or BALB/c. Finally, the Triton-X 100 insoluble/2%

SDS soluble p62 levels (BALB/c to CB6F1/J $p<0.0409$; C57BL/6 to CB6F1/J $p<0.0003$), were significantly dissimilar to either a C57BL/6 or BALB/c.

DISCUSSION

Initially, we thought that the autophagy profiles between different mouse strains would be similar. However, by performing a direct comparison between two different strains, we found that there are substantial differences in the basal autophagic protein profiles between C57BL/6 and BALB/c mice. Young BALB/c mice demonstrate higher levels of pULK1-Ser757 (the inactive or suppressed form of ULK1), p62 (an indication of autophagic flux), Atg7 (associated with both ubiquitin-conjugation systems), Atg12 (component of the atg5/12/16 complex), Atg5/12 (part of the elongation complex), Atg6/Beclin-1 (PI3K complex member associated with nucleation of the autophagosome), Parkin (an E3-ubiquitin ligase associated with mitophagy), pAMPK-Thr172 (the activated form of the kinase AMPK), SirT1 (a deacetylase associated with the FoxO3a transcription factor), and carbonylated protein (an indicator of oxidative stress (ROS)) in addition to reduced expression of LC3-I and LC3-II (the non-incorporated and the autophagosomal membrane-incorporated, lipidated LC3-form) in the heart (Figure 1.1).

Moreover, there appears to be a substantial dysregulation in the autophagy pathway of the young BALB/c, as compared to its C57BL/6 counterpart, resulting in depressed/suppressed autophagy. Although there are similar amounts of total-Ulk1 (associated with the autophagy initiation complex) and total-AMPK (a kinase associated with ATP depletion that activates autophagy), the BALB/c mice have a greater proportion of inactivated ULK1 (pUlk1-Ser757) despite having significantly greater amounts of activated AMPK (pAMPK-Thr172). Furthermore, there are greater amounts

of Atg6/Beclin-1, Parkin, Atg7, Atg12, Atg5/12, and SirT1 in the BALB/c mice, despite an increased amount of aggregated p62 (an indicator of a decline in flux) and carbonylated protein (an indirect indicator of deficient mitophagy via an accumulation of ROS). Additionally, in the C57BL/6 and BALB/c mice there are similar levels of Atg3 (part of the LC3 ubiquitin-like conjugation system), Atg4D (associated with GABARAP processing and mitochondrial targeting), Atg5 (part of the Atg5/12/16 complex), and LAMP2A (facilitates autophagosomal-lysosomal binding), yet LC3-I and LC3-II levels are lower in the BALB/c. This indicates that the autophagy pathway in the BALB/c mice is being activated and inactivated simultaneously (pAMPK-Thr172 and pUlk1-Ser757) despite possessing sufficient Atg3, Atg4D, Atg5, LAMP2A, Atg6/Beclin-1, Atg7, Atg12, Atg5/12 to allow basal autophagy to occur. Moreover, the increase in Atg6/Beclin-1, Parkin, Atg7, Atg12, Atg5/12, and SirT1 may be a compensatory mechanism to try to promote more autophagy in an attempt to overcome the suppression. However, the pathway is heavily suppressed in BALB/c mice as indicated by the decline in LC3-I, LC3-II, and an increase in aggregated p62/SQSTM1 and oxidized proteins. This conclusion is further supported by the approximately 8,000-fold difference in basal *atg8* transcription between C57BL/6 and BALB/c mice (Figure 1.2).

It was expected that by analyzing the progeny of a C57BL/6 and BALB/c cross that autophagy would either be more like one of the parental strains or would show an intermediate phenotype. Interestingly, that hypothesis proved incorrect. The total upstream regulators of autophagy AKT, AMPK, and FoxO3 remained constant between the strains. However, lower levels of pAMPK-Thr172, AKT-Ser473, and SirT1 (similar

to the C57BL/6 mice) and greater levels of LC3-II suggest constitutive basal autophagy is increased in the CB6F1/J mice as compared to the BALB/c. However, the CB6F1/J mice display a similarity to the BALB/c solely with respect to pFoxO3a-Ser253, the phospho-form that promotes nuclear exclusion of the FoxO3a transcription factor (Figure 1.3; Appendix 2). Although FoxO3a is not the only transcription factor associated with autophagy gene expression, it is important for transcription of *ulk2, Beclin-1, vps35, atg8(lc3), atg12, gabarap1, and atg4B* under times of cellular stress[74].

Furthermore, CB6F1/J mice share similarity to the C57BL/6 mice with respect to Atg6/Becllin1, Atg4D, Atg12, LC3-I, LC3-II, and the non-glycosylated and immature form of LAMP2A (Figure 1.3; Appendix 2). Additionally, the CB6F1/J mice share similar levels of protein with respect to both of the parental strains with respect to LAMP2A and Atg3. However, the CB6F1/J mice show significant differences in protein expression as compared to the parental strains in total-Ulk1, Atg5, Atg7, and Atg5/12; furthermore, these mice display an intermediate amount of pUlk1-Ser757 and Parkin. Autophagy in the F1 progeny is manifest differently than either of the parental strains, resulting in an intermediate amount of aggregated p62/SQSTM1 and a level of carbonylated proteins similar to the C57BL/6. This indicates that although the CB6F1/J is more similar to C57BL/6 than BALB/c, it will likely behave differently under autophagy-stimulating conditions.

We have established that there are substantial differences in autophagy (at least in basal autophagy) in the hearts of C57BL/6 and BALB/c mice. Interestingly, the van der Borne study (involving 10-12 week old C57BL/6 and BALB/c mice subjected to

myocardial infarction and the strain-related difference in post-infarct fibrosis[103,104] – See Chapter Introduction) suggested that differences in autophagy between the C57BL/6 and BALB/c strains play a role in fibrosis following myocardial infarction. Although we have not yet done any direct autophagy functional studies to verify differential autophagy regulation under stress (autophagy-inducing) conditions, the observed strain difference in autophagy coupled with the fasting studies of cardiac autophagy described in Chapter II do imply substantially different autophagy responses in stress conditions, which could result in different susceptibilities to fibrosis following myocardial infarction.

The myocardial infarction experiment discussed in the paragraph above raises an interesting point. Differences in basal autophagy in the C57BL/6 and BALB/c have far ranging implications with respect to how animal models are chosen for scientific studies and could impact reproducibility of data in studies that are done with different strains, even in experiments that have nothing to do with autophagy. Autophagy is a constitutive process that is upregulated under conditions of cellular stress and impacts virtually all of the major cellular pathways: apoptosis, inflammation, cell cycle, DNA repair, and many others. Autophagy is also active in a large variety of disease states in addition to age-related diseases (Reviewed in Choi et al. and Sridhar et al. for more common diseases, but there are 1090 PubMed review papers gathered from a search "autophagy and disease")[106,107]. Consequently, disease studies could have differing outcomes depending on the strain chosen, which may or may not be representative of what occurs in the human population that the animal studies are supposed to model. Additionally, assuming that at least some of the mouse strains are going to have differences in the way autophagy

is manifest, then the assumption that studies done in one strain can be extrapolated to another strain or the human population may be erroneous.

Another interesting implication of this study involves the possibility that the progeny of a C57BL/6 and BALB/c could mount an autophagy response that is quite different from its parental strains. It is apparent that autophagy genes assort independently of the parents, possibly resulting in a different autophagy phenotype. Autophagy function-based experiments such as fasting and chloroquine studies (see Chapter II) could prove if the autophagy pathway behaves differently in the CB6F1/J mice, potentially indicating a differential response or contribution to disease relative to its parental strains. If so, as autophagy research begins to design therapeutics to modulate autophagy in the context of treating human disease, then this could demonstrate the need for generating an autophagy profile in patients before initiating such a treatment. In other words, generating an autophagy profile will become vital in order to tailor treatment of disease to the patient (personalized medicine).

Chapter I, in part, is currently being prepared for submission for publication of this material. Gurney, M.A., Gottlieb, R.A., and Linton, P.J. The dissertation author was the primary investigator and author of this material.

	PROTEIN	BALB/c vs. C57BL/6
Phagophore Formation	total ULK1	
	p(ser757)-ULK1	
	Atg6	
Elongation	Atg3	
	Atg4D	
	Atg5	
	Atg7	
	Atg12	
	Atg5/12	
	LC3-I	
	LC3-II	
Fusion	Lamp2a	
	Lamp2A N.G.	
Targeting Protein	p62/SQSTM1	
	Ubiquitinated protein	
	Parkin	
Upstream Regulators	total-AKT	
	p(308thr)-AKT	
	p(473ser)-AKT	
	total-AMPK	
	p(172thr)-AMPK	
	total FOXO-3a	
	p(253ser)-FOXO-3a	
	SirT1	
Oxidative Damage	Carbonyl. Prot.	

BALB/c > C57BL/6

BALB/c = C57BL/6

C57BL/6 > BALB/c

Figure 1.1: Differences in Proteins Associated with Autophagy in Young BALB/c and C57BL/6 Mice. The hearts of 2.5-3 month old BALB/c and C57BL/6 (n=4) were removed and subjected to western blot analysis for the detection of several autophagy proteins, proteins associated with the regulation of autophagy and carbonylated protein (See Common Methods for details). Protein expression was normalized to its actin control. Comparing protein levels in both mouse strains, a white cell indicates significantly greater expression in BALB/c, a black cell indicates significantly greater expression in C57BL/6, and a gradient cell indicates similar protein expression (significance was established by Student's T-Test ($p<0.05$)). Source data (original blots and graphs derived from ImageJ quantification) are found in Appendix 2.

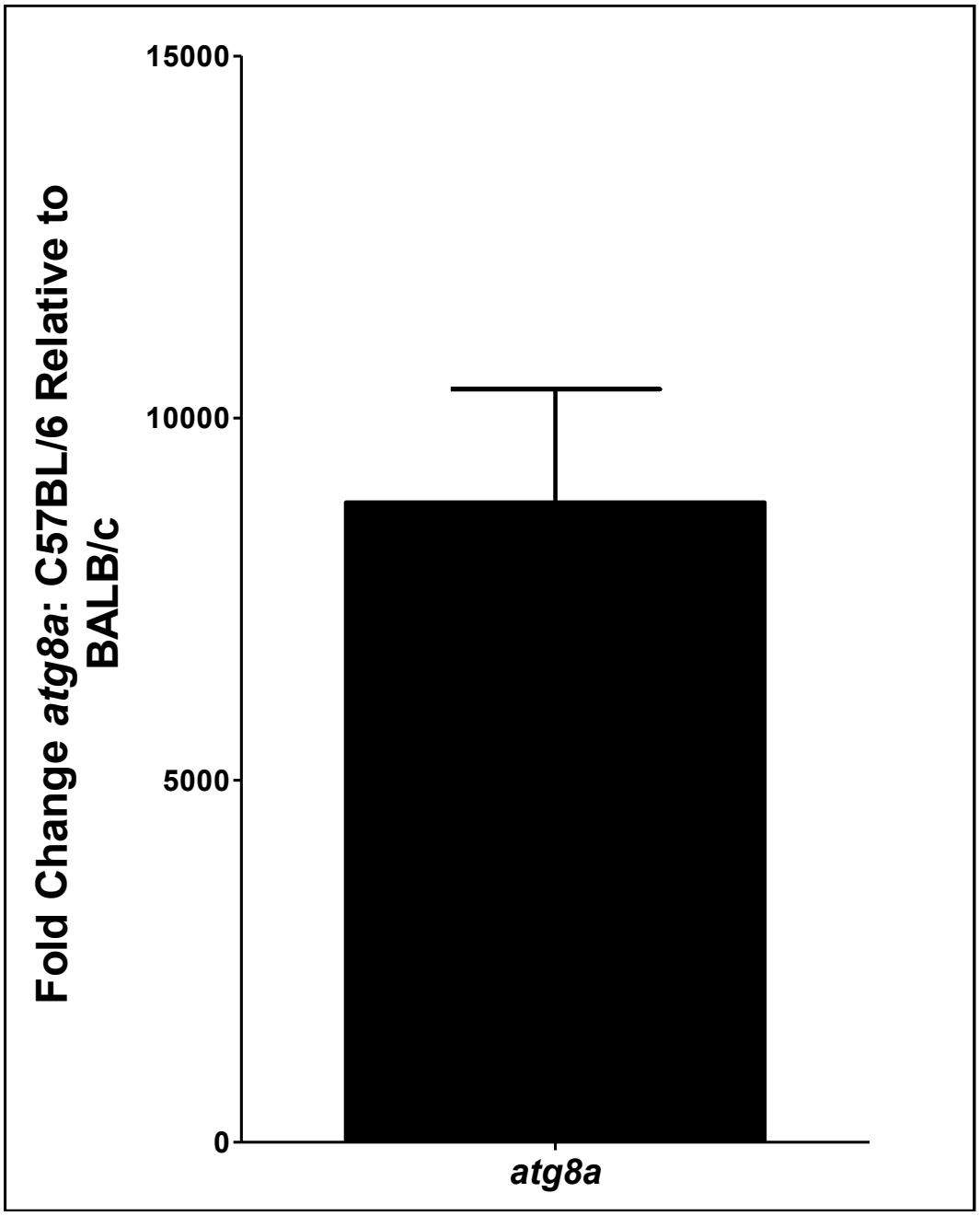

Figure 1.2: RT-qPCR Analysis of *atg8a* Expression in C57BL/6 Relative to BALB/c Mice. RT-qPCR analysis is described in detail in Common Methods. Briefly, RNA was extracted using Nucleospin RNA extraction kit, cDNA was synthesized with iScript Reverse Transcription Supermix for RT-qPCR, and RT-qPCR was performed using *β-actin* as a house keeping gene. The fold induction or fold difference was calculated using the Pfaffl method and verified using the $\Delta\Delta C_t$ method. Value shown is the means of four mice +/- SEM. A value of 2.5 fold or greater is considered significant.

	PROTEIN	CB6F1/J is More Similar to:
Phagophore Formation	total ULK1	**CB6F1/J**
	p(ser757)-ULK1	**Intermediate**
	Atg6	**C57BL/6**
Elongation	Atg3	**C57BL/6 & BALB/c**
	Atg4D	**C57BL/6**
	Atg5	**CB6F1/J**
	Atg7	**CB6F1/J**
	Atg12	**C57BL/6**
	Atg5/12	**CB6F1/J**
	LC3-I	**C57BL/6**
	LC3-II	**C57BL/6**
Fusion	Lamp2a	**C57BL/6 & BALB/c**
	Lamp2A N.G.	**C57BL/6**
Targeting Protein	p62/SQSTM1	**CB6F1/J**
	Ubiquitinated protein	**C57BL/6 & BALB/c**
	Parkin	**Intermediate**
Upstream Regulators	total-AKT	**C57BL/6 & BALB/c**
	p(308thr)-AKT	**C57BL/6 & BALB/c**
	p(473ser)-AKT	**C57BL/6**
	total-AMPK	**C57BL/6 & BALB/c**
	p(172thr)-AMPK	**C57BL/6**
	total FOXO-3a	**C57BL/6 & BALB/c**
	p(253ser)-FOXO-3a	**BALB/c**
	SirT1	**C57BL/6**
Oxidative Damage	Carbonyl. Prot.	**C57BL/6**

Figure 1.3: CB6F1/J Autophagy Protein Profile. The hearts of BALB/c (n=4), C57BL/6 (n=4), and CB6F1/J (n=6, n=5 for Carbonylation Assay) were removed and subjected to western blot analysis as detailed in Common Methods. Autophagy protein expression was normalized to its actin control and significance was established by Student's T Test ($p<0.05$). The mouse strain listed in each cell indicates which strain the CB6F1/J protein was expression similar to, i.e., BALB/c, C57BL/6, or both. A cell labeled "Intermediate" indicates protein expression levels ranging between those found in the BALB/c and C57BL/6. A cell labeled CB6F1/J indicates a significant dissimilarity to either C57BL/6 or BALB/c. Source data (original blots and graphs) are found in Appendix 2.

CHAPTER II:

Age-Related Differences in Cardiac Autophagy: C57BL/6 and BALB/c Mice

INTRODUCTION

Cardiovascular diseases are the leading cause of morbidity and mortality in Western societies, particularly in the aged population and despite the years of research, little progress has been made to determine therapies that alleviate or prevent this disease. To date, most studies of ischemia/reperfusion (IR) injury and cardioprotection have relied on healthy, young animals, yet aging has been shown to predispose an individual to increased injury following acute myocardial infarction[108]. As a result, many therapeutics developed to ameliorate the damage associated with myocardial ischemia/reperfusion injury show efficacy in animal models but fail in clinical trials, likely because the efficacy studies are done in a non-relevant population, namely the young and healthy.

Aging is a consequence of dysregulated cellular pathways that over time result in less efficient cell responses or stress management[109]. It is manifest by a drastic phenotypic change over a lifespan and an increase in the so called aging-associated diseases: cardiovascular disease, Type II diabetes, neurodegenerative diseases like Alzheimer's, cancer, arthritis, and so on[110]. There are a variety of theories concerning how organisms/cells age (reviewed by Jin)[111]. Generally, the aging theories are classified into one of two broad themes: aging follows a programmed timeline that alters the cellular behavior and responses to stimuli (Programmed Theories) or aging is the result of the accumulation of damage that alters the aforementioned behaviors and responses (Damage Theories)[111].

Of the myriad of theories, we decided to focus on a refined version of The Free Radical Theory of Aging proposed by Denham Harman in 1956, The Mitochondrial Oxidative Stress Theory of Aging[112-114], as a model for our aging heart studies. Briefly, this theory states that dysfunctional mitochondria accumulate in aged cells and promote the formation of reactive oxygen species (ROS), which negatively modifies DNA, proteins, membranes, and organelles, leading to further accumulation of damaged mitochondria and a ROS cascade contributing to more ROS that results in the "aged" phenotype[64,114-116]. Some have suggested that the decline in the clearance of dysfunctional mitochondria is due to a reduction in autophagy (specifically mitophagy)[116,117]. In fact, Droge and colleagues posit that autophagy has three critical functions in the aging cell, the provision/regulation of amino acids and the reduction of damaged proteins and organelles[118]. The heart has high metabolic activity and is therefore rich in mitochondria. Moreover, cardiomyocytes require a steady supply of oxygen to function and are replaced infrequently[119], making them candidates for oxidative damage and stress[116,120]. Several mechanisms to survive hypoxic stress have evolved. This includes the transition from oxidative phosphorylation to glycolysis with autophagy maintaining ATP levels[121] and limiting the accumulation of ROS[116,117]. Autophagy, specifically macroautophagy, is the process that maintains cellular homeostasis through the renewal/recycling of cytoplasmic materials, organelles (such as mitochondria), removal of aggregated proteins, and the provision of energy and biomolecules to cells[28]. Consequently, autophagy is widely thought to be a vital process in the heart, which functions basally to remove defective cytoplasmic materials and organelles and acutely to try to maintain ATP homeostasis[115,122] and limit ROS damage[116,117].

We decided to focus on the Mitochondrial Oxidative Stress Theory of Aging[112-114], specifically with respect to the role of autophagy, for our aging heart studies for a myriad of reasons. First, it is well established that as the heart ages, basal ROS levels increase[120] and a large number of mitochondria from aged post-mitotic cells are enlarged and typically suffer from a loss of function and turnover mechanisms, i.e. fission, fusion, protein quality control, and removal by autophagy (reviewed in Terman et al.)[123]. Second, autophagy, and by extension mitophagy, has been shown to be a vital component of cellular homeostasis by degrading dysfunctional mitochondria, thus limiting ROS production and making the study of autophagy relevant to many cardiovascular diseases, e.g. ischemia/reperfusion injury[124]. Third, ROS has been shown to induce autophagy *in vitro* via AMPK activation[125] (HeLa cells with amino acid deprivation) and/or by regulating Atg4 activity (CHO or HeLa with H_2O_2)[126], establishing a link between the two processes. Finally, interactions between ROS and iron-containing macromolecules have been shown to promote the formation and accumulation of intralysosomal pigment, Lipofuscin, as cells age (a well described hallmark of aging)[115,123,127,128]. Lipofuscin is indigestible, contributes to dysregulation of lysosomal pH, and possibly prevents/limits autophagy by disrupting lysosomal/autophagosome interaction[127,128]. Taken together, these studies demonstrate a link between autophagy, ROS, and aging with an age-related dysregulation of autophagy at its core. To that end, we decided to characterize autophagy in the aging heart as a preliminary step to understand the contribution of an age-related change in cardiac autophagy in the broader context of myocardial infarction.

Although it is generally accepted that macroautophagy declines with age based on the Lipofuscin and ROS studies[123,127,129-135], there are some inconsistencies in the reported heart autophagy data. Inuzuka et al. have shown that LC3-II declines when comparing 3 to 20-24 month old FVB mice[134]. Additionally, Taneike et al. showed that LC3-II levels decline when comparing 2.5 mo and 26 mo C57BL/6 mice[135]. However Boyle and colleagues showed an increase in LC3-II and Beclin-1 levels when comparing 2 mo and 18 mo C57BL/6 mice[132]. Finally, Wohlgemuth et al. compared 6 mo and 26 mo Fisher 344 rat hearts and showed an age-related increase in Beclin-1, LC3-I, LC3-II, no change in Atg7, and a decline in Atg9[131]. Additionally, the autophagy literature is rife with review papers declaring that autophagy declines as mice age. Surprisingly, many review article authors do not distinguish between CMA and MA, so Anna Marie Cuervo's work focusing on the age-related decline in chaperone-mediated autophagy[20] is often misinterpreted as covering all facets of autophagy, which is incorrect.

Although myocardial infarct is not the focus of this dissertation, we believe that an understanding how autophagy changes in the aged heart will help in the development of therapeutics and cardioprotective interventions that could help minimize the likelihood of having a heart attack or mitigate the tissue damage associated with an acute cardiac event, specifically by minimizing ROS levels. Several studies suggest that the upregulation of autophagy (mitophagy) following cardiac stress mitigates cardiac damage[136,137] and is thought to be a response to minimize further ROS damage by dysfunctional mitochondria[137]. Additionally, reports testing an intervention involving a series of repeated brief ischemic events, presumably to promote a sustained increase in

autophagy proteins or flux have been described in neurons[138,139] and in the heart[140-142]. These interventions seem to be effective in limiting I/R-associated damage in the murine and rat heart in most cases[5,143]. Unfortunately, it is now known that the effects of ischemic preconditioning appear to be limited to the young[144] (reviewed in Wojtovich et al.)[145]. However, long-term dietary modifications, such as caloric restriction, have been shown to improve cardiac function (reviewed in Speakman et al.)[61]. Moreover, Abete and colleagues demonstrated that "physical activity or caloric restriction is partially capable to preserve the cardioprotective effect of ischemic preconditioning in the aging [human] heart."[146]. This brings up an interesting question that we decided to follow up on, "Could such a dietary modification modulate autophagy in the aging heart?"

To our knowledge we are the first to undertake a comprehensive analysis of autophagy in the aging murine heart. In fact, Ana Maria Cuervo, a prominent autophagy researcher, called for such an analysis in 2005[127]. Consequently, we undertook a global approach where we would not only confirm that autophagy declines in the aging heart, but determine how those changes are manifest as a consequence of aging. Consequently, we examined basal levels of key autophagy and autophagy regulation proteins in both a long-lived (C57BL/6 - mean/max lifespan is 30/36 mo) and shorter-lived (BALB/c - mean/max lifespan is 24/30 mo) strain and undertook functional assays designed to detect if autophagy activity in the aged differs from young mice with respect to initiating an autophagy response to an acute stressor (fasting), clearance of autophagosomes or autophagic flux, and an accumulation of oxidative damage that indirectly reports dysfunctional mitochondrial clearance via mitophagy. These experiments allowed us to

answer the following questions: 1) How does autophagy change with age? 2) Are those age-related changes manifest similarly between the C57BL/6 and BALB/c mice (as observed in the mice in Chapter I)? 3) Can aged mice induce autophagy as readily as in young mice? 4) Is autophagic flux and mitophagy altered with age? and 5) Can initiating an intermittent fasting protocol modulate autophagy such that autophagic function can be restored or partially restored in the aged?

METHODS

Basal Aging

Hearts were extracted from 2.5, 8, 13, 18, and 24 month old C57BL/6 and 3, 8, 13, 19, and 25 month old BALB/c mice for lifespan autophagy analysis of p62/SQSTM1 and ubiquitin ($n \geq 3$ each age group) in the Triton X-100 soluble/2% SDS insoluble fraction by western blot (See Common Methods).

All of the remaining studies (e.g. basal protein expression) examined hearts from young, middle-aged, and old C57BL/6 (aged 3, 13, and 23 month old) and BALB/c (aged 3, 14, and 24 month old) mice (purchased from the NIA Colony at Charles River Laboratories) (n=4 in each age group). The hearts were extracted and subjected to autophagy protein analysis by western blot (See Common Methods).

Fasting Protocol

2.5-3 month old and 18 month old C57BL/6 were fasted for 0, 24, or 48 hrs (n=4 for each group). Additionally, approximately 5 month old and 23-25 month old BALB/c mice were subjected to a similar fasting protocol (n=4 for each group, except n=5 for young 24 hr fast). Upon the initiation of the fast at 10 A.M., mice were moved into fresh cages without food and sacrificed 24 or 48 hrs later. Water availability was not restricted. Tissue treatment and western blot analysis was performed in accordance with the procedure found in the Common Methods.

Intermittent Fasting

Middle-aged males and females (13 month old) BALB/c or C57BL/6 mice were subjected to a twice a week 24 hr fast. The mice were placed in a fresh cage without food on fasting days (5 P.M. Monday to 5 P.M. Tuesday and 5 P.M. Thursday to 5 P.M. Friday).

Intermittent fasting of BALB/c mice started with approximately 13 month old mice (n=29 intermittent fasted, n=14 controls). Mouse weights were recorded in week 9, 15, and 16. Mice were harvested 4 and (17 months old) 6.5 months (19.5 months old) following the initiation of intermittent fasting and LC3-I and LC3-II levels (n = 3 ad libitum control, n = 5 for intermittently fasted mice) were measured by western blot as previously described in the Common Methods section (Tissue Lysis and Preparation for Gene and Proteins Analysis; SDS PAGE and western blot analysis – TETN Buffer). Additionally, 24-25 month old intermittently fasted BALB/c mice (intermittently fasted for 49 weeks) and their ad libitum counterparts were subjected to chloroquine treatment to determine flux levels (n=4) (See Method Below). The spleens and lymph nodes in the intermittently fasted mice exhibited pathology, i.e., splenomegaly and lymphadenopathy and all mice discarded.

Intermittent fasting of C57BL/6 mice started with approximately 13 month old mice (n=29 control and n=35 intermittent fasted mice). Mouse weights were recorded weekly or daily depending on experimental requirements (see Results/Discussion section). Tissue was harvested from age/sex matched mice that were fed ad libitum or intermittently fasted for 3 weeks (n=5), 6 weeks (n=5), and 16 weeks (n=5) and the

prepared tissue lysates were probed for LC3/Actin by western blot (See Common Methods). For these studies, the animals were sacrificed 3 days following their last fast. Finally, 19.5 month old intermittently fasted C57BL/6 mice (intermittently fasted for 25 weeks) and their ad libitum counterparts were subjected to chloroquine treatment to determine flux levels (n=4) (See Method Below).

Autophagic Flux

Mice were fasted to induce maximal autophagy (C57BL/6 48 hrs and BALB/c 24 and 36 hrs). The fast was timed and the assay was timed so that tissue harvest started at 11 AM.

Five hrs prior to the end of the fast, mice were weighed. A 10 mg/mL chloroquine diphosphate (Sigma-Aldrich, C6628-100G) stock solution was prepared fresh in 1X PBS (Gibco, 14200-075) and filter sterilized. The chloroquine diphosphate solution was adjusted for each animal so that a 50 mg/kg body weight dose would be administered in a 200 μL injection. Four hours prior to the end of the fast, mice were injected intraperitoneally with either chloroquine or PBS. At 11AM, the mice were killed, the ventricles were extracted, lysed, and LC3-II protein expression was determined by western blot (See Common Methods).

The twenty-four hour fast with chloroquine-treated BALB/c mouse assay was done with both young (approximately 3.5 month old) and aged (19 month old) mice (n=4). The thirty-six hour fast with chloroquine treatment in the BALB/c mice was done with 4.5-5 month old mice (young) and 21.5-22 month old (aged) mice (n=4). Finally,

the forty-eight hour fast with the C57BL/6 was done in 3.5 month old (young) and 24-25 month old (aged) mice (n=4).

Carbonylation

The carbonylation assay is previously described in the Carbonylation section of the Common Methods.

RT-qPCR Analysis of Autophagy Gene Expression

Gene expression by real time quantitative PCR is described in the Common Methods portion of this dissertation.

RESULTS

Basal Autophagy Protein Profile of Young and Aged C57BL/6 and BALB/c Mice

To understand potential differences in basal autophagy in the murine heart across age, we analyzed basal autophagy as well as its upstream regulatory proteins. To do so, the hearts (ventricles) of 2.5-3 month old and 24 month old C57BL/6 or BALB/c mice (n=4) were subjected to analysis by western blot using antibodies to proteins associated with autophagy induction, phagophore formation, phagophore elongation, autophagosome/lysosome fusion, autophagosome targeting, upstream regulation of autophagy, and oxidative damage.

Age-Related Changes in Basal Autophagy Profile in C57BL/6 Mice:

A decline in Atg5 (a protein associated with the Atg5/12/16L1 complex - $p<0.0085$) and LC3-II (a protein integrated into the autophagosomal membrane - $p<0.0235$) was observed. However, the Triton X-100 insoluble/2% SDS soluble p62 and ubiquitin (proteins associated with aggregate clearance via autophagy) was found to increase with increasing age (p62 $p<0.0069$; ubiquitin $p<0.0005$). Additionally, pAKT-Ser473 was found to increase with age (pAKT-Ser473 $p<0.0256$) and the amount of oxidative damage in the form of carbonylated protein was significantly greater in the aged versus young mice. Additionally, we found no significant age-related changes in total-ULK1, pULK1-Ser757, Atg6, Atg3, Atg4D , Atg7, Atg12, Atg5/12, LC3-I , LAMP2A , the non-glycosylated or immature form of LAMP2A, Parkin, total-AKT,

pAKT-Thr308, total-AMPK, pAMPK-Thr172, total-FoxO3a, pFoxO3a-Ser253, and SirT1.

Age-Related Changes in Basal Autophagy Profile in BALB/c Mice:

We observed that both pULK1-Ser757 (the inactive or suppressed form of ULK1) and Atg6 (Beclin-1 - PI3K complex member associated with nucleation of the autophagosome) increased with age (pULK1-Ser757 $p<0.0158$; Atg6 (Beclin-1) $p<0.0057$). Furthermore, an increase in Atg3 (part of the LC3 ubiquitin-like conjugation system - $p<0.0022$), Atg4D (associated with mitochondrial targeting and GABARAP processing - $p<0.0010$), Atg7 (associated with both ubiquitin-conjugation systems - $p<0.0147$), Atg12 (component of the Atg5/12/16 complex - $p<0.0004$), LC3-I (the non-membrane associated form of LC3 - $p<0.0111$), and LC3-II (the autophagosomal membrane associated form of LC3 - $p<0.0064$) was observed in the aged versus the young. Moreover, the Triton X-100 insoluble/2% SDS soluble p62 was found to decrease with increasing age (a protein associated with autophagic flux - p62 $p<0.0197$) and Parkin (an E3-ubiquitin ligase associated with mitophagy - $p<0.0112$) levels were increased in the aged mice relative to the young. Finally, pAKT-Thr308 (an activated kinase that suppresses autophagy - $p<0.038$), pAKT-Ser473 (an activated form of AKT that suppresses autophagy - $p<0.0029$), pAMPK-Thr172 (the activated form of the kinase AMPK - $p<0.0040$), and pFoxO3a-Ser253 (phosphorylated FoxO3a form that promotes nuclear exclusion - $p<0.0090$) levels were increased in the aged versus the young. Furthermore, we found no significant age-related changes in total-ULK1, Atg5, Atg5/12, LAMP2A, total-AKT, total-AMPK, total-FoxO3a, or SirT1.

Neither significant age-related change in the Triton X-100 insoluble/2% SDS soluble ubiquitin nor the amount of oxidative damage in the form of carbonylated protein was observed. Unfortunately, the immature non-glycosylated form of LAMP2A could not be observed on the blot; consequently, it was not reported.

RT-qPCR Analysis of Basal Young and Aged C57BL/6 and BALB/c Mice

The autophagy protein profiles comparing basal young to aged mice in C75BL/6 and BALB/c has demonstrated substantial differences in protein expression across age. This begs the question, "If autophagy protein levels are changing, how is autophagy gene transcription affected?" In other words, is the root change in autophagy driven by a transcriptional decline? To answer this question, total RNA was extracted from the hearts of basal young and aged C57BL/6 and BALB/c mice (the same mice sacrificed for the basal autophagy protein study) and converted to template for RT-qPCR analysis (See Common Methods). The RT-qPCR plates were loaded such that each plate contained both young and old samples from both strains, allowing for both a direct comparison of age-related differences in addition to strain-related differences with respect to each autophagy primer set (*atg1, atg3, atg5, atg6, atg7, atg4a, atg4b, atg4c, atg4d, atg8a, atg8b, atg12, atg16l1, LAMP2a, parkin, p62/sqstm1, and nrf2,* with *β-actin* as the housekeeping gene). The data demonstrated no significant age-related differences in any of the autophagy primer sets (See Table I.2 for primer sequences).

LC3 Profile of Young and Aged C57BL/6 and BALB/c Mice (Figure 2.2)

In the first half of this chapter, a dysregulation in the autophagy pathway was evident as an organism ages, particularly in the case of BALB/c mice. This prompts the following question, "If changes in the autophagy pathway occur with increasing age, will those changes result in a noteworthy change in the autophagic response to acute induction of the pathway?" Fasting is the gold standard for inducing autophagy because it is known to upregulate autophagy without the off-target effects associated with drugs[147]. Therefore, to determine if autophagy induction differs across age and/or strain, both young and aged C57BL/6 (3 and 18 mo, respectively) and BALB/c (3 and 24-25 mo, respectively) mice were fasted for 24 and 48 hours and their LC3 protein profiles analyzed by western blot (Figure 2.2A-D; Appendix 4).

We found that in young C57BL/6 mice, levels of LC3-II were elevated at 24 hrs and sustained through 48 hrs (Figure 2.2A) (C57BL/6 young - LC3-I: Fed versus 24 hrs $p<0.0178$; LC3-II: Fed versus 24 hrs $p<0.0017$, Fed versus 48 hrs $p<0.0026$; note: no change in LC3-II at 24 vs. 48 hrs). The aged C57BL/6 mice also responded upon fasting with an increase in LC3-II (Figure 2.2B); however, the maximal response was observed at 48 hrs rather than 24 hrs (Fed versus 24 hrs $p< 0.0026$, Fed versus 48 hrs $p<0.0018$, 24 hrs versus 48 hrs $p<0.0052$) suggesting an intact inducible autophagic response in older mice although slower to peak. Although young BALB/c mice also demonstrated an increase in LC3-II upon fasting, the response was similar to that of aged C57BL/6 mice in that peak levels in LC3-II were not attained until 48 hrs (Figure 2.2C) (Fed versus 24 hrs $p<0.0002$, Fed versus 48 hrs $p<0.0007$, 24 hrs versus 48 hrs $p<0.0115$). A similar

delay in reaching maximal LC3-II levels was noted in the old BALB/c mice but unlike the findings in the other groups, the response in aged BALB/c mice was less robust (note the scale difference) (Figure 2.2 D) (Fed versus 24 hrs $p<0.0104$, Fed versus 48 hrs $p<0.0045$, 24 hrs to 48 hrs $p<0.0384$).

Autophagy Protein Profile of Fasting Young and Aged C57BL/6 and BALB/c Mice

The fasting study looking solely at LC3 in the hearts of C57BL/6 and BALB/c mice (Figure 2.2; Appendix 4) gives a limited static indication or snapshot of autophagy induction and progression. However, by extending the study to include a more comprehensive list of autophagy proteins (such as proteins associated with the initiation of phagophore formation, phagophore elongation, autophagosome/lysosome fusion, and autophagosome targeting) an analysis of both age- and strain-related changes in the whole pathway under an autophagy-inducing stimulus (fasting) can be undertaken (Figure 2.3 and Figure 2.4; Appendix 4).

Autophagy in fasting C57BL/6 mice (Figure 2.3; Appendix 4):

We observed that in young mice both total-ULK1 (associated with the autophagy initiation complex) and pULK1-Ser757 (the inactive or suppressed form of ULK1) increase upon initiation of the fast and remain greater than in the fed controls (total-ULK1 Fed versus 24 hrs $p<0.0012$, Fed versus 48 hrs $p<0.0221$; pULK1-Ser757 Fed versus 24 hrs $p<0.0284$, Fed versus 48 hrs $p<0.0042$). In the young, total-ULK1 levels are high initially, but significantly decrease by 48 hrs (24 hr versus 48 hr $p<0.0053$) while pULK1-Ser757 levels remain constant over the course of the fast. In the aged, both total

and pULK1-Ser757 levels were increased and maintained for the duration of the fast (total-ULK1 Fed versus 24 hrs $p<0.0301$, Fed versus 48 hrs $p<0.0240$; pULK1-Ser757 Fed versus 24 hrs $p<0.0011$, Fed versus 48 hrs $p<0018$). Additionally, Atg6/Beclin-1 (PI3K complex member associated with nucleation of the autophagosome) levels in young animals were significantly greater than the fed controls at 24 hrs ($p<0.0011$), but returned to levels comparable to the fed levels by 48 hrs. However, Atg6/Beclin-1 in the aged mice demonstrated a delay relative to its young counterpart, increasing only at 48 hrs ($p<0.0135$).

There were no significant changes observed in the young with Atg4D (associated with GABARAP processing and mitochondrial targeting); however, the aged animals demonstrated an increase in Atg4D at 48 hrs ($p<0.0102$). Both the young and aged animals displayed an increase in Atg5 (part of the Atg5-12-16 complex) at 48 hrs (young $p<0.0048$; aged $p<0.0038$)). An analysis of Atg7 (associated with both ubiquitin-conjugation systems) showed an increase at 24 hrs in the young mice only ($p<0.0154$). Both the young and aged showed a robust response with respect to Atg12 (component of the atg5/12/16 complex) in that levels increased upon the initiation of the fast and were maintained through the 48 hr time point (young Fed versus 24 hrs $p<0.0120$, Fed versus 48 hrs $p<0.0026$; aged Fed versus 24 hrs $p<0.0271$, Fed versus 48 hrs $p<0.0063$). Finally, Atg5/12 levels (part of the elongation complex) remained unchanged in the young while there was a slight, but significant, increase in Atg5/12 at the 48 hr time point in the aged ($p<0.0467$).

The young animals demonstrated an increase in LAMP2A at 24 hrs ($p<0.0086$) and a significant decrease in both LAMP2A (facilitates autophagosomal-lysosomal binding) and the immature or non-glycosylated form of LAMP2A as compared to the fed controls at 48 hrs (LAMP2A $p<0.0006$, LAMP2A N.G. $p<0.0019$). Conversely, no significant changes in LAMP2A or the non-glycosylated form of LAMP2A in the aged were observed during the course of the fast. Finally, Parkin levels (an E3-ubiquitin ligase associated with mitophagy) were found to be greater than the fed control mice in both the young and aged (Young Fed versus 24 hrs $p<0.0011$, Fed versus 48 hrs $p<0.0327$; Aged Fed versus 24 hrs $p<0.0030$, Fed versus 48 hrs $p<0.0045$).

Autophagy in fasting BALB/c mice (Figure 2.4; Appendix 4):

Unlike young C57BL/6 mice, we noticed marked differences in the expression of autophagy proteins, especially those involved in the initiation of phagophore formation, following a fast. In young mice, both total and pULK1-Ser757 decreased upon initiation of the fast, reaching significance at the 48 hr time point (total-ULK1 Fed versus 48 hrs $p<0.0430$; pULK1-Ser757 Fed versus 48 hrs $p<0.0030$). In the aged, both total and pULK1-Ser757 significantly decreased upon initiation of the fast (total-ULK1 Fed versus 24 $p<0.0001$, Fed versus 48 hrs $p<0.0001$; pULK1-Ser757 Fed versus 24 $p<0.0003$, Fed versus 48 hrs $p<0.0001$). Additionally, Atg6/Beclin-1 levels in the young animals were significantly less than the fed controls at 48 hrs ($p<0.0084$). Atg6/Beclin-1 remained unchanged in the aged mice. Moreover, young BALB/c mice demonstrate a significant reduction in Atg6/Beclin-1 ($p<0.0084$) while the aged mice show no change in Atg6/Beclin-1 levels.

Additionally, the mice displayed opposing responses to the fast with respect to Atg4D. The young showed a robust increase in Atg4D (Fed versus 24 $p<0.0009$, Fed versus 48 hrs $p<0.0008$) while the aged mice demonstrated a decline in Atg4D at 48 hrs of fasting ($p<0.00043$). With respect to Atg5, the young mice increased protein levels (Fed versus 24 hrs $p<0.0046$, Fed versus 48 hrs $p<0.0006$) while the aged mice displayed no change. Atg7 was again expressed in an opposing fashion with a significant increase in the young peaking at 24 hrs ($p<0.0204$) and a significant decrease in the aged at 48 hrs ($p<0.0088$). Atg12 was upregulated in both ages with a significant increase at both 24 and 48 hrs in the young (Fed versus 24 hrs $p<0.0173$, Fed versus 48 $p<0.0024$) and 48 hrs ($p<0.0213$) in the aged. Finally, the young BALB/c mice showed no difference in Atg5/12 while the aged demonstrated a significant decline at 48 hrs ($p<0.0092$).

Both the young and aged animals demonstrated a change in LAMP2A at 48 hrs; however, the young animals demonstrated a decrease ($p<0.0343$) and the aged displayed an increase ($p<0.0275$) in LAMP2A levels. The young animals demonstrated a robust suppression of the immature form of LAMP2A at both 24 and 48 hrs (Fed versus 24 hrs $p<0.0358$, Fed versus 48 hrs $p<0.0003$) while the aged showed no change in non-glycosylated LAMP2A. Finally, Parkin levels did not differ in the young or aged at 24 or 48 hrs of fasting.

Determination of Autophagic Flux in Young and Aged C57BL/6 and BALB/c Mice

So far static measurements have been utilized to help elucidate the age-associated changes in autophagy; however, autophagy is a dynamic process. The fasting data (Figure 2.2, 2.3, and 2.4; Appendix 4) suggests that both young and aged BALB/c and

aged C57BL/6 can mount an autophagic response to fasting, a potent autophagy-inducing stimulus. However, the LC3-II data (Figure 2.2; Appendix 4) demonstrates that despite the ability of the aged C57BL/6, and young and aged BALB/c mice to mount an autophagic response to a fast, this response is delayed and less robust. This prompts an interesting question, "Is autophagic flux (the ability of autophagy to clear materials targeted for removal by the autophagy machinery) changing with age?" Consequently, a chloroquine flux assay was performed. Mice were injected with chloroquine, a drug that blocks autophagosome/lysosome fusion[147], 4 hrs prior to the end of a fast. This promotes the accumulation of autophagosomes that would normally be degraded by the lysosome, allowing for the quantification of autophagic flux by determining an increase in levels of LC3-II in the presence of chloroquine vs. no chloroquine[148].

Autophagic flux was examined at 48 hrs since maximal fasted levels of LC3-II were observed in both young and aged C57BL/6 mice (Figure 2.2; Appendix 4). We found that a two-fold increase in LC3-II was observed in young treated vs. the untreated C57BL/6 mice, indicating robust flux ($p<0.0025$) (Figure 2.5A; Appendix 5). Conversely, the aged C57BL/6 mice demonstrated no detectible change in LC3-II with chloroquine treatment (Figure 2.5A; Appendix 5). Chloroquine treatment did not induce autophagy in the heart tissue since no significant change was detected in the expression of other autophagy proteins e.g. Beclin-1 (Atg6), LAMP2A, Parkin, Atg5/12, Atg5, or total-ULK1, with the exception of pULK1-Ser757 did show a significant decline in only the aged C57BL/6 ($p<0.0121$).

Although maximal fasted levels of LC3-II were observed in both young and aged BALB/c mice at 48 hrs, the mice had difficulty tolerating a 48 hr fast. Therefore, autophagic flux was assessed following a 24 and 36 hr fast. There was no significant accumulation of LC3-II in young or aged mice upon chloroquine treatment with either a 24 hr (Figure 2.2B; Appendix 5) or 36 hr (Figure 2.2C; Appendix 5) fast.

Long-Term Intermittent Fasting in BALB/c Mice

It has been documented that periodic bouts of autophagic upregulation in tissues prior to an ischemic event have a protective effect in neurons[138,139] and in the heart[140-142]. Additionally, long-term dietary modifications, such as caloric restriction, have been shown to improve cardiac function (reviewed in Speakman et al.)[61]. To determine if long-term intermittent fasting (IF) initiated in middle age mice could modulate autophagy, we subjected 13 mo BALB/c mice to a 24 hr fast (Mon/Thurs 5 PM to Tues/Fri 5 PM) twice a week for 6.5 months. Initially, n=9 ad libitum (AL) and n=19 intermittently fasted (IF) mice were enrolled in the study. To ensure that the mice were responding well to the fast, i.e., not experiencing excess weight loss, we measured the daily weights of the mice for 8 days (Figure 2.6A). The intermittently fasted group experienced an approximate and sustained 1.5% loss in body weight following the initial measurement. On the days fasted the IF mice experienced an approximate 10% loss in weight that is recovered within 48 hrs.

To determine if intermittent fasting was modulating basal autophagy, IF and AL mice were sacrificed following 4 and 6.5 months of intermittent fasting and the hearts were probed for LC3 by western blot (See Common Methods) (Figure 2.6 and Appendix

6). Although no significant difference in LC3-II levels were detected after 4 months of intermittent fasting, there was an approximate 5-fold increase in LC3-II by 6.5 months (Figure 2.6B). Anecdotally, when we examined 24 month old BALB/c mice that began an intermittent fast protocol at 13 months of age, we found that all mice had developed pathology (i.e., splenomegaly or lymphadenopathy) as compared to ~10% incidence in their ad libitum cohorts.

Long-Term Intermittent Fasting in C57BL/6 Mice

It has been documented that periodic bouts of autophagic upregulation in tissues prior to an ischemic event have a protective effect in neurons[138,139] and in the heart[140-142]. Additionally, long-term dietary modifications, such as caloric restriction, have been shown to improve cardiac function (reviewed in Speakman et al.)[61]. To determine if long-term intermittent fasting initiated in middle age mice could modulate autophagy, we subjected 13 mo mice to a twice weekly 24 hr fast (Mon/Thurs 5 PM to Tues/Fri 5 PM) for up to 29 weeks. Initially, n=29 ad libitum (AL) and n=35 intermittently fasted (IF) mice were enrolled in the study. To ensure that the mice were not responding adversely to the fast, the mice were weighed daily for 15 days starting at 6 weeks following the initiation of the fasting protocol and weekly over the course of the 29 week fast (Figures 2.7A and 2.7B, respectively). As shown in Figure 2.7A, during the 24 hr fast, the fasted mice lost approximately 10% of their initial weight, which they immediately regained when food was replaced in the cage. Over the 29 week treatment period, both groups of mice gained weight as they aged (Figure 2.7B). Interestingly, an approximate 4.5-5% divergence in weight was observed between AL and IF mice between 2 and about 6

weeks of IF. IF mice gained weight up through the first 3 weeks and then leveled out until 8 weeks when the weight of the AL group caught up. Thereafter, there was no significant difference in the continued weight gain between the two groups.

To determine if intermittent fasting changed the level of basal autophagy, IF and AL mice were sacrificed following 3, 6, and 16 weeks of intermittent fasting and the hearts were probed for LC3 by western blot (See Common Methods) (Figure 2.7C and Appendix 6). At 3 weeks, there was a significant 2-fold increase in LC3-II ($p<0.0026$). However, at 6 and 16 weeks a significant difference in LC3-II was no longer observed between the AL and IF groups.

Although there was no change in LC3-II between the AL and IF mice at 16 weeks of intermittent fasting, the basal autophagy set points could conceivably change, resulting in autophagy functioning at a higher level without demonstrating an increase in basal LC3-II levels. Consequently, a chloroquine flux assay was performed on the fasted mice following approximately 25 weeks of intermittent fasting (See Common Methods), but no difference was observed in the LC3-II levels of the AL versus the IF mice (Figure 2.7D).

DISCUSSION

Autophagy in the Aged C57BL/6 Heart:

Overall, the C57BL/6 mice displayed an age-related decline in autophagy at both the basal and functional levels. An increase in levels of Triton X-100 Insoluble/2% SDS Soluble p62/SQSTM1 and ubiquitinated proteins are indicative of diminished autophagic flux, and similar changes were detected in old C57BL/6 mice. Under basal conditions, we found a decline in LC3-II as C57BL/6 mice age, consistent with the observations of Taneike et al. and Inuzuka et al.[134,135] We also found that the C57BL/6 mice demonstrated a decline in basal levels of Atg5, a molecule associated with phagophore elongation. Although it is tempting to try to tie the basal decline of Atg5 to a reduction in autophagy, this may not be the case because both the young and aged C57BL/6 mice can upregulate the protein by 48 hrs during a fast. Furthermore, an increase in the autophagy suppressive regulatory protein pAKT-Ser473 is observed with increasing age. AKT is associated with cellular senescence, growth (increases in cellular mass), and age[26,42,48,49]. If there is a decline in basal autophagy, then by extension there should be a decline in mitophagy, a specialized form of autophagy. It is well established that as the heart ages, basal ROS levels increase[120], presumably in part due to a decline in mitophagy[123], and cause oxidative protein damage, i.e. protein carbonylation[149]. To that end, we analyzed levels of carbonylated proteins in basal hearts by western blot, finding that carbonylated protein levels increase (and by extension ROS levels) in the aged. Altogether, these results support a decline in autophagy with increasing age (Figure 2.1) in the C57BL/6 mice.

Interestingly, our results confirm those of Hua et al. who also described a decline in Atg5, Triton Insoluble p62, and the LC3-II/LC3-I ratio in aged mice (24-26 months old), a condition that was exacerbated by AKT overexpression (with the exception of Atg5)[150]. Hua and colleagues also noted a decline in Atg6/Beclin-1 (protein associated with nucleation of the pre-autophagosomal membrane) with their aged mice[150], which we could not confirm. However, this is not surprising because we have previously noted that Atg6/Beclin-1 protein expression can vary between assays (data not shown).

Although we found age-related changes in the autophagic protein profile, surprisingly, we did not observe significant differences in autophagy message levels of *atg1 atg3, atg5, atg6, atg7, atg4a, atg4b, atg4c, atg4d, atg8a, atg8b, atg12, atg16l1, LAMP2a, parkin, p62/sqstm1, and nrf2* including the FoxO3a-mediated genes, *atg12, atg4B, ulk1, atg6/bcln1, atg8A, and atg8B*[74](data not shown). There are several ways to explain this observation. First, there was no age-related change observed in the autophagic/metabolic transcriptional regulatory protein levels of SirT1 (a deacetylase presumably associated with FoxO3a activation)[62-64], total-FoxO3a (a transcription factor), or pFoxO3a-Ser253 (the cytoplasmic localized phospho-form of FoxO3a mediated by the kinase AKT) (Figure 2.1)[65,67,68]. If there are no changes in these proteins, then it is conceivable that there would be no corresponding change in gene transcription at least with the FoxO3a-mediated genes mentioned above. Second, there are a variety of transcription factors (at least 37 associated with different cellular stresses alone – See Pietrocola et al.)[74] associated with a variety of autophagy genes that could compensate for an age-related decline independent of FoxO3a involvement. In any case, the autophagy

mRNA analysis indicates that the age-related changes in autophagy are manifest at the protein level and not driven by apparent changes in the FoxO3a-dependent transcriptional program.

Fasting induced the upregulation of autophagy in both young and old C57BL/6 mice as evidenced by increased expression of a number of autophagy proteins, including Parkin (E3 ubiquitin ligase associated with mitophagy), Atg12 (part of the Atg5-12-16L1 complex associated with elongation), Atg5 (same as Atg12), Atg6/Beclin-1, total ULK1 (the kinase that initiates autophagy induction), and pULK1-Ser757 (a suppressive phospho-form of ULK1 that suppresses autophagy induction).

However, similar to the basal studies, the data support an age-related functional decline in the autophagy pathway following a fast. Whereas young C57BL/6 mice mounted a robust and sustained increase in LC3-II conversion, aged mice demonstrate a slower response. In young mice, the constant pULK1-Ser757 and declining total-ULK1 levels suggests that the induction of autophagy is suppressed as the fast progresses, presumably to prevent runaway autophagy ("runaway" autophagy is a phenomenon that is hypothesized to occur during excessive autophagy when its pro-survival aspects transition to pro-apoptotic signals[151]). This is likely confirmed with Atg6/Beclin-1 and Atg7 (part of both ubiquitin-conjugation complexes – See Below) where the initial protein levels increase, but then decrease to control levels presumably to suppress autophagy. In contrast, in old mice total-ULK1 and pULK1-Ser757 increase and are maintained at similar levels, indicating a delayed response to the fast relative to the young animals. This is confirmed by the delay in Atg6/Beclin-1 level upregulation and a

lack of Atg7 upregulation. Interestingly, it is worth noting that the decline in Atg7 induction, a protein associated with both ubiquitin-like conjugating systems (the machinery associated with both the preparation of LC3 and its subsequent incorporation into the blossoming autophagosomal membrane and the formation of the Atg5-12-16L1 complex). It is conceivable that the delay in Atg7 could result in the step-wise LC3-II profile observed in the aged mice.

Moreover, changes in the levels of LAMP2A may also be indicative of functional changes in autophagy. A reduction in LAMP2A following a fast is suggestive of increased LAMP2A degradation following autophagosomal/lysosomal fusion. Cuervo et al. reported that LAMP2A is continuously cycled from the lysosomal membrane to the matrix[152]. In the matrix, some LAMP2A is degraded and some is recycled back to the lysosomal membrane; however, under serum starvation LAMP2A degradation is reduced, so the majority of LAMP2A remains in the lysosomal membrane to facilitate chaperone mediated autophagy and macroautophagy[152]. This most likely results in the observed increase in LAMP2A at 24 hrs and the subsequent decline to well below fed levels by 48 hrs in the young C57BL/6 mice. In order to keep up with LAMP2A degradation, it appears that new LAMP2A protein is synthesized as demonstrated by the increase in the non-glycosylated form (immature form) of LAMP2A. Interestingly, there is no change in LAMP2A or the non-glycosylated form of LAMP2A in the aged C57BL/6 animals. It is apparent that the elderly response to a fast is slowed; however, in the case of LAMP2A these data indicate a very low level of autophagic flux in the aged relative to their young counterpart as indicated by the lack of a decline in LAMP2A associated depletion in

autophagosomes (which is confirmed by the chloroquine assay). The above fasting data suggest that both young and aged C57BL/6 animals are capable of undergoing autophagy following the initiation of a fast; however, autophagy occurs with slower or delayed kinetics in the aged C57BL/6.

The accumulation of carbonylated protein (defective mitochondrial clearance) and p62/ubiquitinated protein (defective Triton X-100 Insoluble/2% SDS Soluble protein aggregate clearance) in the aged C57BL/6 mice suggests deficient autophagic flux. Additionally, the step-wise patterning of LC3-II, the delay in Atg7 upregulation, and the insignificant change in LAMP2A in the aged mice also suggest an autophagic decline.

Finally, the findings with LC3-II in the presence and absence of chloroquine treatment support that the autophagy pathway is functioning in the young but is deficient in the aged. It has been suggested that autophagy flux inhibitors such as chloroquine could induce autophagy because the drug would promote dysregulated lysosomal function. To ensure that the chloroquine treatment was not inducing autophagy during the C57BL/6 flux assays, we analyzed the changes in Beclin-1 (Atg6), LAMP2A, Parkin, Atg5/12, Atg5, or total-ULK1 protein expression following the 4 hr treatment with chloroquine (data not shown), finding no significant differences the young or aged in any of the aforementioned proteins, save a decline in pULK1-Ser757 in the old. This indicates that autophagy induction is triggered by the release of mTOR repression on ULK1 in the aged C57BL/6 mice, yet there is still no detectible flux, which lends further support to a broken autophagy pathway in elderly mice.

In all, age-related deficiencies in autophagy in the C57BL/6 mice are apparent under basal and fasting conditions. However, it is uncertain at which point or points the pathway breaks in the aged, but the regulation of the AKT-AMPK-mTOR pathways as being a major contributor to the aging phenotype in the heart is an interesting lead, particularly with respect to the role of preventing the accumulation of dysfunctional mitochondria, protein aggregates, and lipofuscin.

Autophagy in the Aging BALB/c Heart

In marked contrast to the findings in C57BL/6 mice, the data from the BALB/c mice demonstrate a drastically different aging profile. Of interest are the simultaneous autophagy-inducing and repressing signals observed in the regulatory and initiation complexes in the aged animals. The suppression of autophagy is supported by an increase in the following proteins: pAKT-Ser473 and pAKT-Thr308 (active forms of AKT that suppress autophagy),[42,48-52] pFoxO3-Ser253 (the phosphorylated form of FoxO3a that sequesters the autophagy-related transcription factor in the cytoplasm)[67,68], and pULK1-Ser757 (phosphorylation of this member of the autophagy-initiation complex by mTOR suppresses autophagy)[28,29]. Conversely, the observed increase in pAMPK-Thr172 (a kinase activated with a variety of cellular stresses and known activator of autophagy) in the aged promotes autophagy induction[44-47]. Although it is tempting to speculate that the age-related increase in Atg6/Beclin promotes upregulation of autophagy, the complex that Atg6/Beclin-1 is associated with will determine behavior and not necessarily the level of Atg6/Beclin-1. Consequently, further analysis of the

Atg6/Beclin-1 complex would have to be undertaken to determine if Beclin-1 is contributing to the induction of autophagy.

A substantial number of the proteins associated with elongation of the phagophore membrane are significantly upregulated in the aged BALB/c mice (e.g., Atg3, Atg4D, Atg7, Atg12, and both forms of LC3), but it is difficult to determine how these proteins contribute to basal levels of autophagy. Two possible interpretations are possible. The first interpretation is that increasing levels of these proteins in the aged is a compensatory mechanism to make up for insufficient autophagy in the aged animals. The second is that basal autophagy increases in the aged BALB/c mice, and that increase is reflected in levels of elongation proteins. In support of the latter interpretation, there is an observed increase in Parkin (an E3 ubiquitin ligase associated with targeting deficient mitochondria for autophagic degredation), a decline in oxidative damage (carbonylated protein) coupled with a concordant decline in Triton X-100 Insoluble/2% SDS Soluble p62/SQSTM1, and a lack of accumulated ubiquitinated protein, all of which are indicative of functional autophagy. In all, the aging BALB/c mice demonstrate substantial dysregulation of the pathway relative to C57BL/6 mice. Surprisingly, it also appears that autophagy is constitutively active in aged BALB/c mice, although there is an attempt to suppress it at the regulatory, initiation, and possibly the nucleation parts of the pathway.

Similar to our findings with the C57BL/6 mice, the RT-qPCR demonstrated no significant age-related change in any of the autophagy genes tested. As stated before, there are a variety of transcription factors associated with a variety of autophagy genes

that could compensate for any age-related effects (at least 37 transcription factors have been associated with different cellular stresses alone – See Pietrocola et al.)[74]. In any case, the autophagy mRNA analysis indicates that the age-related changes in autophagy are manifest at the protein level and not driven by apparent changes in the autophagy transcriptional program.

At least by basal analysis, there is an apparent dysregulation in autophagy as BALB/c mice age. How is this age-related dysregulation in autophagy manifest when the animals are put under autophagy-inducing conditions i.e. an assay looking at functional aspects of autophagy? Upon the initiation of a 24 or 48 hr fast, we found that young BALB/c mice demonstrated an upregulated and delayed LC3-II response whereas the response in old BALB/c mice was additionally diminished. This suggests that both young and aged animals are capable of undergoing autophagy following the initiation of a fast; however, the autophagic process occurs with slower kinetics. These data suggest two possible conclusions. The step-wise patterning of LC3-II observed in these mice may be indicative of a deficiency in autophagy that results in a delayed response. However, it is equally plausible that the slowed/diminished increase in LC3-II after fasting BALB/c mice is a consequence of an autophagy pathway that is constitutively upregulated. Indeed, the substantial dysregulation in the autophagy-aging profile coupled with indications of functional autophagy in the aged (i.e., reduced accumulation of aggregate p62/SQSTM1 and carbonylated proteins) suggest that basal autophagy is already robust in fed BALB/c mice. Further induction of the response would lead to a downregulation to prevent “runaway” autophagy and preserve cellular integrity.

As expected, the fast is upregulating autophagy in young and old BALB/c mice as demonstrated by changes in expression in several autophagy proteins, e.g., LAMP2A, Atg12, Atg7, Atg4D, total-ULK1, and pULK1-Ser757. Thus, autophagy is functional in the aged. However, of primary interest is that the relative levels of proteins associated with autophagy initiation and nucleation (total-ULK1, pULK1-Ser757, and Atg6/Beclin-1) with respect to the fed control are opposite of those seen in the C57BL/6 (levels are less than control in the BALB/c and greater than control in the C57BL/6). Not only does this suggest that the mechanisms regulating autophagy during a fast are very different between C57BL/6 and BALB/c mice, but importantly, it appears that in the BALB/c mice the initiation and nucleation complexes are autophagy suppressive, presumably downregulated to prevent excessive autophagy that would lead to apoptosis. The basal autophagic protein profile in the BALB/c mice demonstrates dysregulation of the autophagic regulatory proteins, AMPK and AKT, which serve to stimulate and suppress autophagy simultaneously. We would expect that both processes operating simultaneously might result in a unique way of modulating autophagy to prevent "runaway" autophagy.

It should be noted that there are other examples of opposing trends in the expression of autophagy proteins that are observed when comparing young to aged BALB/c mice. For example, Atg7 is significantly increased in the young at 24 hrs and significantly decreased by 48 hrs in the aged. Since Atg7 is a protein used in both ubiquitin conjugation systems, specifically to process and guide the incorporation of LC3 into the autophagosomal membrane, it may be responsible for the decline in the relative

induction or magnitude of LC3-II relative to the young animals. In other words, Atg7 may be rate limiting in the aged BALB/c mice. Additionally, Atg5 is upregulated at both 24 and 48 hrs in the young, yet demonstrates no significant change in the aged. Again, this indicates a response to the fast in the young by promoting autophagosome formation, which is lacking in the aged, suggesting that Atg5 may be rate limiting as well. Since both Atg7 and Atg5 have roles in LC3 processing and autophagosome formation, the muted but significant induction of LC3-II in the aged relative to the young BALB/c mice may be attributed to those proteins. Finally, the autophagy protein expression includes LAMP2A, suggesting further age-related changes in the autophagy pathway upon fasting, though it is difficult to assign a functional significance to this difference.

The finding that neither carbonylated protein nor aggregate p62/ubiquitinated protein accumulated in the aged BALB/c mice is suggestive of sufficient autophagic flux. However, autophagic flux was not detected by chloroquine treatment following a 24 or 36 hr fast in young or old BALB/c mice. It is conceivable that flux is functioning below the detection threshold of the chloroquine assay.

In all, autophagy is manifest differently in C57BL/6 versus BALB/c mice. The BALB/c mice demonstrate a substantial dysregulation in aged basal autophagic protein profiles relative to the young. Additionally, the BALB/c mice demonstrate a difference in autophagy regulation with initiation and nucleation proteins relative to the C57BL/6 mice, which may account for the step-wise induction of LC3-II and a lack of detectible flux in both the young and old mice. It appears that autophagy is constitutive across age leading to the clearance of protein aggregates (via p62/SQSTM1) and the lack of

carbonylated proteins (indicating functional mitophagy and the clearance of ROS-damaged proteins).

Intermittent Fasting

Reports testing an intervention involving a series of repeated brief ischemic events, presumably to promote a sustained increase in autophagy proteins or flux, seems to be effective in limiting I/R-associated damage in the murine and rat heart in most cases[5,143]. Unfortunately, it is now known that the effects of ischemic preconditioning appear to be limited to the young[144] (reviewed in Wojtovich et al.)[145]. However, long-term dietary modifications, such as caloric restriction, have been shown to improve cardiac function (reviewed in Speakman et al.)[61]. Moreover, Abete and colleagues demonstrated that "physical activity or caloric restriction is partially capable to preserve the cardioprotective effect of ischemic preconditioning in the aging [human] heart.[146]" Additionally, it has been recently shown that the upregulation of mitophagy will minimize ROS damage by dysfunctional mitochondria[137].

If dietary restrictions can improve heart function in the aged[61,146] and AKT is known to be responsive to the metabolic/energetic state of the cell, then we thought that dietary restriction initiated in middle age (13 months of age) may reverse or partially reverse the observed age-related decline in autophagy. Therefore, C57BL/6 mice subjected to intermittent fasting gained weight relative to the AL group between weeks 2 and 6 (Figure 2.7 B) and at the point of maximal weight divergence between the AL and IF groups (3 weeks) there was a corresponding a two-fold increase in LC3-II (Figure 2.7 C). However, no differences in LC3-II or mouse weight at 6 and 16 weeks or autophagic

flux at 25 weeks (Figure 2.7 D) were observed between the AL or IF mice. These data taken together suggest a correlative relationship between weight and changes in the autophagy protein LC3-II. Although our results with dietary restriction in middle-aged animals are highly correlative, it is possible that a three week intermittent fasting regimen (where a two-fold increase in LC3-II was observed – Figure 2.7 C) could help upregulate mitophagy in the aged heart and combat ROS accumulation and the subsequent increase in cardiac basal inflammation. Consequently, when/if the ischemic event then occurs, the cells would be better protected against cardiac damage and dysregulated wound healing. Recent evidence suggests that over the short term, very short bouts of cardiovascular exercise (very slow running such as >10 minutes/mile) can protect the heart for up to five years[164], presumably by upregulating autophagy. We believe that if the intermittent fasting protocol were adapted to humans and performed periodically over the life of the individual, it may be sufficient to confer cardioprotection in the elderly if they have the appropriate autophagic disposition (see below).

Curiously, the BALB/c mice subjected to the same intermittent fasting profile as the C57BL/6 demonstrated a robust increase in LC3-II following 6.5 months of fasting (Figure 2.6 B). However, when the mice were sacrificed there were signs of rampant pathology (most likely cancer), specifically enlarged spleens and lymph nodes (splenomegaly and lymphadenopathy), and the tissues had to be discarded. This prompted the following question: “Can chronic modulation of autophagy via dietary modification promote cancer?”

There is evidence in the literature that suggests that the activation of the upstream autophagy regulatory protein AMPK can either prevent or promote tumorigenesis, depending on context (Reviewed in Faubert et al.)[153]. Additionally, it is well established that the upregulation of the AKT/PI3K pathway is associated with a large variety of cancers (Reviewed by Vara et al. and Davies)[154,155]. Additionally, a presentation at the 2014 Keystone Meeting Autophagy: Fundamentals to Disease in Austin, TX one presenter (could have been Dr. Kroemer) stated that treatment of mice with the known autophagy inducer, spermidine, protected mice from tumorigenesis; however, if spermidine treatment was initiated after tumorigenesis, cancer growth progressed very rapidly. Although at this point any association of the spleen and lymph node abnormalities with cancer and dysregulation of autophagy and its upstream regulators is highly anecdotal, we did observe some tantalizing clues that this may be the case.

We initiated the intermittent fasting protocol in middle aged BALB/c mice (13 months) and maintained it for more than 6.5 months. First, we know that at least initially the fasting promoted autophagy (Figure 2.2) in both young and aged animals and would expect in middle aged animals as well, but we would need to verify to be certain. Additionally, the aged BALB/c mice demonstrated a substantial dysregulation in the autophagy regulatory proteins as demonstrated by the upregulation of both the AMPK and AKT pathways relative to the young BALB/c and C57BL/6 (Figures 2.1). It is difficult to tell with certainty if this dual and dueling upregulation promotes or suppresses autophagy (the data suggests upregulates), but by having both pathways active the likelihood of developing cancer must certainly increase, a condition potentially verified

in all of our BALB/c mice at the study's terminal time point. The drastic increase in LC3-II at 6.5 months of intermittent fasting is an interesting observation. Upon gross analysis, the splenic and lymph node pathology was likely associated with white blood cells. Is it possible that the heart was responsive to the blood-borne cancer and upregulated autophagy, just like autophagy in the white blood cells is upregulated in response to cardiac stress (See Chapter III)? As stated before, the link between IF in the BALB/c mice and the possibility of developing cancers is highly correlative, but it bears further examination. This is important because autophagy researchers tend to think of autophagy upregulation as protective against age-related diseases. In Chapter I we found that the offspring of two autophagy-dissimilar mouse strains (C57BL/6 and BALB/c mice) demonstrated a unique basal autophagy protein profile relative to its parents. This prompted us to argue that autophagy profiles would be important metrics for determining personalized treatment methodologies for disease. If the autophagy profiles in the human are as varied as in the murine population, the above finding indicates that in some cases it may be possible to upregulate autophagy to prevent one disease while promoting another.

Chapter II, in part, is currently being prepared for submission for publication of this material. Gurney, M.A., Gottlieb, R.A., and Linton, P.J. The dissertation author was the primary investigator and author of this material.

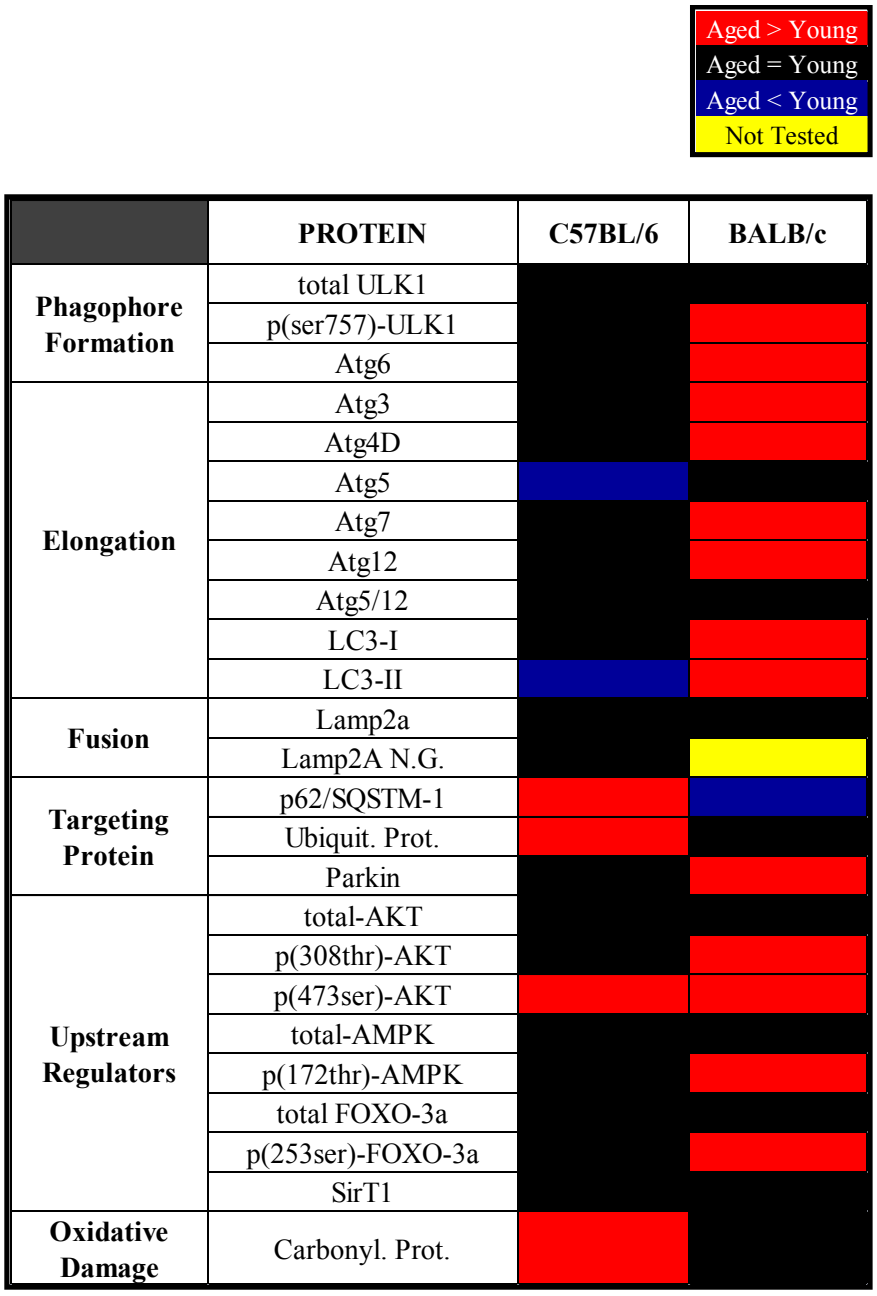

Figure 2.1: Autophagy Protein Expression in the Hearts of Aged vs. Young Mice. The expression of autophagy proteins and upstream regulators was determined in the hearts of 2.5-3 vs. 24-25 month old BALB/c and C57BL/6 (n=4) using the western blot protocol described in Common Methods. Additionally, the samples were subjected to the OxiSelect Protein Carbonyl Immunoblot Kit to determine relative carbonylated protein expression. Protein expression was normalized to its actin control and significance was established by $p<0.05$ using Student's T Test. A red, blue, or black cell indicates significantly greater protein expression in the aged vs. the young, the young vs. the aged, or no age-related difference in protein expression, respectively. Source data (original blots and graphs derived from ImageJ quantification) are found in Appendix 3.

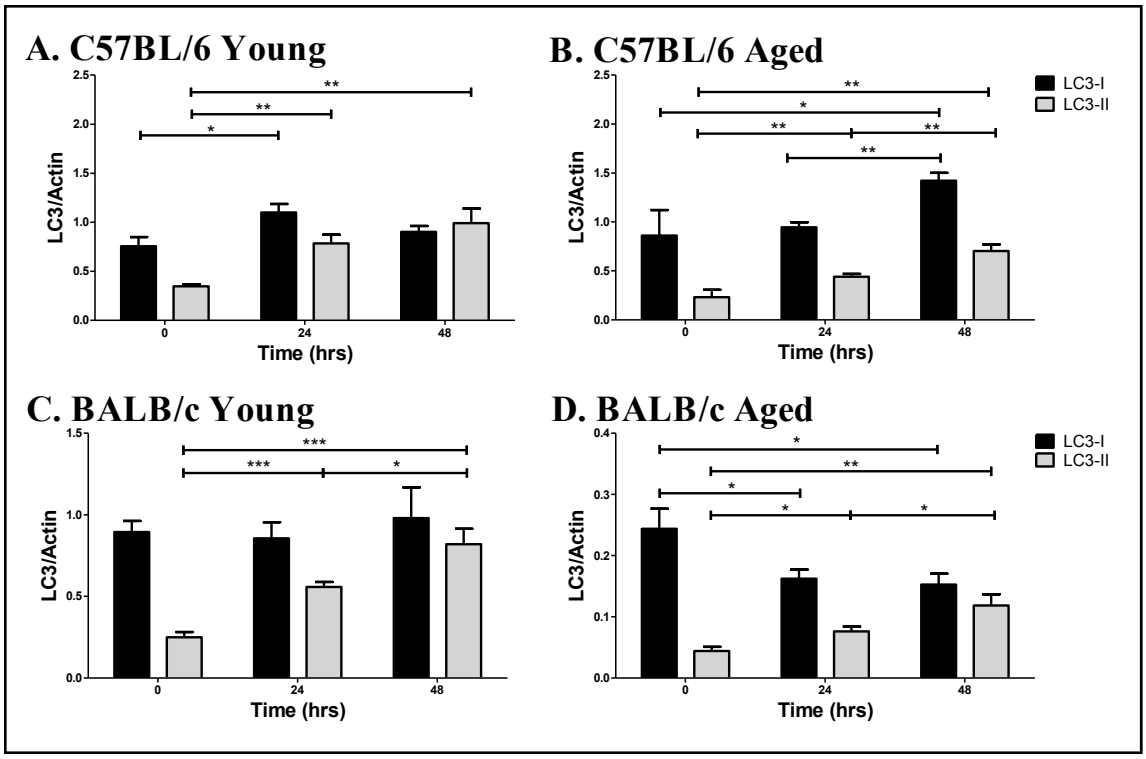

Figure 2.2: LC3 Profile in Fasting Young and Old C57BL/6 and BALB/c Mice. 3 and 18 mo C57BL/6 (panels A & B) or 3 and 24-25 mo BALB/c mice (panels C & D) were fasted for 0, 24, and 48 hrs. Hearts were harvested, homogenized, and lysed. 30 µg total protein was loaded onto a 4-20% Tris-HCl gel and transferred to a PVDF membrane. Blots were probed with rabbit anti-LC3AB antibody followed by goat anti-rabbit Ig, stripped, and reprobed with mouse anti-actin antibody followed by goat anti-mouse Ig. LC3-I and LC3-II are normalized to actin. Shown are the mean +/- SEM. Significance was determined using Student's T Test, with significance set at $0.01<p<0.05$, $0.001<p<0.01$, or $0.001<p<0.001$ are denoted by 1, 2, or 3 asterisks, respectively. Relative level of LC3 indicates the LC3/Actin ratio normalized to non-fasted controls. Source data (original blots) are found in Appendix 4.

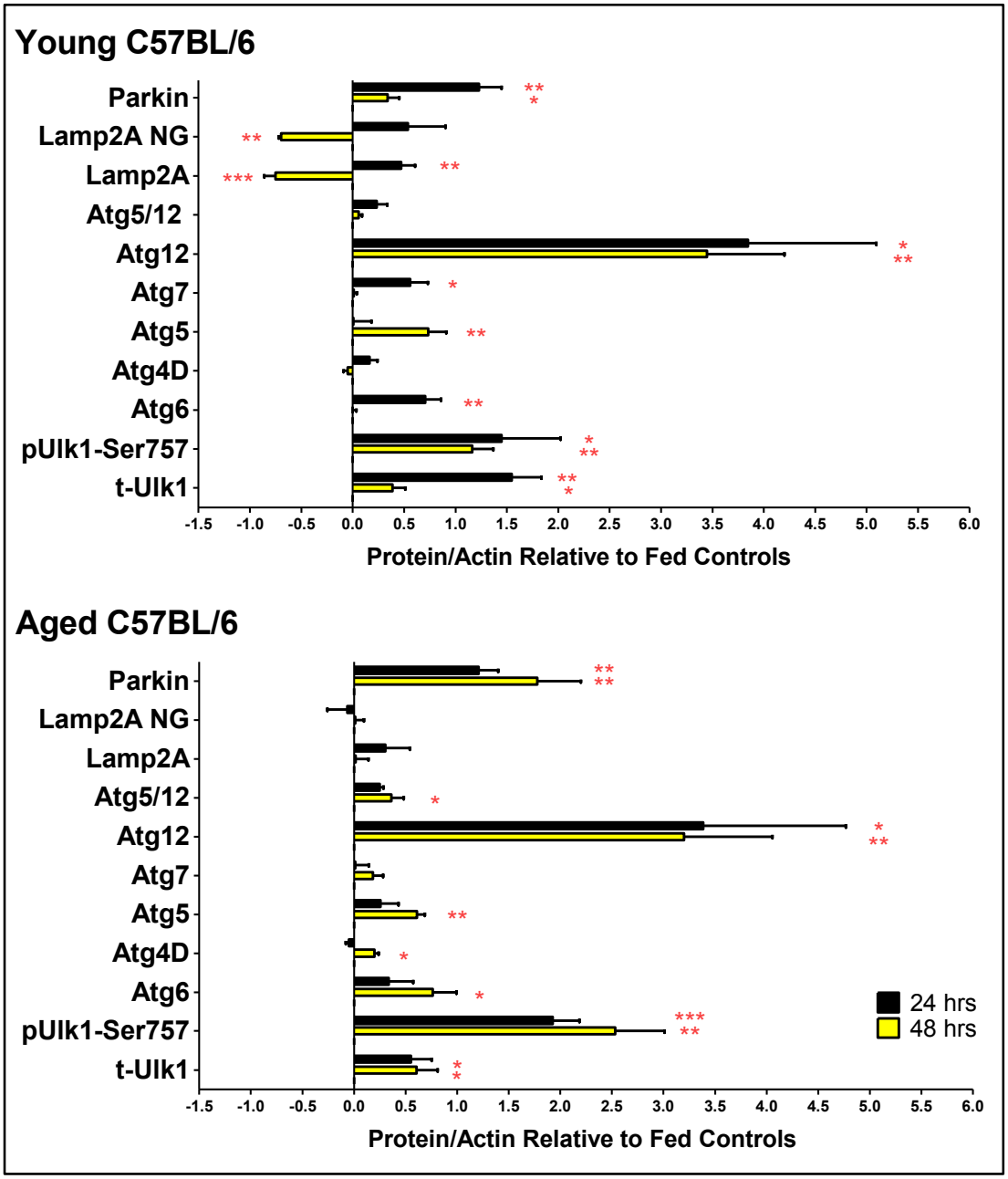

Figure 2.3: Autophagy Profile in Fasting Young and Old C57BL/6 Mice. 3 month old (top panel) and 18 month old (bottom panel) C57BL/6 were fasted for 0, 24, or 48 hrs. Autophagy protein levels were determined as described in Common Methods. Protein levels were normalized to their respective actin control and the values were adjusted so that the fed controls were set to "0.0". Shown are the mean +/- SEM. Significance was established by Student's T Test wherein fasted vs. non-fasted control were compared. ($0.01<p<0.05$, $0.001<p<0.01$, or $p<0.001$ are denoted by 1, 2, or 3 asterisks, respectively). Source data (original blots) are found in Appendix 4. [LAMP2A NG – non glycosylated form of LAMP2A].

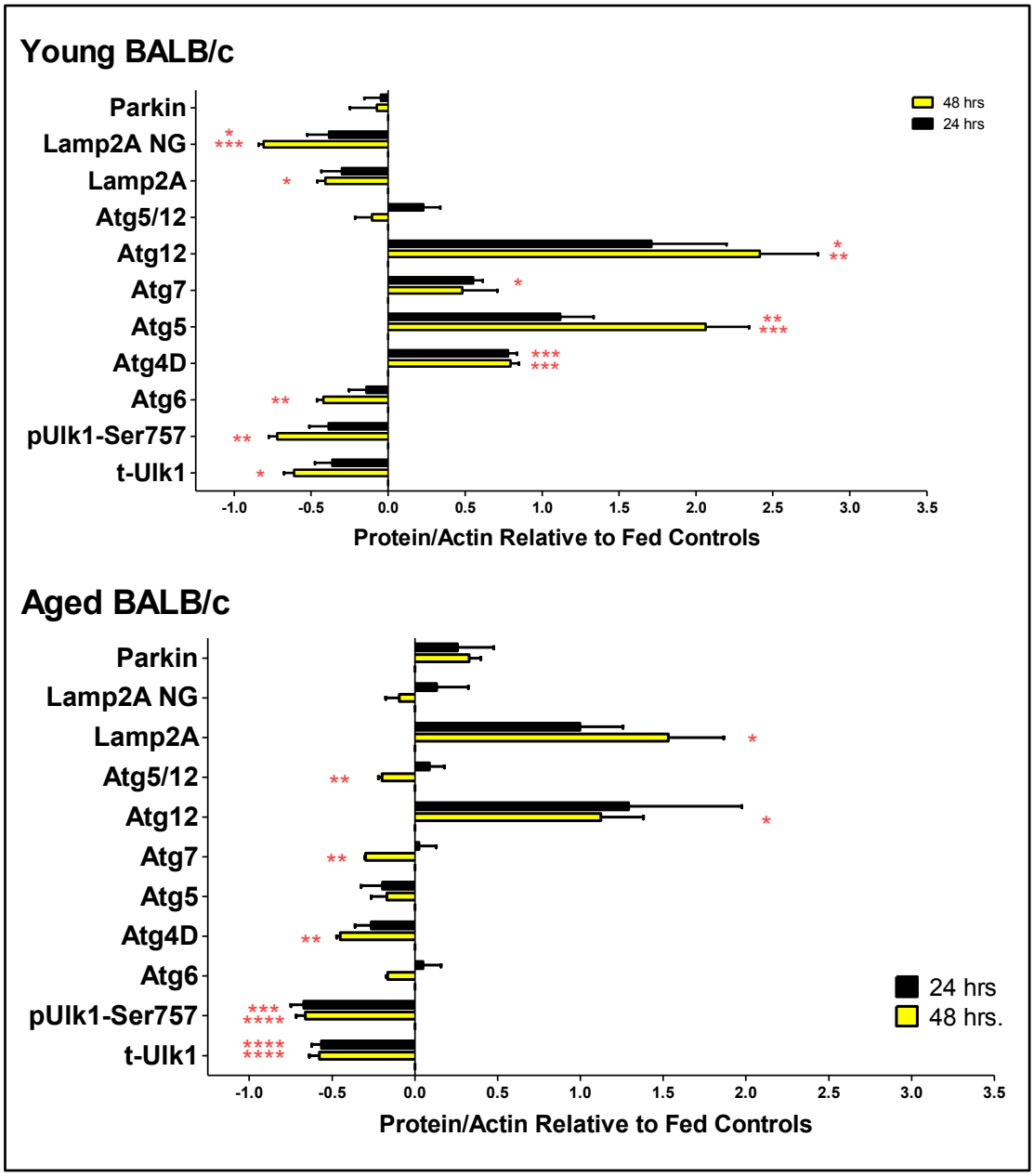

Figure 2.4: Autophagy Profile in Fasting Young and Old BALB/c Mice. 3 month old (top panel) and 18 month old (bottom panel) BALB/c were fasted for 0, 24, or 48 hrs. Autophagy protein levels were determined as described in Common Methods. Protein levels were normalized to their respective actin control and the values were adjusted so that the fed controls were set to "0.0". Shown are the mean +/- SEM. Significance was established by Student's T Test wherein fasted vs. non-fasted control were compared. ($0.01<p<0.05$, $0.001<p<0.01$, $0.0001<p<0.001$, or $p<0.0001$ are denoted by 1, 2, 3, and 4 asterisks, respectively). Source data (original blots) are found in Appendix 4. [LAMP2A NG – non glycosylated form of LAMP2A].

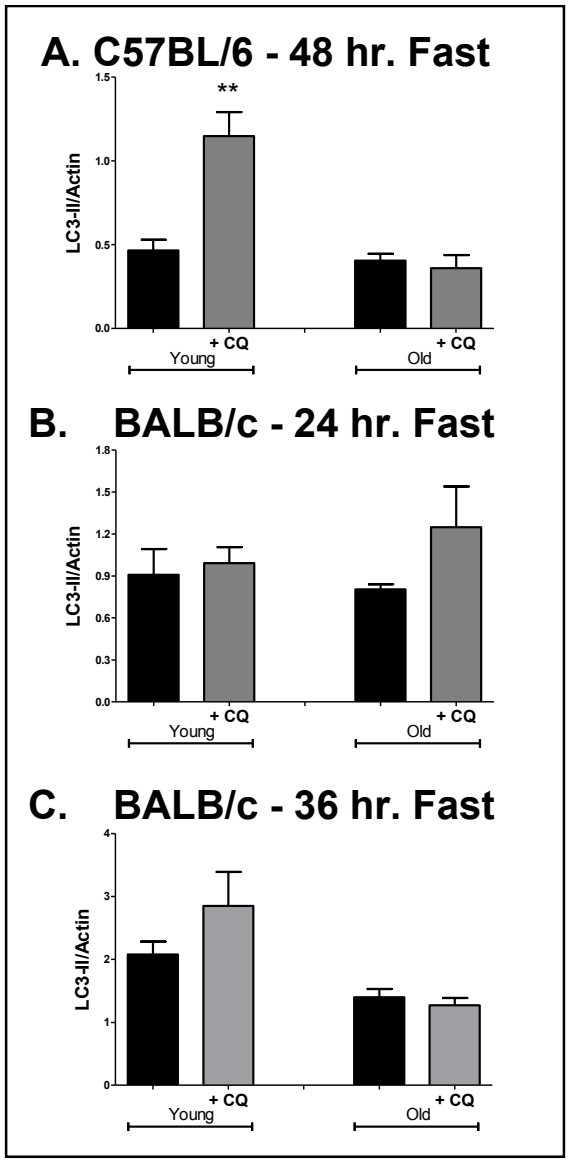

Figure 2.5: Autophagic Flux in Young and Aged C57BL/6 and BALB/c Mice Following a Fast. C57BL/6 mice were fasted for 48 hrs (3.5 and 24-25 months old – Panel A) and BALB/c mice were fasted for 24 or 36 hrs (Panel B. 3.5 and 19 months old for 24 hrs; Panel C. 4.5 and 21.5-22 mo for 36 hrs). Four hours prior to the termination of the fast, mice were injected i.p. with either 50 mg/kg chloroquine suspended in phosphate buffered saline or phosphate buffered saline as a control. Hearts were harvested, homogenized, and lysed. 30 μg of total protein was loaded onto a 10-20% Tris-HCl gel and transferred to a PVDF membrane. Blots were probed with rabbit anti-LC3AB antibody followed by goat anti-rabbit Ig, stripped, and reprobed with mouse anti-actin antibody followed by goat anti-mouse Ig. LC3-II was normalized to actin. Shown are the mean +/- SEM. Significance was determined using Student's T Test comparing chloroquine treated mice with respective untreated controls (**=$p<0.0025$); All other data are not significant). Source western blots are found in Appendix 5.

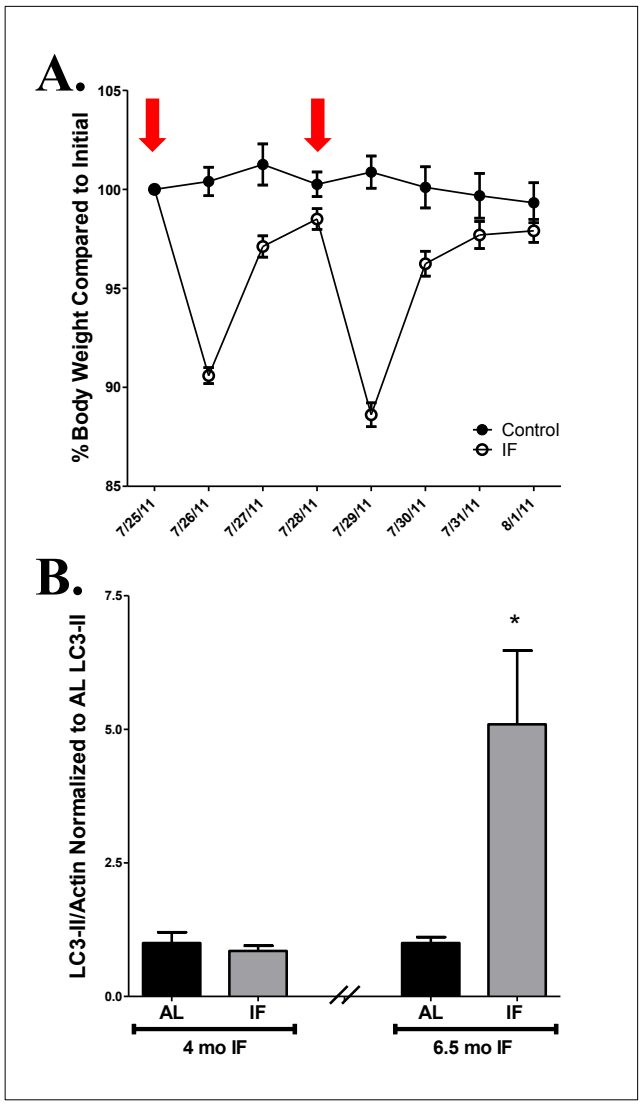

Figure 2.6: Intermittent Fasting with BALB/c Mice. 13 month old (middle aged) mice were subjected to a 24 hr fast twice a week, 5 PM to 5 PM for 4 or 6.5 months. A. Weights of IF (n=19) and AL mice (n=9) were measured in the morning and recorded daily for 8 days. Weight was graphed as the percent body weight compared to the initial weight for each mouse, with AL mice denoted by closed and the IF, mice as open circles. Red arrows denote the start of the fast. B. Following 4 or 6.5 months of IF mice were sacrificed 3 days following their last fast (n=3 AL control; n=5 IF mice). Hearts were harvested, homogenized, and lysed. 30 µg of total protein was loaded onto a 4-20% Tris-HCl gel and transferred to a PVDF membrane. Blots were probed with rabbit α-LC3AB and mouse α-β-actin. Protein expression was normalized to its actin control and relative expression to the non-fasted control is shown (mean +/- S.E.M.). Graph is a composite of two blots (separated by hash marks) with LC3-II for each IF time point normalized to its AL LC3-II counterpart. Significance was established by $p<0.05$ by Student's T Test relative to the AL control. $p<0.05$ is denoted by an asterisks. Source data (original blots) are found in Appendix 6.

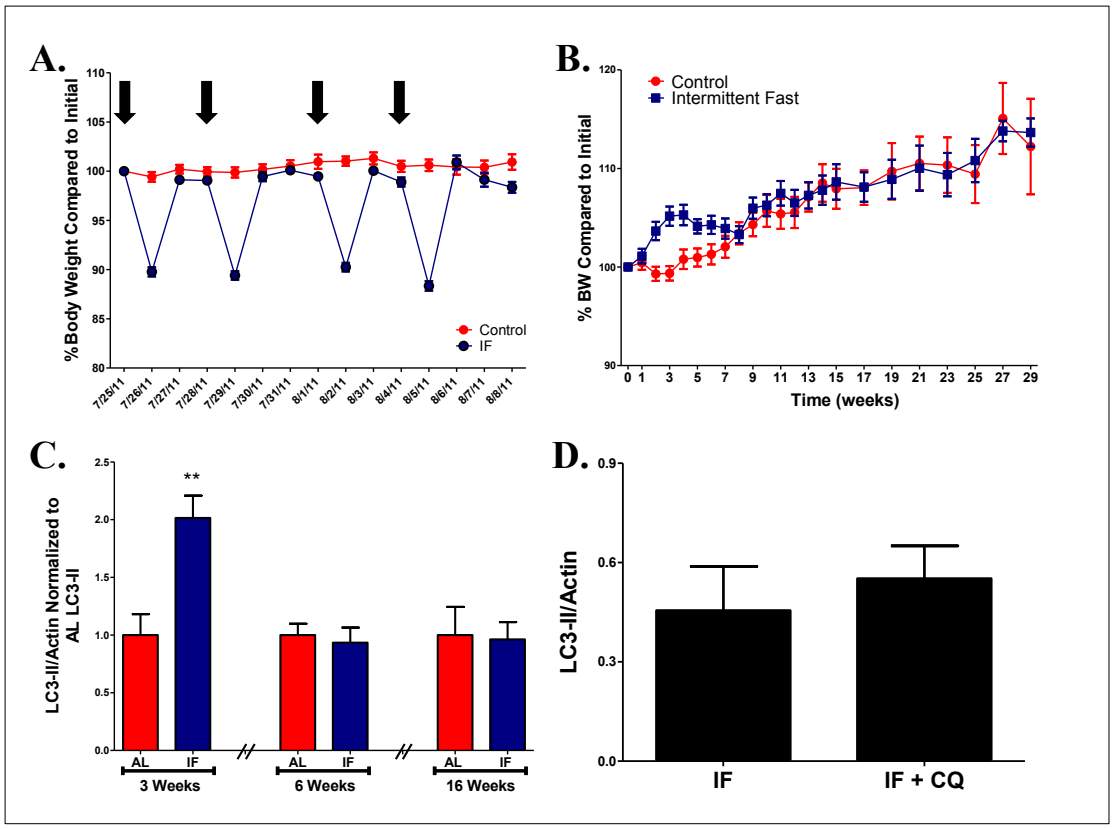

Figure 2.7: Intermittent Fasting with C57BL/6 Mice. 13 month old mice were subjected to a 24 hr fast twice a week, 5 PM to 5 PM for 6.7 months. A. Weights of IF (n=30) and control mice (fed ad librium, n=24) were measured in the morning and recorded daily for 15 days (week 6 through 8 of the 29 week study) (n=30/24 initially, but 5 from each group were removed for experiments prior to the end of the 15 days). Weight was graphed as the percent body weight compared to the initial weight for each mouse AL mice are denoted by red and the IF mice as blues circles. Black arrows indicate the start of a fast. B. Weights of AL (initial n=29; final n=9) and IF mice (initial n=35; final n=13) were recorded weekly for 15 weeks, then every two weeks until week 29. The reduction in n was due to the removal of mice for experimentation and not death by natural causes. Weight was graphed as the percent body weight compared to the initial weight for each mouse, with the control mice denoted by red and the IF mice as blue. C. Following a 3, 6, or 16 weeks of IF, mice were sacrificed 3 days following their last fast (n=5 AL and IF), hearts removed, and subjected to western blot. Graph is a composite of multiple blots (separated by hash marks) with LC3-II for each IF (blue) time point normalized to its AL (red) control. D. Following 25 weeks of IF, mice were fasted 24 hrs and injected with 50 mg/kg chloroquine or PBS i.p. to determine autophagic flux (n=4). 4 hrs later mice were sacrificed, hearts removed and subjected to western blot. Hearts were homogenized and lysed. 30 µg total protein was loaded onto a 4-20% Tris-HCl gel and transferred to a PVDF membrane and probed with rabbit α-LC3AB and mouse α-β-actin. Protein expression was normalized to its actin control. In panels C & D, the mean expression of LC3-II +/- S.E.M. are shown with $p<0.01$ denoted by two asterisk (Student's T Test) Source data (original blots) are found in Appendix 6.

CHAPTER III:

Development of a Fluorescence Based Autophagy Detection Protocol to Monitor Autophagy *in vitro* and *in vivo*

INTRODUCTION

A current obstacle to *in vivo* and *in vitro* high throughput autophagy studies is the lack of suitable tools to measure autophagy in a rapid, reproducible, and quantitative manor. Biochemical assays, such as western blot, are useful for characterizing autophagy in cells/tissues; however, harvesting the tissue used for analysis results in the death of the animal or would require repeated biopsies from human patients. Unfortunately, this makes longitudinal studies difficult, if not impossible, to perform. For example, studies looking at how or if autophagy has an impact on health or lifespan or how autophagy changes during long-term drug therapies or dietary modifications require repeated testing of the subject. Moreover, western blot analysis is both time and labor intensive and is relatively expensive, making western blot analysis impractical for use with high-throughput drug screens looking for autophagy modulating compounds. Finally, the translational applications of autophagy research are manifold, provided viable reagents are available for detecting and quantifying autophagy in living patients. Defects in autophagy have been implicated in a variety of diseases, including cancer, cardiovascular disease, Alzheimer's, metabolic disorders, inflammatory diseases, infection, developmental disorders, and so on.

As autophagy research transitions from basic science to drug design to translational applications such as diagnosis and development of treatment strategies, a reagent/methodology needs to be developed that can quickly and reliably quantitate autophagy in the hospital. In order to maximize marketability and standardize autophagosome counts and/or flux to specific disease states, finding a single, versatile

compound capable of detecting/quantifying autophagy on a variety of different platforms, plate reader (for *in vitro* drug screens), microscopy (basic science), and flow cytometry (clinical diagnosis and treatment *in vivo*) is desirable.

We sought to determine if AlexaFluor-488^{TM}-cadaverine plus spermidine (we coined the name Fluormidine for the combination) could be used to detect autophagy and be adapted for use in basic science, high throughput screening, and clinical applications. We have verified that the reagent responds appropriately to autophagy modulation stimulus in a variety of cell lines under a variety of conditions. Furthermore, we have demonstrated a loss of fluorescent puncta in autophagy deficient cells and have demonstrated putative co-localization between Fluormidine and the protein Rab9, which is active in the late endosomal and autophagosomal compartments.

Additionally, we tested Fluormidine in order to address the need for a reagent that can detect and quantitate autophagosomes for diagnostic, therapeutic, and *in vivo* research applications. Previous research has demonstrated that elderly patients with angina have lower levels of LC3-II in their cardiac tissue and blood cells than age-matched controls, indicating that peripheral blood sampling might reflect autophagic processes in other organs including the heart[156]. Thus, Fluormidine flow cytometry analysis of peripheral blood lymphocytes might serve as a surrogate indicator of autophagy in solid organs, such as the heart. Upon the injection of the autophagy inducing compound, rapamycin, we were able to detect an increase in Fluormidine staining of peripheral blood mononuclear cells by flow cytometry and a corresponding increase in LC3-II (a measure of autophagy) by western blot in male mice.

Finally, we adapted and optimized this protocol for work with a variety of detection equipment such as fluorescent and confocal microscopes, fluorescent plate readers, and flow cytometers, making Fluormidine a viable candidate to be developed as a tool to aide *in vivo* research, drug design, and in the clinic.

METHODS

Common Solutions

Norepinephrine Solution: 20 mL of ascorbic acid was prepared by dissolving 105.7 mg ascorbic acid in 20 mL water. 60 mg of norepinephrine bitartrate salt (Sigma-Aldrich, A0937-1G) was added to the 20 mL of ascorbic acid to yield a 10 mM stock. The solution is stored in aliquots at -20°C.

Gelatin-Fibronectin Solution: 0.02% Gelatin in water was prepared and autoclaved. 0.5 mL fibronectin was added to 99.5 mL of the gelatin solution and used to treat all tissue culture flasks. The solution is stored in aliquots at -20°C.

Krebs Starvation Buffer: Dissolve 1 vial Krebs-Henseleit (Sigma – K3753-10X1L), 2.1 g $NaHCO_3$, 2.4 g HEPES, and 0.373 g $CaCl_2$ in 0.950 L water. pH to 7.0, fill to 1L, and filter sterilize. Keep at 4°C for no longer than 1 month.

Complete Claycomb Media: 217.5 mL Claycomb Media (SAFC, 51800C-500ML), 10% Fetal Bovine Serum, 0.1 mM norepinephrine, 2 mM glutamine, and Anti-Anti [final concentration 100 U/mL Penicillin, 100 mg/mL Streptomycin, and 0.25 µg/mL Fungizone (Gibco, 15240-062)].

Complete RPMI Media: 1X RPMI-1640 (Gibco, 11875-093), 10% FBS, 2 mM glutamine, and 1X Anti-Anti [final concentration 100 U/mL Penicillin, 100 mg/mL Streptomycin, and 0.25 µg/mL Fungizone (Gibco, 15240-062)].

Complete DMEM Media: 1X DMEM Media (Gibco, 11885-084), 10% FBS, 2 mM glutamine, and 1X Anti-Anti [final concentration 100 U/mL Penicillin, 100 mg/mL Streptomycin, and 0.25 µg/mL Fungizone (Gibco, 15240-062)].

AlexaFluor-488™-cadaverine: AlexaFluor-488™-cadaverine (Life Technologies, A-30676) was resuspended in water to a stock concentration of 25 mM. Dye was aliquoted and kept in desiccant in the dark at -20°C.

Fluorescence and Confocal Microscopy

Nikon TE300 Fluorescent Microscope: Cells were imaged on a Nikon TE300 fluorescent microscope outfitted with a cooled charge-coupled device camera (Orca-ER, Hamamatsu), a Z-motor (ProScan II, Prior Scientific), an automated excitation/emission filter wheel controlled by a LAMBDA 10-2 (Sutter Instrument), and operated by MetaMorph 6.2 software (Molecular Devices Co.). Fluorescent images were captured with primary mirror/filter mirror set (Chroma, 61002) with the addition of excitation/emission filters (Chroma HQ480/x40 and D535/50m, respectively). Imaging conditions, exposure time and illumination, were held constant across samples within an experiment.

Fluorescent Microscopy: Zeiss Axio Observer D1 Fluorescent Microscope: Cells were imaged on a Zeiss Axio Observer D1 (Oberkochen, Germany) inverted fluorescent microscope with an attached Zeiss MRc camera. Imaging conditions, exposure time, and illumination were held constant across samples within an experiment.

Leica Sp2 Confocal Microscope: Cells were imaged on a Leica Sp2 Confocal Microscope (Wetzlar, Germany) outfitted with LAS AF software. Imaging conditions, exposure time, and illumination were held constant across samples within an experiment.

Maintaining the *in vitro* Cell Lines

HL-1 (AT-1 Mouse Atrial Cardiomyocyte Line): HL-1 cells were developed and maintained as previously described[157]. HL-1 cells we maintained in filter sterilized Complete Claycomb Media. T75 flasks (Corning Incorporated, 3526) were pre-treated with a gelatin-fibronectin solution for a minimum of 24 hrs prior to use. For passage, the cells were incubated in 5 mL pre-warmed 0.05% Trypsin-EDTA for 5 minutes (Gibco, 25300-054), incubated 5 min. at 37°C, diluted in 5 mL Complete Claycomb Media, and centrifuged for 5 minutes at 4°C. The cells were then resuspended in 10 mL Complete Claycomb Media and maintained at 37°C/5% CO_2 at 100% relative humidity in a T75 flask (Corning Incorporated, 3526) or used for experiments.

Jurkat Cells (Human T Cell Cancer Line): Cells were maintained in Complete RPMI Media. For passage, the cells non-adherent cells are collected, centrifuged at 1100 rpm, and resuspended in fresh complete media. The cells were then resuspended in 10-12 mL Complete RPMI Media and maintained at 37°C/5% CO_2 at 100% relative humidity in a T75 flask (Corning Incorporated, 3526) or used for experiments. The cells were seeded at 2 x 10^5 cells/mL and were considered confluent at 2 x 10^6 cells/mL.

J774 Cells (Mouse Monocyte/Macrophage Line): Cells (ATCC, Tib-67) are maintained in Complete DMEM Media. For passage, the cells non-adherent cells were

removed, leaving adherent cells. Adherent cells were scraped in the presence of Complete Media, centrifuged at 1100 rpm, and resuspended in fresh complete media. The cells were then resuspended in 10-12 mL Complete Media and maintained at 37°C/5% CO_2 at 100% relative humidity in a T75 flask (Corning Incorporated, 3526) or used for experiments.

Maintaining HEK293T Cells (Human Embryonic Kidney Line), NIH/3T3 (Mouse Fibroblast Line), and HeLa (Human Cervical Cancer Line): Cells (ATCC, CRL-11268 - HEK293T; CLR-1658 – NIH/3T3; CCL-2 - HeLa) are maintained in Complete DMEM Media. For passage, the cells were incubated in 5 mL pre-warmed 0.05% Trypsin-EDTA for 5 minutes (Gibco, 25300-054), incubated 5 min. at 37°C, diluted in 5 mL Complete Media, and centrifuged for 5 minutes at 4°C. The cells were then resuspended in 12 mL Complete Media and maintained at 37°C/5% CO_2 at 100% relative humidity in a T75 flask (Corning Incorporated, 3526) or used for experiments.

GFP-LC3 Adenovirus Transfection of HL-1 Cells

200,000 Hl-1 cells were plated on a 0.02% gelatin/fibronectin pre-treated 35 mm glass bottom culture dish (MatTek, P35G-1.5-14-C) and allowed to grow overnight to approximately 400,000 cells/dish at 37°C/5% CO_2. MatTek dishes were washed twice with 1.5 mL pre-warmed 2% FBS-Claycomb (217.5 mL Claycomb Media (SAFC, 51800C-500ML), 2% Fetal Bovine Serum, 0.1 mM norepinephrine, 2 mM glutamine, and 1X Anti-Anti [final concentration 100 U/mL Penicillin, 100 mg/mL Streptomycin, and 0.25 μg/mL Fungizone – Gibco, 15240-062]). 1 mL 2% FBS-Claycomb supplemented with GFP-LC3 Adenovirus (MOI of 10) was added to the cells and incubated at 37°C/5%

CO_2 for 3 hrs Cells were washed twice with Complete Claycomb Media and incubated 20 hrs in Complete Claycomb Media to allow cellular recovery/protein expression. Cells were washed 1-2 times with 2 mL pre-warmed Complete Media or Krebs Starvation Buffer. Cells were then incubated at 37°C/5% CO_2 for 3 to 4 hrs Cells were washed 1-2 times with 2 mL 1X PBS (Gibco, 14200-075) and fixed 15 min. in 4% paraformaldehyde/1X PBS at room temperature. Cells were washed once with room temperature 1X PBS. Coverslips (Fisher, 12-545-80) were mounted with 1 drop Aqua Poly/Mount (Polysciences Inc., 18606) placed in the center of the MatTek dish (Polysciences, 186-06-20). Cells were imaged using the Nikon TE300 fluorescent microscope.

AlexaFluor-488™ Time Course and Dose Response in HL-1 Cells

300,000 HL-1 cells were plated on a Gelatin-Fibronectin pre-treated 35 mm glass bottom culture dish (MatTek, P35G-1.5-14-C) and allowed to grow over night to approximately 500,000 cells. Cells were washed twice with pre-warmed Complete Claycomb Media (control cells) or Krebs Starvation Media. Cells were then incubated in Complete Claycomb Media or Krebs Starvation Buffer at 37°C/5% CO_2 for 4 hrs. Cells were quickly washed twice with pre-warmed 1% FBS in 1X PBS (Gibco, 14200-075). 1 mL pre-warmed Complete Claycomb or Krebs Starvation Buffer with 150 μM or 50 μM AlexaFluor-488™-cadaverine (Life Technologies, A-30676) was added and cells were incubated for either 20 or 60 minutes at 37°C. The cells were quickly washed twice with pre-warmed 1% FBS in 1X PBS and fixed with a 4% paraformaldehyde solution in 1X PBS for 15 minutes. Cells were again washed twice with 1X PBS. Coverslips (Fisher,

12-545-80) were mounted with 1 drop Aqua Poly/Mount (Polysciences Inc., 18606) placed in the center of the MatTek dish (Polysciences, 186-06-20). Cells were imaged using the Nikon TE300 fluorescent microscope.

Optimization of HL-1/AlexaFluor-488™-cadaverine with Polyamines

Cadaverine, Putrescine, Spermidine, and Spermine Treatments: 300,000 HL-1 cells were plated on a Gelatin-Fibronectin pre-treated 35 mm glass bottom culture dish (MatTek, P35G-1.5-14-C) and allowed to grow over night to approximately 500,000 cells at 37°C/5% CO_2. Cells were washed twice with pre-warmed Complete Claycomb Media (control cells) or Krebs Starvation Media. Cells were then incubated in Complete Claycomb Media or Krebs Starvation Buffer at 37°C for 4 hrs Cells were quickly washed twice with pre-warmed 1% FBS in 1X PBS (Gibco, 14200-075). 1 mL pre-warmed Complete Claycomb or Krebs Starvation Buffer with 50 μM AlexaFluor-488™-cadaverine (Life Technologies, A-30676), Hoechst 33342 (10 μM), and 20 or 50 μM cadaverine or putrescine was added and cells were incubated for 20 minutes at 37°C/5% CO_2. The cells were quickly washed twice with pre-warmed 1% FBS in 1X PBS and fixed with a 4% paraformaldehyde solution in 1X PBS for 15 minutes. Cells were again washed twice with 1X PBS. Coverslips (Fisher, 12-545-80) were mounted with 1 drop Aqua Poly/Mount (Polysciences Inc., 18606) placed in the center of the MatTek dish (Polysciences, 186-06-20). Cells were imaged using the Nikon TE300 fluorescent microscope.

Optimization of Polyamine Inhibitors in 96 Well MatTek Plates

Pretreated 96 well MatTek plate with 80 µL 0.02% gelatin/0.5% fibronectin was incubated over night at 37°C/5% CO_2. 5000 HL-1 cells in Complete Claycomb Media were seeded into each well and incubated over night at 37°C/5% CO_2. Each well was washed twice with 200 µL 1%FBS in 1X PBS (Gibco, 14200-075). 200 µL Complete Claycomb or Krebs Starvation Media was added to each well and incubated at 37°C/5% CO_2 for 4 hrs Cells were carefully washed twice with Complete Claycomb or Krebs Starvation Buffer and incubated in Complete Claycomb or Krebs Starvation Buffer supplemented with 50 or 100 µM AlexaFluor-488™-cadaverine and 100, 75, 50, 25, and 10 µM polyamine (cadaverine, putrescine, spermidine, or spermine). Cells were observed using the Nikon TE300 fluorescent microscope.

HL-1/AlexaFluor-488™-cadaverine Time Course with Spermidine

HL-1 cells were plated on a 0.02% gelatin/0.5% fibronectin pre-treated coverslip (Fisher Scientific, 12-545-80) overnight in a 24 well plate (Corning Incorporated, 3526) at 37°C/5% CO_2. The cells were washed with Complete Claycomb Media or Krebs Starvation Buffer. Complete Media or Krebs Starvation Buffer was added and the cells were incubated 4 hrs at 37°C/5% CO_2. 15 minutes prior to the end of the assay, 50 µM AlexaFluor-488™-cadaverine (Life Technologies, A-30676) and 25 µM spermidine were added and cells were incubated for 2.5, 5, 7.5, 10, or 15 minutes at 37°C. The cells were washed twice with PBS (Gibco, 14200-075), fixed with a 4% paraformaldehyde solution in 1X PBS for 15 minutes, washed twice with 1X PBS, and mounted with Prolong Gold

Anti-Fading Reagent (Life Technologies, P36930) on glass slides (Fisher Scientific, 12-550-15). The slides were imaged using the TE300 fluorescent microscope.

Comparison of Monodansylcadaverine and Fluormidine

Approximately 1-2 x 10^5 HL-1 cells/well were plated into 0.02% gelatin/0.5% fibronectin pre-treated coverslips (Fisher Scientific, 12-545-80) overnight in a 24 well plate (Corning Incorporated, 3526) maintained at 37°C/5% CO_2. The cells were washed three times with Complete Claycomb Media or Krebs Starvation Buffer. Complete Media or Krebs Starvation Buffer was added and the cells were incubated 4 hrs at 37°C/5% CO_2.

AlexaFluor-488™-cadaverine or Fluormidine: 15 minutes prior to end of assay 50 µM AlexaFluor-488™-cadaverine was added. 5 minutes prior to assay end, 25 µM spermidine was added to half of the samples. 1:1000 Hoechst 33342 was added to all of the samples. The cells were washed three times with 1X PBS (Gibco, 14200-075) and incubated in 4% paraformaldehyde 15 minutes at room temperature. The cells were washed twice in 1X PBS (Gibco, 14200-075) and mounted with Prolong Gold Anti-Fading Reagent (Life Technologies, P36930) on glass slides (Fisher Scientific, 12-550-15). The slides were imaged using the Zeiss Axio Observer D1 fluorescence microscope.

Monodansylcadaverine: 15 minutes prior to end of assay 50 or 100 µM (2 or 4 µL of a 25 mM stock) Monodansylcadaverine (Sigma-Aldrich, D4008-1G) was added. 5 minutes prior to assay end, 1:1000 Hoechst 33342 was added to the samples. The cells were washed three times with 1X PBS (Gibco, 14200-075) and incubated in 4%

paraformaldehyde for 15 minutes at room temperature. The cells were washed twice in 1X PBS (Gibco, 14200-075) and mounted with Prolong Gold Anti-Fading Reagent (Life Technologies, P36930) on glass slides (Fisher Scientific, 12-550-15). The slides were imaged using the Zeiss Axio Observer D1 fluorescence microscope (See Above).

HeLa, HEK293T, and NIH/3T3 Cells Starved and Labeled with Fluormidine*

Approximately 5 x 10^4 and 1 x 10^5 HL-1 cells/well were plated on coverslips (Fisher Scientific, 12-545-80) overnight in a 24 well plate (Corning Incorporated, 3526) maintained at 37°C/5% CO_2. The cells were washed three times with Complete Claycomb Media or Krebs Starvation Buffer. Complete Media or Krebs Starvation Buffer was added and the cells were incubated 2 or 4 hrs at 37°C/5% CO_2. 15 minutes prior to end of assay 25 μM AlexaFluor-488™-cadaverine was added. 5 minutes prior to assay end, 25 μM spermidine and 1:1000 Hoechst 33342 were added to all of the samples. The cells were washed twice with 1X PBS (Gibco, 14200-075) and incubated in 4% paraformaldehyde 15 minutes at room temperature. The cells were washed three times in 1X PBS (Gibco, 14200-075) and mounted with Aqua/Poly Mount (Polysciences, 18606) on glass slides (Fisher Scientific, 12-550-15). The slides were imaged using the Zeiss Axio Observer D1 fluorescence microscope.

*These assays were done with 25 μM AlexaFluor-488-™-cadaverine, instead of the 50 μM typically associated with Fluormidine.

HeLa, HEK293T, and NIH/3T3 Treatment with Chloramphenicol and Fluormidine Labeling*

Approximately 5 x 10^4 HeLa or HEK293T cells/well were plated on coverslips (Fisher Scientific, 12-545-80) overnight in a 24 well plate (Corning Incorporated, 3526) maintained at 37°C/5% CO_2. The cells were washed three times with Complete DMEM Media or Krebs Starvation Buffer. Complete DMEM Media supplemented with 30 μM Chloramphenicol (100mM stock in DMSO) or an equivalent amount of DMSO (control cells) was added and the cells were incubated 1, 2, or 3 hrs at 37°C/5% CO_2. 15 minutes prior to end of assay 25 μM AlexaFluor-488™-cadaverine was added. 5 minutes prior to assay end, 25 μM spermidine and 1:1000 Hoechst 33342 were added to all of the samples. The cells were washed twice with 1X PBS (Gibco, 14200-075) and incubated in 4% paraformaldehyde 15 minutes at room temperature. The cells were washed three times in 1X PBS (Gibco, 14200-075) and mounted with Aqua/Poly Mount (Polysciences, 18606) on glass slides (Fisher Scientific, 12-550-15). The slides were imaged using the Zeiss Axio Observer D1 fluorescence microscope.

*These assays were done with 25 μM AlexaFluor-488-™-cadaverine, instead of the 50 μM typically associated with Fluormidine.

Transient Transfection of HL-1 Cells with mCherry-Atg5-K130R

pmCherry-C1 and the autophagy deficient mutant mCherry-Atg5-K130R plasmids (Clonetech, PT3975 Cat# 632524) were transformed into HL-1 cells. 2 x 10^5 cells were plated on pre-treated 0.02% gelatin/0.5% fibronectin coverslips (Fisher

Scientific, 12-545-80) overnight at 37°C/5% CO_2. The HL-1 cells were transfected using the Effectine Transfection Reagent Kit (Qiagen, 301427) for 6 hrs. The transfection media was removed, replaced with Complete Claycomb Media, and the cells were incubated overnight at 37°C/5% CO_2. The following morning, the cells were first washed in and then incubated in Complete Claycomb or Krebs Starvation Buffer for 4 hrs Fifteen minutes prior to end of assay 50 μM AlexaFluor-488™-cadaverine was added. 5 minutes prior to assay end, 25 μM spermidine was added to the cells in addition to 1:1000 Hoechst 33342. The cells were washed two-three times with 1X PBS (Gibco, 14200-075) and incubated in 4% paraformaldehyde for 15 minutes at room temperature. The cells were washed three times in 1X PBS (Gibco, 14200-075) and mounted with Prolong Gold Anti-Fading Reagent (Life Technologies, P36930) on glass slides (Fisher Scientific, 12-550-15). The slides were imaged using the Zeiss Axio Observer D1.

HL-1 Cell Treatment with Chloramphenicol and Fluormidine

Plated approximately 5 x 10^5 HL-1 cells/well into 0.02% gelatin/0.5% fibronectin pre-treated coverslips (Fisher Scientific, 12-545-80) overnight in a 24 well plate (Corning Incorporated, 3526) maintained at 37°C/5% CO_2. The cells were washed three times with Complete Claycomb Media or Krebs Starvation Buffer supplemented with either 300 μM or 30 μM chloramphenicol (Sigma-Aldrich, C0378-5G -- dissolved in absolute ethanol) or an equivalent volume of ethanol (control cells) and incubated 2, 4, or 6 hrs at 37°C/5% CO_2. 15 minutes prior to end of assay 50 μM AlexaFluor-488™-cadaverine was added. 5 minutes prior to assay end, 25 μM spermidine was added to the cells. The cells were washed three times with 1X PBS (Gibco, 14200-075) and incubated in 4%

paraformaldehyde for 15 minutes. The cells were washed once in 1X PBS (Gibco, 14200-075) and mounted with Prolong Gold Anti-Fading Reagent (Life Technologies, P36930) on glass slides (Fisher Scientific, 12-550-15). The slides were imaged using the TE300 fluorescent microscope.

J774 Cell Treatment with Chloramphenicol and Fluormidine

Plated approximately 1 x 10^5 HL-1 cells/well into 0.02% gelatin/0.5% fibronectin pre-treated coverslips (Fisher Scientific, 12-545-80) overnight in a 24 well plate (Corning Incorporated, 3526) maintained at 37°C/5% CO_2. The cells were washed three times with Complete Media or Krebs Starvation Buffer supplemented with either 300 μM/30 μM chloramphenicol (Sigma-Aldrich, C0378-5G -- dissolved in DMSO) or an equivalent volume of DMSO (control cells) and incubated 1, or 2 hrs at 37°C/5% CO_2. 15 minutes prior to end of assay 50 μM AlexaFluor-488™-cadaverine was added. 5 minutes prior to assay end, 25 μM spermidine was added to the cells. The cells were washed twice with 1X PBS (Gibco, 14200-075) and incubated in 4% paraformaldehyde for 15 minutes. The cells were washed twice in 1X PBS (Gibco, 14200-075) and mounted with Prolong Gold Anti-Fading Reagent (Life Technologies, P36930) on glass slides (Fisher Scientific, 12-550-15). The slides were imaged using the TE300 fluorescent microscope.

Starved J774 Cell Labeling with Fluormidine

Plated approximately 1 x 10^5 HL-1 cells/well into 0.02% gelatin/0.5% fibronectin pre-treated coverslips (Fisher Scientific, 12-545-80) overnight in a 24 well plate (Corning Incorporated, 3526) maintained at 37°C/5% CO_2. The cells were washed three times

with Complete Claycomb Media or Krebs Starvation Buffer and incubated 2, 4, or 6 hrs at 37°C/5% CO_2. 15 minutes prior to end of assay 50 μM AlexaFluor-488™-cadaverine was added. 5 minutes prior to assay end, 25 μM spermidine was added to the cells. The cells were washed twice with 1X PBS (Gibco, 14200-075) and incubated in 4% paraformaldehyde for 15 minutes. The cells were washed twice in 1X PBS (Gibco, 14200-075) and mounted with Prolong Gold Anti-Fading Reagent (Life Technologies, P36930) on glass slides (Fisher Scientific, 12-550-15). The slides were imaged using the TE300 fluorescent microscope.

Colocalization Experiment: LysoTracker Red and Fluormidine

Coverslips (Fisher Scientific, 12-545-80) were pretreated overnight with 0.02% gelatin/0.5% fibronectin in a 24 well plate (Corning, 3526) at 37°C/5% CO_2. 300,000-400,000 HL-1 cells were plated overnight on the coated coverslips at 37°C/5% CO_2. Cells were washed three times with 1 mL Complete Claycomb or Krebs Starvation Media. 1 mL Complete Claycomb or Krebs Starvation Media was added and the cells were incubated 4 hrs at 37°C/5% CO_2. The media was supplemented with 50 μM AlexaFluor-488™-cadaverine, 25 μM spermidine, and/or 1:1000 LysoTracker Red (Molecular Probes, L7528) for 10 minutes prior to the end of the assay. Cells were washed three times with 1% FBS in 1X PBS (Gibco, 14200-075). Cells were fixed in 1 mL 4% paraformaldehyde and incubated at room temperature or 10 minutes. The cells were then washed twice with 1X PBS. Coverslips were then mounted on slides (Fisher Scientific, 12-550-15) using VectaShield (Vector Laboratories, H-1000) and sealed with nail polish. Images were obtained using the Leica Sp2 Confocal.

Colocalization of Autophagy-Related Proteins and Fluormidine

Approximately 1 x 10^5 HL-1 cells/well were plated onto 0.02% gelatin/0.5% fibronectin pre-treated coverslips (Fisher Scientific, 12-545-80) overnight in a 24 well plate (Corning Incorporated, 3526) maintained at 37°C/5% CO_2. The cells were washed three times with Complete Claycomb Media or Krebs Starvation Buffer and incubated 4 hrs at 37°C/5% CO_2. 15 minutes prior to end of assay 50 µM AlexaFluor-488™-cadaverine was added. 5 minutes prior to assay end, 25 µM spermidine was added to the cells in addition to 1:1000 Hoechst 33342. The cells were washed two-three times with 1X PBS (Gibco, 14200-075) and incubated in 4% paraformaldehyde for 15 minutes at room temperature. Cells were again washed with 1X PBS and then incubated in 5% goat serum in 1X PBS for approximately 1-2 hrs at room temperature. Cells were washed three times with 1X PBS. Antibody of interest was diluted in 1X PBS (See Table 4 for dilutions used in the course of these experiments), 1% Bovine Serum Albumin, and 0.3% Triton-X 100 overnight at 4°C. Coverslips were washed in 1X PBS for 15 minutes. 2 µg of a goat-anti-rabbit-AlexaFluor-647™ (Life Technologies, A21244) or goat-anti-mouse-AlexaFluor-647™ (Life Technologies, 21235) diluted in 200 µL 1X PBS containing 1% Bovine Serum Albumin and 0.3% Triton-X 100 was applied to each slide for 2 hrs at room temperature, washed three times in 1 mL 1X PBS for 15 minutes, and mounted on slides (Fisher Scientific, 12-550-15) using Prolong Gold Anti-Fading Reagent (Life Technologies, P36930). Slides were saved at 4°C until they could be imaged on the Leica Sp2 Confocal Microscope (See Above) or by the Zeiss Axio Observer D1 fluorescent microscope.

Fluormidine Colocalization with Rab9: Approximately 5 x 10^4 HL-1 cells/well were plated onto 0.02% gelatin/0.5% fibronectin pre-treated coverslips (Fisher Scientific, 12-545-80) in a 24 well plate (Corning Incorporated, 3526) maintained overnight at 37°C/5% CO_2. The cells were washed three times with Complete Claycomb Media or Krebs Starvation Buffer and incubated 1, 2, 3, 4, or 5 hrs at 37°C/5% CO_2. 15 minutes prior to end of assay, 25 μM AlexaFluor-488™-cadaverine was added. 5 or 15 minutes prior to assay end, 10, 25, 50 or 75 μM spermidine was added to the cells in addition to 1:1000 Hoechst 33342. The cells were washed three times with 1X PBS (Gibco, 14200-075) and incubated in 4% paraformaldehyde in 1X PBS for 15 minutes at room temperature. Cells were again washed with 1X PBS for 20 minutes and washed three times for 5 minutes in 1X PBS. The cells were incubated in 5% goat serum in 1X PBS for 2 hrs at room temperature. Cells were washed three times with 1X PBS. 1:250 dilution of Rab9 antibody (See Table 4) diluted in 1X PBS, 1% Bovine Serum Albumin, and 0.3% Triton-X 100 overnight at 4°C. Coverslips were washed in 1X PBS for 3x5 minutes. 1 μg/mL of a goat-anti-rabit-AlexaFluor-647™ (Life Technologies, A21244) or goat-anti-mouse-AlexaFluor-647™ (Life Technologies, 21235) diluted in 200 μL 1X PBS containing 1% Bovine Serum Albumin and 0.3% Triton-X 100 was applied to each slide for 90 minutes at room temperature, washed three times in 1 mL 1X PBS for 5 minutes, and mounted on slides (Fisher Scientific, 12-550-15) using Aqua Poly/Mount (Poly Sciences Inc., 18606). Slides were saved at 4°C until they could be imaged on the Zeiss Axio Observer D1 fluorescent microscope.

Fluormidine Treatment of Starved Jurkat Cells

1.5 x 10^5 Jurkat cells (ATCC, CRL-2063) in 500 µL Complete RPMI Media or Krebs Starvation Buffer in a 48 well plate (Corning Incorporated, 3548). 5 µM Rapamycin (CalBioChem, 553210) was added to appropriate wells. The cells were incubated for 4 hrs at 37°C/5% CO_2. 15 minutes prior to end of assay 50 µM AlexaFluor-488™-cadaverine was added. 5 minutes prior to assay end, 25 µM spermidine was added to the cells in addition to 1:1000 Hoechst 33342. Cells were aspirated from well and centrifuged 7 minutes at 1400 rpm; media was aspirated and cells were washed/resuspended in 350 µL 1X PBS (Gibco, 14200-075), and placed on a Shandon Cytospin 3 (Waltham, MA) at 800 rpm for 6 minutes. Slides were immersed in 4% paraformaldehyde in 1X PBS for 10 minutes. Slides were rehydrated overnight in 1X PBS at room temperature and mounted with VectaShield Hardset Mounting Medium (Vector Laboratories, H-1400). Cells were imaged with TE300 Fluorescent Microscope.

Fluormidine Labeling of Lymph Node-Derived Lymphocytes

Lymph nodes were isolated from a euthanized 3 month old male C57BL/6 mouse and homogenized in 2-3% FBS in RPMI supplemented with 25 mM HEPES. The cell suspension was split (750,000 cells in 500 µL media per well in a 48 well plate (Corning Incorporated, 3548)), and placed in either Complete Media (10% FBS, 1X Glutamine, and 25 mM HEPES in 1X RPMI) or Krebs Starvation Buffer with or without 5 µM Rapamycin (CalBioChem, 553210). The cells were incubated 4 or 6 hours at 37°C/5% CO_2. 15 minutes prior to end of assay 50 µM AlexaFluor-488™-cadaverine was added. 5 minutes prior to assay end, 25 µM spermidine was added to the cells in addition to

1:1000 Hoechst 33342. Cells were aspirated from well, centrifuged 7 minutes at 1400 rpm, the media was aspirated, and the cells were washed/resuspended in 400 μL 1X PBS (Gibco, 14200-075), and placed on cytospin at 800 rpm for 6 minutes. Slides were immersed in 4% paraformaldehyde in 1X PBS for 10 minutes. Slides were rehydrated overnight in 1X PBS at room temperature, then mounted with VectaShield Hardset Mounting Medium (Vector Laboratories, H-1400). Cells were imaged with TE300 Fluorescent Microscope.

FACS Analysis of HL-1 and Jurkat Cells treated with Fluormidine

Jurkat cells and HL-1 cells were plated at approximately 10^5 cells and incubated overnight at 37°C/5% CO_2. The cells were washed in Complete Media or Krebs Starvation Buffer and starved for 2 (Jurkat Cells) or 4 (HL-1 Cells) hrs. 15 minutes prior to end of assay 50 μM AlexaFluor-488™-cadaverine was added. 5 minutes prior to assay end, 25 μM spermidine was added to the cells in addition to 1:1000 Hoechst 33342.

Jurkat cells were centrifuged at 1400 rpm for 7 minutes to pellet cells, washed twice with 1X PBS (Gibco, 14200-075), and fixed in 4% paraformaldehyde/1X PBS solution for 10-15 minutes. The cells were then washed once in 1X PBS and resuspended in a 1% BSA/1X PBS solution. The cells were run on a FACS Aria 2 (Becton Dickinson, Franklin Lakes, NJ) – FITC vs. Pacific Blue.

HL-1 cells were scraped, collected, and centrifuged at 1100 rpm for 5 minutes to pellet cells, washed twice with 1X PBS (Gibco, 14200-075), and fixed in 4% paraformaldehyde/1X PBS solution for 10-15 minutes. The cells were then washed once

in 1X PBS and resuspended in a 1% BSA/1X PBS solution. The cells were run on a FACS Aria 2 (Becton Dickinson, Franklin Lakes, NJ) – FITC vs. Pacific Blue.

Detecting Autophagy *ex vivo* using Rapamycin and Chloroquine with Fluormidine

Young male C57BL/6 mice were injected with the following: 5 mg/kg rapamycin solution in vehicle (5% PEG/5% Tween-80 in 200 µL 1X PBS), 5 mg/kg rapamycin solution in vehicle and 60 mg/kg chloroquine diphosphate (n=1 mouse each condition), or vehicle alone. In a second assay 2 female C57BL/6 mice were subjected solely to the aforementioned rapamycin and vehicle control conditions (total of 6 mice).

4.5 hours later (4 hours with female mice) the mice were sacrificed and the heart and blood were removed. The hearts were frozen in liquid nitrogen for western blot analysis (See Common Methods) and the blood was placed in a heparinized tube. 450 µL of Hank's Balanced Salt Solution (HBSS) was added to 50 µL of blood (n=3 blood samples per condition; 0, 25, or 50 µM AlexaFluor-488^{TM}-cadaverine). 0.25 µg of APC-α-mouse CD3ϵ (T Cells; BioLegend, 100311), PE-α-mouse CD11b (Macrophages; BioLegend, 101207), and PerCP-α-mouse CD19 (B Cells; BioLegend, 115531) were added to each sample. 0, 25, or 50 µM AlexaFluor-488^{TM}-cadaverine was added and incubated in the dark on ice for 15 minutes and 25 µM spermidine for 5 minutes, centrifuged 1300 rpm for 7 minutes, and washed in 1 mL 1X PBS (Gibco, 14200-075). The cells were resuspended in 4% paraformaldehyde in 1X PBS for 15 minutes at room temperature in the dark. The cells were centrifuged at 1300 rpm for 7 minutes, washed in 1X PBS, and resuspended in 1% FBS in 1X HBSS. The cells were run on an Accuri C6 Flow Cytometer (BD Biosciences, Franklin Lakes, NJ).

Rapamycin Solution: The rapamycin solution was made and administered as previously described[158]. Briefly, 5 mg rapamycin (LC Laboratories, R-5000) was dissolved in absolute ethanol to a concentration of 20 mg/mL. The rapamycin solution was diluted 1:25 in a 5% PEG-400/5% Tween-80 solution and injected at 5 mg/kg intraperitoneally.

Chloroquine Solution: A 10 mg/mL solution of chloroquine diphosphate (Sigma-Aldrich, C6628-100G) was prepared fresh in 1X PBS (Gibco, 14200-075) and filter sterilized. Syringes were then prepared with the chloroquine diphosphate stock diluted in sterile 1X PBS to administer 60 mg chloroquine per kg body weight in a 200 µL injection or 1X PBS as a vehicle control.

Visualizing Autophagy in HL-1 Cells Using a Spectrofluorometer

2 x 10^5 cells were plated in a 0.02% gelatin/0.5% fibronectin pre-treated 60 mm dishes (BD Falcon, 353003) and incubated overnight at 37°C/5% CO_2. The cells were washed three times with Complete Claycomb Media or Krebs Starvation Buffer and incubated 4 hrs at 37°C/5% CO_2. 15 minutes prior to end of assay 25 or 50 µM AlexaFluor-488™-cadaverine was added. 5 minutes prior to assay end 25 µM spermidine was added to the cells in addition to 1:1000 DAPI (1 mg/mL stock). The cells were washed twice with 1X PBS (Gibco, 14200-075) and scraped/lysed in ice-cold RIPA Buffer (50 mM Tris, 150 mM NaCl, 0.1% SDS, 0.5% sodium deoxycholate, 1% NP-40). The lysate was centrifuged for 5 min at 21,000 rpm at 4°C. 200 µL was loaded into a 96 well glass bottom plate (BD Falcon, 353219) and read at AlexaFluor-488™-cadaverine (excitation = 495 nm, emission = 519 nm) and 1:1000 DAPI (1 mg/mL)

(excitation = 358 nm, emission = 461 nm) on a Spectramax Gemini EM spectrofluorometer (Molecular Devices, Sunnyvale, CA).

RESULTS & DISCUSSION

Assays that measure *in situ* autophagy in cells or tissues are often laborious, require special instrumentation, and highly technical manipulation. Consequently, we set out to develop a fluorescence-based autophagy detection protocol that works with a variety of different platforms, including microscopy, flow cytometry, and the spectrofluorometric plate reader. In short, under conditions known to induce autophagy in cells, such as nutrient deprivation, puncta (autophagosomes) form, which can be stained and counted in order to quantify autophagy. One method for detection of autophagosomes requires transient transfection with GFP-LC3 or infection with adenovirus or lentivirus for GFP-LC3. Although autophagosomes can be detected and quantified (See Figure 3.1 A & B), this technique is limited to *in vitro* studies or GFP-LC3 transgenic animals. One pitfall of using this reagent is that the constitutive expression of GFP may be toxic to cells, leading to possible artifacts, and overexpression can result in protein aggregates that can be mistaken for autophagosomes. Also, infection of cells with adenovirus has been demonstrated to upregulate autophagy[159] (data not shown). Constitutive expression of GFP-LC3 likely contributes to the diffuse background fluorescence that makes this technique unsuitable for flow cytometry (Compare Figure 3.1 A & B; flow cytometry data not shown), and the response to adenoviral infection can result in increased autophagic puncta formation in "control" cells. Finally, in approximately 5% of HL-1 cells there is "super-expression" where the cell glows too intensely to quantify puncta (Figure 3.1 C).

AlexaFluor-488™-cadaverine

Monodansyl cadaverine (MDC) was proposed as a label for autophagosomes, but it has fallen out of favor in the autophagy community because it can label acidic compartments in addition to autophagosomes[147]. Moreover, it exhibits high nonspecific fluorescence, fixation results in >75% loss of fluorescence, and the dansyl moiety undergoes rapid photobleaching. Previously, research by former members of the Gottlieb lab indicated that the fluorescent reagent AlexaFluor-488™-cadaverine (a polyamine conjugated to a fluorophore) could be substituted for MDC with improved results, i.e., increased puncta counts and decreased background (Figure 3.2). We sought to determine if AlexaFluor-488™-cadaverine is a viable alternative to MDC. Nutrient deprivation (fasting/starving) i.e. culture media without serum and/or amino acid is typically used to induce autophagy *in vivo*. Therefore, HL-1 cells (neonatal mouse cardiomyocytes) were cultured in complete media (control) or media without serum and amino acids (Krebs Starvation Buffer) for 4 hrs and then stained with 50 and 100 μM AlexaFluor-488™-cadaverine for 20 and 60 minute (Figure 3.3). We found that 50 μM AlexaFluor-488™-cadaverine incubation for 20 minutes demonstrated the best staining; however, the AlexaFluor-488™-cadaverine resulted in relatively high cytoplasmic background staining, making it unsuitable for imaging and FACS analysis.

Optimization of Polyamines with AlexaFluor-488™-cadaverine

We correctly hypothesized that the addition of an unlabeled polyamine (cadaverine, putrescine, spermidine, or spermine) would compete for nonspecific binding and improve the specific labeling of autophagosomes. Consequently, we incubated HL-1

cells with the aforementioned polyamines, finding that addition of spermidine or spermine yielded the lowest background fluorescence and clearest puncta. Next, we performed a study to determine which polyamine (spermine or spermidine) and at which dose would result in optimal AlexaFluor-488^{TM}-cadaverine staining (96 Well MakTek Plate Assay – Data Not Shown). We found that 25 μM spermidine was optimal. Next, we undertook a spermidine time course study in HL-1 cells, determining that 5 minutes was the minimum time to observe clear puncta in HL-1 cells (Figure 3.5). Through trial and error across a variety of experiments, we decided that 50 μM ALexaFluor-488^{TM}-cadaverine for 15 minutes and 25 μM spermidine for 5 minutes were the optimal conditions for HL-1 cells – a combination of compounds that we have titled Fluormidine. To demonstrate the superiority of Fluormidine relative to MDC, we starved (serum and amino acid withdrawal) HL-1 cells for 4 hrs and stained with MDC or Fluormidine. The sensitivity of Fluormidine is much greater than MDC and the background observed in the AlexaFluor-488^{TM}-cadaverine plus spermidine samples is much less than what is observed in the AlexaFluor-488^{TM}-cadaverine samples (Figure 3.2).

Staining with Fluormidine *in vitro* under Autophagy-Modulating Conditions

Fluormidine labeling detects autophagy in a variety of cells with autophagy inducing conditions. We subjected NIH 3T3 (embryonic fibroblasts), HeLa (cervical cancer), HEK 293 (human embryonic kidney), and J774 (mouse monocytes/macrophage) to serum and amino acid withdrawal for 2 hrs (Figure 3.6) and Jurkat (human T cells) for 4 hrs (Figure 3.7). As shown in Figures 3.6 and 3.7, the numbers of puncta increased after induction of autophagy via starvation. Moreover HEK 293, HeLa, and J774 (1 hr

incubation, 30 μM) and HL-1 cells (2 hr incubation, 300 μM) treated with chloramphenicol, a known autophagy inducer, in complete media also showed an increase in puncta formation (Figure 3.8). A similar result is observed with Jurkat cells subjected to starvation or rapamycin treatment (Figure 3.7).

Fluormidine and Autophagy-Deficient HL-1 Cells: mCherry-Atg5-K130R Transfection

The aforementioned data demonstrates that Fluormidine staining correlated with autophagy modulating events. However, is autophagy directly involved in the formation of the Fluormidine-labeled puncta? To definitively demonstrate a link between autophagy and Fluormidine-labeled puncta, we transfected HL-1 cells with a dominant negative Atg5K130R plasmid and assayed for puncta formation following a 4 hr fast (Figure 3.9). No differences in the number of puncta were detected between the mCherry-Atg5K130R-transfected fed and starved cells where there were significant differences in puncta numbers between the fed and starved cells (Figure 3.9). This indicates that the puncta labeled by Fluormidine are Atg5-dependent and therefore autophagy related.

Fluormidine Colocalization with Autophagy Proteins

We can conclude that Fluormidine labeling is proportional to and dependent on autophagy induction, making Fluormidine a viable marker for quantification of autophagy by microscopy. Although we have demonstrated a strong correlation between the numbers of Fluormidine labeled puncta with conditions known to induce autophagy,

we need to establish the identity of the puncta labeled by Fluormidine. While we believe that Fluormidine is labeling autophagosomes, we cannot rule out other structures including other vesicle compartments. Consequently, colocalization studies of fluormidine and a variety of autophagy proteins (including possible sources for autophagosomal membrane) were undertaken. An ungodly number of antibodies (LC3B, LC3AB, Transglutaminase-2, Apg5, Apg12, Atg5, LAMP1, LAMP2A, Atg7, Atg16L1, γ-tubulin, Rab7, Wipi1(Atg18), VPS34, Atg9, p62/SQSTM1, Atg4B, PDI, Cyclophilin S, mTOR, Pink1, S6K, Beclin-1, and TOM-70) and the reagent LysoTracker Red (a lysosomal stain) were used in an attempt to link Fluormidine-positive structures to the autophagy machinery (Data Not Shown; See Table 3.1 for a list of antibodies). Finally one of the antibodies, Rab9, tested demonstrated a large degree of, but not universal, colocalization with Fluormidine (Figure 3.10). According to Shimizu et al., the GTPase Rab9 is important in shuttling membrane between the trans-Golgi Network and late endosomes and has been found to be essential for alternative autophagy (Atg5/7 independent autophagy)[160,161]. It appears to be essential during alternative autophagy for membrane elongation by supplementing the isolation membranes with membrane generated by the trans-Golgi and late endosomes in gene knockdown studies (it is thought to act like Atg5); however, Rab9 is not essential for canonical autophagy[160,161]. The details of conventional vs. alternative autophagy are still being elucidated. Consequently, it remains unknown if both pathways are constitutive with one predominating over the other depending on conditions or if solely one pathway is active at a time depending on cell type and stimulus. Interestingly, a recent paper reports that hearts from type-I diabetic mice demonstrate a suppression of conventional autophagy, presumably to

prevent cardiac dysfunction, and a concomitant increase in alternative autophagy (hallmarked by increasing Rab9 levels)[162]. This indicates that at least in the adult mouse heart, both autophagy pathways are operational. Since we do not observe universal colocalization between Fluormidine and Rab9, we suspect that Fluormidine may label structures formed in both autophagy pathways.

Measuring Autophagy by Flow Cytometer

Having established that the Fluormidine could measure autophagy in cell culture, we sought to determine if Fluormidine could be used to measure autophagy in lymphocytes isolated from peripheral blood. Previous research has demonstrated that elderly patients with angina have lower levels of LC3-II in their cardiac tissue and blood cells than age-matched controls, indicating that peripheral blood sampling might reflect autophagic processes in other organs including the heart[156]. Thus, Fluormidine flow cytometry analysis of peripheral blood lymphocytes might serve as a surrogate indicator of autophagy in solid organs.

While Fluormidine works well for microscopic analysis, it would be preferable to use flow cytometry. Previous experiments with Jurkat cells demonstrated Fluormidine-labeled puncta following serum and amino and deprivation and 5 μM rapamycin treatment (Figure 3.7). Additionally, primary mouse lymphocytes, isolated from lymph nodes, treated *ex vivo* displayed Fluormidine-labeled puncta following starvation and rapamycin treatment (Figure 3.11). These results suggested that differences in Fluormidine intensity following an autophagy-inducing stimulus could be detected by flow cytometry. As proof of principle we used Fluormidine to stain Jurkat and HL-1

cells under control conditions or after nutrient deprivation and performed FACS analysis. We found a significant shift between the fed and fasted cell populations in Jurkat cells, but not in HL-1 cells (Data Not Shown), indicating that FACS can detect differences in puncta levels indicative of autophagy induction following nutrient starvation in at least one cell type (Figure 3.12). Klionsky et al., in his seminal work "Guidelines for the use and Interpretations of Assays for Monitoring Autophagy," has cautioned autophagy researchers that autophagy can change when normally adherent cells lines become non-adherent, which could explain why we see a significant change Fluormidine-labeled puncta in Jurkat, but not HL-1 cells[147]. Additionally, Jurkat cells have a large nucleus with a relatively low volume of cytoplasm; conversely, HL-1 cells are large, polynuclear cells with a greater cytoplasmic volume relative to Jurkat cells. Consequently, these differences in cells may contribute to the differential detection of autophagy i.e. greater puncta per unit volume, making a brighter cell. In all, we have determined that murine lymphocytes can respond to autophagy induction *ex vivo* and that we can detect changes in Fluormidine labeling via FACS analysis in Jurkat cells.

Next, to test if Fluormidine could label murine lymphocytes *ex vivo* we injected male C57BL/6 mice with 5 mg/kg rapamycin or 5 mg/kg rapamycin and 60 mg/kg chloroquine. Four hours later blood and hearts were isolated in order to see if autophagy was induced in the deep tissues (heart) and in the lymphocytes. The blood cells were stained with Fluormidine and antibodies labeling T Cells and macrophages and were run on a flow cytometer (the B cell staining did not work). Both the rapamycin and rapamycin plus chloroquine treatment resulted in a substantial shift in mean fluorescence

in both T Cells and macrophages as compared to the control (See Figure 3.13), indicating that Fluormidine could be used for detection of autophagy in the blood by flow cytometry. Of note, chloroquine, which blocks lysosomal clearance of autophagosomes, did not result in increased Fluormidine staining, suggesting that the label is incorporated into autophagosomes as they form and is therefore insensitive to impaired flux. Thus, Fluormidine appears to have utility as a specific indicator of autophagic initiation. Further work will be needed to buttress this assertion. To determine if changes in autophagy in peripheral blood cells mirrored changes in the heart, the hearts were isolated and analyzed by western blotting for LC3. We observed an increase in LC3-II (indicator of autophagy) in the hearts of mice treated with rapamycin compared to controls, suggesting that analysis of autophagy in peripheral blood cells responding to a systemic stimulus might reflect similar processes in other organs.

Incidentally, upon repeating the experiment with female C57BL/6 mice we observed no shift in the Fluormidine mean fluorescence (Data Not Shown). Moreover, western blot LC3 analysis of the isolated hearts demonstrated no significant change in LC3-II (indicator of autophagy) in the female hearts (Figure 3.14). This implies gender differences between genders in response to rapamycin, which is confirmed in the literature[163]. Consequently, these experiments should be repeated using another method of inducing autophagy.

Measuring Autophagy by Spectrofluorometer

To determine if Fluormidine could be adapted to a plate reader-based spectrofluorometer assay, we treated HL-1 cells (in 60 mm dishes) under nutrient and

serum starvation conditions, stained with Fluormidine (with 25 or 50 μM AlexaFluor-488^{TM}-cadaverine) and DAPI, lysed the cells with RIPA buffer, and loaded the lysates into wells of a glass bottomed 96 well plate. DAPI was added to each sample to control for potential differences in cell numbers. We found a robust difference in fluorescence between fasted and fed cells, indicating that Fluormidine is a viable reagent for detecting autophagy via plate reader (Figure 3.15). This assay needs to be repeated several more times, but it is looking promising.

Chapter III, in part, is currently being prepared for submission for publication of this material. Gurney, M.A., Linton, P.J., and Gottlieb, R.A. The dissertation author was the primary investigator and author of this material.

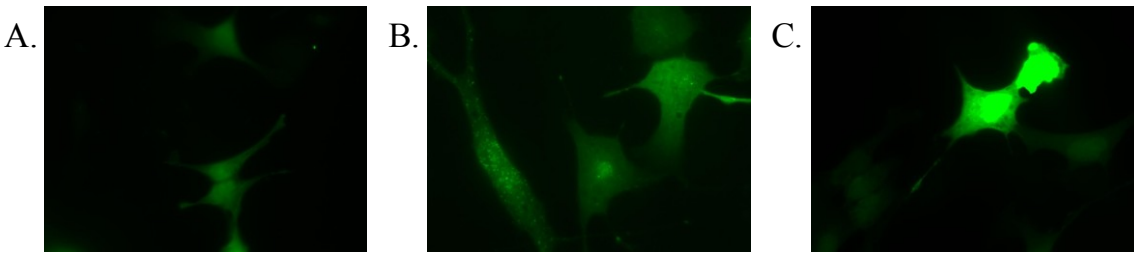

Figure 3.1: GFP-LC3 Transfected HL-1 Cells. 200,000 HL-1 cells were plated on pre-treated 0.02% gelatin/0.5% fibronectin MakTek plates. Cells were transfected with GFP-LC3 and subjected to a four hr incubation at 37°C, 5% CO_2 in complete media (A) or Krebs Starvation Buffer (serum/amino acid deprivation) (B), washed with phosphate buffered saline, fixed with 4% paraformaldehyde (15 min), and imaged. C. An example of a GFP-LC3 "super-expression" artifact.

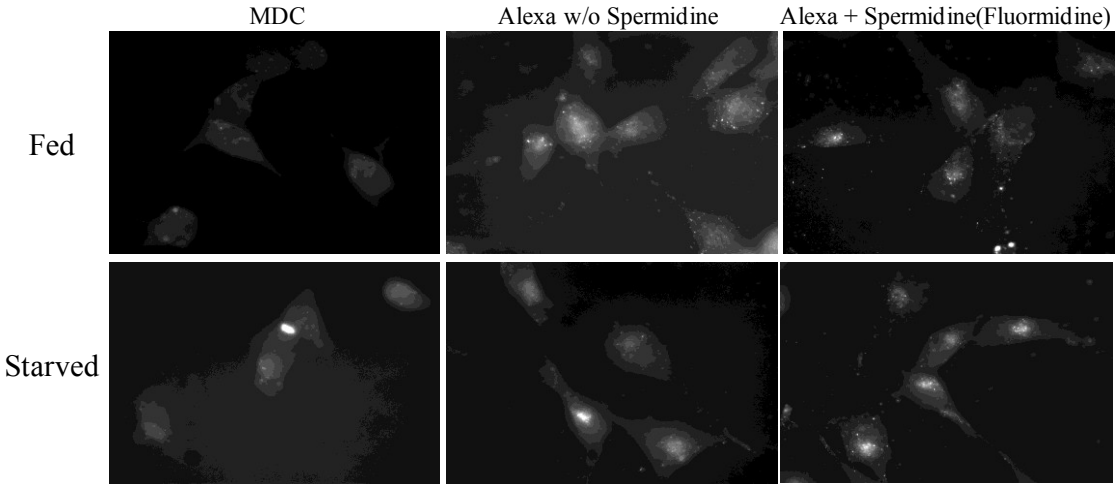

Figure 3.2: Characterization of Fluormidine. Representative comparison of Monodansyl cadaverine (MDC) , Alexafluor-488^{TM}-cadaverine, and Alexafluor-488^{TM}-cadaverine + spermidine. HL-1 cells are plated on glass cover slips coated overnight with 0.02% gelatin supplemented with 0.5% fibronectin. HL-1 cells were subjected to amino acid/serum starvation for 4 hrs at 37°, 5% CO_2. Cells were stained with 50 µM MDC, 50 µM Alexafluor-488^{TM} cadaverine (for 15 min), or 50 µM Alexafluor-488^{TM}-cadaverine (15 min) and 25 µM spermidine (5 minutes). The samples were washed with phosphate buffered saline, fixed with 4% paraformaldehyde (15 min), and imaged.

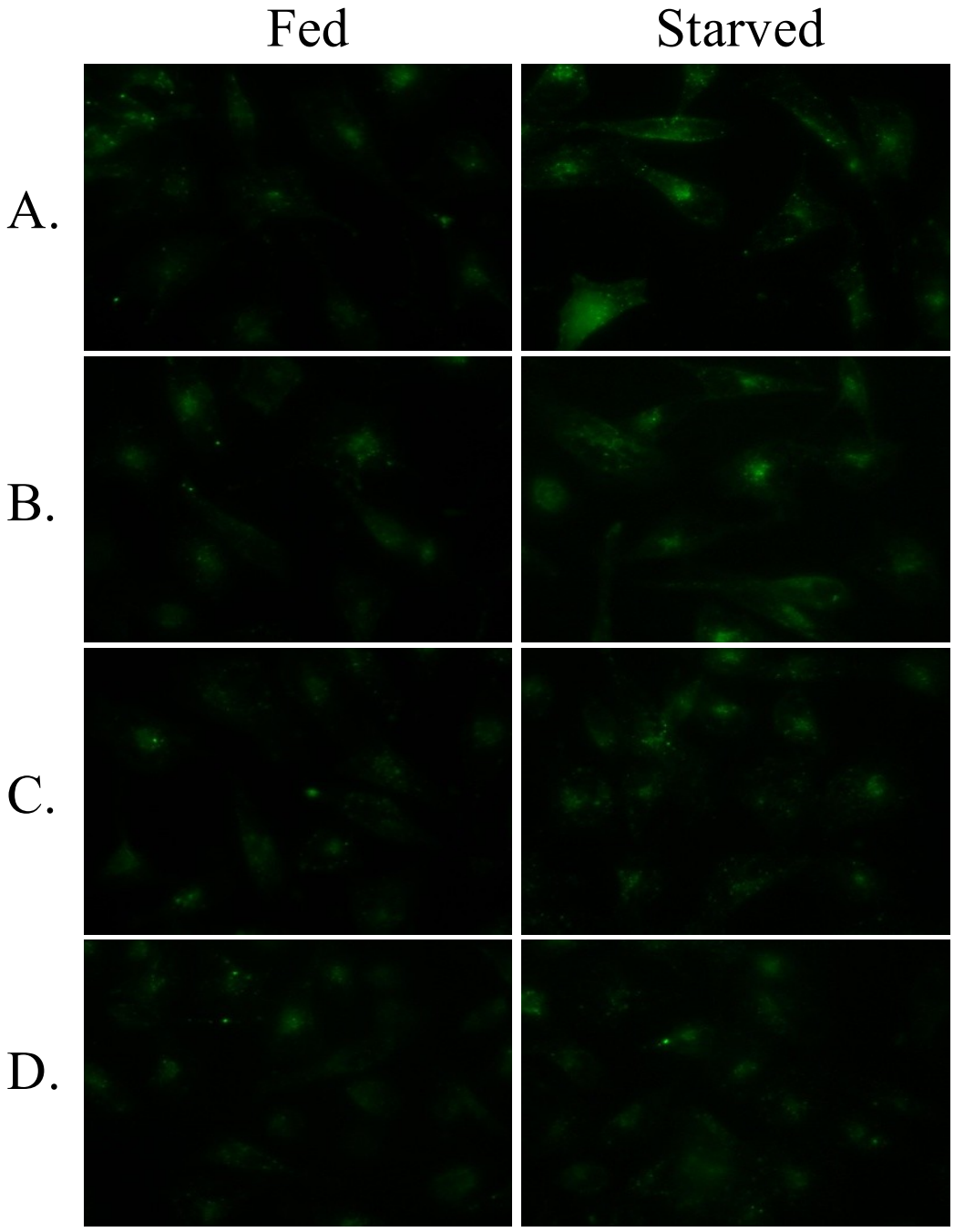

Figure 3.3: AlexaFluor-488^{TM}-cadaverine Time Course/Dose Response in HL-1 Cells. HL-1 cells are plated on glass cover slips treated overnight in a 0.02% gelatin supplemented with 0.5% fibronectin. HL-1 cells were subjected to amino acid/serum starvation for 4 hrs at 37°, 5% CO_2. Cells were stained with 150μM (A) or 50 μM (B) Alexafluor-488^{TM} cadaverine for 60 min or 150 μM (C) or 50 μM (D) Alexafluor-488^{TM}-cadaverine for 20 minutes. The samples were washed with phosphate buffered saline, fixed with 4% paraformaldehyde (15 min), and imaged.

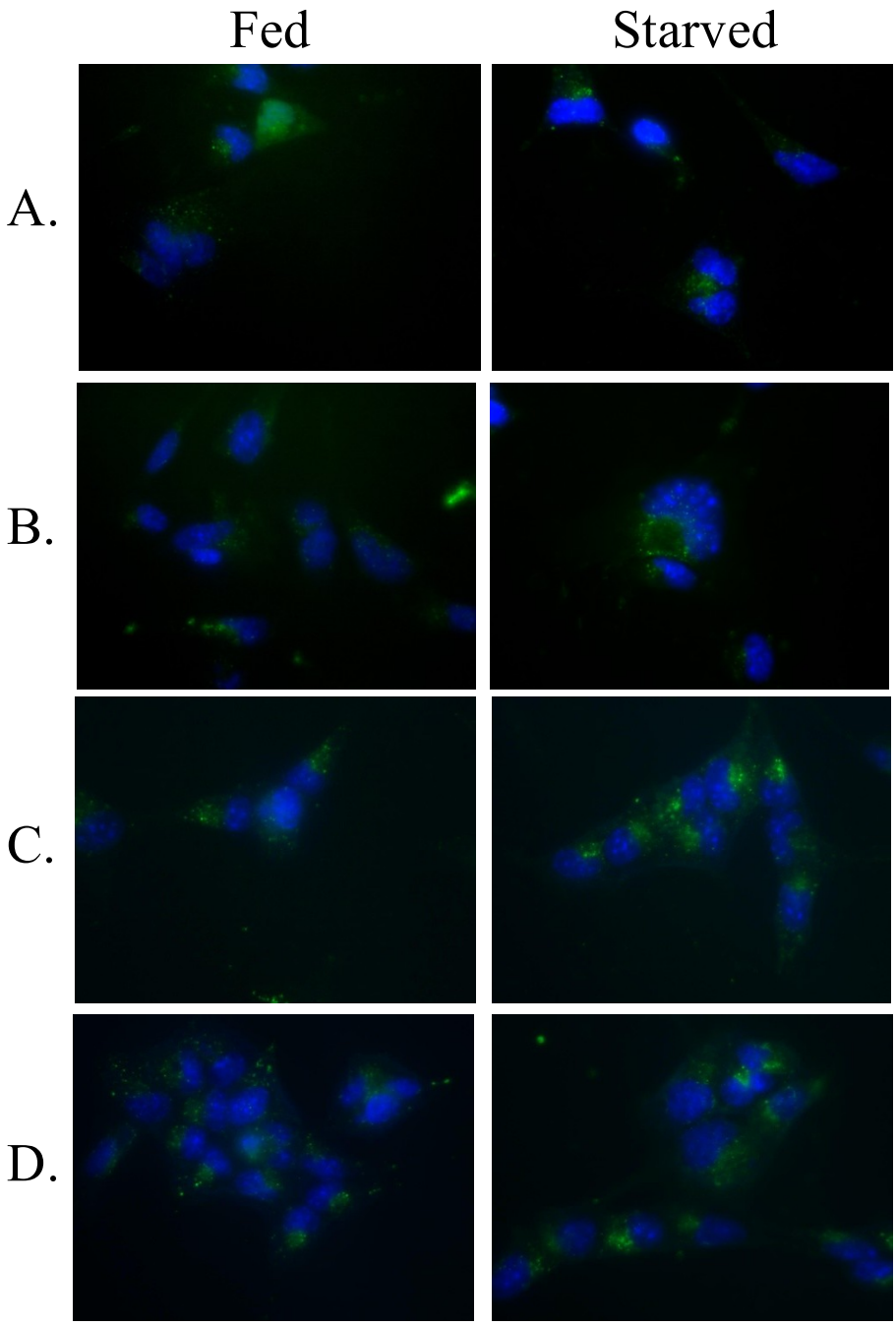

Figure 3.4: Optimization of AlexFluor-488^{TM}-cadaverine with Polyamines. 300,000 HL-1 cells were plated on a Gelatin-Fibronectin pre-treated 35 mm glass bottom culture dish overnight. HL-1 cells were subjected to amino acid/serum starvation for 4 hrs at 37°, 5% CO_2. Cells were stained with 50 μM Alexafluor-488^{TM} cadaverine for 20 minutes and 20 μM cadaverine (A), 20 μM putrescine (B), 50 μM spermine (C), or 50 μM spermidine. The samples were washed with phosphate buffered saline, fixed with 4% paraformaldehyde (15 min), and imaged.

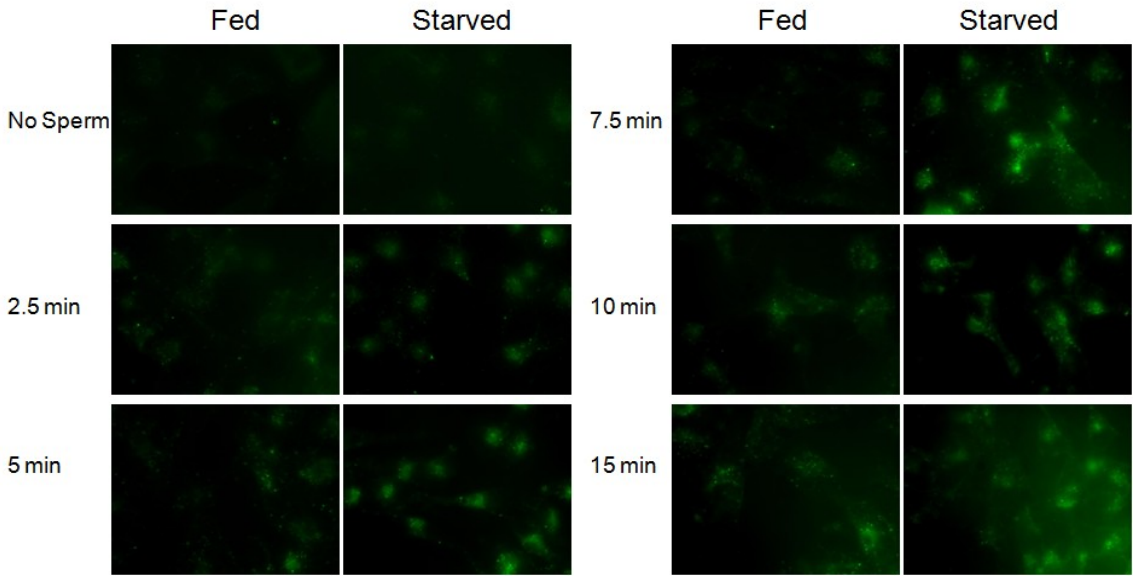

Figure 3.5: AlexaFluor-488^{TM}-cadaverine Spermidine Time Course. HL-1 cells were plated on a 0.02% gelatin/0.5% fibronectin pre-treated coverslip overnight. The cells were incubated with Complete Claycomb Media or Krebs Starvation Buffer for 4 hrs at 37ºC/5% CO_2. 15 minutes prior to assay end, 50 µM AlexaFluor-488^{TM}-cadaverine and 25 µM spermidine were added and cells were incubated for 2.5, 5, 7.5, 10, or 15 minutes at 37°C. The cells were washed with 1X PBS, fixed with a 4% paraformaldehyde solution in 1X PBS for 15 minutes, washed again in 1X PBS, and imaged.

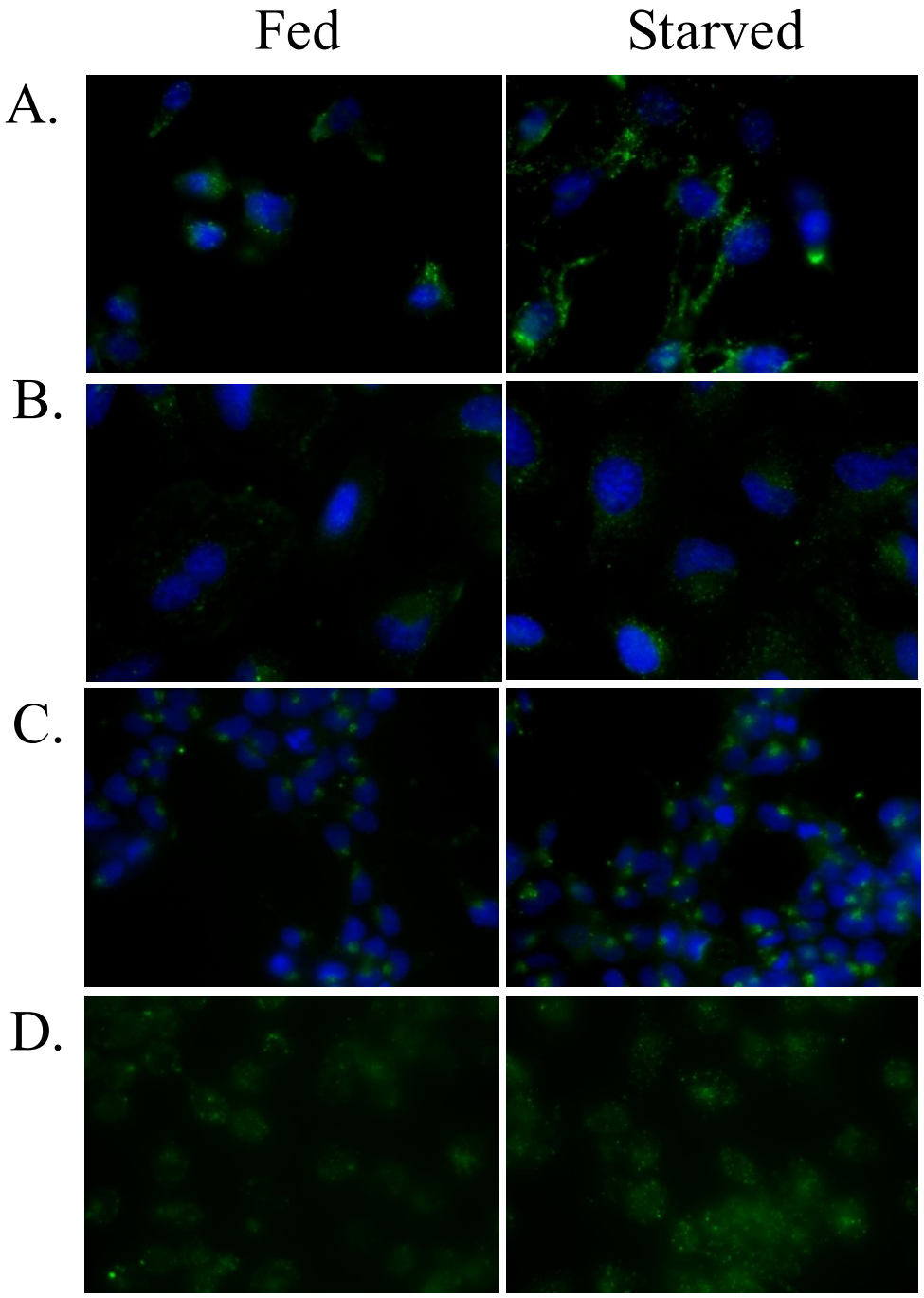

Figure 3.6: Autophagy induction increases Fluormidine labeling of puncta in multiple cell types. A. NIH 3T3, B. HeLa, C. HEK 293, and D. J774. 1 x 10^5 cells/well overnight on glass coverslips. Cells were starved for 2 hrs, stained with Fluormidine (25 μM AlexFluor-488™-cadaverine 3T3, HeLa, and HEK 293 and 50 μM AlexaFluor-488™-cadaverine J774), washed in PBS, fixed in 4% paraformaldehyde, and imaged.

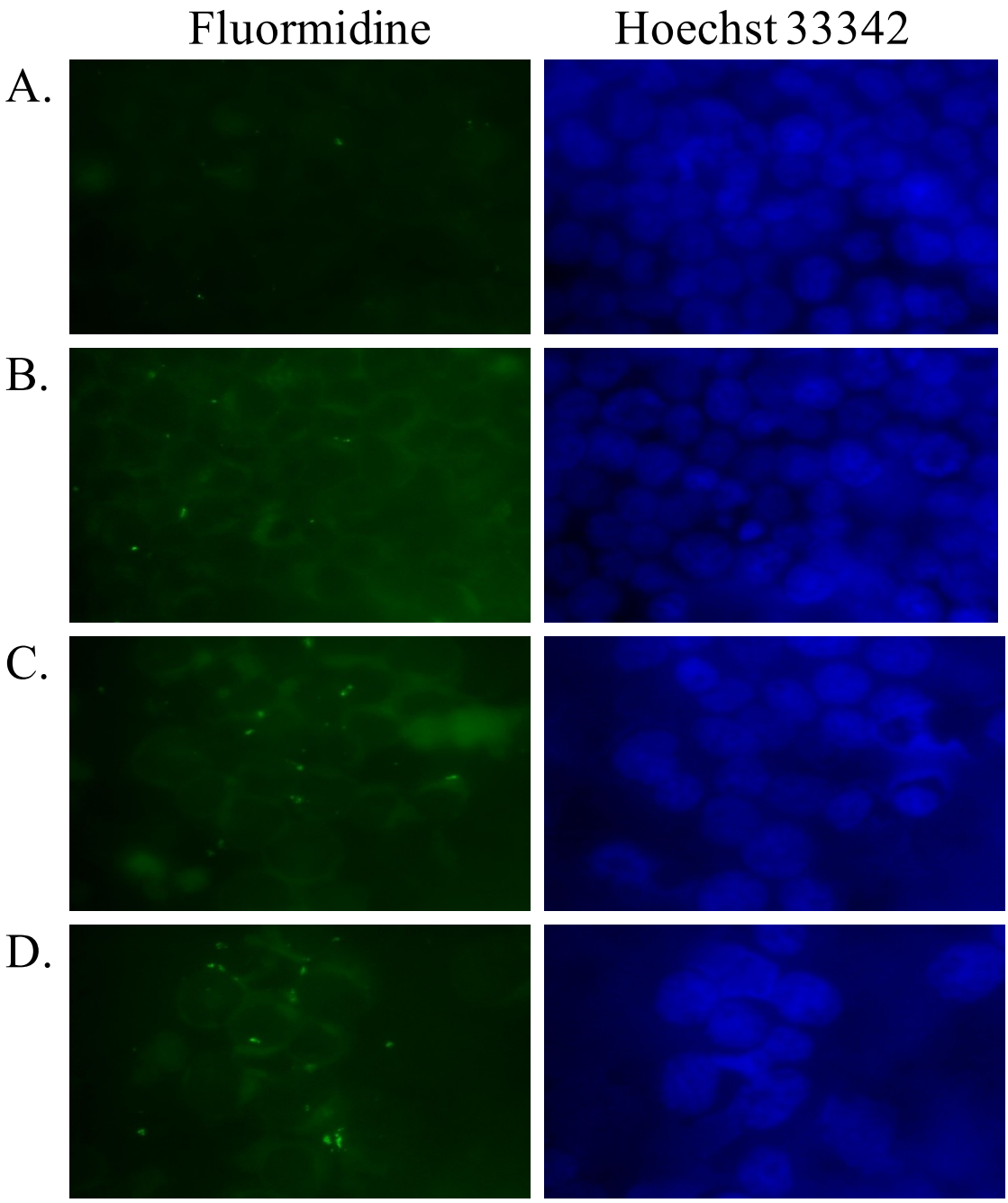

Figure 3.7: Fluormidine Treatment of Starving Jurkat Cells +/- Rapamycin. 1.5 x 10^5 Jurkat cells were starved for 4 hrs with and without 5 μM rapamycin, stained with Fluormidine and Hoechst 33432, washed in PBS, subjected to cytospin, fixed in 4% paraformaldehyde, and imaged. A. Complete media, B. Complete media supplemented with 5 μM rapamycin, C. Starvation buffer, and D. Starvation buffer supplemented with 5 μM rapamycin.

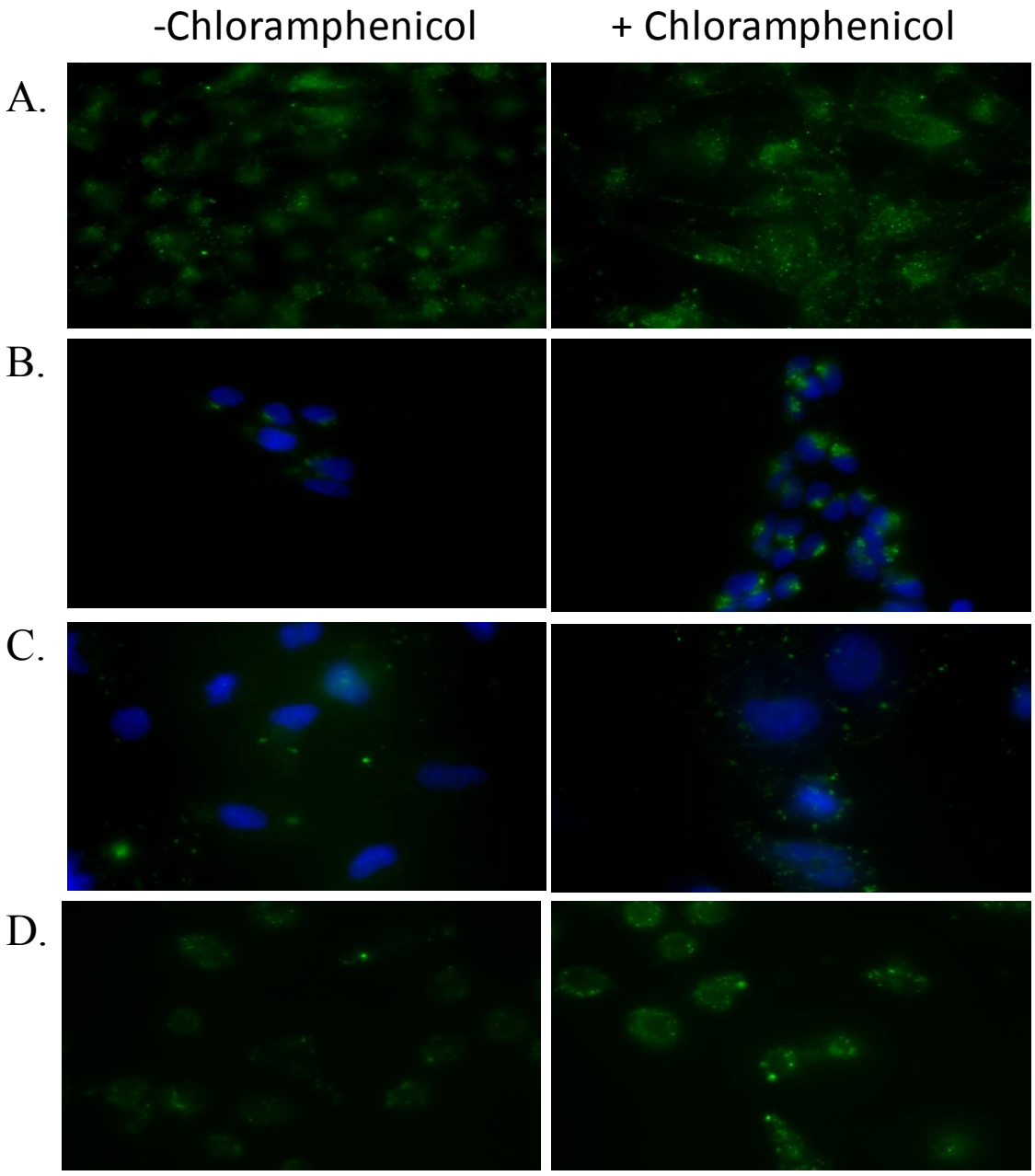

Figure 3.8: *In vitro* Induction of Autophagy by Chloramphenicol Treatment. A. HL-1, B. HEK 293, C. HeLa, and D. J774. 1 x 10^5 cells/well (5 x 10^5 for HL-1) overnight on glass coverslips. Cells were treated with 30 μM chloramphenicol (suspended in DMSO – 0.03% final DMSO concentration in media) for 2 hrs (HL-1) or 1 hr (HEK 293, HeLa, and J774), stained with Fluormidine (50 μM – HL-1 and J774, 25 μM – HeLa and HEK 293), washed in PBS, fixed in 4% paraformaldehyde, and imaged.

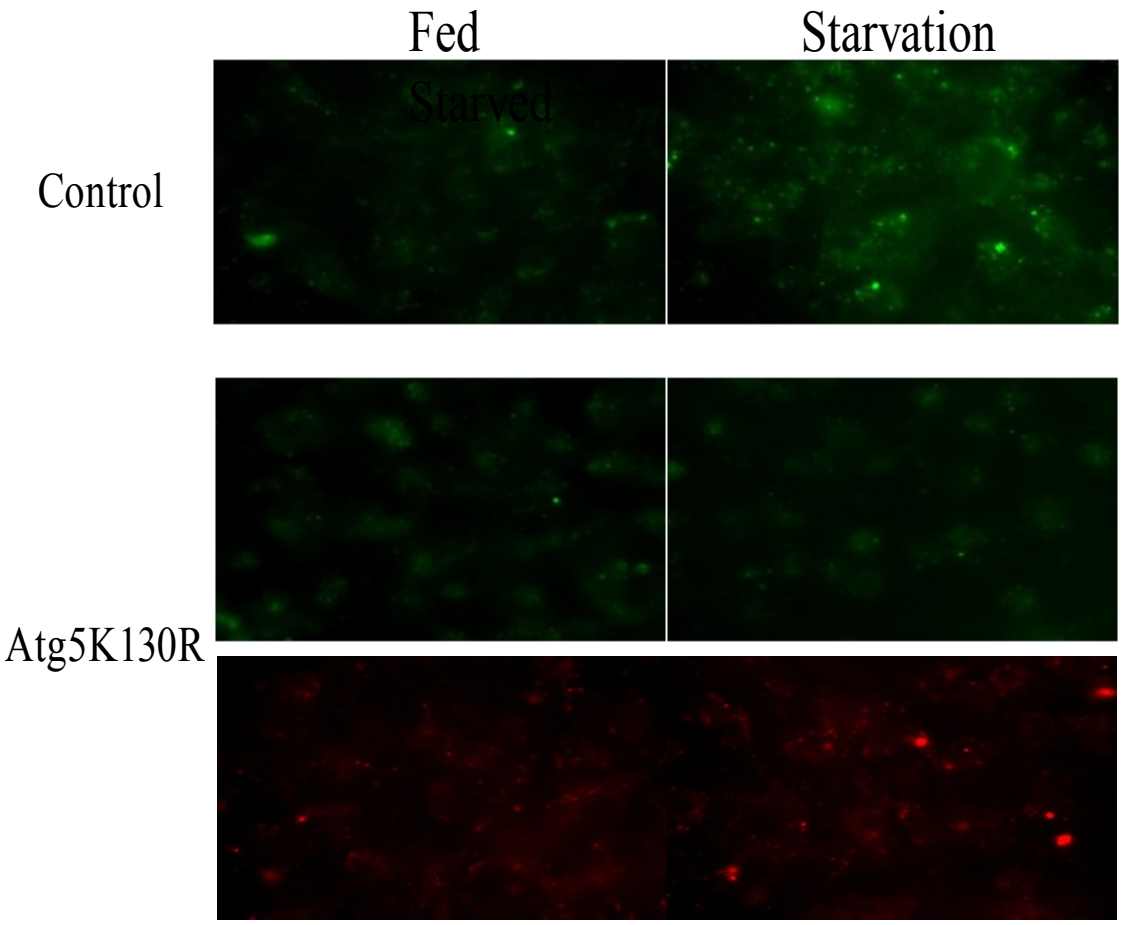

Figure 3.9: Atg5K130R Treatment of HL-1 Cells Under Fed or Starved Conditions. HL-1 cells are plated on glass cover slips coated overnight in a 0.02% gelatin supplemented with 0.5% fibronectin. The cells were transfected with 0.2 ng of the Atg5K130R plasmid for 8 hrs before the media was replaced and the cells were incubated overnight. The transfected and control cells were either subjected to amino acid/serum starvation for 4 hrs or maintained in complete media at 37° and 5% CO_2, stained with Fluormidine, washed with phosphate buffered saline, fixed with 4% paraformaldehyde (15 min), and imaged. Shown below are the images demonstrating mCherry-Atg5K130R expression in the fed and starved cells.

Table 3.1: Antibodies Used for AlexaFluor-488™-cadaverine Colocalization Assays

Name	Cat. #	Manufacturer	Dilution
LC3B	2775	Cell Signaling	1:400, 1:500
LC3AB	4108	Cell Signaling	1:400, 1:1000
Transglutamiase-2	ab421	Abcam	1:400, 1:500
APG5	sc-33210	Santa Cruz Biotechnology	1:200, 1:400, 1:1000
Apg12	sc-68884	Santa Cruz Biotechnology	1:200, 1:400, 1:1000
Atg5	AP1812a	Abgent	1:100, 1:200, 1:1000
LAMP1	Ab24170	Abcam	1:400, 1:500, 1:1000
LAMP2A	PA1-655	Thermo Scientific	1:400, 1:500, 1:1000
Atg7	AP1813b	Abgent	1:400, 1:1000
Atg16L1	AP1817b	Abgent	1:1000
γ-tubulin	ab-11320	Abcam	1:500, 1:1000
Rab7	9367	Cell Signaling	1:100, 1:500, 1:1000
Wipi1(Atg18)	W2394	Sigma-Aldrich	1:250, 1:1000
VPS34	V9764	Sigma-Aldrich	1.6λ:500λ, 1:1000
Atg9	A0732	Sigma-Aldrich	1:250, 1:1000
p62/SQSTM1	03-GP62-C	American Research Products	1:500, 1:1000
Atg4B	1809c	Abgent	1:500, 1:1000
PDI	2446	Cell Signaling	1:500, 1:1000
Cyclophillin D	MSA04	MitoSciences	1:500
mTOR	2972	Cell Signaling	1:500
Pink	ab23707	Abcam	1:500
S6K	9202	Cell Signaling	1:500
Beclin-1 (Atg6)	3738	Cell Signaling	1:500
TOM70	Ap-1058-50ug	CalBioChem	1:500, 1:1000
Rab9	5118	Cell Signaling	1:100, 1:250

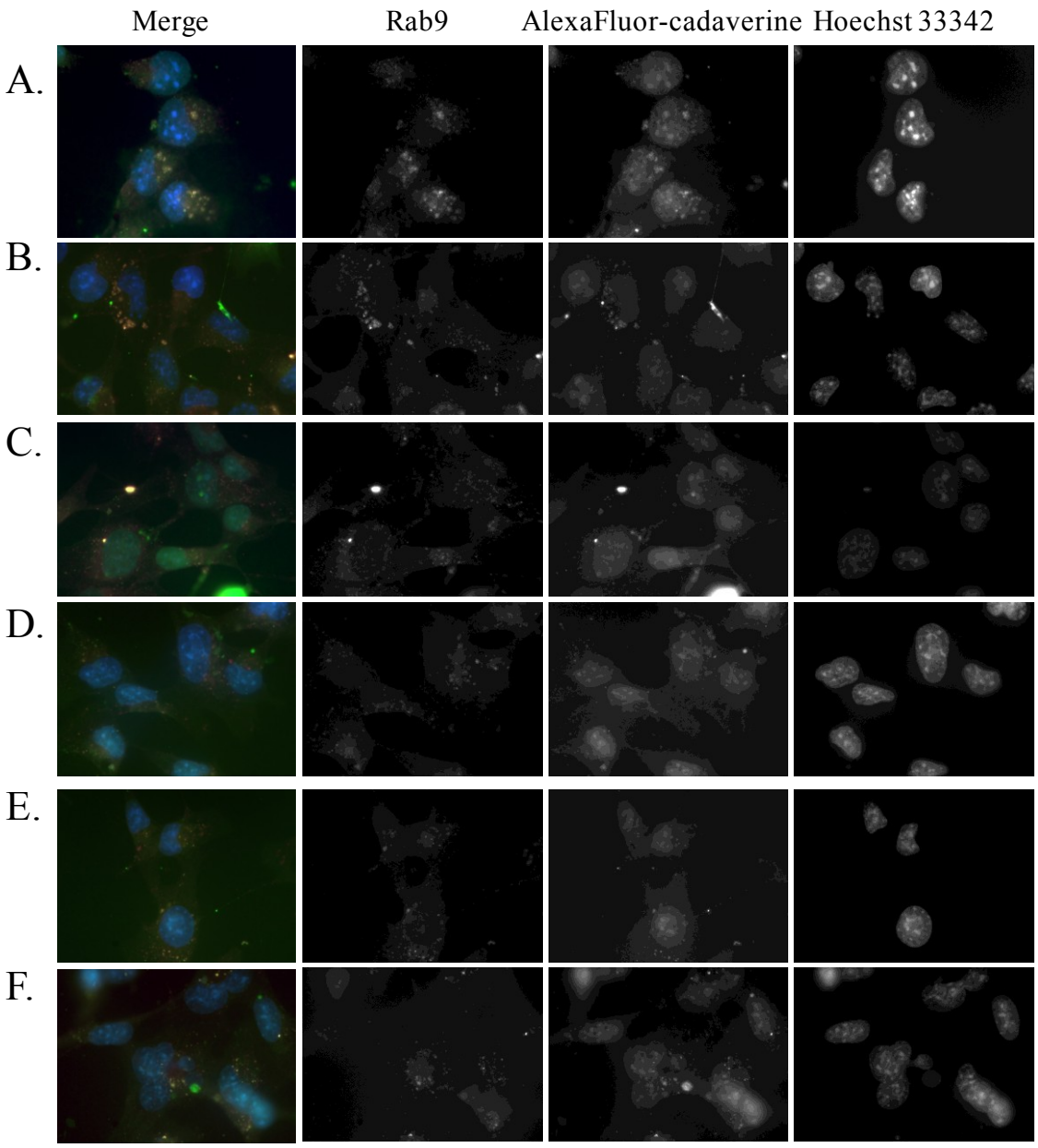

Figure 3.10: Rab9 Colocalization with AlexaFluor-488™-cadaverine in HL-1 Cells. HL-1 cells were plated on a 0.02% gelatin/0.5% fibronectin pre-treated coverslip overnight. The cells were incubated in Krebs Starvation Buffer for 4 hrs at 37°C/5% CO_2. 15 minutes prior to assay end, 25 µM AlexaFluor-488™-cadaverine and 0 (A), 10 (B), 25 (C), 50 (D), and 75 (E & F) µM spermidine was added and cells were incubated for 15 minutes at 37°C. The cells were washed with 1X PBS, fixed with a 4% paraformaldehyde solution in 1X PBS and imaged.

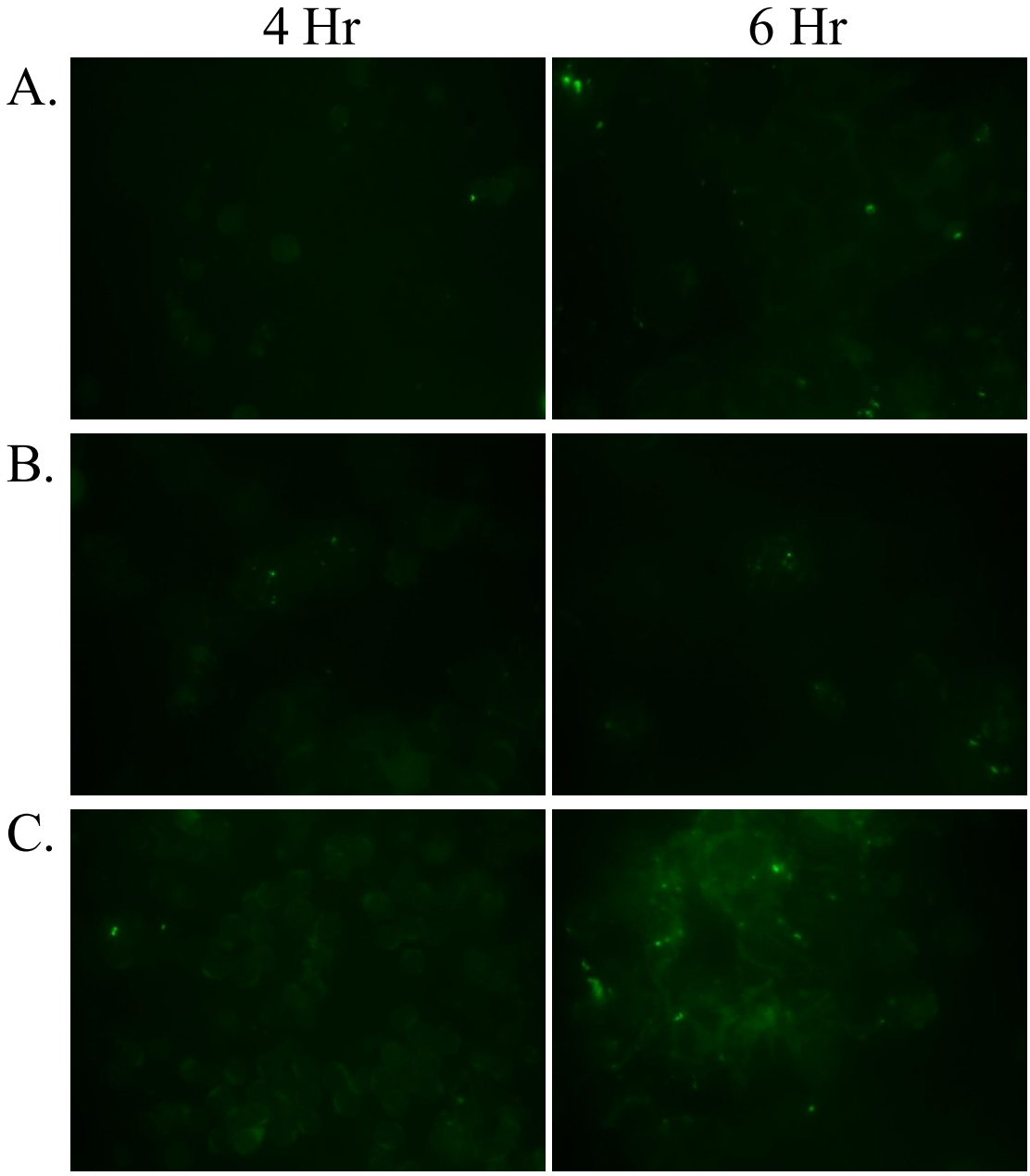

Figure 3.11: Fluormidine Treatment of Lymph Node-Derived Lymphocytes. Lymph Nodes were isolated from a 3 month old male C57BL/6 mouse and homogenized in 2-3% FBS in RPMI supplemented with 25 mM HEPES. The cell suspension was divided and placed in either Complete Media (A) or Krebs Starvation Buffer (B & C) with (C) or without (B) 5 μM Rapamycin. The cells were incubated 4 or 6 hours at 37°C/5% CO_2, treated with Fluormidine, cyto-spun, and fixed in 4% paraformaldehyde for 10 minutes. The slides were mounted and imaged.

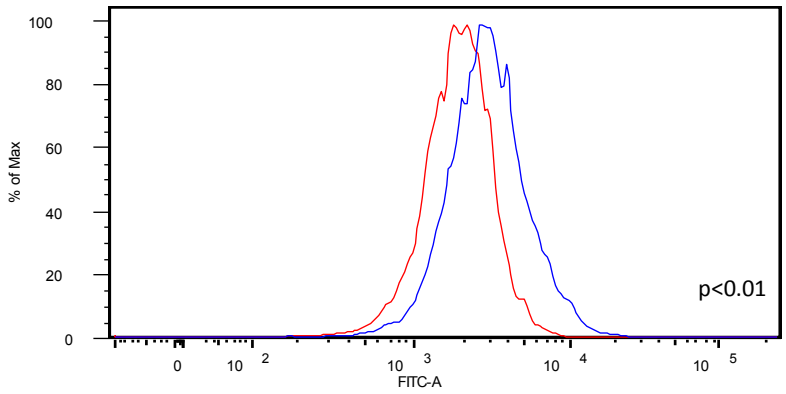

Figure 3.12: FACs Analysis of Starved Jurkat Cells. Jurkat cells were stained with Fluormidine following incubation for 2 hr in full medium (red line) or deprived of serum and amino acids (blue line). The cells were washed in 1X PBS, fixed in 4% paraformaldehyde, and run on a DB FACS Aria flow cytometer. Significance was calculated using the Chi Squared Test.

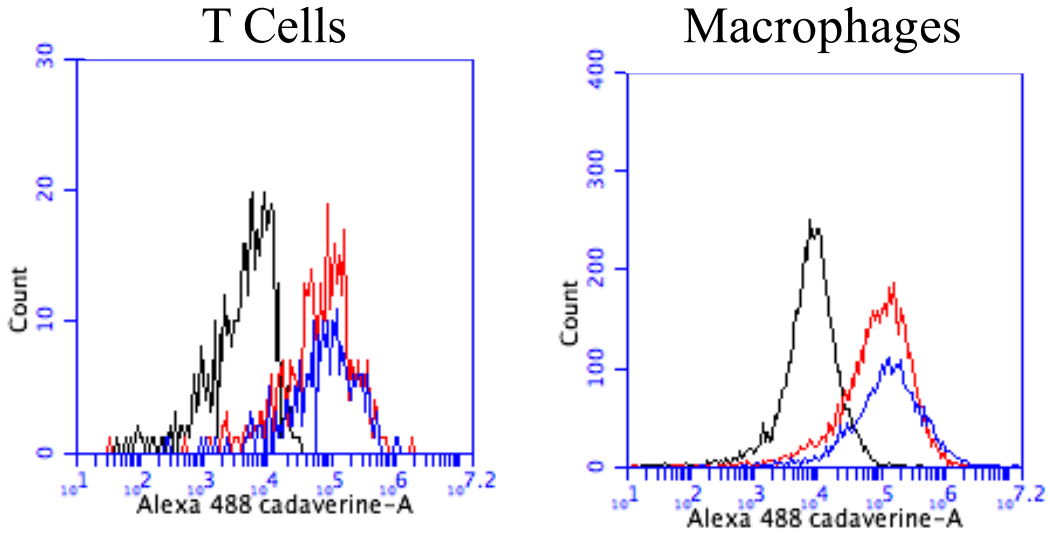

Figure 3.13: Fluormidine Analysis of Autophagy in T Cells and Macrophages from Rapamycin Treated Mice. Young male C57BL/6 mice were injected with vehicle control (5% PEG/5% Tween-80 and 200 µL 1X PBS) (black line), 5 mg/kg rapamycin solution and 200 µL PBS (red line), or 5 mg/kg rapamycin and 60 mg/kg chloroquine diphosphate (blue line) (n=1 mouse/condition). 4.5 hrs later the mice were bled and sacrificed. 450 µL of HBSS was added to 50 µL of blood (n=3 blood samples per condition). 0.25 µg of APC-α-mouse CD3ϵ (to label T Cells) and PE-α-mouse CD11b (to label Macrophages) was added to each sample in addition to Fluormidine, centrifuged 1300 rpm for 7 minutes, washed in PBS, suspended in 4% paraformaldehyde in 1X PBS for 15 minutes, washed, and resuspended in 1% FBS in HBSS. The cells were run on an Accuri C6 Flow Cytometer.

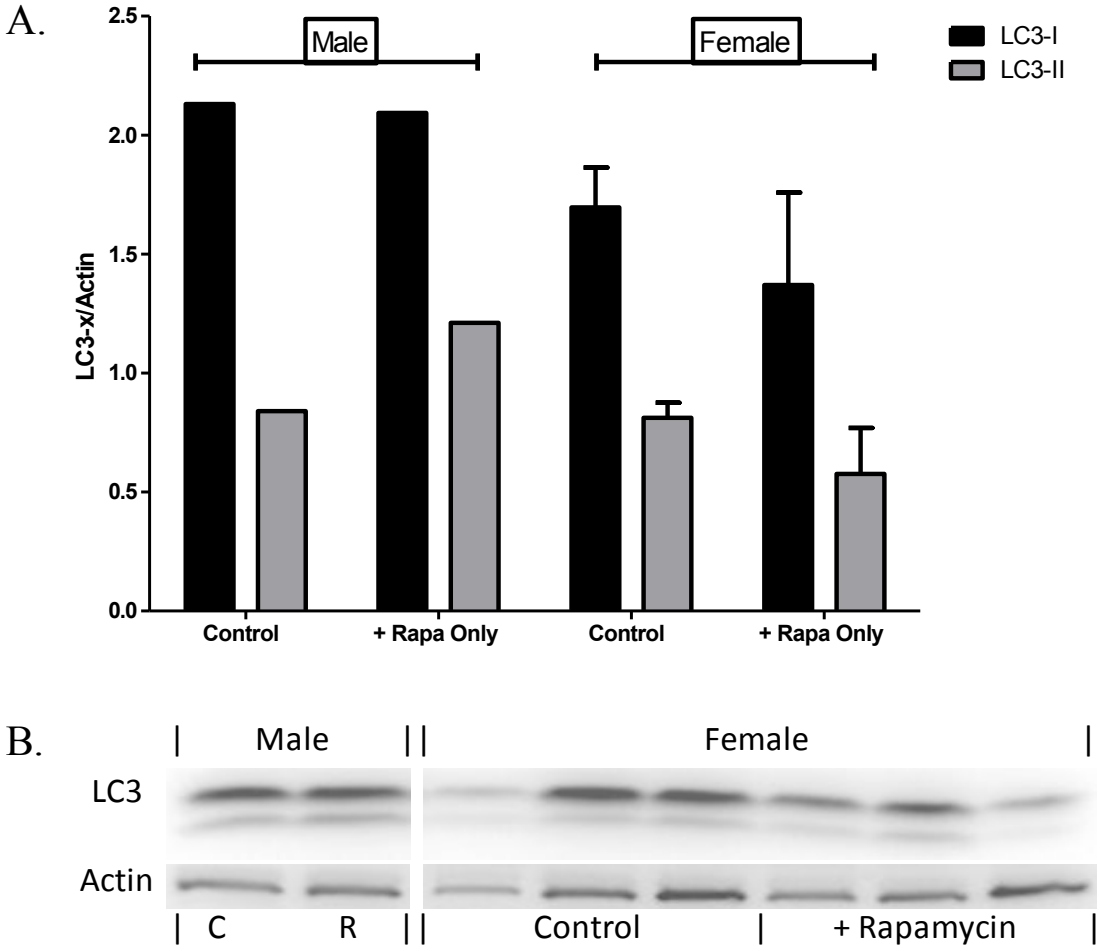

Figure 3.14: Western Blots of Hearts Isolated from the *ex vivo* C57BL/6 Fluormidine Blood Staining Study: (Male & Female Hearts). Young male C57BL/6 mice were injected with 5 μg/kg rapamycin solution for 4.5 hrs (n=1/condition). Additionally, young female C57BL/6 mice were injected with 5 μg/kg rapamycin solution for 4 hrs (n=3/condition). The mice were sacrificed, the hearts removed, and frozen in liquid nitrogen. The hearts were lysed in RIPA buffer and subjected to PAGE, western blot, and probed for LC3 (B). The blots were quantified with ImageJ using actin as a loading control (A).

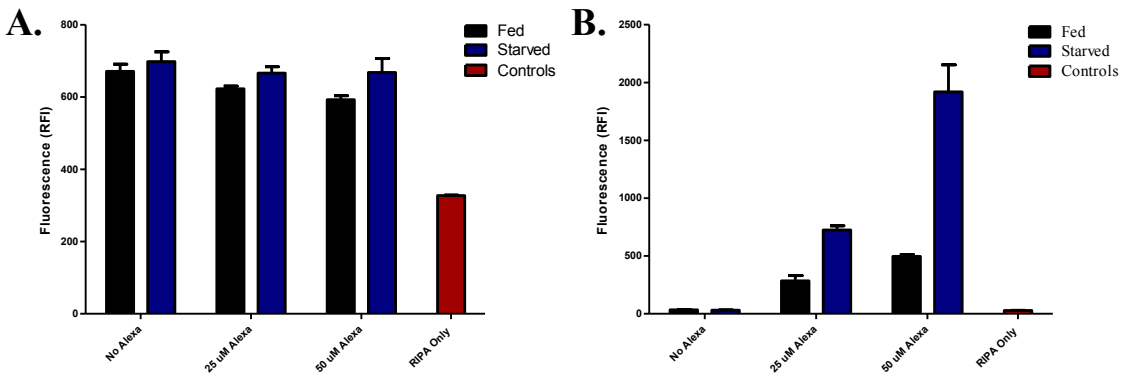

Figure 3.15: Autophagy Detection by Fluormidine using a Spectrofluorometer. 2 x 10^5 cells were plated in a 0.02% gelatin/0.5% fibronectin pre-treated 60 mm dishes and incubated overnight at 37°C/5% CO_2. The cells were washed three times with Complete Media or Krebs Starvation Buffer and incubated 4 hrs at 37°C/5% CO_2. 15 minutes prior to end of assay 25 or 50 µM AlexaFluor-488™-cadaverine was added. 5 minutes prior to assay end, 25 µM spermidine was added to the cells in addition to 1:1000 DAPI (1 mg/mL stock). The cells were washed with PBS and scraped/lysed in ice-cold RIPA Buffer. The lysate was centrifuged and 200 µL of the lysate was loaded into a 96 well glass bottom plate and read for (A) DAPI (excitation = 358 nm, emission = 461 nm) and (B) AlexaFluor-488™-cadaverine (excitation = 495 nm, emission = 519 nm) and fluorescence on a Spectramax Gemini EM spectrofluorometer.

CONCLUSION OF THE DISSERTATION

Autophagy is a cellular process that has been demonstrated to play an important role in an array of age-related diseases such as neurodegenerative disorders[1], muscle disorders[2], cancer[3,4], cardiovascular disease[5], metabolic syndrome[6,7], obesity[7], infection[8-10], and many others. It is generally assumed in the literature that autophagy declines in the murine heart with increasing age. To determine if this is the case, we performed a comprehensive analysis of how changes in autophagy are manifest in the aged by observing both basal and induced or stimulated autophagy and to see if reactive oxygen species (ROS) levels change as a result of changes in autophagy (mitophagy). Originally, we thought that undertaking a direct comparison of the autophagic proteins of C57BL/6 and BALB/c mice (a long-lived versus a short-lived mouse strain) would yield similar profiles, albeit with the short-lived strain displaying similar trends with a more compressed profile, relative to the longer-lived strain. This is most definitely not the case. In fact, we found that there are substantial differences in how autophagy is manifest/regulated in both a strain and age related fashion (BALB/c versus the C57BL/6 mice).

First, we observed substantial strain-related differences between C57BL/6 and BALB/c mice. Overall, the autophagic protein and gene analysis of the BALB/c mice versus the C57BL/6 mice indicated a considerable derangement of the autophagy pathway and its upstream regulatory components in the BALB/c mice, resulting in diminished autophagy in those mice relative to the C57BL/6's. An analysis of the progeny of a C57BL/6 and BALB/c mouse cross revealed an autophagy "phenotype" different from its parental strains.

Second, we observed substantial age-related differences in autophagy in both the C57BL/6 and BALB/c mice. We found that in the aged C57BL/6 heart, basal autophagy declined with age; upon nutrient deprivation (fasting), aged mice demonstrated a delayed increase in autophagy relative to young mice and had impaired autophagic flux. Therefore, there is a definite age-related decline in autophagy in the C57BL/6 mice. In an attempt to rescue or restore autophagy in the aged, we subjected middle-aged C57BL/6 mice to intermittent fasting (twice a week) and found that following three weeks of intermittent fasting, the autophagy marker LC3 was upregulated; however, it returned to baseline levels after six weeks, suggesting the development of compensatory mechanisms to suppress excessive autophagy between fasts. This indicates that intermittent fasting is not a viable means of modulating autophagy over the long-term but may be useful in short-term periodic bouts. Conversely, basal BALB/c mice demonstrated substantial derangement of the autophagy pathway with age, yet demonstrated life-long constitutive autophagy (albeit below the detection threshold of our chloroquine flux assays). Furthermore, the BALB/c fasting studies revealed divergent profiles of protein expression in C57BL/6 and BALB/c with respect to autophagic induction and nucleation proteins (indicating fundamental differences in autophagy regulation between strains) and differences in some of the elongation proteins in the aged versus young BALB/c mice (indicating important rate limiting proteins in the aged response). An intermittent fasting study in the BALB/c mice resulted in a cadre of mice demonstrating pathology in the spleen and lymph nodes, which may be due to the dysregulation of the upstream autophagy regulators, AKT and AMPK.

The larger implications of these findings are four-fold. First, autophagy plays an important role in a variety of diseases, so strain-related differences in autophagy could impact the selection of animal models, interpretation of results, the comparability of data across different strains, and whether studies done in a specific strain can be generalized to the human population. Second, aging mice demonstrate changes in autophagy relative to their younger counterparts (although how those changes are manifest differs between strains), indicating that results obtained from young animals used for experiments concerning age-related diseases (like myocardial infarct or Alzheimer's) may not be applicable to an elderly population. Third, a dietary intervention designed to upregulate autophagy in the aged also showed strain-related differences, with C57BL/6 mice demonstrating a temporary upregulation of autophagy, and BALB/c demonstrating tissue pathology over the long-term. This disparity in outcome between strains subjected to intermittent fasting raises concerns that if autophagic capacity also differs in the far more genetically diverse human population, then disease treatments specifically targeting the autophagic pathway will need to be tailored to the individual.

To that end, we have developed an autophagy detection reagent, which we named Fluormidine, that may prove useful for generating a personalized autophagic profile. It can be used to determine the viability of autophagy modulating compounds or in the treatment of autophagy-associated disease. Fluormidine offers a number of advantages over GFP-LC3 or MDC. It is brighter and more photostable than mono dansyl cadaverine, and does not require transfection. Additionally, Fluormidine is specific for autophagy because: it colocalizes with a known autophagy protein (Rab9): its staining is

abolished in an autophagy knockdown: and varies directly with known autophagy modulators in a variety of cell lines. Fluormidine has been shown to be a viable reagent for use with a variety of different platforms, such as the spectrofluorometer, the fluorescent and confocal microscope, and the flow cytometer. Although early and requiring more testing, Fluormidine appears to be able to quantitatively report on autophagy in the peripheral blood, which could enable the clinician to assess whether a particular drug modulates autophagy, paving the way for therapeutic interventions targeting autophagy as a way to treat a particular disease.

Although myocardial infarction was not the focus of this dissertation, we believe that understanding how autophagy changes in the aged heart will help in the development of therapeutics and cardioprotective interventions that could minimize the tissue damage associated with myocardial ischemia and reperfusion, in part by minimizing ROS levels, which contribute to apoptosis, necrosis, and inflammation.

The excessive ROS in the aged C57BL/6 heart promotes or contributes to the "aging" phenotype via oxidative damage to the various cells in the heart[120] as well as activation of inflammatory signaling pathways through NF-κB and the NLRP3 inflammasome. This study was done as a prelude to a much larger study to establish a link between mitophagy, ROS, and inflammasome activation in the context of the aged, infarcted heart, in order to design interventions to upregulate autophagy and thereby mitigate the tissue damage post-myocardial infarct in the elderly.

INTRODUCTION TO THE APPENDICES

The Appendices consist of the cropped western blots and the graphs of the protein quantifications that were used as source material in the dissertation.

Appendix 1: Age-Related Changes in Autophagy Proteins in a Variety of Murine Tissues in C57BL/6 and BALB/c Mice

The brains, hearts, livers, spleens, thymuses, lymph nodes, and/or lungs of the animals were extracted from 2.5/3 and 24/25 month old (n=3 or n=4) C57BL/6 and BALB/c mice, respectively, were removed and subjected to western blot analysis (See Common Methods – TETN and the Triton X-100 soluble/2%SDS insoluble extraction). Protein expression was normalized to its actin control and significance was established by $p<0.05$ by Student's T Test ($0.01<p<0.05$, $0.001<p<0.01$, or $0.001<p<0.001$ $p<0.05$, $p<0.01$, $p<0.001$, and $p<0.0001$ are denoted by 1, 2, or 3 asterisks, respectively).

Appendix 2: Strain-Related Differences in Young C57Bl/6, BALB/c, and CB6F1/J Mice

The hearts of BALB/c (n=4), C57BL/6 (n=4), and CB6F1/J (n=6, n=5 for Carbonylation Assay) were removed and subjected to western blot analysis as detailed in Common Methods (RIPA extraction). Autophagy protein expression was normalized to its actin control and significance was established by $p<0.05$ by Student's T Test ($0.01<p<0.05$, $0.001<p<0.01$, or $0.001<p<0.001$ $p<0.05$, $p<0.01$, $p<0.001$, and $p<0.0001$ are denoted by 1, 2, or 3 asterisks, respectively).

Appendix 3: Age-Related Differences in the Hearts of Basal Young and Aged C57BL/6 and BALB/c Mice

The expression of autophagy proteins and upstream regulators was determined in the hearts of 2.5-3 vs. 24-25 month old BALB/c and C57BL/6 (n=4) using the western blot protocol in Common Methods (RIPA extraction). Additionally, the samples were subjected to the OxiSelect Protein Carbonyl Immunoblot Kit to determine relative carbonylated protein expression (See Common Methods). Shown are the mean +/- S.E.M. Protein expression was normalized to its actin control and significance was established by Student's T Test ($p<0.05$).

Appendix 4: Autophagy Profiles in the Hearts of Fasting Young and Aged C57BL/6 and BALB/c Mice

LC3 Fasting Assay. The expression of autophagy proteins of 3 and 18 mo C57BL/6 or 3 and 24-25 mo BALB/c mice were fasted for 0, 24, and 48 hrs. Hearts were harvested, homogenized, lysed, and probed for LC3 by western blot (See Common Methods – TETN extraction). Shown are the mean +/- S.E.M. Significance was determined using Student's T Test, with significance set at $0.01<p<0.05$, $0.001<p<0.01$, or $0.001<p<0.001$ are denoted by 1, 2, or 3 asterisks, respectively. Relative level of LC3 indicates the LC3/Actin ratio normalized to non-fasted controls.

The Remainder of Autophagy Proteins: 3 month) and 18 month old C57BL/6 and 3 and 24-25 month old BALB/c mice were fasted for 0, 24, or 48 hrs. Autophagy protein levels were determined (See Common Methods – TETN extraction). Protein levels were

normalized to their respective actin control and the findings in nonfasted control mice were set to the baseline. The non-fasted controls were set to the baseline. Shown are the mean +/- S.E.M.. Significance was established by Student's T Test wherein fasted vs. non-fasted control were compared. ($0.01<p<0.05$, $0.001<p<0.01$, or $0.001<p<0.001$ $p<0.05$, $p<0.01$, $p<0.001$, and $p<0.0001$ are denoted by 1, 2, or 3 asterisks, respectively).

Appendix 5: Autophagic Flux Assays in C57BL/6 and BALB/c Mice

C57BL/6 mice were fasted for 48 hrs (3.5 and 24-25 months old). BALB/c mice were fasted for 24 or 36 hrs. (3.5 and 19 months old - 24 hrs.; 4.5 and 21.5-22 mo - 36 hrs). Four hours prior to the termination of the fast, mice were injected i.p. with either 50 mg/kg chloroquine suspended in phosphate buffered saline or phosphate buffered saline as a control. Hearts were harvested, homogenized, lysed, and probed for LC3 by western blot (See Common Methods). Shown are the mean +/- S.E.M. Significance was determined using Student's T Test comparing chloroquine treated mice with respective untreated controls (**=$p<0.0025$; All other data are not significant).

Appendix 6: Intermittent Fasting in the C57BL/6 and BALB/c Heart

BALB/c Mice: 13 month old (middle aged) mice were subjected to a 24 hr fast twice a week, 5 PM to 5 PM for 4 or 6.5 months. Hearts were harvested, homogenized, lysed, and probed for LC3 by western blot (See Common Methods – TETN extraction).

C57BL/6 Mice: 13 month old mice were subjected to a 24 hr fast twice a week, 5 PM to 5 PM for 6.7 months. Following a 3, 6, or 16 weeks of IF, mice were sacrificed 3

days following their last fast (n=5 AL and IF), hearts removed, and probed for LC3-II by western blot (See Common Methods).

Following 25 weeks of IF, mice were fasted 24 hrs and injected with 50 mg/kg chloroquine or PBS i.p. to determine autophagic flux (n=4). 4 hrs later mice were sacrificed, hearts removed, and LC3-II was analyzed by western blot (See Common Methods).

APPENDIX 1:

Age-Related Changes in Autophagy Proteins in a Variety of Murine Tissues in C57BL/6 and BALB/c Mice

C57BL/6 Brain

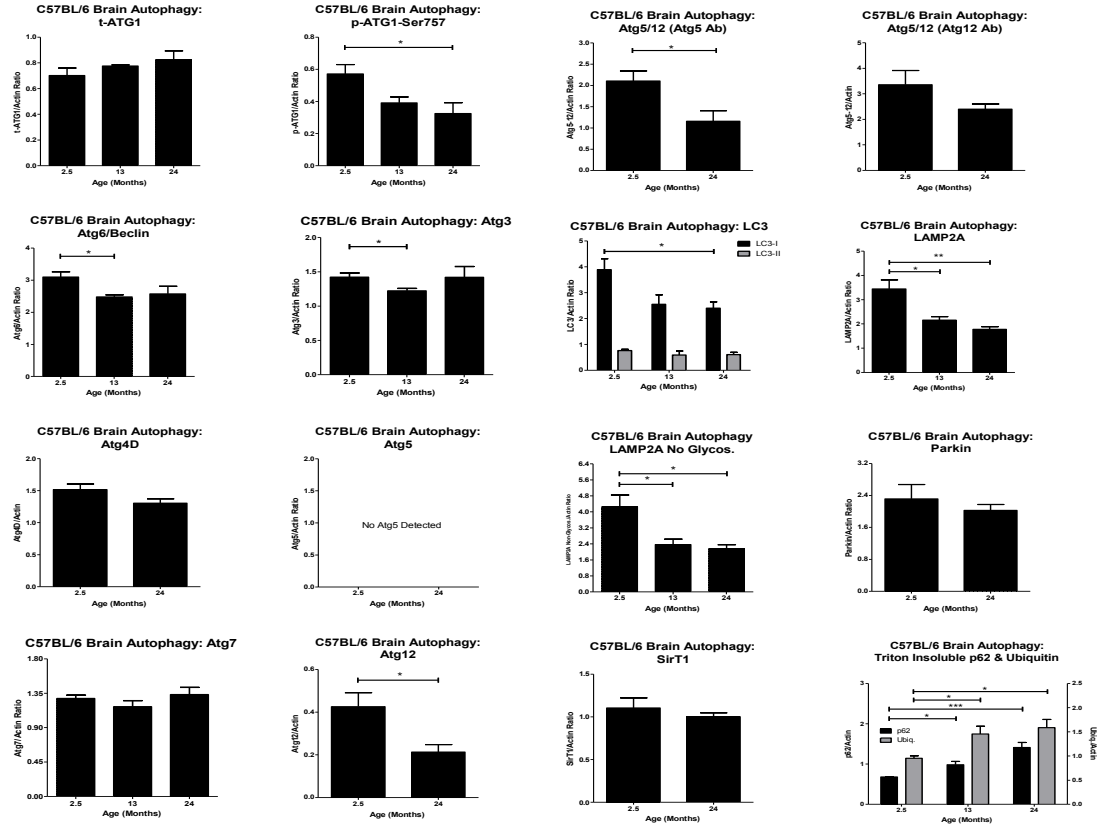

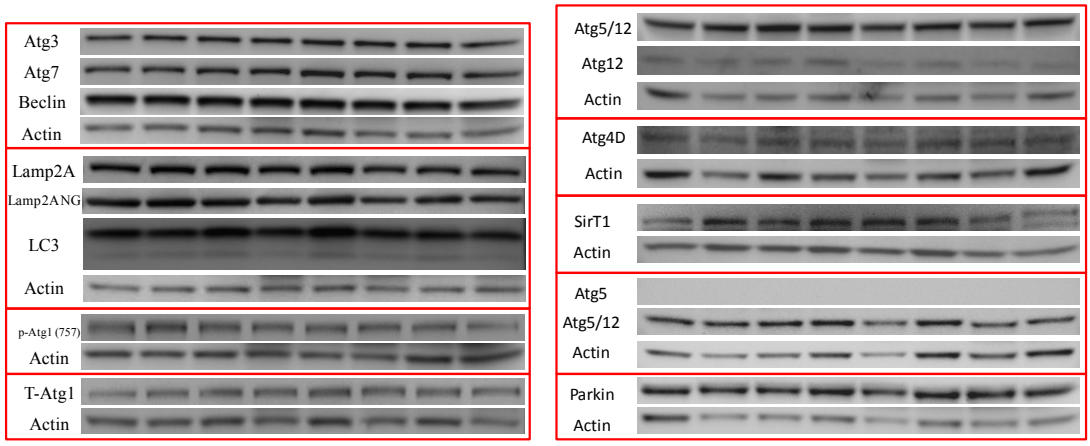

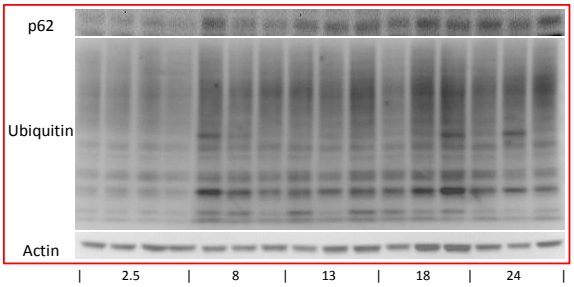

C57BL/6 Liver

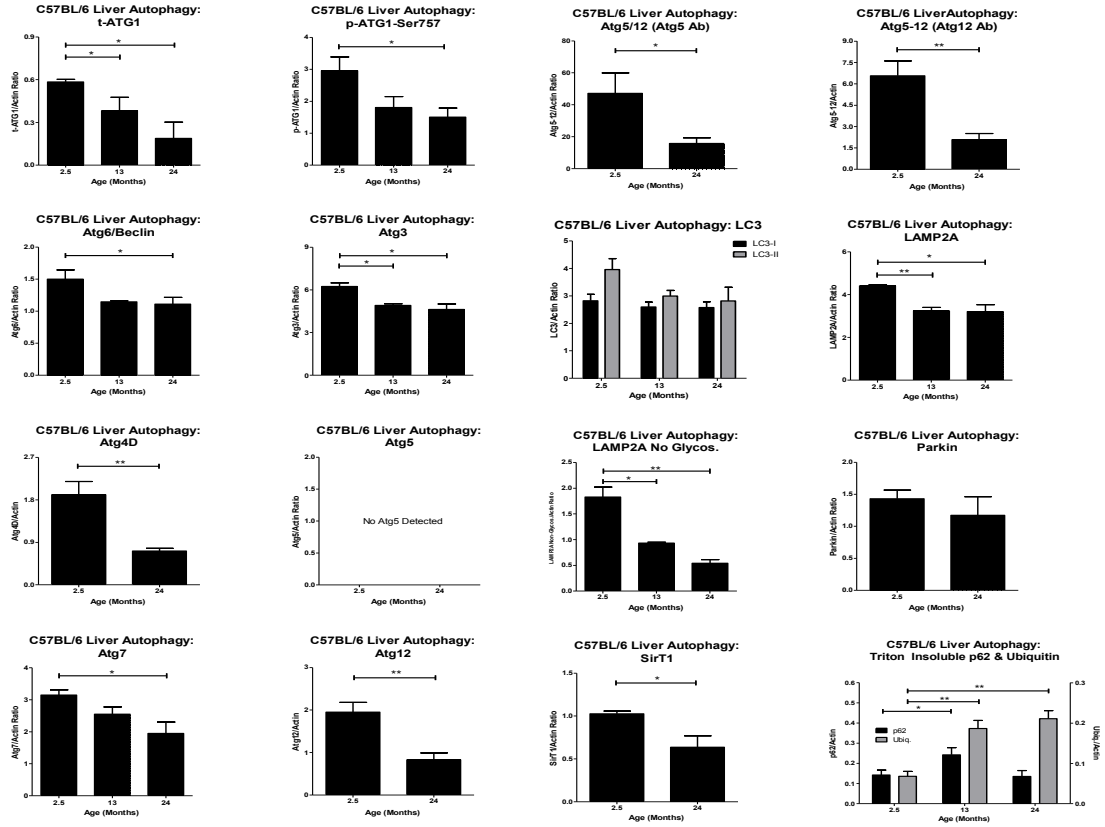

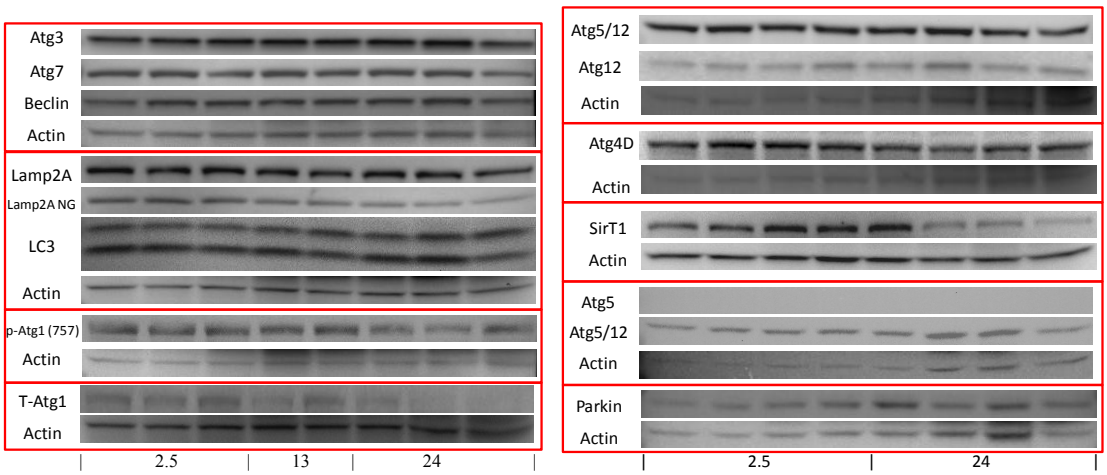

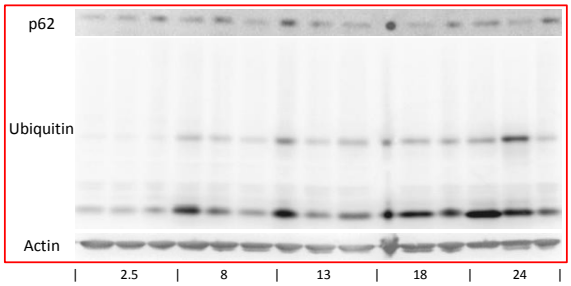

C57BL/6 Spleen

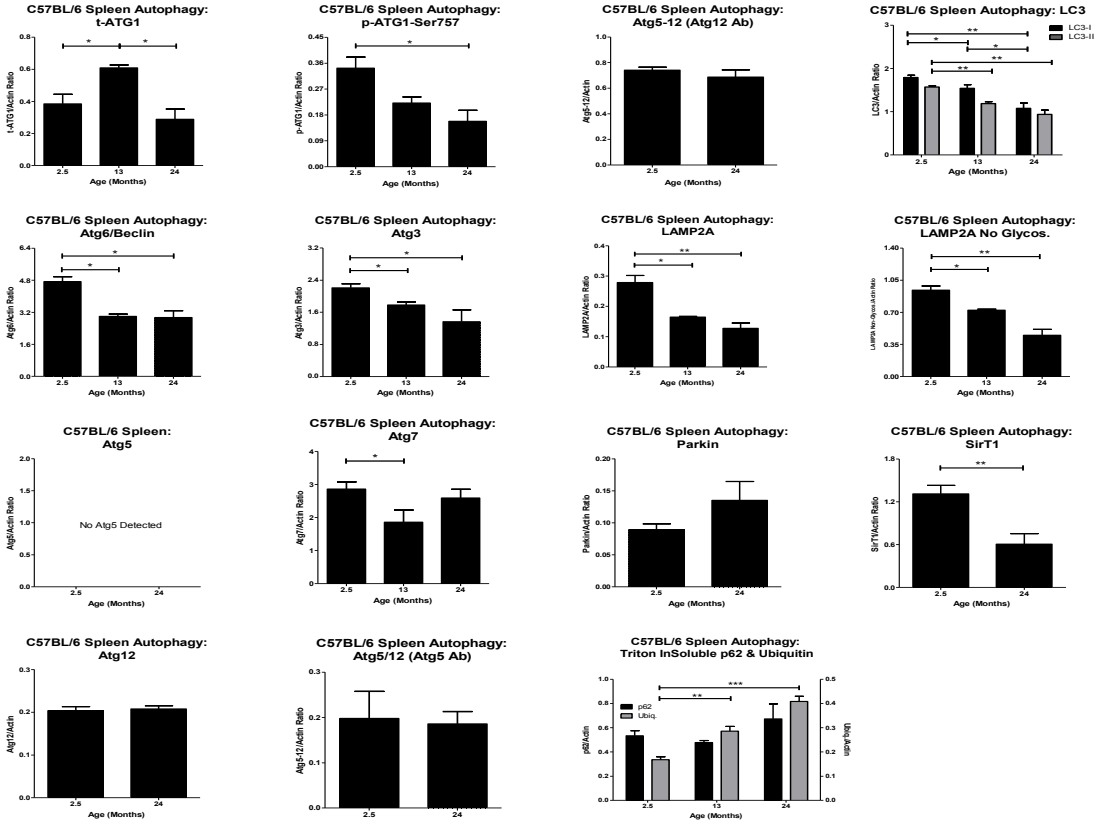

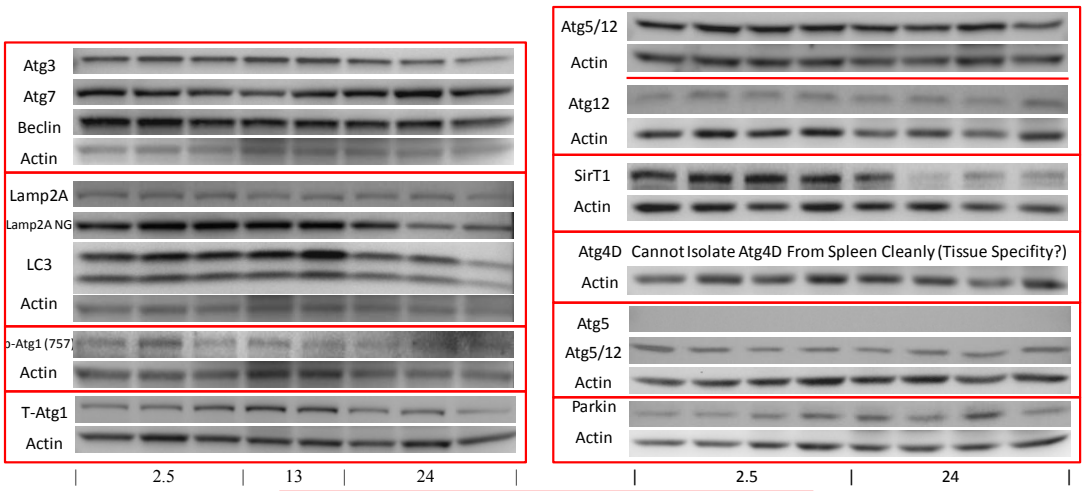

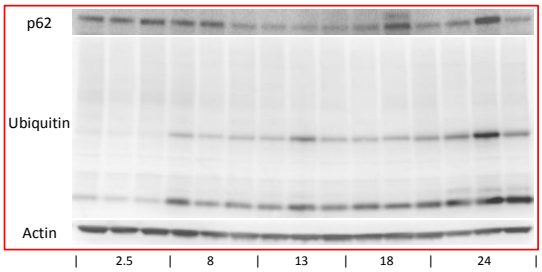

C57BL/6 Thymus

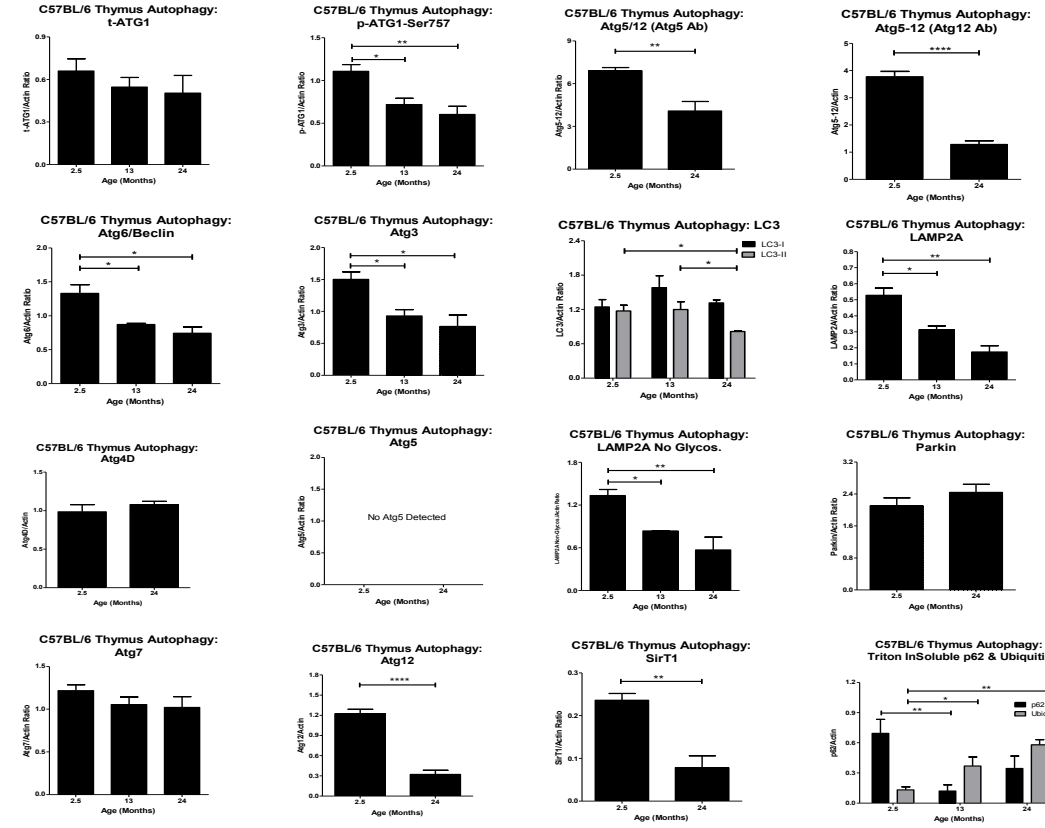

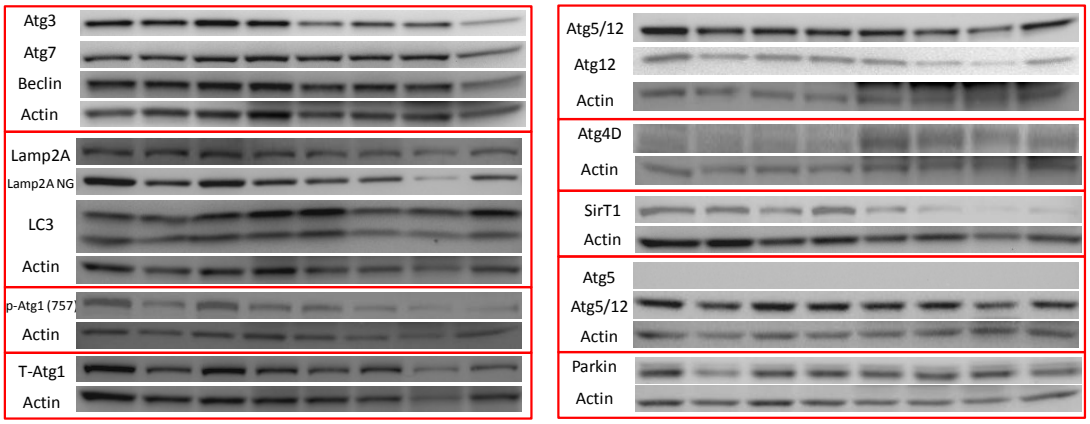

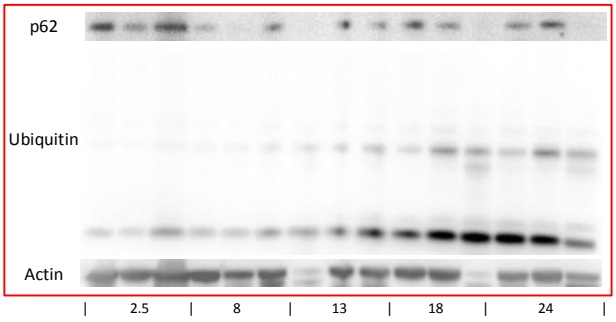

C57BL/6 Lymph Node

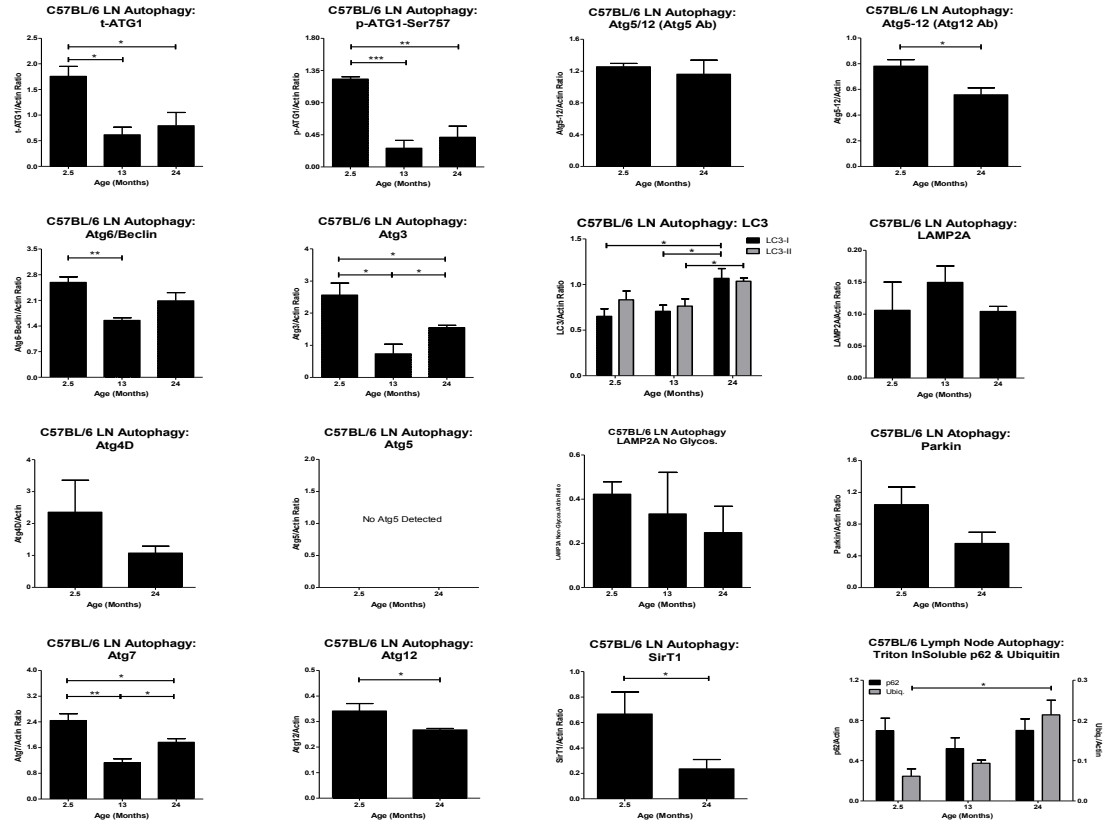

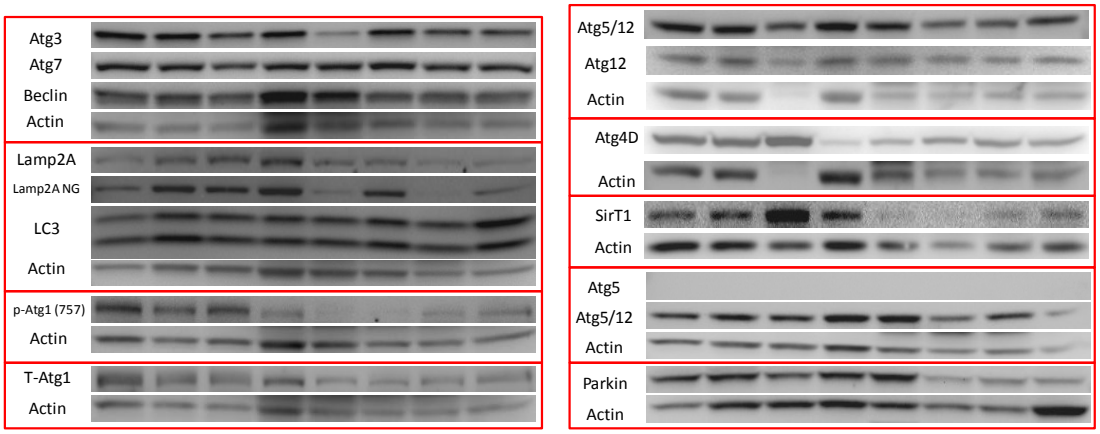

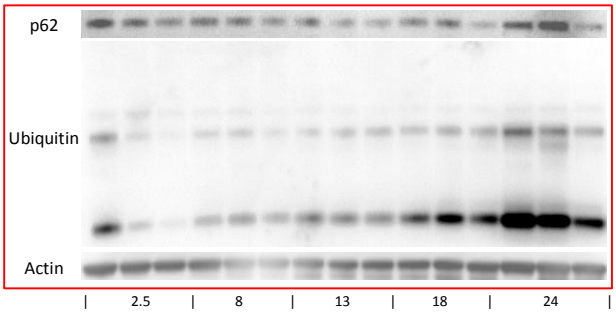

C57BL/6 Lung

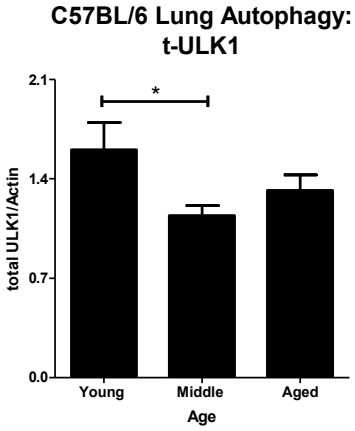
C57BL/6 Lung Autophagy:
t-ULK1
total ULK1/Actin
2.1
1.4
0.7
0.0
*
Young
Middle
Aged
Age

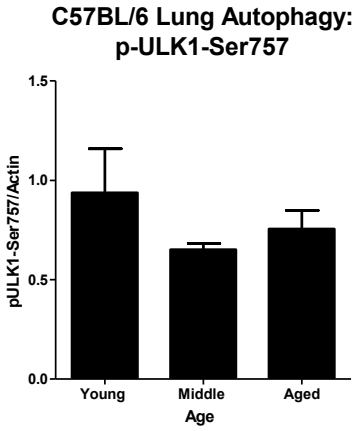
C57BL/6 Lung Autophagy:
p-ULK1-Ser757
pULK1-Ser757/Actin
1.5
1.0
0.5
0.0
Young
Middle
Aged
Age

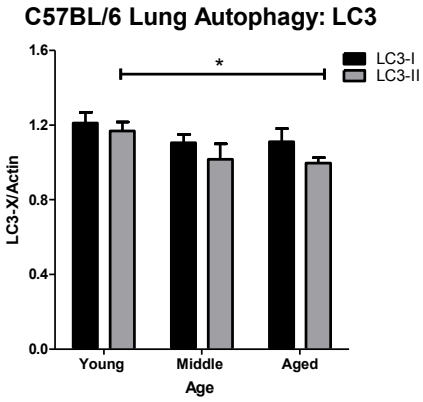
C57BL/6 Lung Autophagy: LC3
LC3-X/Actin
1.6
1.2
0.8
0.4
0.0
*
LC3-I
LC3-II
Young
Middle
Aged
Age

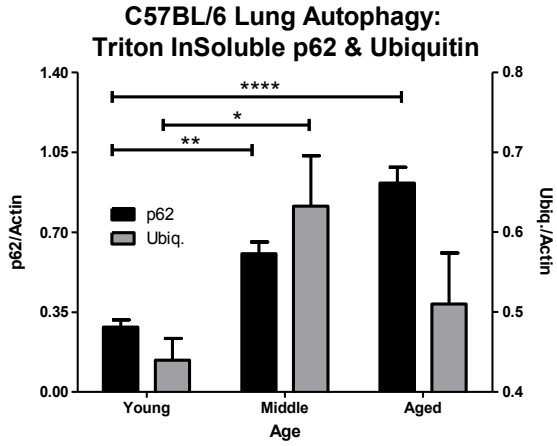
C57BL/6 Lung Autophagy:
Triton InSoluble p62 & Ubiquitin
p62/Actin
Ubiq./Actin
1.40
1.05
0.70
0.35
0.00
0.8
0.7
0.6
0.5
0.4
****
*
**
p62
Ubiq.
Young
Middle
Aged
Age

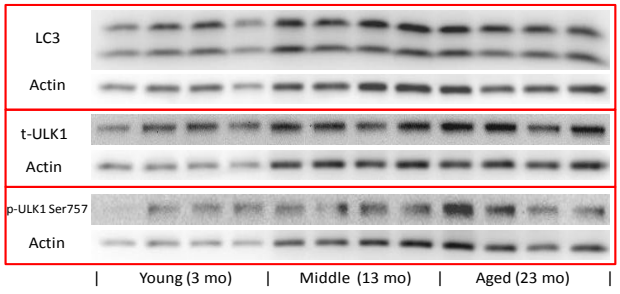
LC3
Actin
t-ULK1
Actin
p-ULK1 Ser757
Actin
Young (3 mo)
Middle (13 mo)
Aged (23 mo)

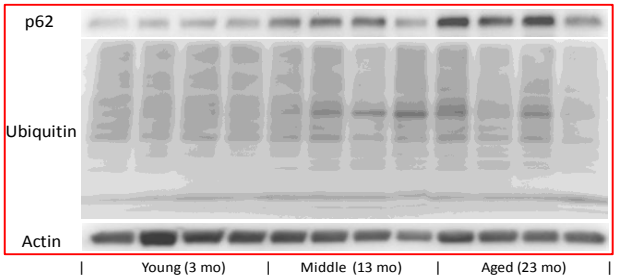
p62
Ubiquitin
Actin
Young (3 mo)
Middle (13 mo)
Aged (23 mo)

BALB/c Brain

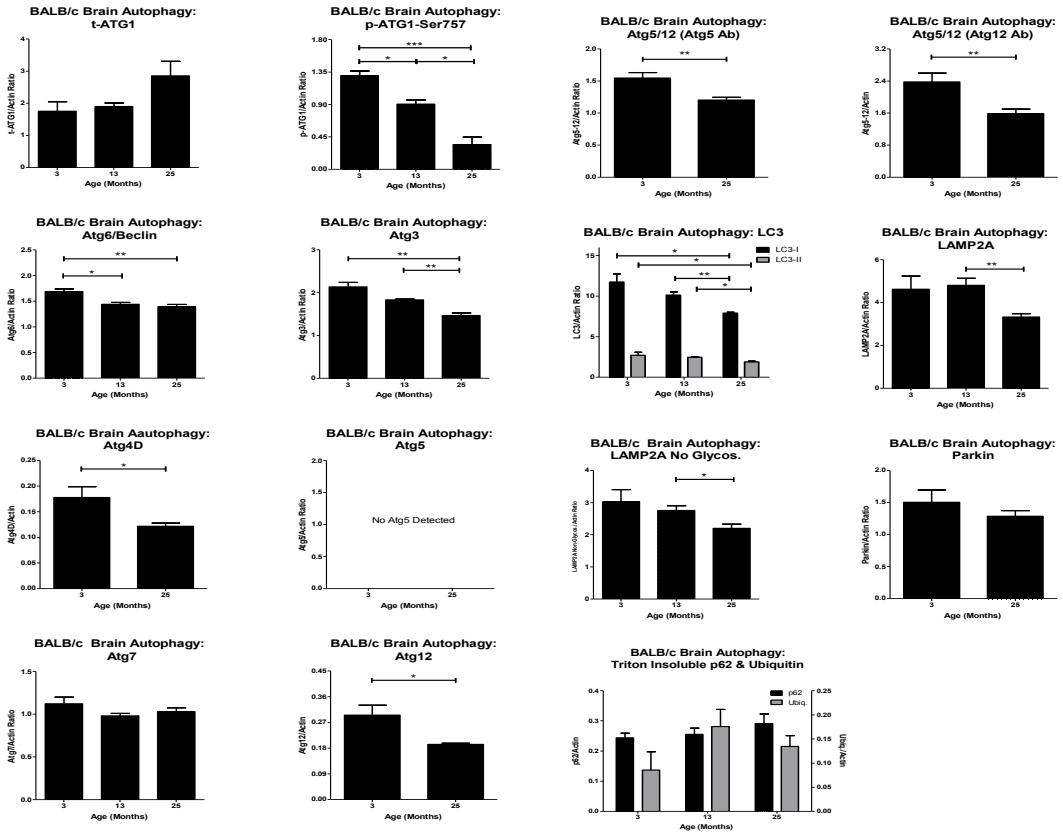
BALB/c Brain Autophagy: t-ATG1
BALB/c Brain Autophagy: p-ATG1-Ser757
BALB/c Brain Autophagy: Atg5/12 (Atg5 Ab)
BALB/c Brain Autophagy: Atg5/12 (Atg12 Ab)
BALB/c Brain Autophagy: Atg6/Beclin
BALB/c Brain Autophagy: Atg3
BALB/c Brain Autophagy: LC3
LC3-I
LC3-II
BALB/c Brain Autophagy: LAMP2A
BALB/c Brain Aautophagy: Atg4D
BALB/c Brain Autophagy: Atg5
No Atg5 Detected
BALB/c Brain Autophagy: LAMP2A No Glycos.
BALB/c Brain Autophagy: Parkin
BALB/c Brain Autophagy: Atg7
BALB/c Brain Autophagy: Atg12
BALB/c Brain Autophagy: Triton Insoluble p62 & Ubiquitin
p62
Ubiq.
Age (Months)

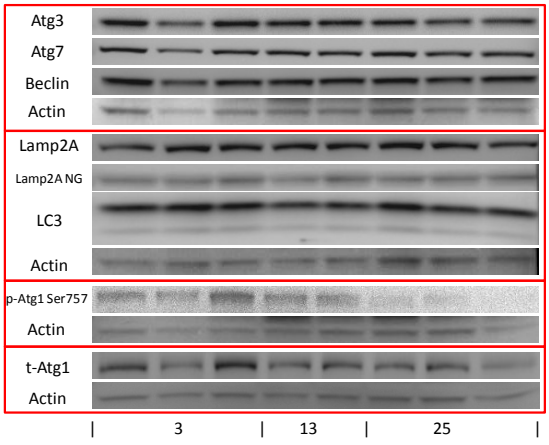
Atg3
Atg7
Beclin
Actin
Lamp2A
Lamp2A NG
LC3
Actin
p-Atg1 Ser757
Actin
t-Atg1
Actin
3
13
25

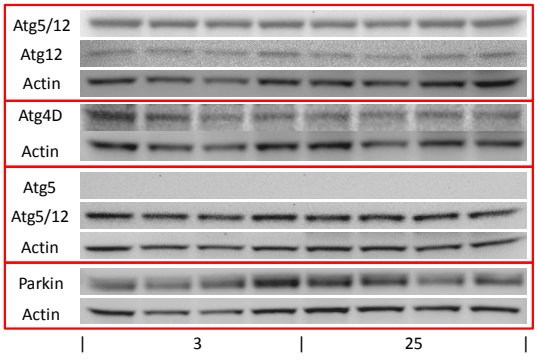
Atg5/12
Atg12
Actin
Atg4D
Actin
Atg5
Atg5/12
Actin
Parkin
Actin
3
25

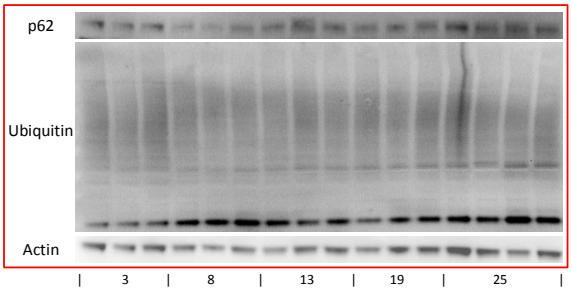
p62
Ubiquitin
Actin
3
8
13
19
25

BALB/c Liver

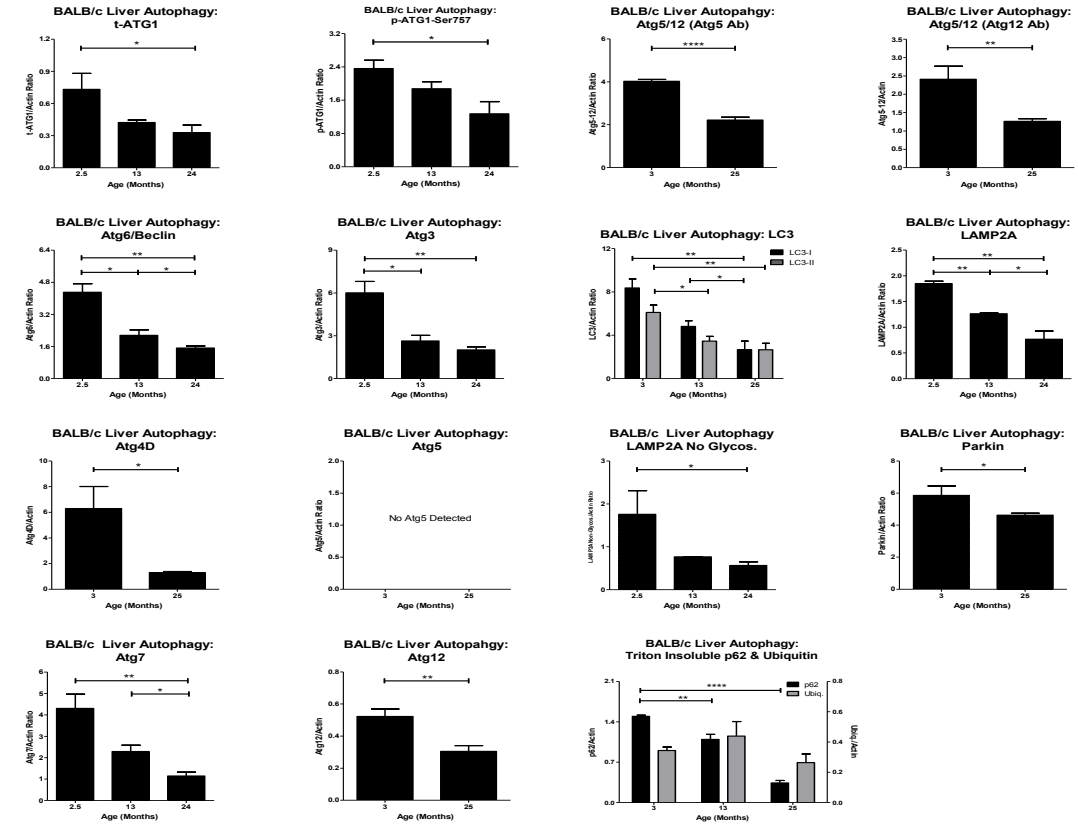
BALB/c Liver Autophagy: t-ATG1
BALB/c Liver Autophagy: p-ATG1-Ser757
BALB/c Liver Autopahgy: Atg5/12 (Atg5 Ab)
BALB/c Liver Autophagy: Atg5/12 (Atg12 Ab)
BALB/c Liver Autophagy: Atg6/Beclin
BALB/c Liver Autophagy: Atg3
BALB/c Liver Autophagy: LC3
BALB/c Liver Autophagy: LAMP2A
BALB/c Liver Autophagy: Atg4D
BALB/c Liver Autophagy: Atg5
No Atg5 Detected
BALB/c Liver Autophagy LAMP2A No Glycos.
BALB/c Liver Autophagy: Parkin
BALB/c Liver Autophagy: Atg7
BALB/c Liver Autopahgy: Atg12
BALB/c Liver Autophagy: Triton Insoluble p62 & Ubiquitin
Age (Months)

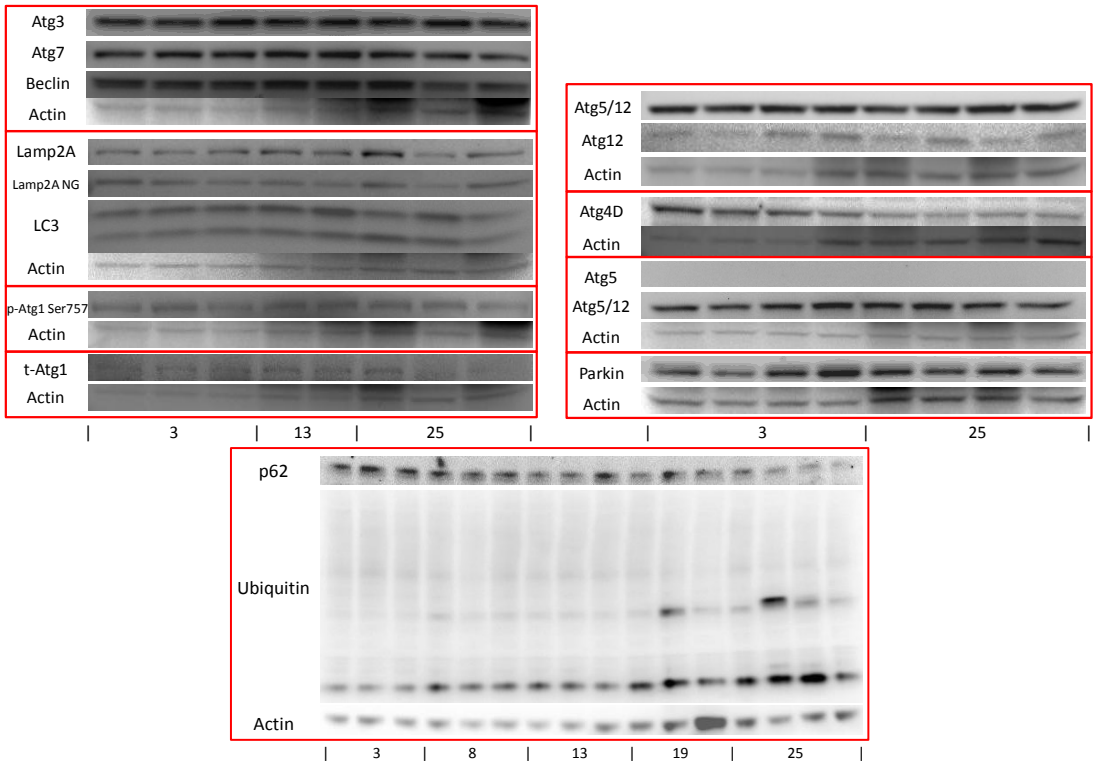
Atg3
Atg7
Beclin
Actin
Lamp2A
Lamp2A NG
LC3
Actin
p-Atg1 Ser757
Actin
t-Atg1
Actin
Atg5/12
Atg12
Actin
Atg4D
Actin
Atg5
Atg5/12
Actin
Parkin
Actin
3
13
25
3
25

p62
Ubiquitin
Actin
3
8
13
19
25

BALB/c Spleen

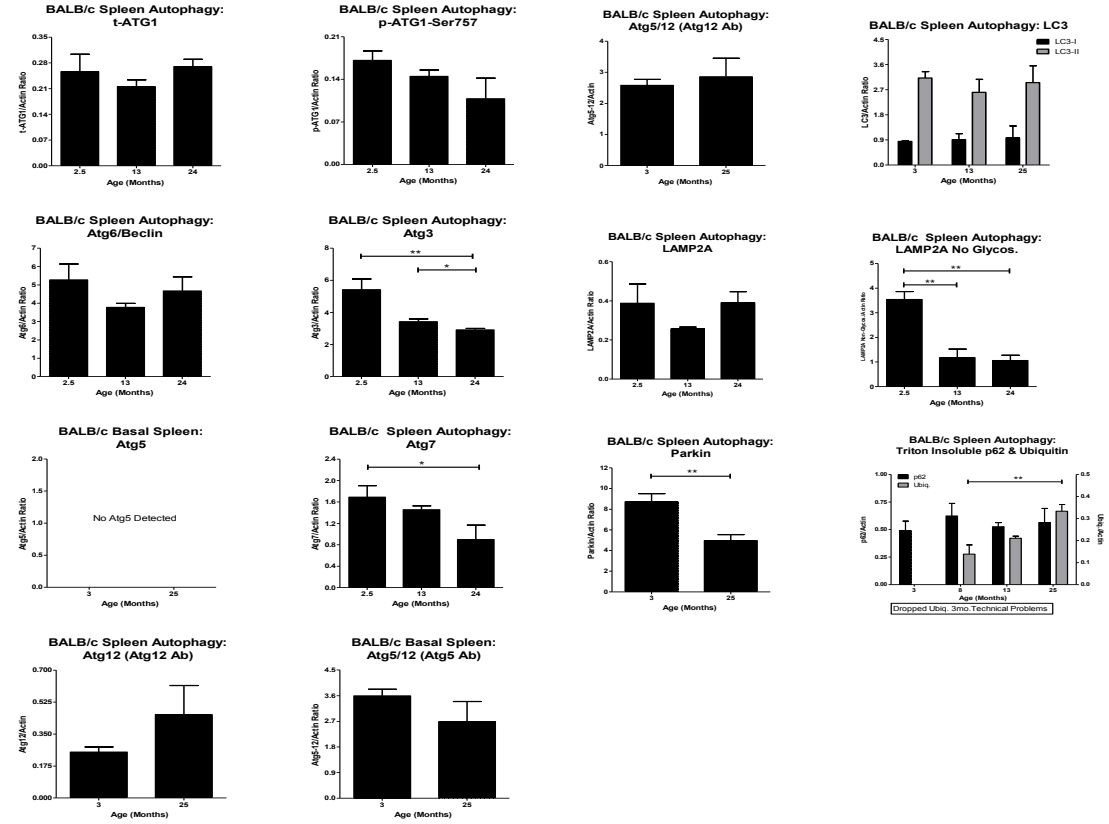

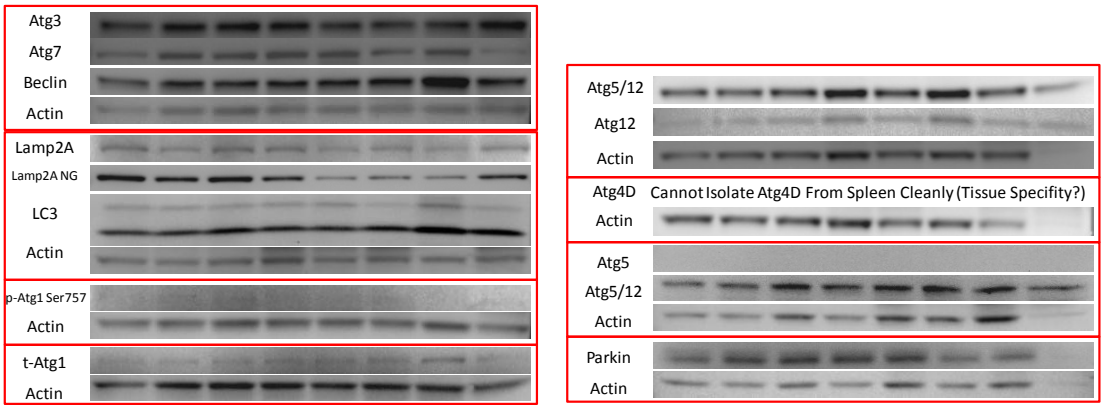

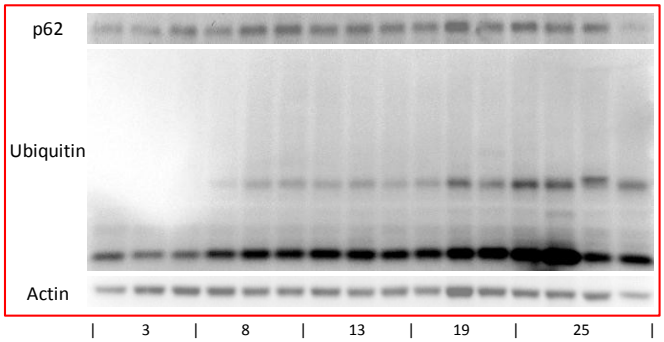

BALB/c Thymus

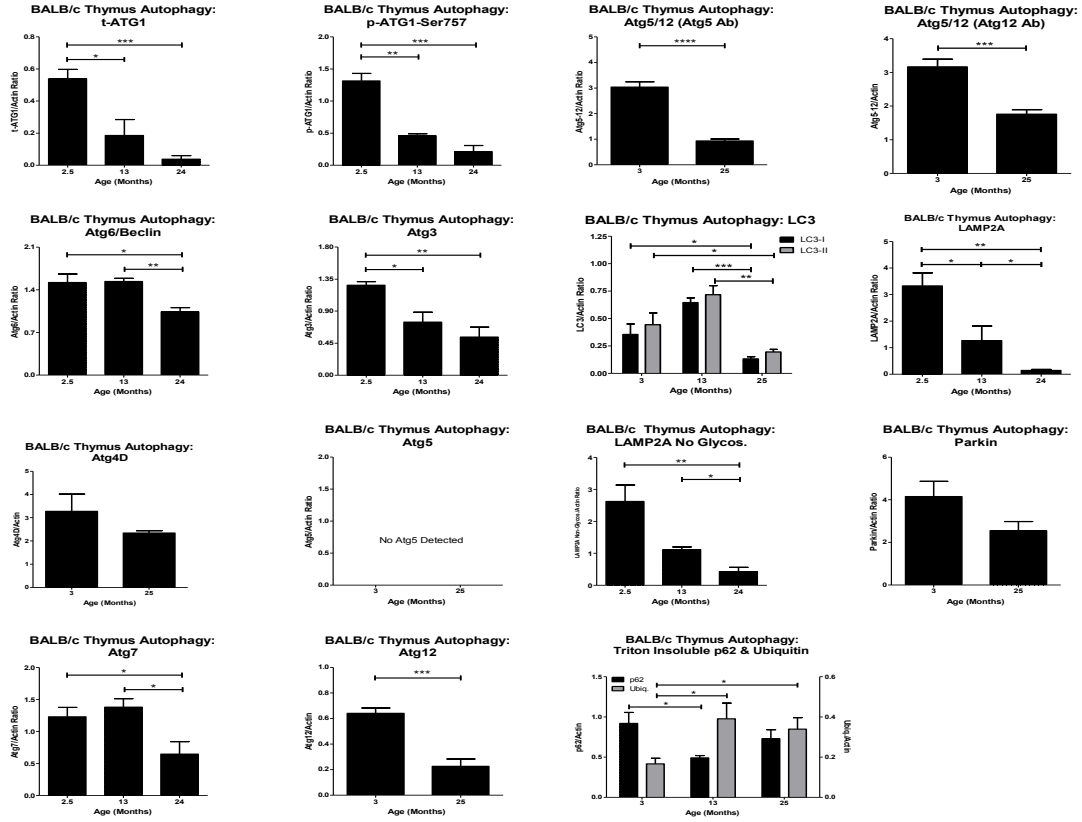

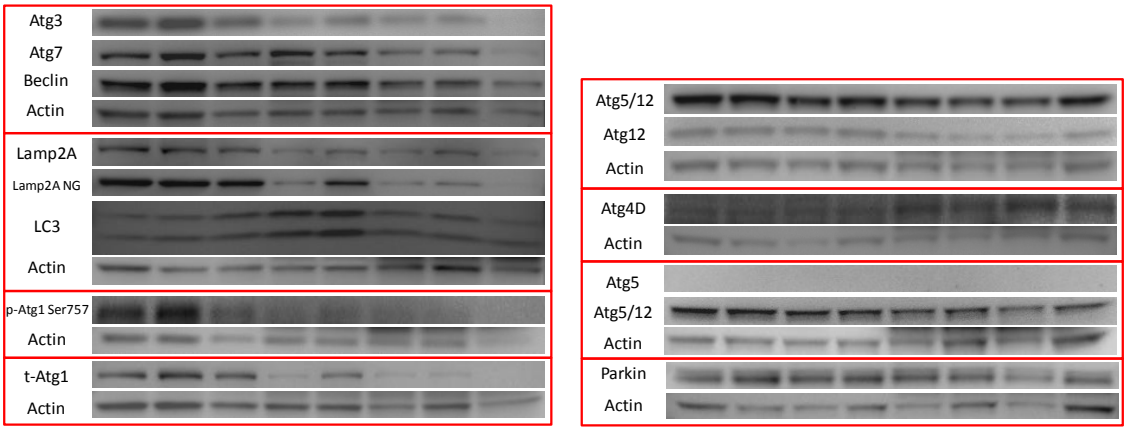

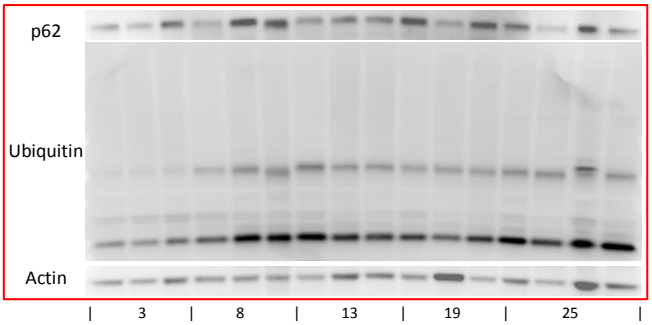

BALB/c Lymph Node

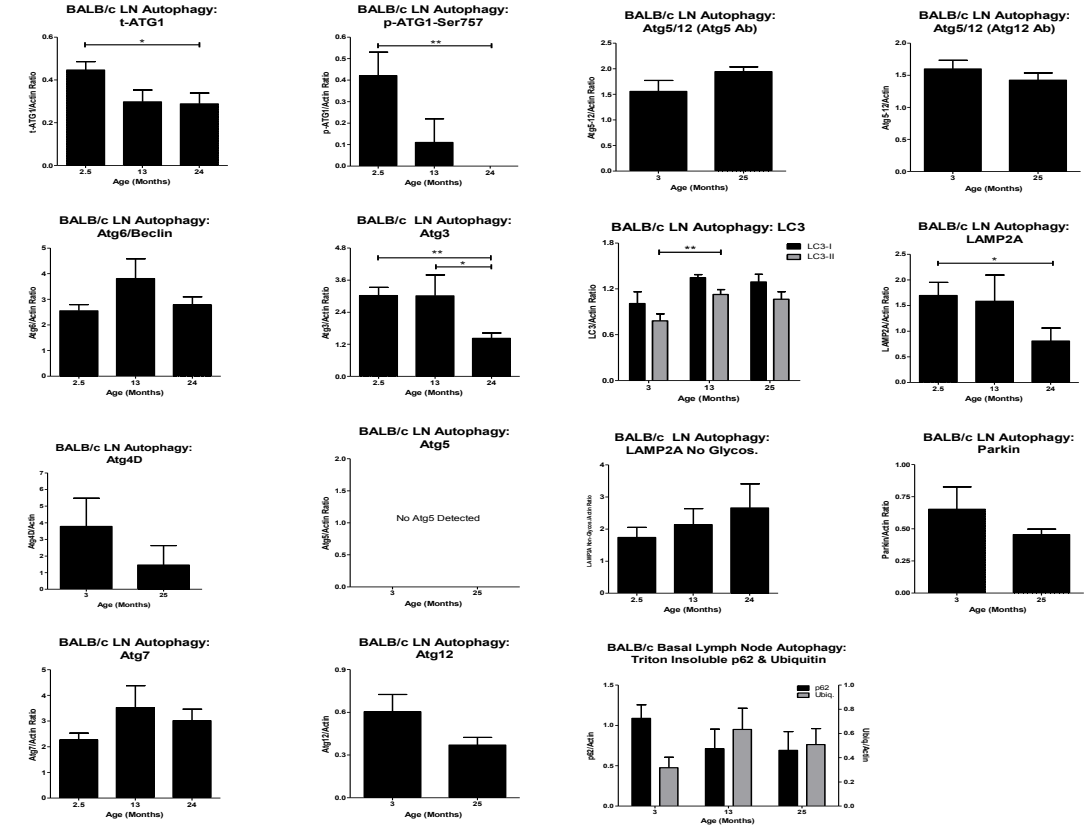

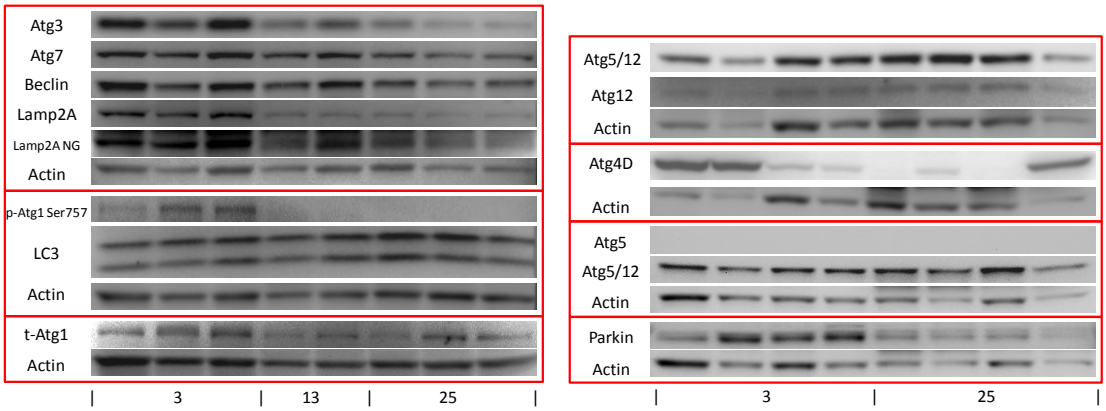

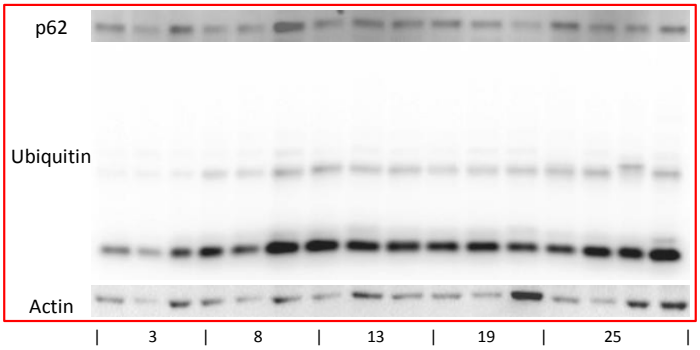

BALB/c Lung

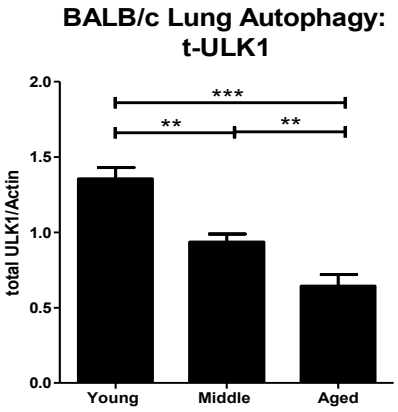
BALB/c Lung Autophagy:
t-ULK1
total ULK1/Actin
2.0
1.5
1.0
0.5
0.0
***
**
**
Young
Middle
Aged

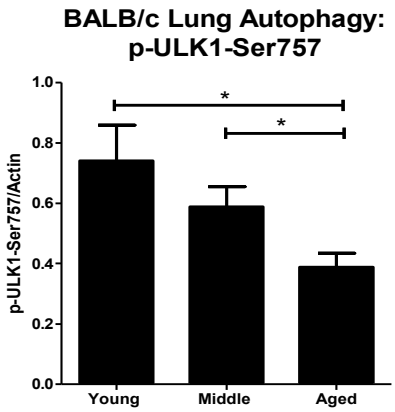
BALB/c Lung Autophagy:
p-ULK1-Ser757
p-ULK1-Ser757/Actin
1.0
0.8
0.6
0.4
0.2
0.0
*
*
Young
Middle
Aged

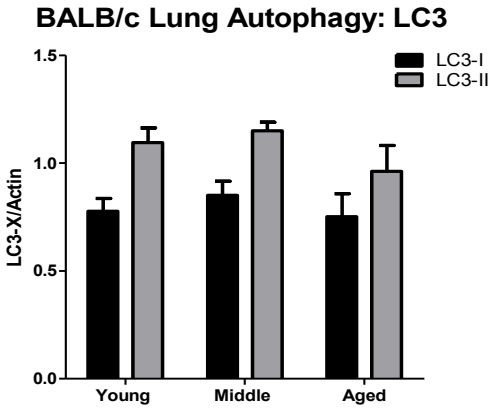
BALB/c Lung Autophagy: LC3
LC3-I
LC3-II
LC3-X/Actin
1.5
1.0
0.5
0.0
Young
Middle
Aged

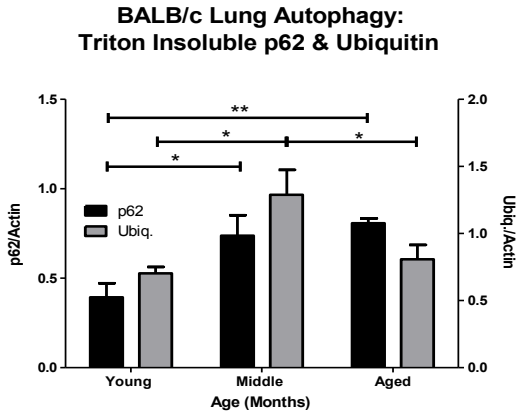
BALB/c Lung Autophagy:
Triton Insoluble p62 & Ubiquitin
p62
Ubiq.
p62/Actin
Ubiq./Actin
1.5
1.0
0.5
0.0
2.0
1.5
1.0
0.5
0.0
**
*
*
*
Young
Middle
Aged
Age (Months)

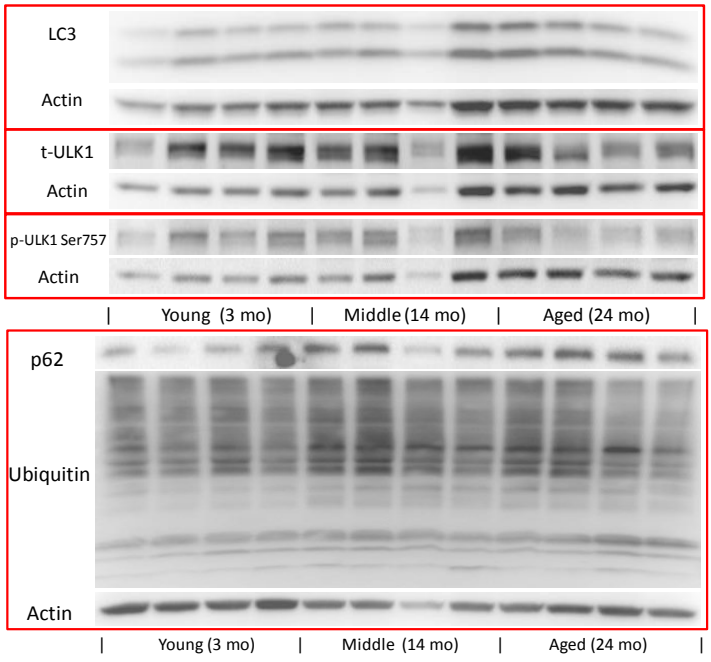
LC3
Actin
t-ULK1
Actin
p-ULK1 Ser757
Actin
Young (3 mo)
Middle (14 mo)
Aged (24 mo)
p62
Ubiquitin
Actin
Young (3 mo)
Middle (14 mo)
Aged (24 mo)

APPENDIX 2:

Strain-Related Differences in Young C57Bl/6, BALB/c, and CB6F1/J Mice

C57BL/6, BALB/c, and CB6F1/J Young Autophagy Profile

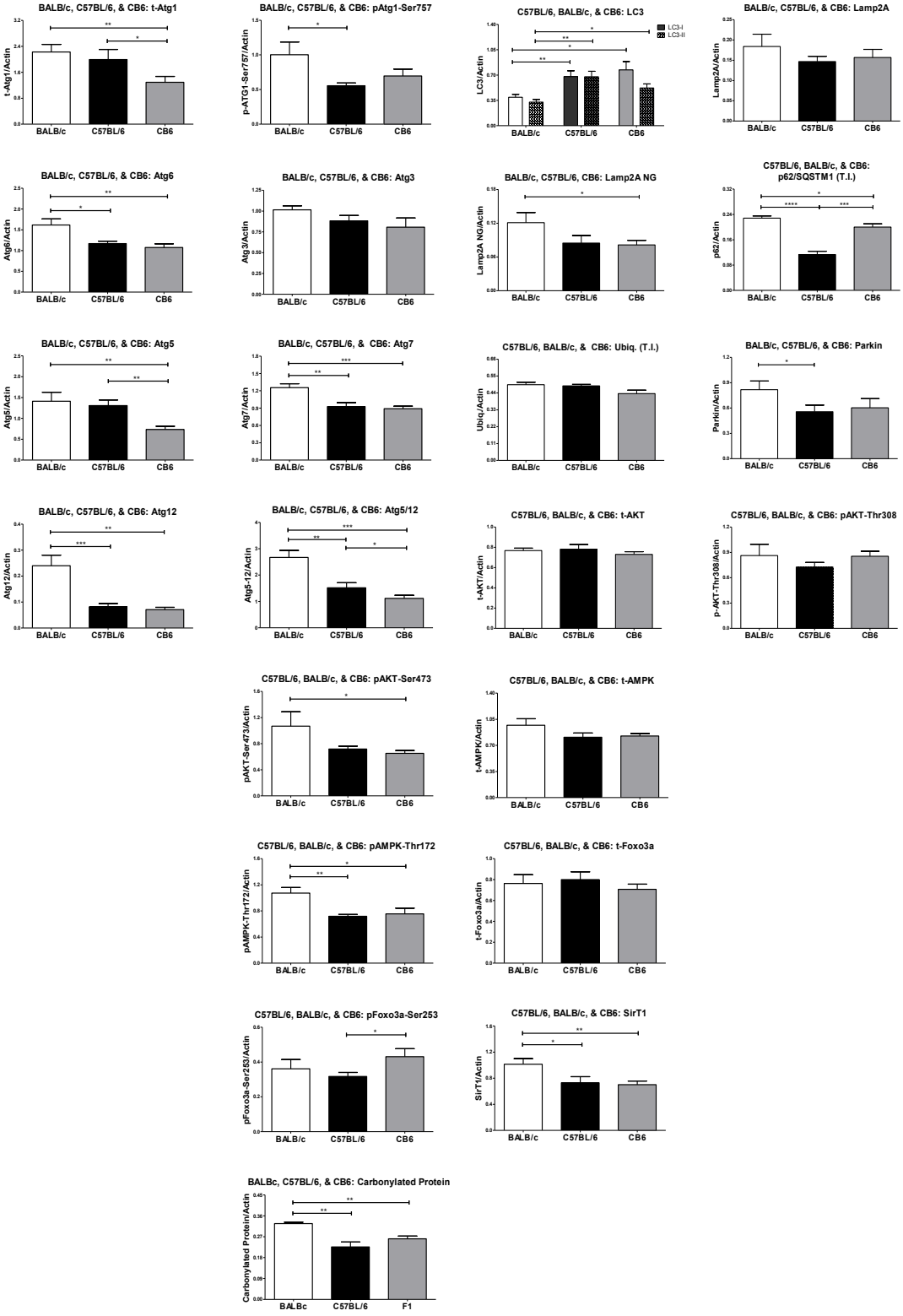

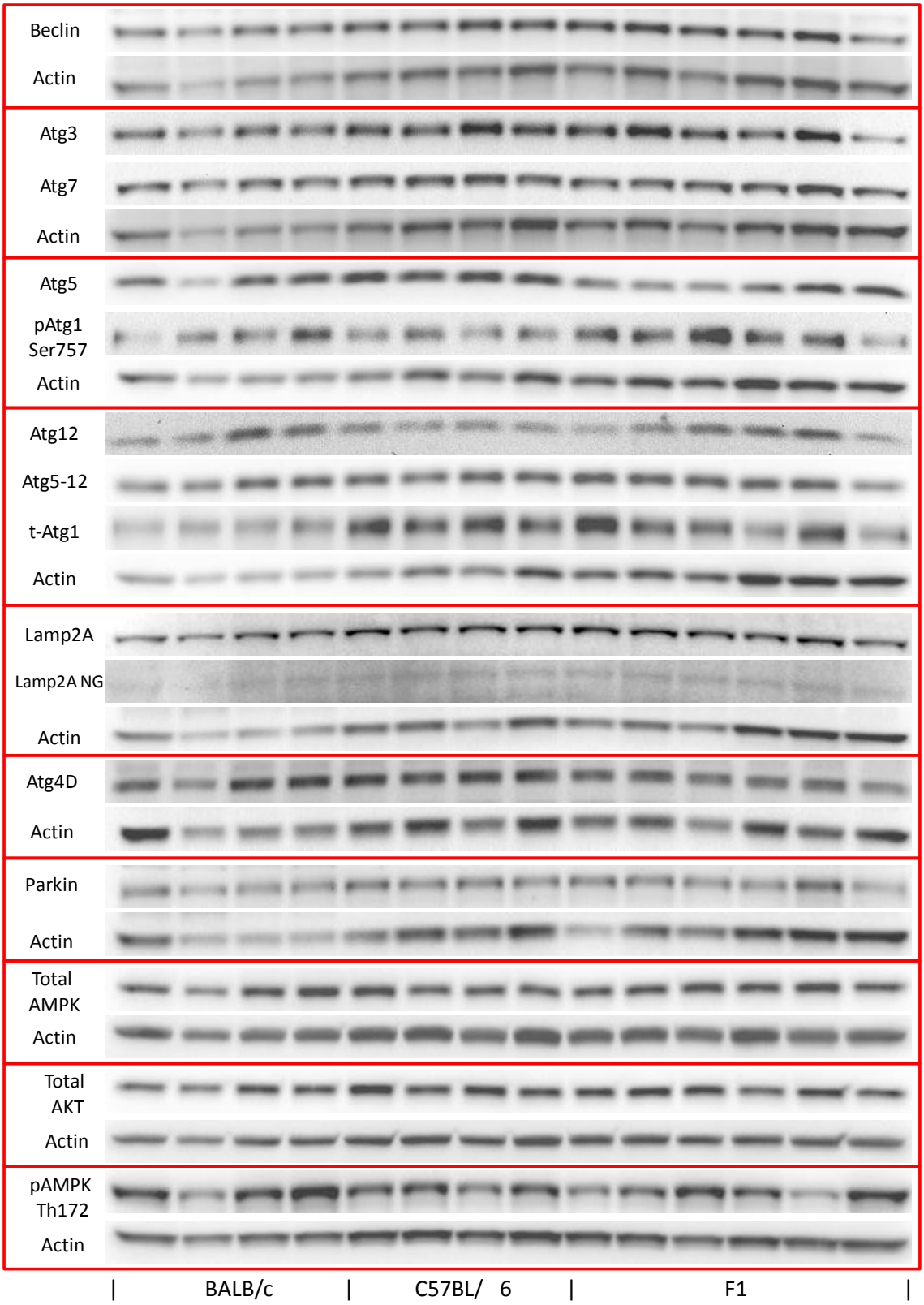
Beclin
Actin
Atg3
Atg7
Actin
Atg5
pAtg1 Ser757
Actin
Atg12
Atg5-12
t-Atg1
Actin
Lamp2A
Lamp2A NG
Actin
Atg4D
Actin
Parkin
Actin
Total AMPK
Actin
Total AKT
Actin
pAMPK Th172
Actin
BALB/c
C57BL/ 6
F1

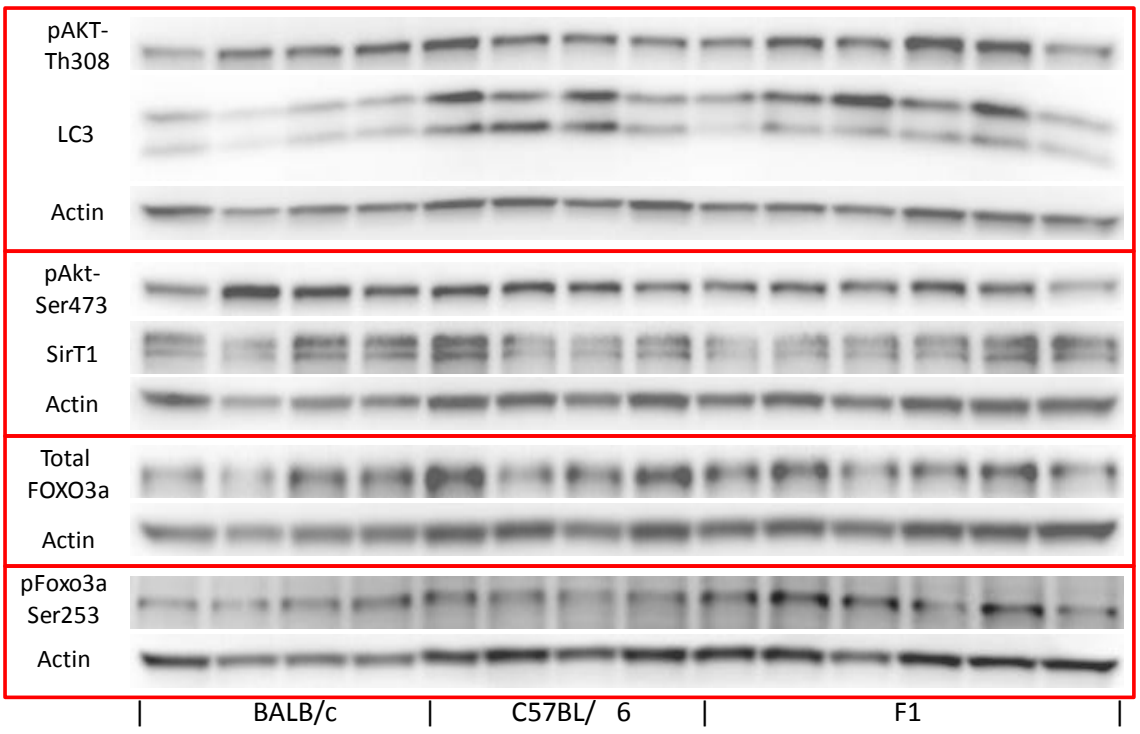
pAKT-Th308
LC3
Actin
pAkt-Ser473
SirT1
Actin
Total FOXO3a
Actin
pFoxo3a Ser253
Actin
BALB/c
C57BL/ 6
F1

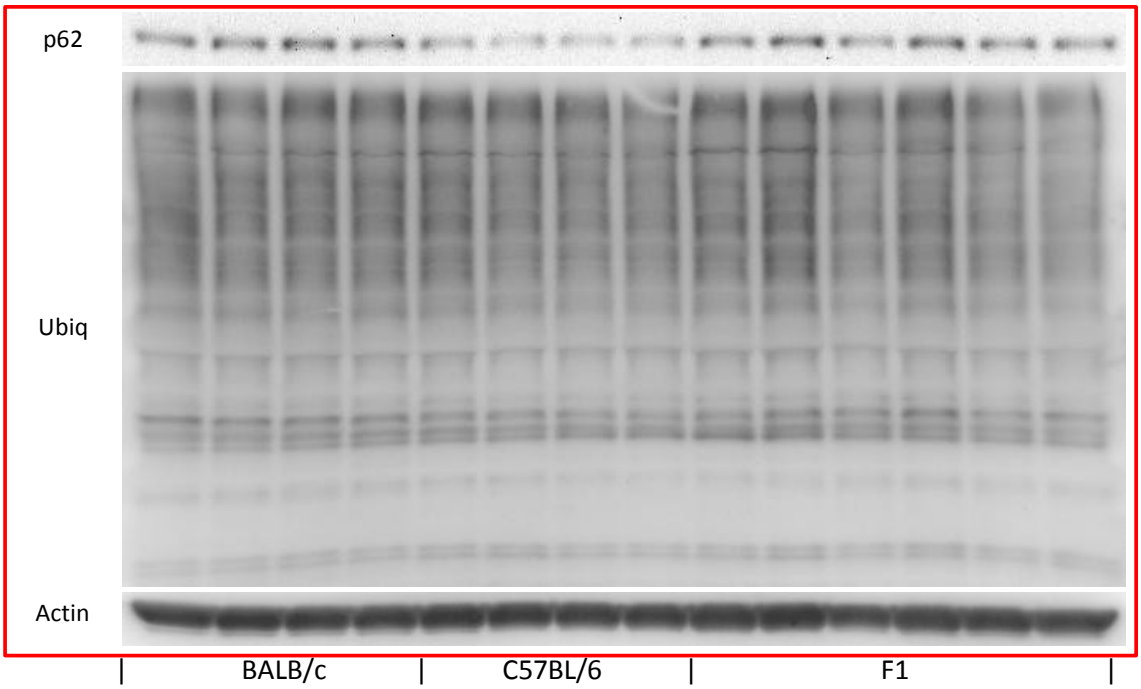
p62
Ubiq
Actin
BALB/c
C57BL/6
F1

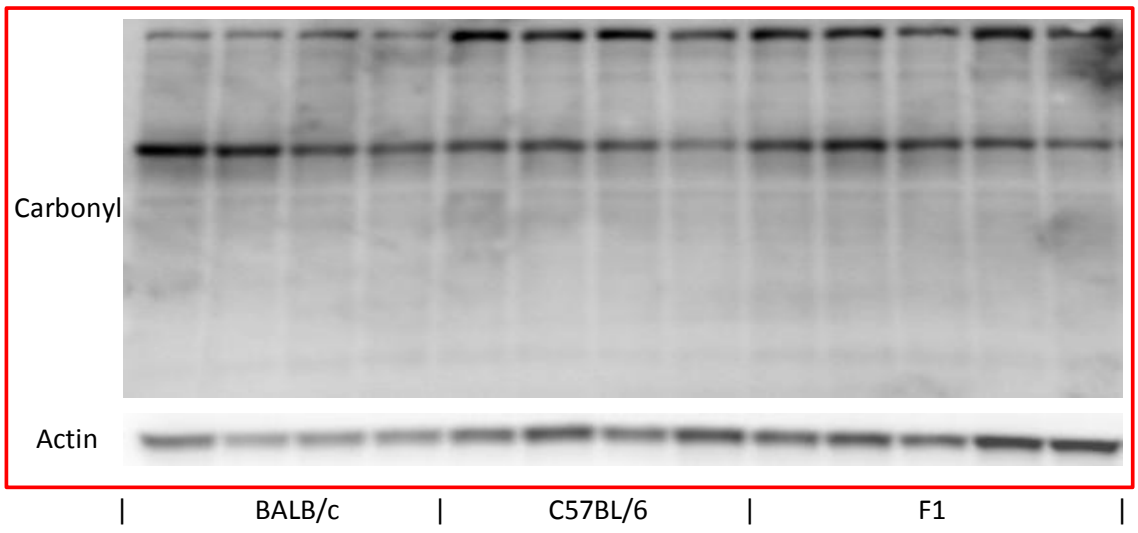
Carbonyl
Actin
| BALB/c | C57BL/6 | F1 |

APPENDIX 3:

Age-Related Differences in the Hearts of Basal Young and Aged C57BL/6 and BALB/c Mice

C57BL/6 Heart

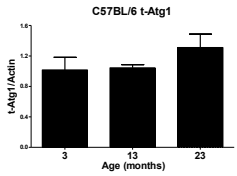

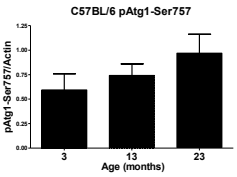

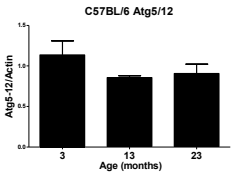

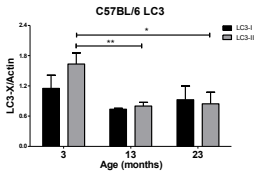

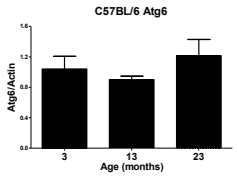

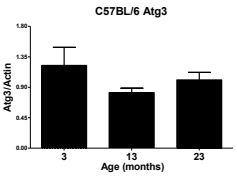

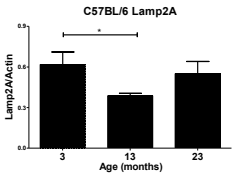

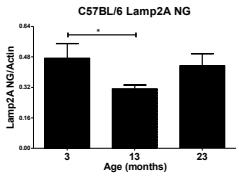

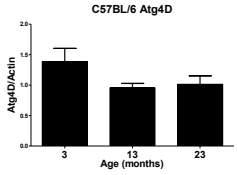

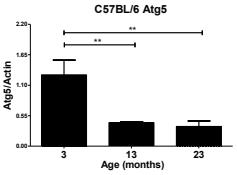

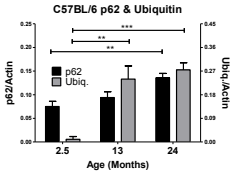

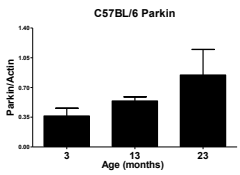

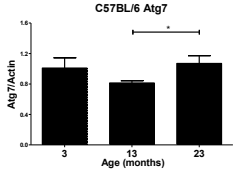

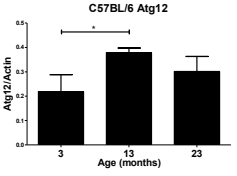

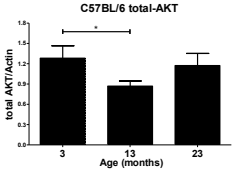

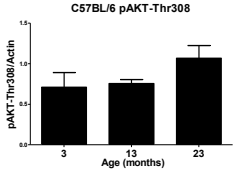

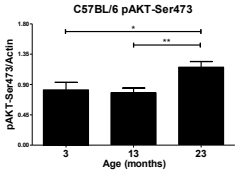

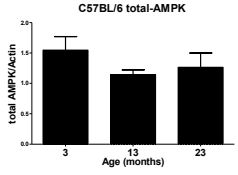

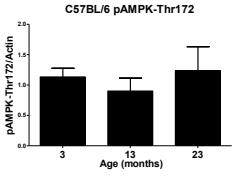

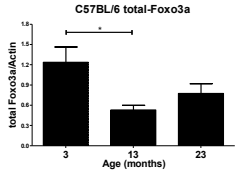

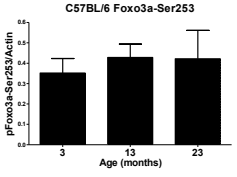

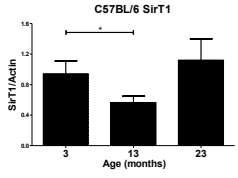

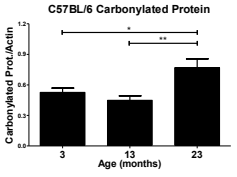

C57BL/6 Heart

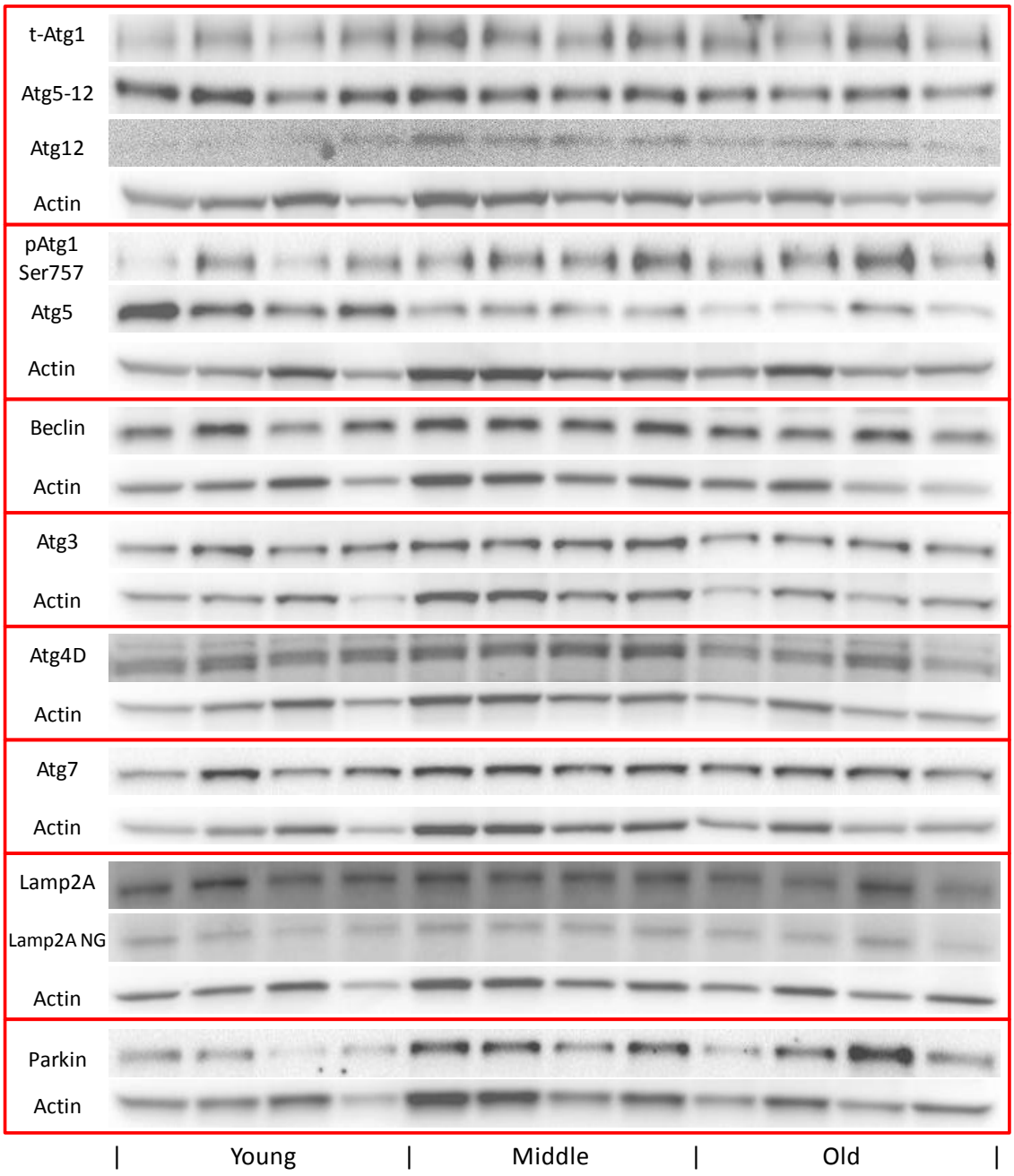

C57BL/6 Heart

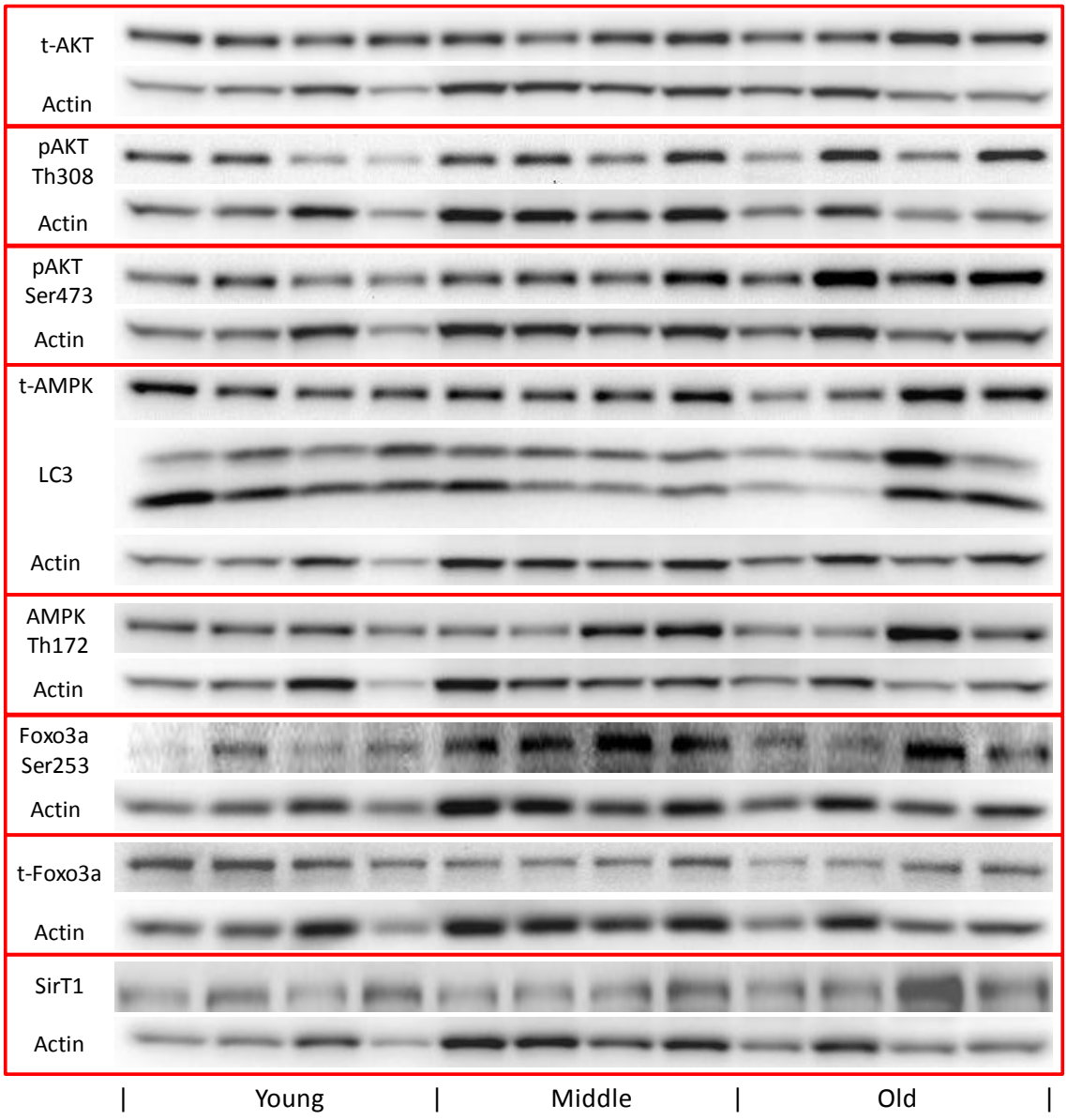

C57BL/6 Heart

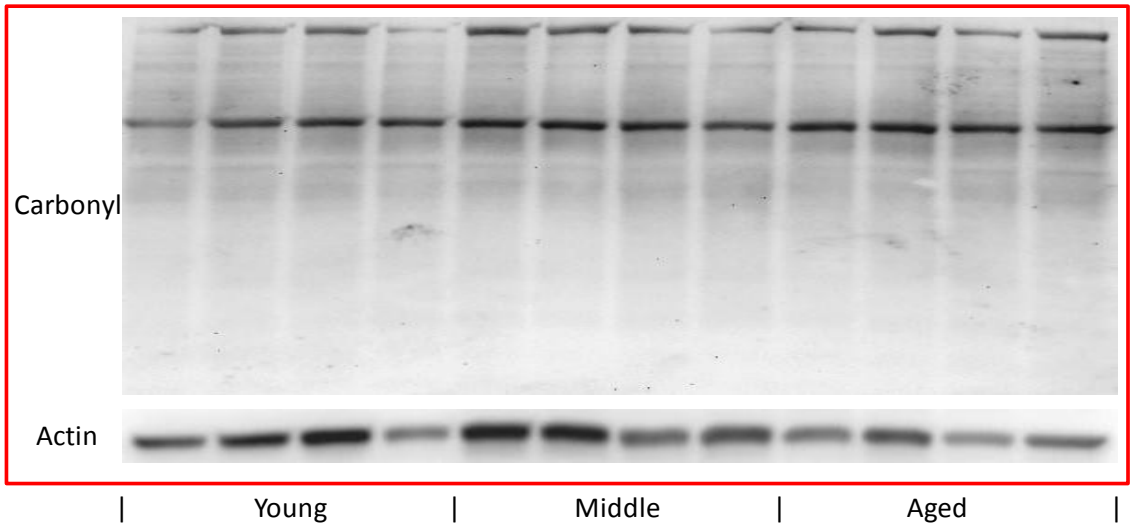

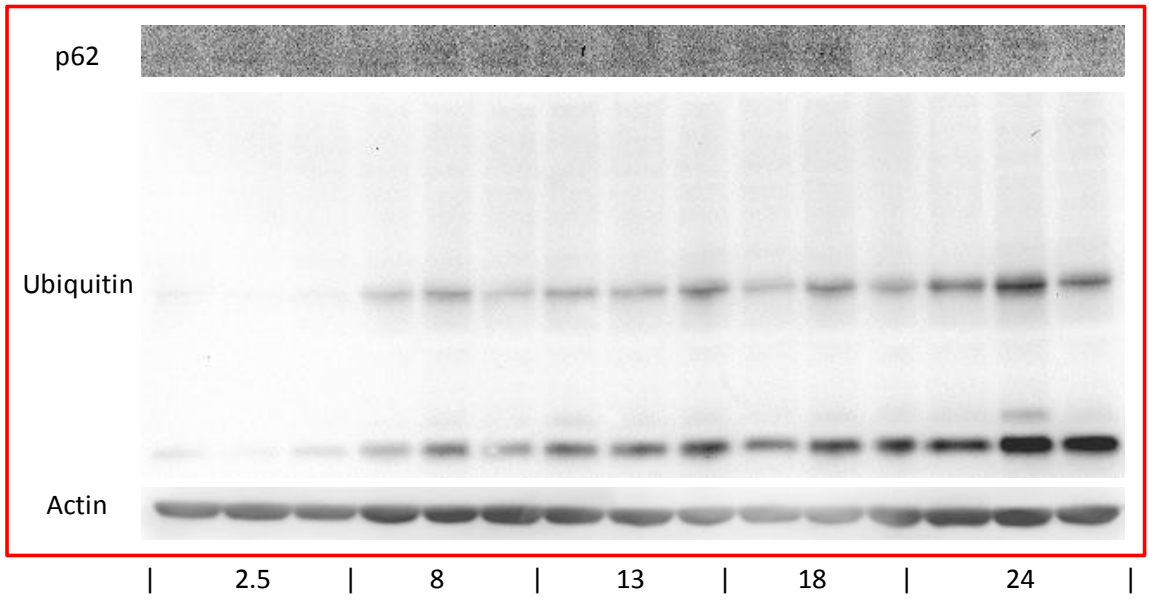

BALB/c Heart

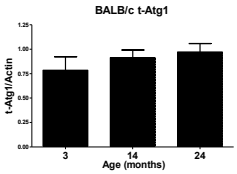
BALB/c t-Atg1
t-Atg1/Actin
Age (months)

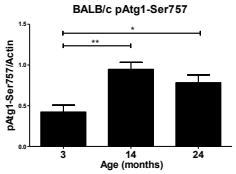
BALB/c pAtg1-Ser757
pAtg1-Ser757/Actin
Age (months)

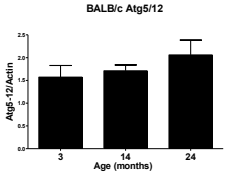
BALB/c Atg5/12
Atg5-12/Actin
Age (months)

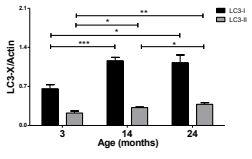
BALB/c LC3
LC3-I
LC3-II
LC3-X/Actin
Age (months)

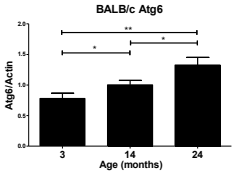
BALB/c Atg6
Atg6/Actin
Age (months)

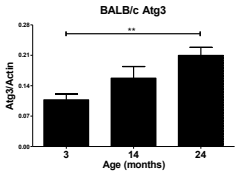
BALB/c Atg3
Atg3/Actin
Age (months)

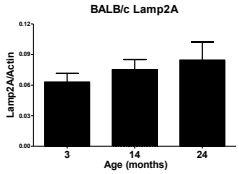
BALB/c Lamp2A
Lamp2A/Actin
Age (months)

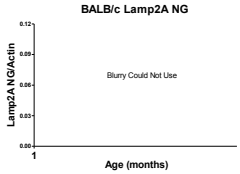
BALB/c Lamp2A NG
Lamp2A NG/Actin
Blurry Could Not Use
Age (months)

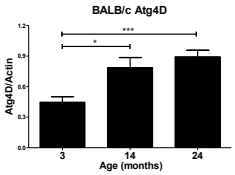
BALB/c Atg4D
Atg4D/Actin
Age (months)

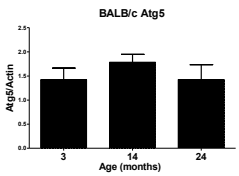
BALB/c Atg5
Atg5/Actin
Age (months)

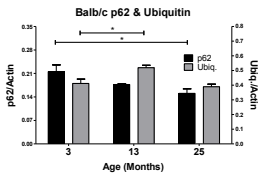
Balb/c p62 & Ubiquitin
p62
Ubiq.
p62/Actin
Ubq./Actin
Age (Months)

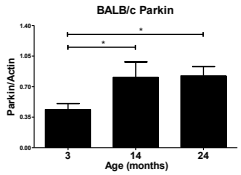
BALB/c Parkin
Parkin/Actin
Age (months)

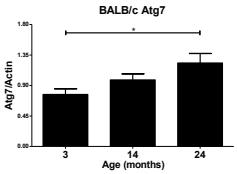
BALB/c Atg7
Atg7/Actin
Age (months)

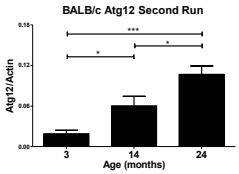
BALB/c Atg12 Second Run
Atg12/Actin
Age (months)

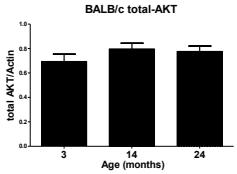
BALB/c total-AKT
total AKT/Actin
Age (months)

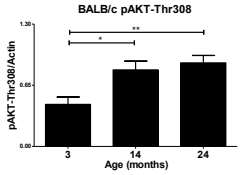
BALB/c pAKT-Thr308
pAKT-Thr308/Actin
Age (months)

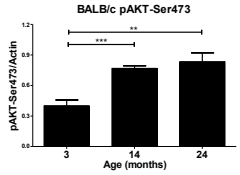
BALB/c pAKT-Ser473
pAKT-Ser473/Actin
Age (months)

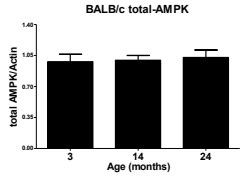
BALB/c total-AMPK
total AMPK/Actin
Age (months)

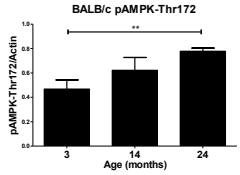
BALB/c pAMPK-Thr172
pAMPK-Thr172/Actin
Age (months)

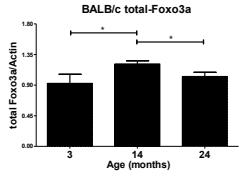
BALB/c total-Foxo3a
total Foxo3a/Actin
Age (months)

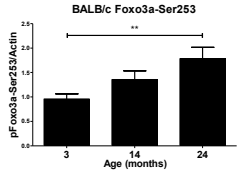
BALB/c Foxo3a-Ser253
pFoxo3a-Ser253/Actin
Age (months)

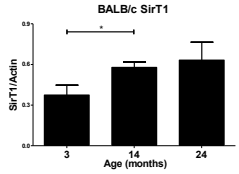
BALB/c SirT1
SirT1/Actin
Age (months)

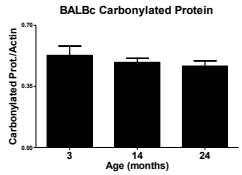
BALBc Carbonylated Protein
Carbonylated Prot./Actin
Age (months)

BALB/c Heart

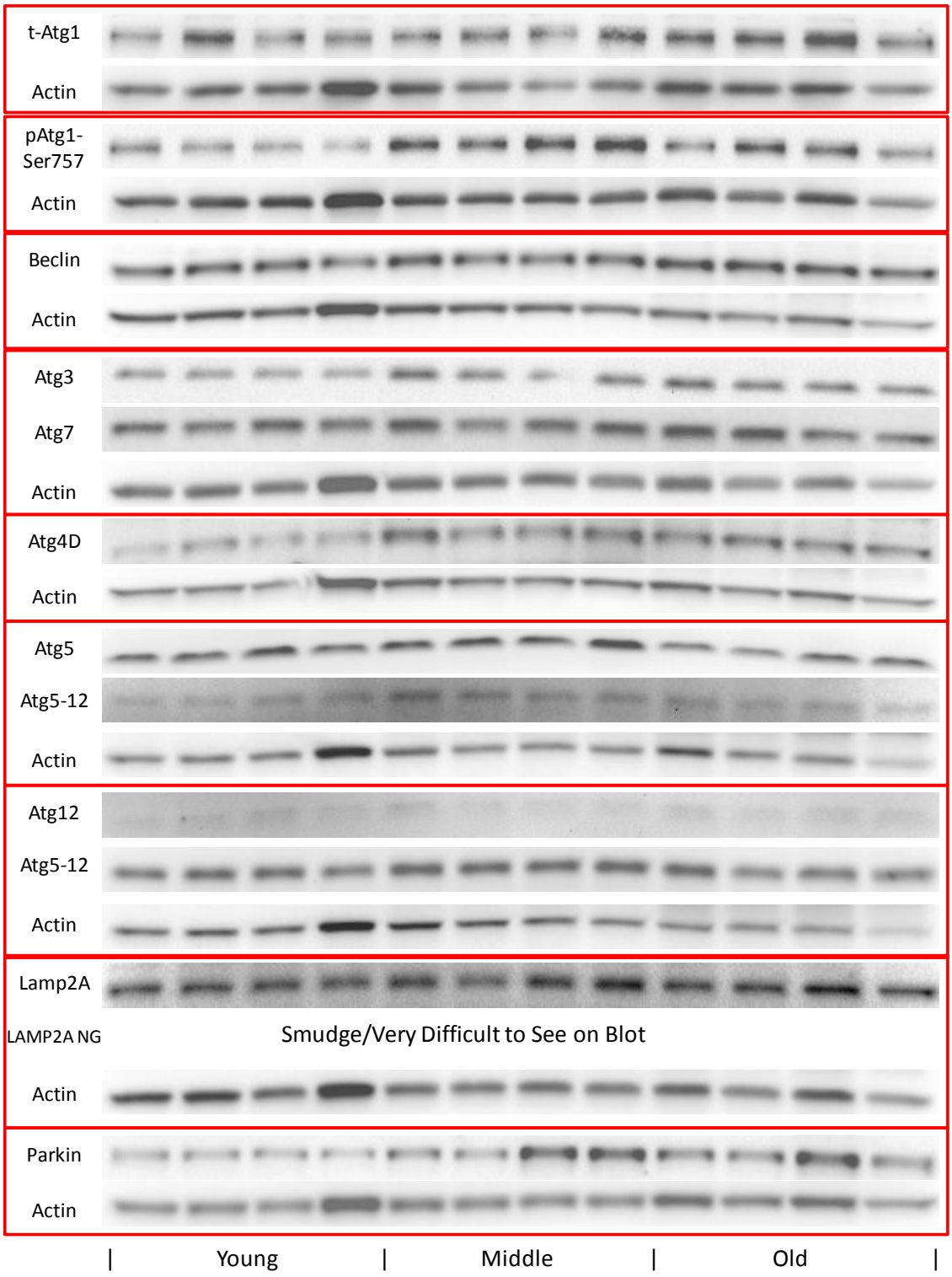
t-Atg1
Actin
pAtg1-Ser757
Actin
Beclin
Actin
Atg3
Atg7
Actin
Atg4D
Actin
Atg5
Atg5-12
Actin
Atg12
Atg5-12
Actin
Lamp2A
LAMP2A NG
Smudge/Very Difficult to See on Blot
Actin
Parkin
Actin
| Young | Middle | Old |

BALB/c Heart

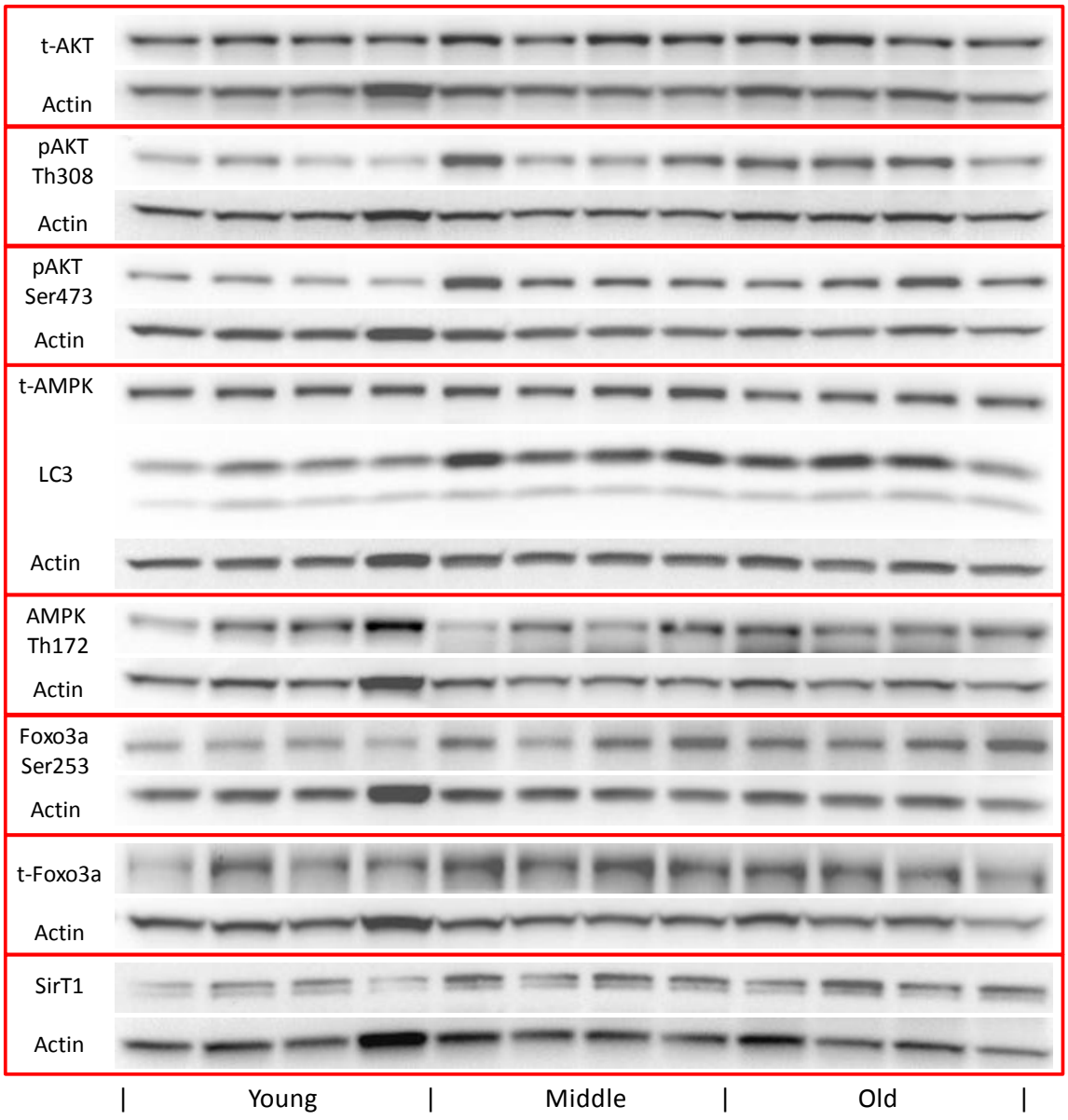
t-AKT
Actin
pAKT Th308
Actin
pAKT Ser473
Actin
t-AMPK
LC3
Actin
AMPK Th172
Actin
Foxo3a Ser253
Actin
t-Foxo3a
Actin
SirT1
Actin
Young
Middle
Old

BALB/c Heart

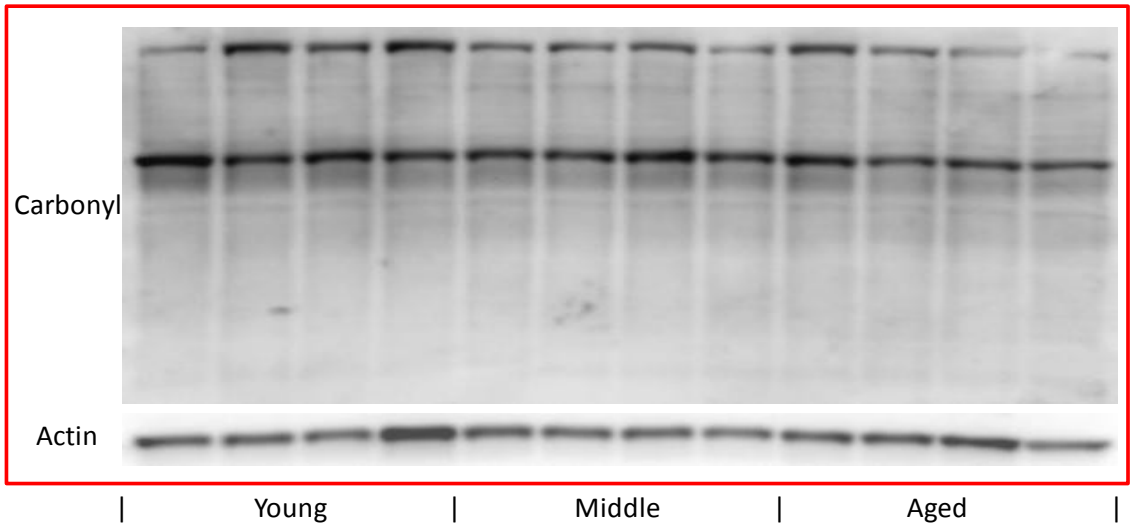
Carbonyl
Actin
Young
Middle
Aged

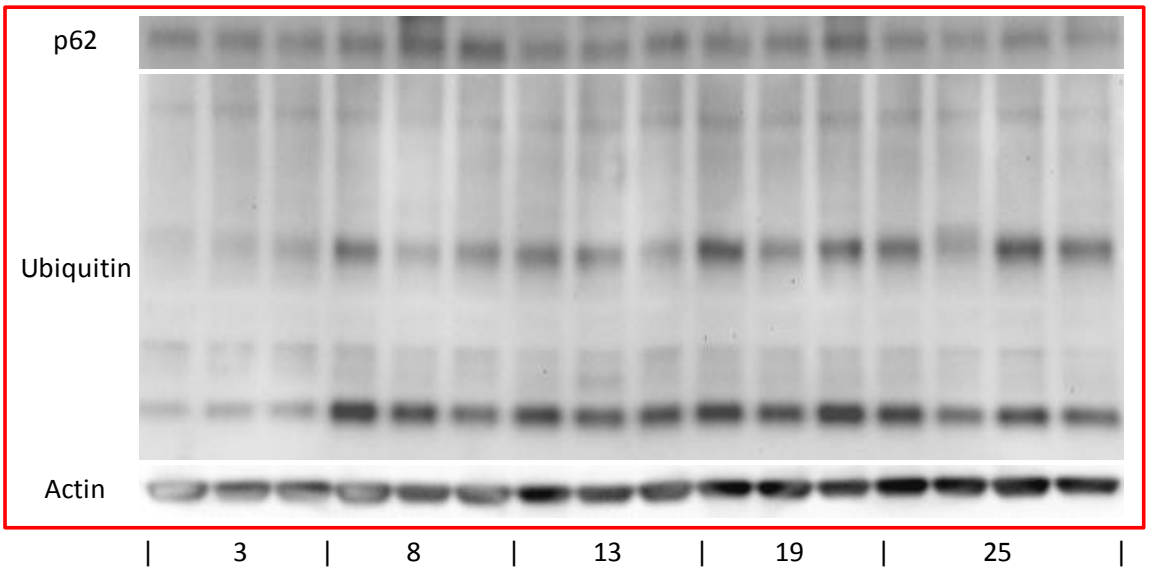
p62
Ubiquitin
Actin
3
8
13
19
25

APPENDIX 4:

Autophagy Profiles in the Hearts of Fasting Young and Aged C57BL/6 and BALB/c Mice

Source Blots for Figure 2.2

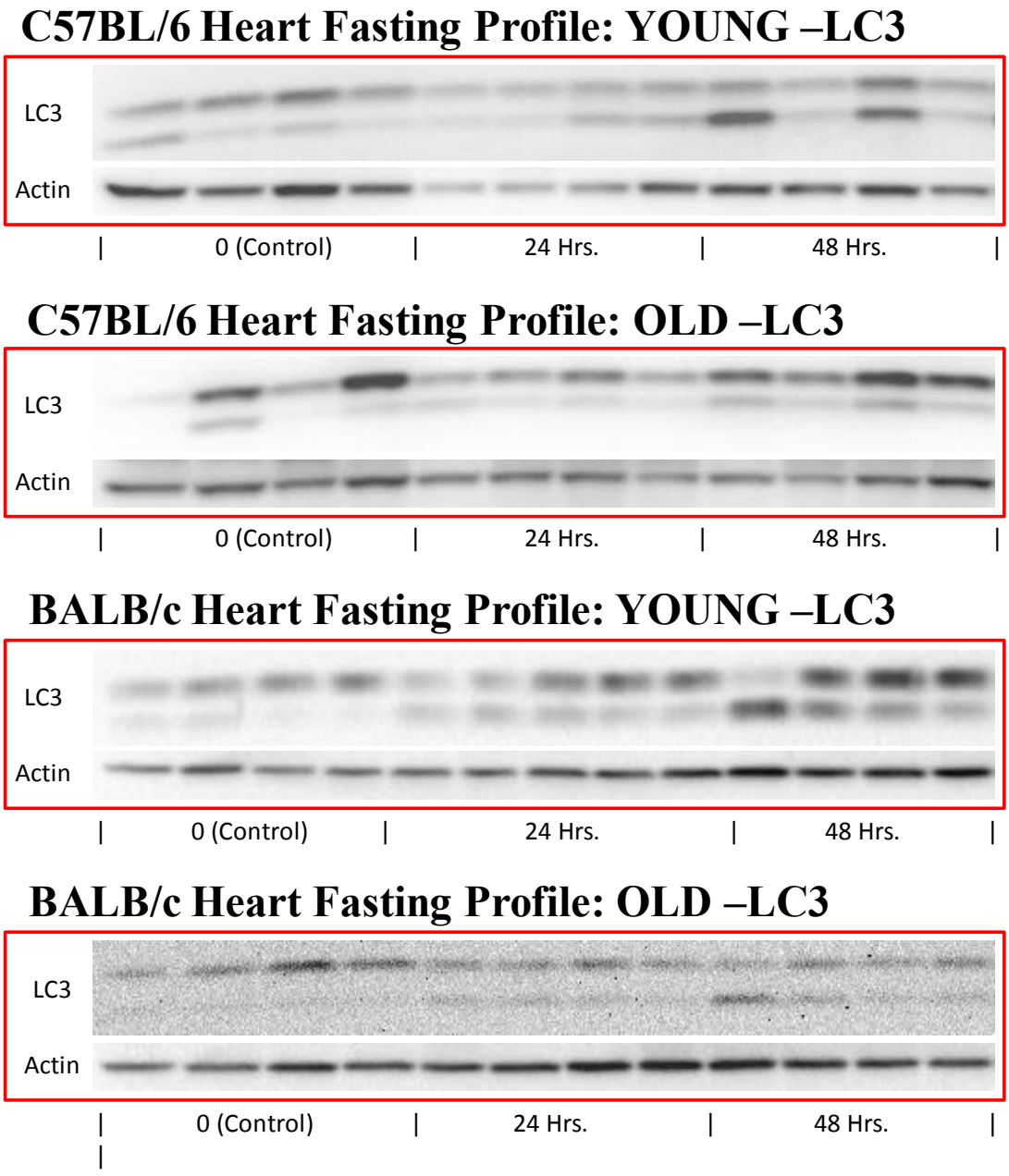

Gel Images and Graphs for Figure 2.4

Fasted Young BALB/c:

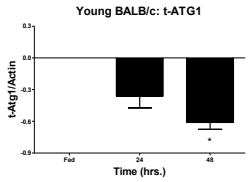

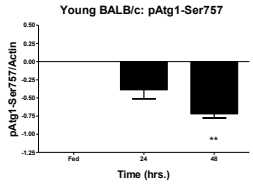

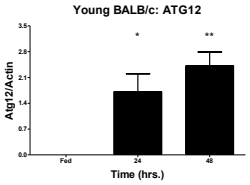

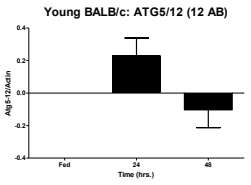

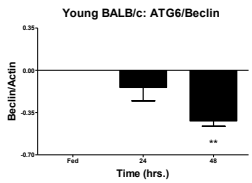

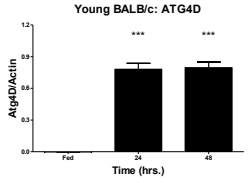

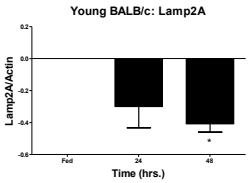

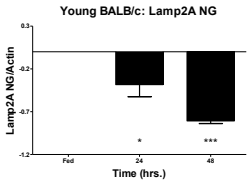

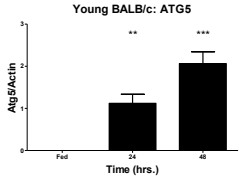

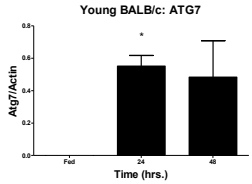

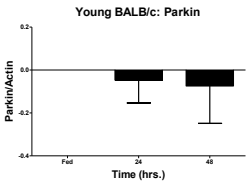

Fasted Aged BALB/c:

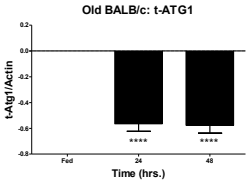

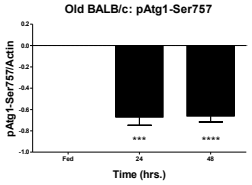

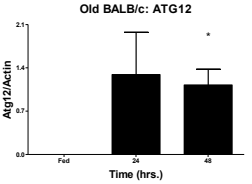

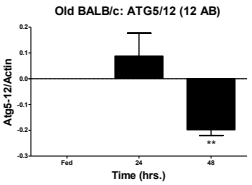

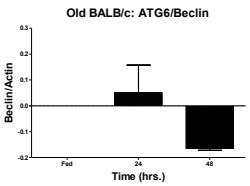

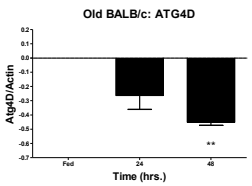

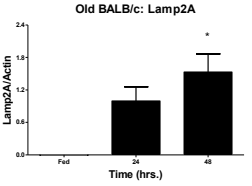

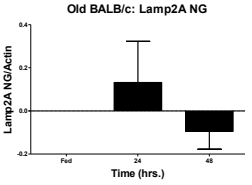

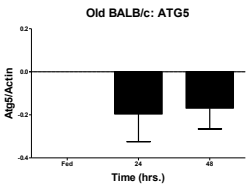

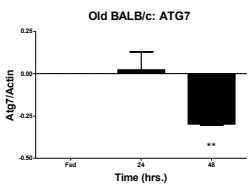

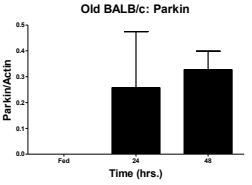

Gel Images for Figure 2.4

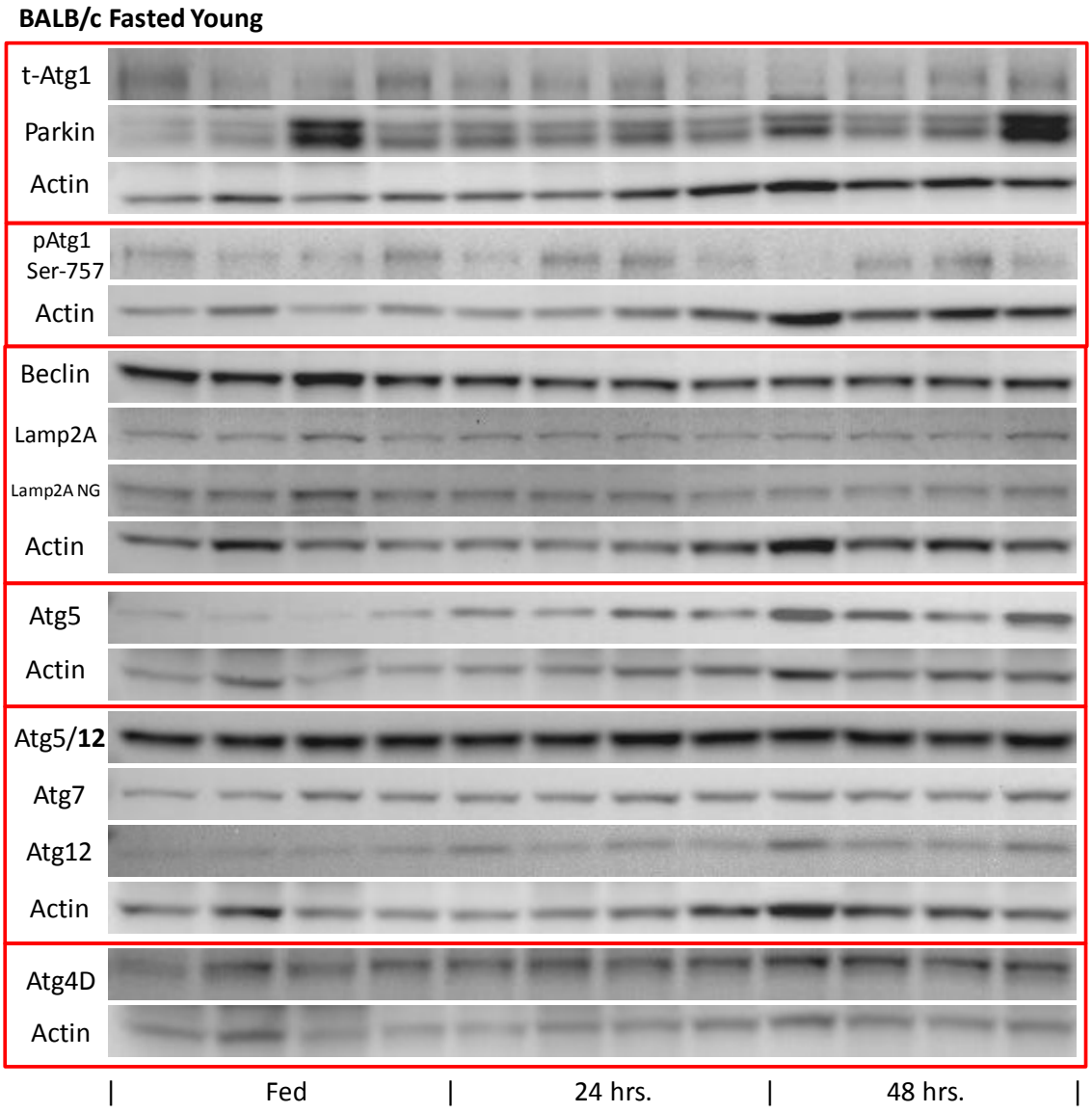

Gel Images for Figure 2.4

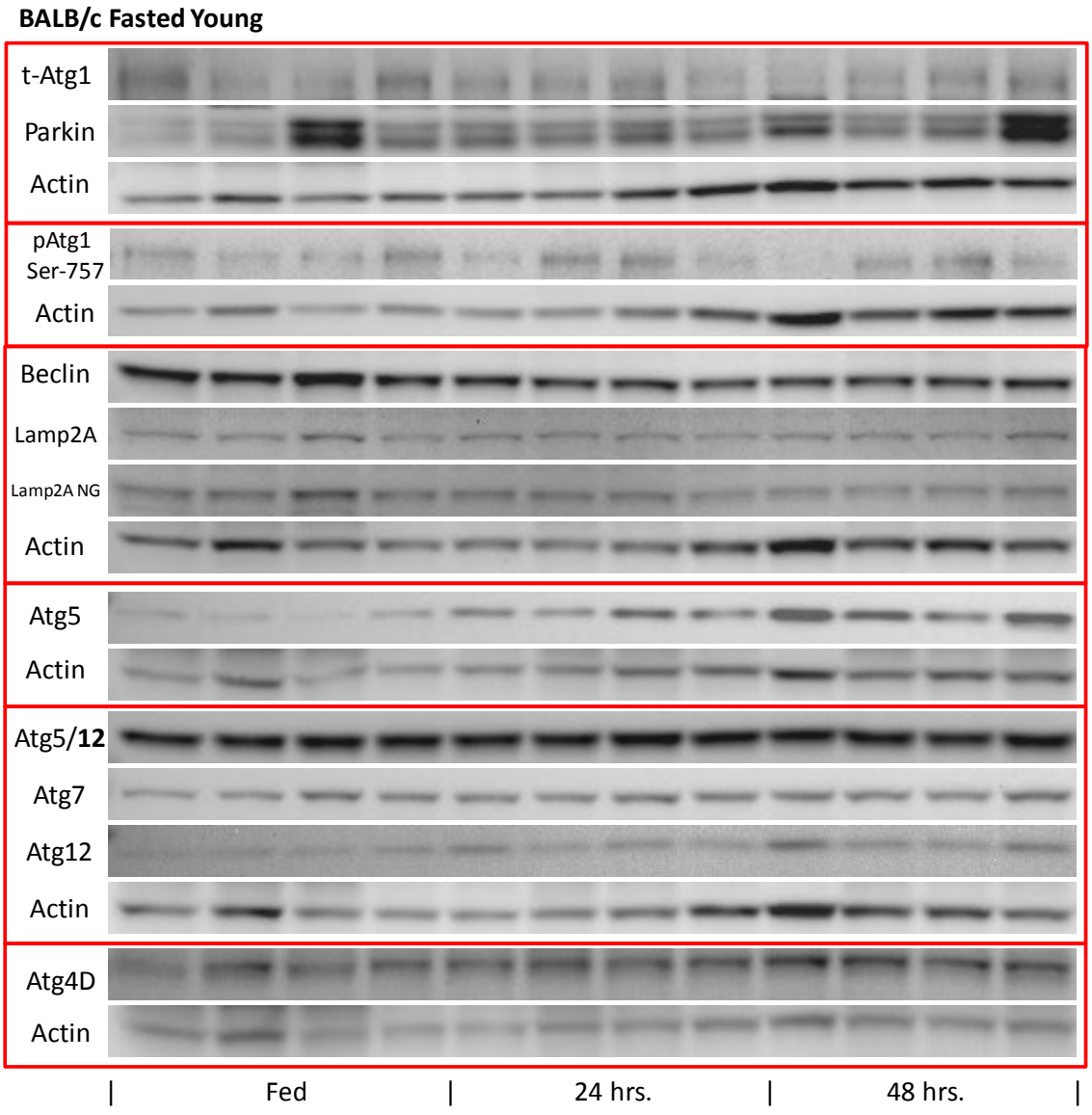

Gel Images and Graphs for Figure 2.3

Fasted Young C57BL/6:

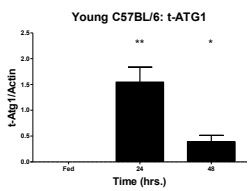

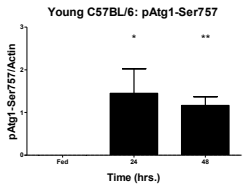

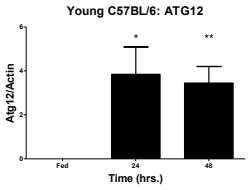

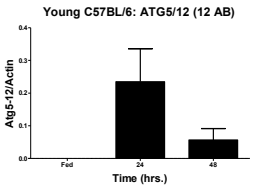

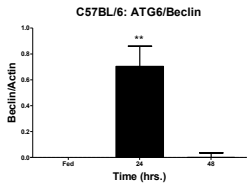

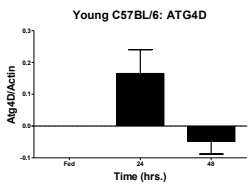

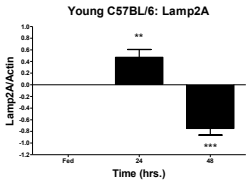

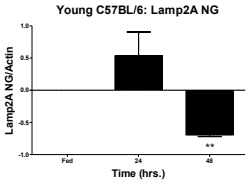

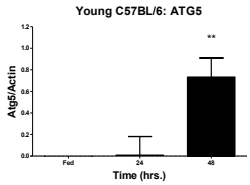

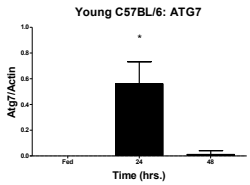

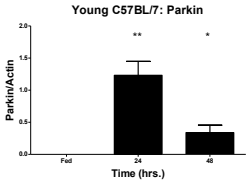

Fasted Aged C57BL/6

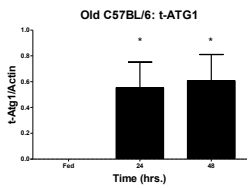

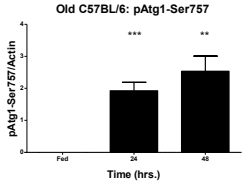

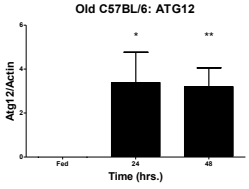

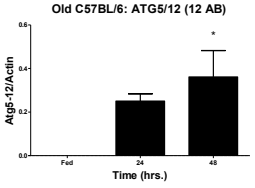

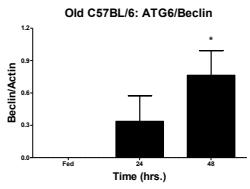

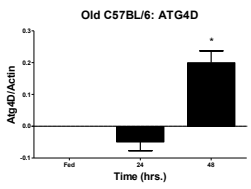

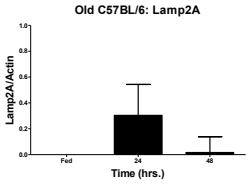

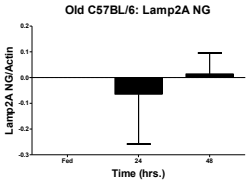

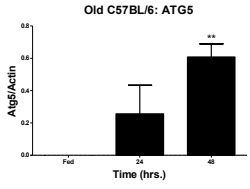

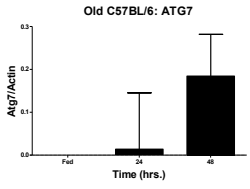

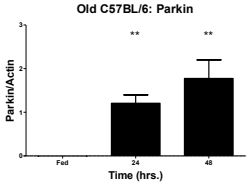

Gel Images for Figure 2.3

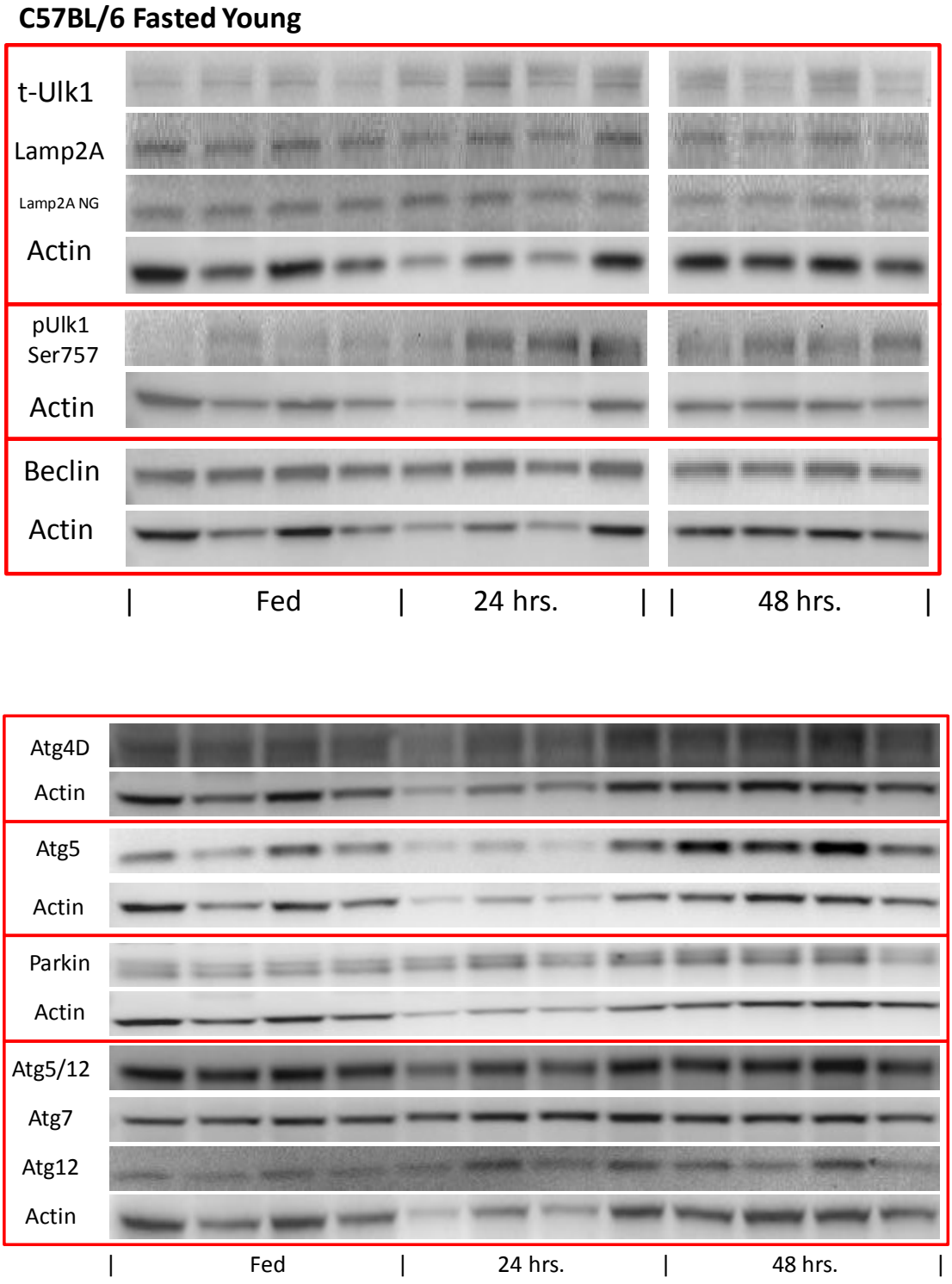

Gel Images for Figure 2.3

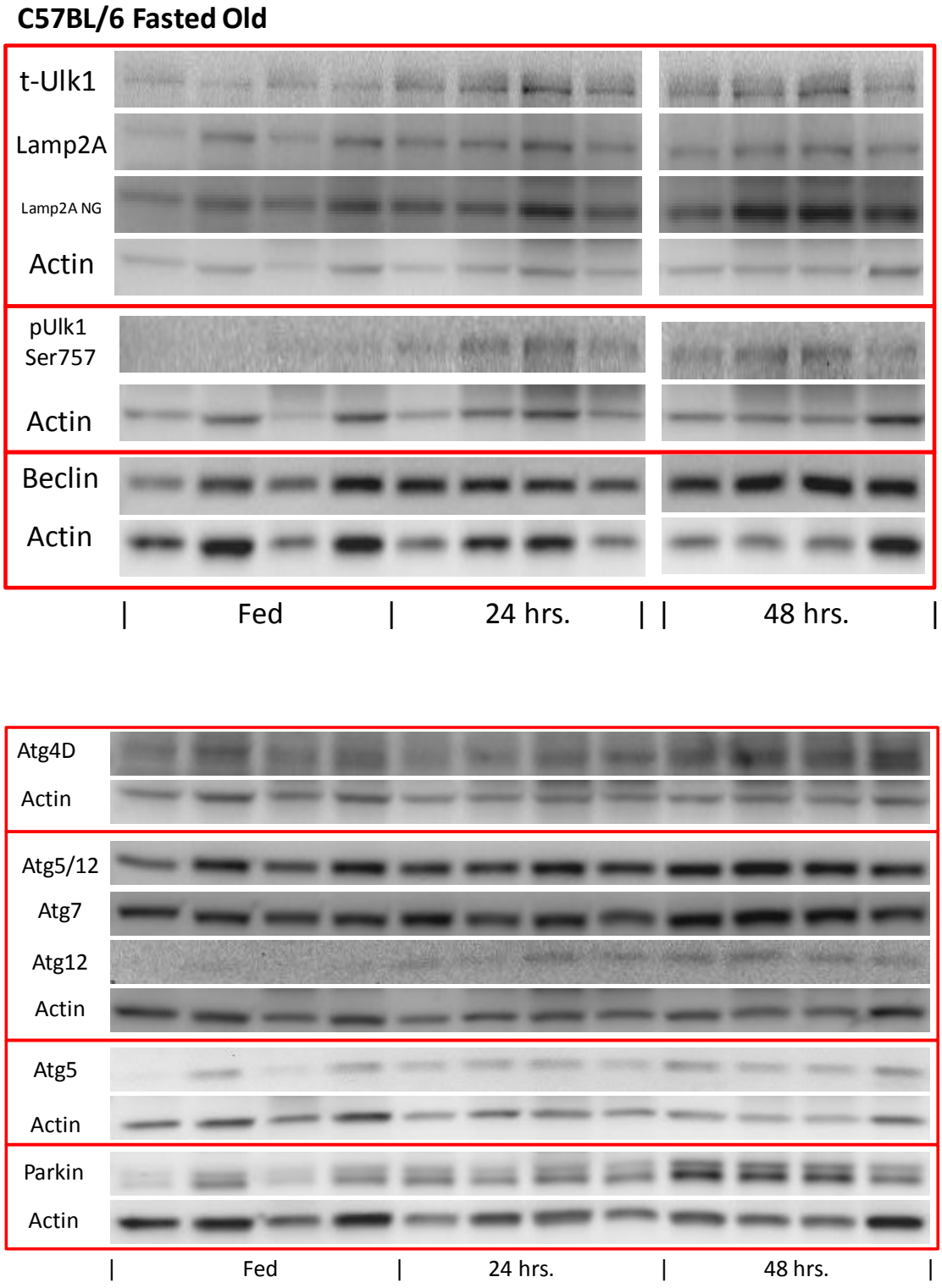

APPENDIX 5:

Autophagic Flux Assays in C57BL/6 and BALB/c Mice

BALB/c 24 Hr. Heart Chloroquine

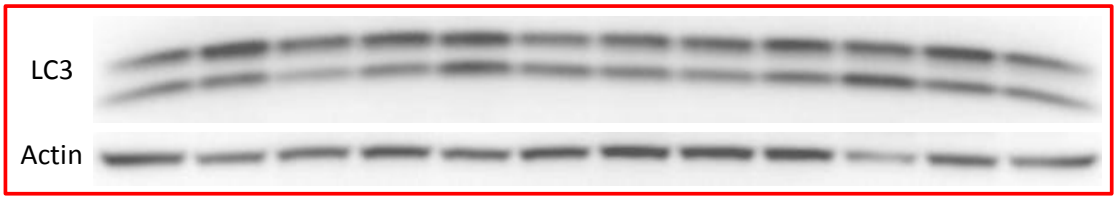

BALB/c 36 Hr. Heart Chloroquine

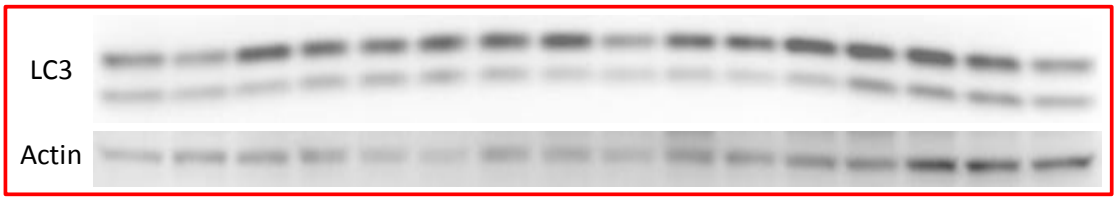

C57BL/6 48 Hr. Heart Chloroquine

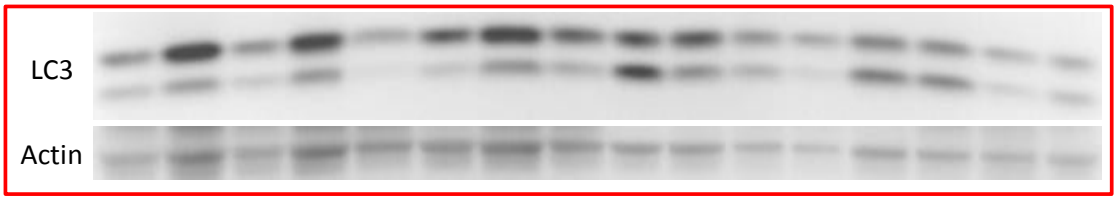

APPENDIX 6:

Intermittent Fasting in the C57BL/6 and BALB/c Heart

BALB/c IF Heart

Heart: 17 m/o Mice – 4 months of IF

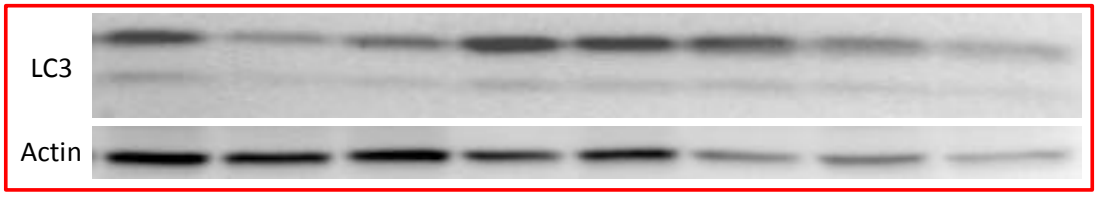

Heart: 19.5 m/o Mice – 6.5 months of IF

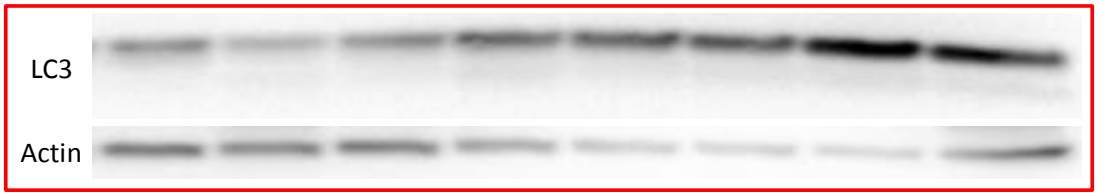

C57BL/6 IF Heart

C57BL/6 IF Heart 3 Week IF

C57BL/6 IF Heart 6 Week IF

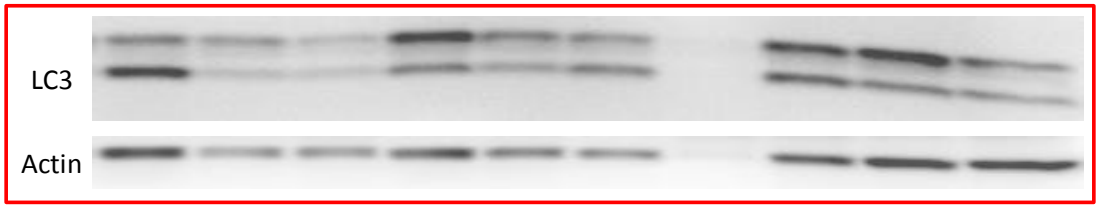

C57BL/6 IF Heart 16 Week IF

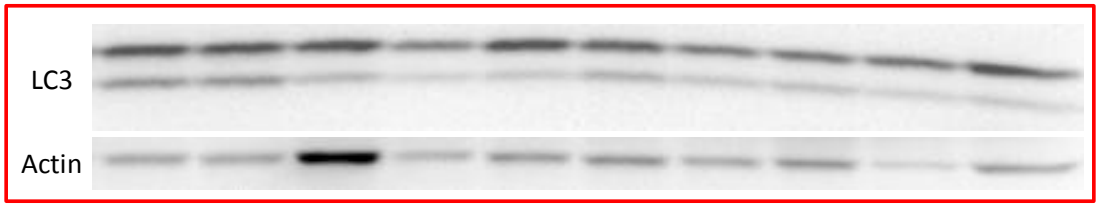

C57BL/6 IF Heart

C57BL/6 IF +/- CQ

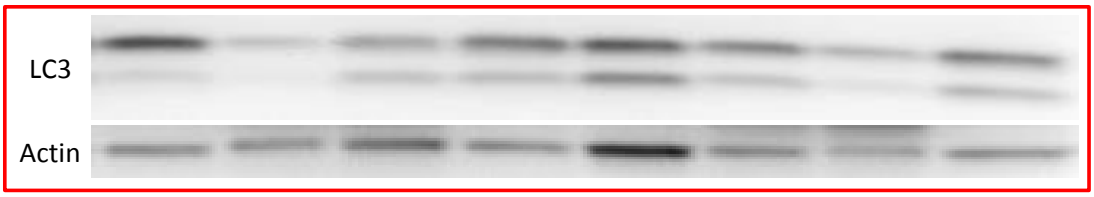

REFERENCES

1. Tanaka, K. & Matsuda, N. Proteostasis and neurodegeneration: the roles of proteasomal degradation and autophagy. *Biochim Biophys Acta* **1843**, 197-204 (2014).

2. Malicdan, M.C., Noguchi, S. & Nishino, I. Monitoring autophagy in muscle diseases. *Methods Enzymol* **453**, 379-96 (2009).

3. Yang, Z.J., Chee, C.E., Huang, S. & Sinicrope, F.A. The role of autophagy in cancer: therapeutic implications. *Mol Cancer Ther* **10**, 1533-41 (2011).

4. Mathew, R., Karantza-Wadsworth, V. & White, E. Role of autophagy in cancer. *Nat Rev Cancer* **7**, 961-7 (2007).

5. De Meyer, G.R. & Martinet, W. Autophagy in the cardiovascular system. *Biochim Biophys Acta* **1793**, 1485-95 (2009).

6. Ren, S.Y. & Xu, X. Role of autophagy in metabolic syndrome-associated heart disease. *Biochim Biophys Acta* (2014).

7. Quan, W. & Lee, M.S. Role of autophagy in the control of body metabolism. *Endocrinol Metab (Seoul)* **28**, 6-11 (2013).

8. Deretic, V., Saitoh, T. & Akira, S. Autophagy in infection, inflammation and immunity. *Nat Rev Immunol* **13**, 722-37 (2013).

9. Yuk, J.M., Yoshimori, T. & Jo, E.K. Autophagy and bacterial infectious diseases. *Exp Mol Med* **44**, 99-108 (2012).

10. Kudchodkar, S.B. & Levine, B. Viruses and autophagy. *Rev Med Virol* **19**, 359-78 (2009).

11. Schneider, J.L. & Cuervo, A.M. Autophagy and human disease: emerging themes. *Curr Opin Genet Dev* **26C**, 16-23 (2014).

12. Li, W.W., Li, J. & Bao, J.K. Microautophagy: lesser-known self-eating. *Cell Mol Life Sci* **69**, 1125-36 (2012).

13. Mijaljica, D., Prescott, M. & Devenish, R.J. Microautophagy in mammalian cells: revisiting a 40-year-old conundrum. *Autophagy* **7**, 673-82 (2011).

14. de Waal, E.J., Vreeling-Sindelárová, H., Schellens, J.P. & James, J. Starvation-induced microautophagic vacuoles in rat myocardial cells. *Cell Biol Int Rep* **10**, 527-33 (1986).

15. Takikita, S., Myerowitz, R., Zaal, K., Raben, N. & Plotz, P.H. Murine muscle cell models for Pompe disease and their use in studying therapeutic approaches. *Mol Genet Metab* **96**, 208-17 (2009).

16. Dice, J.F. et al. A selective pathway for degradation of cytosolic proteins by lysosomes. *Semin Cell Biol* **1**, 449-55 (1990).

17. Kaushik, S. & Cuervo, A.M. Chaperone-mediated autophagy: a unique way to enter the lysosome world. *Trends Cell Biol* **22**, 407-17 (2012).

18. Aniento, F., Roche, E., Cuervo, A.M. & Knecht, E. Uptake and degradation of glyceraldehyde-3-phosphate dehydrogenase by rat liver lysosomes. *J Biol Chem* **268**, 10463-70 (1993).

19. Kiffin, R., Christian, C., Knecht, E. & Cuervo, A.M. Activation of chaperone-mediated autophagy during oxidative stress. *Mol Biol Cell* **15**, 4829-40 (2004).

20. Cuervo, A.M. & Dice, J.F. Age-related decline in chaperone-mediated autophagy. *J Biol Chem* **275**, 31505-13 (2000).

21. Kiffin, R. et al. Altered dynamics of the lysosomal receptor for chaperone-mediated autophagy with age. *J Cell Sci* **120**, 782-91 (2007).

22. Zhang, C. & Cuervo, A.M. Restoration of chaperone-mediated autophagy in aging liver improves cellular maintenance and hepatic function. *Nat Med* **14**, 959-65 (2008).

23. Takemura, G. et al. Autophagy maintains cardiac function in the starved adult. *Autophagy* **5**, 1034-6 (2009).

24. Gustafsson, A.B. & Gottlieb, R.A. Autophagy in ischemic heart disease. *Circ Res* **104**, 150-8 (2009).

25. Betz, C. & Hall, M.N. Where is mTOR and what is it doing there? *J Cell Biol* **203**, 563-74 (2013).

26. Bracho-Valdés, I. et al. mTORC1- and mTORC2-interacting proteins keep their multifunctional partners focused. *IUBMB Life* **63**, 896-914 (2011).

27. Jewell, J.L. & Guan, K.L. Nutrient signaling to mTOR and cell growth. *Trends Biochem Sci* **38**, 233-42 (2013).

28. Kroemer, G., Mariño, G. & Levine, B. Autophagy and the integrated stress response. *Mol Cell* **40**, 280-93 (2010).

29. He, C. & Klionsky, D.J. Regulation mechanisms and signaling pathways of autophagy. *Annu Rev Genet* **43**, 67-93 (2009).

30. Averous, J. & Proud, C.G. When translation meets transformation: the mTOR story. *Oncogene* **25**, 6423-35 (2006).

31. Ma, X.M. & Blenis, J. Molecular mechanisms of mTOR-mediated translational control. *Nat Rev Mol Cell Biol* **10**, 307-18 (2009).

32. Bakan, I. & Laplante, M. Connecting mTORC1 signaling to SREBP-1 activation. *Curr Opin Lipidol* **23**, 226-34 (2012).

33. Peterson, T.R. et al. mTOR complex 1 regulates lipin 1 localization to control the SREBP pathway. *Cell* **146**, 408-20 (2011).

34. Laplante, M. & Sabatini, D.M. An emerging role of mTOR in lipid biosynthesis. *Curr Biol* **19**, R1046-52 (2009).

35. Ben-Sahra, I., Howell, J.J., Asara, J.M. & Manning, B.D. Stimulation of de novo pyrimidine synthesis by growth signaling through mTOR and S6K1. *Science* **339**, 1323-8 (2013).

36. Robitaille, A.M. et al. Quantitative phosphoproteomics reveal mTORC1 activates de novo pyrimidine synthesis. *Science* **339**, 1320-3 (2013).

37. Morita, M. et al. mTORC1 controls mitochondrial activity and biogenesis through 4E-BP-dependent translational regulation. *Cell Metab* **18**, 698-711 (2013).

38. Peña-Llopis, S. et al. Regulation of TFEB and V-ATPases by mTORC1. *EMBO J* **30**, 3242-58 (2011).

39. Iadevaia, V., Huo, Y., Zhang, Z., Foster, L.J. & Proud, C.G. Roles of the mammalian target of rapamycin, mTOR, in controlling ribosome biogenesis and protein synthesis. *Biochem Soc Trans* **40**, 168-72 (2012).

40. Oh, W.J. & Jacinto, E. mTOR complex 2 signaling and functions. *Cell Cycle* **10**, 2305-16 (2011).

41. Wang, S., Song, P. & Zou, M.H. AMP-activated protein kinase, stress responses and cardiovascular diseases. *Clin Sci (Lond)* **122**, 555-73 (2012).

42. Sridharan, S., Jain, K. & Basu, A. Regulation of autophagy by kinases. *Cancers (Basel)* **3**, 2630-54 (2011).

43. Suter, M. et al. Dissecting the role of 5'-AMP for allosteric stimulation, activation, and deactivation of AMP-activated protein kinase. *J Biol Chem* **281**, 32207-16 (2006).

44. Egan, D.F. et al. Phosphorylation of ULK1 (hATG1) by AMP-activated protein kinase connects energy sensing to mitophagy. *Science* **331**, 456-61 (2011).

45. Kim, J., Kundu, M., Viollet, B. & Guan, K.L. AMPK and mTOR regulate autophagy through direct phosphorylation of Ulk1. *Nat Cell Biol* **13**, 132-41 (2011).

46. Inoki, K., Zhu, T. & Guan, K.L. TSC2 mediates cellular energy response to control cell growth and survival. *Cell* **115**, 577-90 (2003).

47. Gwinn, D.M. et al. AMPK phosphorylation of raptor mediates a metabolic checkpoint. *Mol Cell* **30**, 214-26 (2008).

48. Kumar, A., Rajendran, V., Sethumadhavan, R. & Purohit, R. AKT kinase pathway: a leading target in cancer research. *ScientificWorldJournal* **2013**, 756134 (2013).

49. Ravikumar, B. et al. Regulation of mammalian autophagy in physiology and pathophysiology. *Physiol Rev* **90**, 1383-435 (2010).

50. Vincent, E.E. et al. Akt phosphorylation on Thr308 but not on Ser473 correlates with Akt protein kinase activity in human non-small cell lung cancer. *Br J Cancer* **104**, 1755-61 (2011).

51. Gallay, N. et al. The level of AKT phosphorylation on threonine 308 but not on serine 473 is associated with high-risk cytogenetics and predicts poor overall survival in acute myeloid leukaemia. *Leukemia* **23**, 1029-38 (2009).

52. Huang, J., Wu, S., Wu, C.L. & Manning, B.D. Signaling events downstream of mammalian target of rapamycin complex 2 are attenuated in cells and tumors deficient for the tuberous sclerosis complex tumor suppressors. *Cancer Res* **69**, 6107-14 (2009).

53. Wang, L., Harris, T.E., Roth, R.A. & Lawrence, J.C. PRAS40 regulates mTORC1 kinase activity by functioning as a direct inhibitor of substrate binding. *J Biol Chem* **282**, 20036-44 (2007).

54. Sancak, Y. et al. PRAS40 is an insulin-regulated inhibitor of the mTORC1 protein kinase. *Mol Cell* **25**, 903-15 (2007).

55. Haigis, M.C. & Sinclair, D.A. Mammalian sirtuins: biological insights and disease relevance. *Annu Rev Pathol* **5**, 253-95 (2010).

56. Lee, I.H. et al. A role for the NAD-dependent deacetylase Sirt1 in the regulation of autophagy. *Proc Natl Acad Sci U S A* **105**, 3374-9 (2008).

57. Morselli, E. et al. Caloric restriction and resveratrol promote longevity through the Sirtuin-1-dependent induction of autophagy. *Cell Death Dis* **1**, e10 (2010).

58. Cohen, H.Y. et al. Calorie restriction promotes mammalian cell survival by inducing the SIRT1 deacetylase. *Science* **305**, 390-2 (2004).

59. Salminen, A. & Kaarniranta, K. Regulation of the aging process by autophagy. *Trends Mol Med* **15**, 217-24 (2009).

60. Salminen, A. & Kaarniranta, K. SIRT1: regulation of longevity via autophagy. *Cell Signal* **21**, 1356-60 (2009).

61. Speakman, J.R. & Mitchell, S.E. Caloric restriction. *Mol Aspects Med* **32**, 159-221 (2011).

62. Brunet, A. et al. Stress-dependent regulation of FOXO transcription factors by the SIRT1 deacetylase. *Science* **303**, 2011-5 (2004).

63. Kume, S. et al. Calorie restriction enhances cell adaptation to hypoxia through Sirt1-dependent mitochondrial autophagy in mouse aged kidney. *J Clin Invest* **120**, 1043-55 (2010).

64. Mammucari, C. et al. FoxO3 controls autophagy in skeletal muscle in vivo. *Cell Metab* **6**, 458-71 (2007).

65. Chiacchiera, F. & Simone, C. The AMPK-FoxO3A axis as a target for cancer treatment. *Cell Cycle* **9**, 1091-6 (2010).

66. Vogt, P.K., Jiang, H. & Aoki, M. Triple layer control: phosphorylation, acetylation and ubiquitination of FOXO proteins. *Cell Cycle* **4**, 908-13 (2005).

67. Brunet, A. et al. Akt promotes cell survival by phosphorylating and inhibiting a Forkhead transcription factor. *Cell* **96**, 857-68 (1999).

68. Dobson, M. et al. Bimodal regulation of FoxO3 by AKT and 14-3-3. *Biochim Biophys Acta* **1813**, 1453-64 (2011).

69. Greer, E.L. et al. The energy sensor AMP-activated protein kinase directly regulates the mammalian FOXO3 transcription factor. *J Biol Chem* **282**, 30107-19 (2007).

70. Shackelford, D.B. & Shaw, R.J. The LKB1-AMPK pathway: metabolism and growth control in tumour suppression. *Nat Rev Cancer* **9**, 563-75 (2009).

71. Fulco, M. et al. Glucose restriction inhibits skeletal myoblast differentiation by activating SIRT1 through AMPK-mediated regulation of Nampt. *Dev Cell* **14**, 661-73 (2008).

72. Cantó, C. & Auwerx, J. PGC-1alpha, SIRT1 and AMPK, an energy sensing network that controls energy expenditure. *Curr Opin Lipidol* **20**, 98-105 (2009).

73. van der Vos, K.E. & Coffer, P.J. The extending network of FOXO transcriptional target genes. *Antioxid Redox Signal* **14**, 579-92 (2011).

74. Pietrocola, F. et al. Regulation of autophagy by stress-responsive transcription factors. *Semin Cancer Biol* **23**, 310-22 (2013).

75. Bakker, W.J., Harris, I.S. & Mak, T.W. FOXO3a is activated in response to hypoxic stress and inhibits HIF1-induced apoptosis via regulation of CITED2. *Mol Cell* **28**, 941-53 (2007).

76. Kops, G.J. et al. Forkhead transcription factor FOXO3a protects quiescent cells from oxidative stress. *Nature* **419**, 316-21 (2002).

77. Zhao, J. et al. FoxO3 coordinately activates protein degradation by the autophagic/lysosomal and proteasomal pathways in atrophying muscle cells. *Cell Metab* **6**, 472-83 (2007).

78. Sengupta, A., Molkentin, J.D. & Yutzey, K.E. FoxO transcription factors promote autophagy in cardiomyocytes. *J Biol Chem* **284**, 28319-31 (2009).

79. Xiong, X., Tao, R., DePinho, R.A. & Dong, X.C. The autophagy-related gene 14 (Atg14) is regulated by forkhead box O transcription factors and circadian rhythms and plays a critical role in hepatic autophagy and lipid metabolism. *J Biol Chem* **287**, 39107-14 (2012).

80. Zhou, J. et al. FOXO3 induces FOXO1-dependent autophagy by activating the AKT1 signaling pathway. *Autophagy* **8**, 1712-23 (2012).

81. Reggiori, F., Komatsu, M., Finley, K. & Simonsen, A. Selective types of autophagy. *Int J Cell Biol* **2012**, 156272 (2012).

82. Baek, K.H., Park, J. & Shin, I. Autophagy-regulating small molecules and their therapeutic applications. *Chem Soc Rev* **41**, 3245-63 (2012).

83. Mizushima, N., Yoshimori, T. & Ohsumi, Y. The role of Atg proteins in autophagosome formation. *Annu Rev Cell Dev Biol* **27**, 107-32 (2011).

84. Shanware, N.P., Bray, K. & Abraham, R.T. The PI3K, metabolic, and autophagy networks: interactive partners in cellular health and disease. *Annu Rev Pharmacol Toxicol* **53**, 89-106 (2013).

85. Axe, E.L. et al. Autophagosome formation from membrane compartments enriched in phosphatidylinositol 3-phosphate and dynamically connected to the endoplasmic reticulum. *J Cell Biol* **182**, 685-701 (2008).

86. Hayashi-Nishino, M. et al. A subdomain of the endoplasmic reticulum forms a cradle for autophagosome formation. *Nat Cell Biol* **11**, 1433-7 (2009).

87. Ylä-Anttila, P., Vihinen, H., Jokitalo, E. & Eskelinen, E.L. 3D tomography reveals connections between the phagophore and endoplasmic reticulum. *Autophagy* **5**, 1180-5 (2009).

88. Hailey, D.W. et al. Mitochondria supply membranes for autophagosome biogenesis during starvation. *Cell* **141**, 656-67 (2010).

89. Ravikumar, B., Moreau, K., Jahreiss, L., Puri, C. & Rubinsztein, D.C. Plasma membrane contributes to the formation of pre-autophagosomal structures. *Nat Cell Biol* **12**, 747-57 (2010).

90. Otomo, C., Metlagel, Z., Takaesu, G. & Otomo, T. Structure of the human ATG12~ATG5 conjugate required for LC3 lipidation in autophagy. *Nat Struct Mol Biol* (2012).

91. Tooze, S.A. & Yoshimori, T. The origin of the autophagosomal membrane. *Nat Cell Biol* **12**, 831-5 (2010).

92. Bartlett, B.J. et al. p62, Ref(2)P and ubiquitinated proteins are conserved markers of neuronal aging, aggregate formation and progressive autophagic defects. *Autophagy* **7**, 572-83 (2011).

93. Clausen, T.H. et al. p62/SQSTM1 and ALFY interact to facilitate the formation of p62 bodies/ALIS and their degradation by autophagy. *Autophagy* **6**, 330-44 (2010).

94. Rubinsztein, D.C., Mariño, G. & Kroemer, G. Autophagy and aging. *Cell* **146**, 682-95 (2011).

95. Cumming, R.C., Simonsen, A. & Finley, K.D. Quantitative analysis of autophagic activity in Drosophila neural tissues by measuring the turnover rates of pathway substrates. *Methods Enzymol* **451**, 639-51 (2008).

96. LOWRY, O.H., ROSEBROUGH, N.J., FARR, A.L. & RANDALL, R.J. Protein measurement with the Folin phenol reagent. *J Biol Chem* **193**, 265-75 (1951).

97. Pfaffl, M.W. A new mathematical model for relative quantification in real-time RT-PCR. *Nucleic Acids Res* **29**, e45 (2001).

98. Maiuri, M.C. et al. Macrophage autophagy in atherosclerosis. *Mediators Inflamm* **2013**, 584715 (2013).

99. Robinet, P., Ritchey, B. & Smith, J.D. Physiological difference in autophagic flux in macrophages from 2 mouse strains regulates cholesterol ester metabolism. *Arterioscler Thromb Vasc Biol* **33**, 903-10 (2013).

100. Yu, X.H., Fu, Y.C., Zhang, D.W., Yin, K. & Tang, C.K. Foam cells in atherosclerosis. *Clin Chim Acta* **424**, 245-52 (2013).

101. Glass, C.K. & Witztum, J.L. Atherosclerosis. the road ahead. *Cell* **104**, 503-16 (2001).

102. Paigen, B., Ishida, B.Y., Verstuyft, J., Winters, R.B. & Albee, D. Atherosclerosis susceptibility differences among progenitors of recombinant inbred strains of mice. *Arteriosclerosis* **10**, 316-23 (1990).

103. van den Borne, S.W. et al. Mouse strain determines the outcome of wound healing after myocardial infarction. *Cardiovasc Res* **84**, 273-82 (2009).

104. Walkin, L. et al. The role of mouse strain differences in the susceptibility to fibrosis: a systematic review. *Fibrogenesis Tissue Repair* **6**, 18 (2013).

105. Przyklenk, K., Dong, Y., Undyala, V.V. & Whittaker, P. Autophagy as a therapeutic target for ischaemia /reperfusion injury? Concepts, controversies, and challenges. *Cardiovasc Res* **94**, 197-205 (2012).

106. Choi, A.M., Ryter, S.W. & Levine, B. Autophagy in human health and disease. *N Engl J Med* **368**, 1845-6 (2013).

107. Sridhar, S., Botbol, Y., Macian, F. & Cuervo, A.M. Autophagy and disease: always two sides to a problem. *J Pathol* **226**, 255-73 (2012).

108. Jugdutt, B.I. et al. Aging-related early changes in markers of ventricular and matrix remodeling after reperfused ST-segment elevation myocardial infarction in

the canine model: effect of early therapy with an angiotensin II type 1 receptor blocker. *Circulation* **122**, 341-51 (2010).

109. Vellas, B.J., Albarede, J.L. & Garry, P.J. Diseases and aging: patterns of morbidity with age; relationship between aging and age-associated diseases. *Am J Clin Nutr* **55**, 1225S-1230S (1992).

110. Schraml, E. & Grillari, J. From cellular senescence to age-associated diseases: the miRNA connection. *Longev Healthspan* **1**, 10 (2012).

111. Jin, K. Modern Biological Theories of Aging. *Aging Dis* **1**, 72-74 (2010).

112. Harman, D. The biologic clock: the mitochondria? *J Am Geriatr Soc* **20**, 145-7 (1972).

113. HARMAN, D. Aging: a theory based on free radical and radiation chemistry. *J Gerontol* **11**, 298-300 (1956).

114. Dai, D.F., Chiao, Y.A., Marcinek, D.J., Szeto, H.H. & Rabinovitch, P.S. Mitochondrial oxidative stress in aging and healthspan. *Longev Healthspan* **3**, 6 (2014).

115. Terman, A. & Brunk, U.T. Autophagy in cardiac myocyte homeostasis, aging, and pathology. *Cardiovasc Res* **68**, 355-65 (2005).

116. Rezzani, R., Stacchiotti, A. & Rodella, L.F. Morphological and biochemical studies on aging and autophagy. *Ageing Res Rev* **11**, 10-31 (2012).

117. Mammucari, C. & Rizzuto, R. Signaling pathways in mitochondrial dysfunction and aging. *Mech Ageing Dev* **131**, 536-43 (2010).

118. Dröge, W. Autophagy and aging--importance of amino acid levels. *Mech Ageing Dev* **125**, 161-8 (2004).

119. Bergmann, O. et al. Evidence for cardiomyocyte renewal in humans. *Science* **324**, 98-102 (2009).

120. Judge, S., Jang, Y.M., Smith, A., Hagen, T. & Leeuwenburgh, C. Age-associated increases in oxidative stress and antioxidant enzyme activities in cardiac interfibrillar mitochondria: implications for the mitochondrial theory of aging. *FASEB J* **19**, 419-21 (2005).

121. Ingwall, J.S. & Weiss, R.G. Is the failing heart energy starved? On using chemical energy to support cardiac function. *Circ Res* **95**, 135-45 (2004).

122. Nishida, K., Kyoi, S., Yamaguchi, O., Sadoshima, J. & Otsu, K. The role of autophagy in the heart. *Cell Death Differ* **16**, 31-8 (2009).

123. Terman, A., Kurz, T., Navratil, M., Arriaga, E.A. & Brunk, U.T. Mitochondrial turnover and aging of long-lived postmitotic cells: the mitochondrial-lysosomal axis theory of aging. *Antioxid Redox Signal* **12**, 503-35 (2010).

124. Misra, M.K., Sarwat, M., Bhakuni, P., Tuteja, R. & Tuteja, N. Oxidative stress and ischemic myocardial syndromes. *Med Sci Monit* **15**, RA209-219 (2009).

125. Li, L., Chen, Y. & Gibson, S.B. Starvation-induced autophagy is regulated by mitochondrial reactive oxygen species leading to AMPK activation. *Cell Signal* **25**, 50-65 (2013).

126. Scherz-Shouval, R. et al. Reactive oxygen species are essential for autophagy and specifically regulate the activity of Atg4. *EMBO J* **26**, 1749-60 (2007).

127. Martinez-Vicente, M., Sovak, G. & Cuervo, A.M. Protein degradation and aging. *Exp Gerontol* **40**, 622-33 (2005).

128. Brunk, U.T., Jones, C.B. & Sohal, R.S. A novel hypothesis of lipofuscinogenesis and cellular aging based on interactions between oxidative stress and autophagocytosis. *Mutat Res* **275**, 395-403 (1992).

129. Gottlieb, R.A. & Carreira, R.S. Autophagy in health and disease. 5. Mitophagy as a way of life. *Am J Physiol Cell Physiol* **299**, C203-10 (2010).

130. Rajawat, Y.S., Hilioti, Z. & Bossis, I. Aging: central role for autophagy and the lysosomal degradative system. *Ageing Res Rev* **8**, 199-213 (2009).

131. Wohlgemuth, S.E. et al. Autophagy in the heart and liver during normal aging and calorie restriction. *Rejuvenation Res* **10**, 281-92 (2007).

132. Boyle, A.J. et al. Cardiomyopathy of aging in the mammalian heart is characterized by myocardial hypertrophy, fibrosis and a predisposition towards cardiomyocyte apoptosis and autophagy. *Exp Gerontol* **46**, 549-59 (2011).

133. Uddin, M.N., Nishio, N., Ito, S., Suzuki, H. & Isobe, K. Autophagic activity in thymus and liver during aging. *Age (Dordr)* **34**, 75-85 (2012).

134. Inuzuka, Y. et al. Suppression of phosphoinositide 3-kinase prevents cardiac aging in mice. *Circulation* **120**, 1695-703 (2009).

135. Taneike, M. et al. Inhibition of autophagy in the heart induces age-related cardiomyopathy. *Autophagy* **6**, 600-6 (2010).

136. Kanamori, H. et al. Autophagy limits acute myocardial infarction induced by permanent coronary artery occlusion. *Am J Physiol Heart Circ Physiol* **300**, H2261-71 (2011).

137. Kubli, D.A. et al. Parkin Deficiency Exacerbates Cardiac Injury and Reduces Survival Following Myocardial Infarction. *J Biol Chem* (2012).

138. Fan, J. et al. Ischemic preconditioning enhances autophagy but suppresses autophagic cell death in rat spinal neurons following ischemia-reperfusion. *Brain Res* **1562**, 76-86 (2014).

139. Park, H.K. et al. Autophagy is involved in the ischemic preconditioning. *Neurosci Lett* **451**, 16-9 (2009).

140. Huang, C. et al. Autophagy induced by ischemic preconditioning is essential for cardioprotection. *J Cardiovasc Transl Res* **3**, 365-73 (2010).

141. Yan, L., Sadoshima, J., Vatner, D.E. & Vatner, S.F. Autophagy in ischemic preconditioning and hibernating myocardium. *Autophagy* **5**, 709-12 (2009).

142. Yan, L. et al. Autophagy in chronically ischemic myocardium. *Proc Natl Acad Sci U S A* **102**, 13807-12 (2005).

143. Hamacher-Brady, A., Brady, N.R. & Gottlieb, R.A. Enhancing macroautophagy protects against ischemia/reperfusion injury in cardiac myocytes. *J Biol Chem* **281**, 29776-87 (2006).

144. Boengler, K. et al. Cardioprotection by ischemic postconditioning is lost in aged and STAT3-deficient mice. *Circ Res* **102**, 131-5 (2008).

145. Wojtovich, A.P., Nadtochiy, S.M., Brookes, P.S. & Nehrke, K. Ischemic preconditioning: the role of mitochondria and aging. *Exp Gerontol* **47**, 1-7 (2012).

146. Abete, P. et al. Ischemic preconditioning in the younger and aged heart. *Aging Dis* **2**, 138-48 (2011).

147. Klionsky, D.J. et al. Guidelines for the use and interpretation of assays for monitoring autophagy. *Autophagy* **8**, 445-544 (2012).

148. Klionsky, D.J., Elazar, Z., Seglen, P.O. & Rubinsztein, D.C. Does bafilomycin A1 block the fusion of autophagosomes with lysosomes? *Autophagy* **4**, 849-950 (2008).

149. Dalle-Donne, I., Giustarini, D., Colombo, R., Rossi, R. & Milzani, A. Protein carbonylation in human diseases. *Trends Mol Med* **9**, 169-76 (2003).

150. Hua, Y. et al. Chronic Akt activation accentuates aging-induced cardiac hypertrophy and myocardial contractile dysfunction: role of autophagy. *Basic Res Cardiol* **106**, 1173-91 (2011).

151. Kourtis, N. & Tavernarakis, N. Autophagy and cell death in model organisms. *Cell Death Differ* **16**, 21-30 (2009).

152. Cuervo, A.M. & Dice, J.F. Regulation of LAMP2a levels in the lysosomal membrane. *Traffic* **1**, 570-83 (2000).

153. Faubert, B., Vincent, E.E., Poffenberger, M.C. & Jones, R.G. The AMP-activated protein kinase (AMPK) and cancer: Many faces of a metabolic regulator. *Cancer Lett* (2014).

154. Fresno Vara, J.A. et al. PI3K/Akt signalling pathway and cancer. *Cancer Treat Rev* **30**, 193-204 (2004).

155. Davies, M.A. Regulation, role, and targeting of Akt in cancer. *J Clin Oncol* **29**, 4715-7 (2011).

156. Wu, G. et al. Decreased gene expression of LC3 in peripheral leucocytes of patients with coronary artery disease. *Eur J Clin Invest* **41**, 958-63 (2011).

157. Claycomb, W.C. et al. HL-1 cells: a cardiac muscle cell line that contracts and retains phenotypic characteristics of the adult cardiomyocyte. *Proc Natl Acad Sci U S A* **95**, 2979-84 (1998).

158. Hartman, A.L., Santos, P., Dolce, A. & Hardwick, J.M. The mTOR inhibitor rapamycin has limited acute anticonvulsant effects in mice. *PLoS One* **7**, e45156 (2012).

159. Rodriguez-Rocha, H. et al. Adenoviruses induce autophagy to promote virus replication and oncolysis. *Virology* **416**, 9-15 (2011).

160. Shimizu, S., Arakawa, S. & Nishida, Y. Autophagy takes an alternative pathway. *Autophagy* **6**, 290-1 (2010).

161. Nishida, Y. et al. Discovery of Atg5/Atg7-independent alternative macroautophagy. *Nature* **461**, 654-8 (2009).

162. Xu, X. et al. Diminished autophagy limits cardiac injury in mouse models of type 1 diabetes. *J Biol Chem* **288**, 18077-92 (2013).

163. Leontieva, O.V., Paszkiewicz, G.M. & Blagosklonny, M.V. Mechanistic or mammalian target of rapamycin (mTOR) may determine robustness in young male mice at the cost of accelerated aging. *Aging (Albany NY)* **4**, 899-916 (2012).

164. A.D.A.M. "Exercise In-Depth Report" New York Times. June 17, 2013. New York Times Health Guides. <http://www.nytimes.com/health/guides/specialtopic/physical-activity/exercise%27s-effects-on-the-heart.html> Last Accessed: 28 August 2014.